Mathematical models and numerical methods for XVA in multicurrency setting

Author: Roberta Simonella

Doctoral Thesis UDC / Year 2023

Supervisors: Íñigo Arregui Álvarez

Carlos Vázquez Cendón

Doctoral Programme in Mathematical Methods and Numerical Simulation in Engineering and Applied Sciences

UNIVERSIDADE DA CORUÑA

UNIVERSIDADE DA CORUÑA

Ph.D. Thesis

Mathematical models and numerical methods for XVA in multicurrency setting

AUTORA:

Roberta Simonella

DIRECTORES:

Íñigo Arregui Álvarez

Carlos Vázquez Cendón

TESE PRESENTADA PARA A OBTENCIÓN DO TÍTULO DE DOUTOR NA UNIVERSIDADE DA CORUÑA

DEPARTAMENTO DE MATEMÁTICAS

FACULTADE DE INFORMÁTICA, A CORUÑA (SPAIN)

May, 2023

UNIVERSIDADE DA CORUÑA

Los abajo firmantes hacen constar que son directores de la Tesis Doctoral titulada **"Mathematical models and numerical methods for XVA in multicurrency setting"** desarrollada por Roberta Simonella, cuya firma también se incluye, dentro del programa de doctorado **"Métodos Matemáticos y Simulación Numérica en Ingeniería y Ciencias Aplicadas"** en el Departamento de Matemáticas (Universidade da Coruña), dando su consentimiento para su presentación y posterior defensa.

The undersigned hereby certify that they are supervisors of the Thesis entitled **"Mathematical models and numerical methods for XVA in multicurrency setting"** developed by Roberta Simonella, whose signature is also included, in the Ph.D. Program **"Mathematical Methods and Numerical Simulation in Engineering and Applied Sciences"** at the Department of Mathematics (University of A Coruña), consenting to its presentation and posterior defense.

May, 2023

Directores:

Íñigo Arregui Álvarez

Carlos Vázquez Cendón

Doctoranda:

Roberta Simonella

Roberta Simonella

Funding

This research has been partially funded by:

- European Union, through the grant ABC-EU-XVA: Valuation adjustments for improved risk management, inside the call H2020-MSCA-ITN-2018 (Grant Agreement 813261).
- Spanish Ministry of Science and Innovation, through the grant PID2019-108584RB-I00, including FEDER financial support.
- Galician Government through the grant ED431C2018/033, including FEDER financial support.

This research also received the support from the Centro de Investigación de Galicia (CITIC), funded by Xunta de Galicia and the European Union (European Regional Development Fund - Galicia 2014-2020 Program), by grant ED431G 2019/01.

A Mirco

Acknowledgements

First and foremost, I would like to express my gratitude to my supervisors, Professor Carlos Vázquez Cendón and Professor Íñigo Arregui Álvarez, for their constant support and guidance. The expertise of Carlos, along with his ability to provide great insights, has been fundamental during my research activity. Íñigo's knowledge in numerical methods and his authentic interest in my progress have played an essential role throughout the progress of the thesis. I feel truly honored to have had the opportunity to work with both of you and I hope to carry on this collaboration in future research further advancing our shared passion for Applied Mathematics.

I am grateful to Dr. Marco Di Francesco for his expertise in insurance industry and his ability to connect theoretical Mathematics and real world business problems. Thank you for your enthusiastic teaching and all the knowledge you have largely shared with me.

I would also like to acknowledge all the members of the ABC-EU-XVA project for giving me the opportunity to be part of this stimulating experience and for their dedication to create a supportive research environment, also organizing initiatives that have significantly contributed to my personal and professional growth.

Additionally, I would like to extend my appreciation to the Universidade da Coruña and to the charming city of A Coruña for providing a welcoming and vibrant atmosphere that has made my time here truly memorable.

I would like to offer my thank to all the people I had the opportunity to meet during the PhD who have contributed to my growth and learning in some way or another.

I am also grateful to my friends who have been there for me in numerous ways, from lending an ear to my thoughts, accompanying me on walks, or just engaging in simple talks.

Last but not least, I would like to express my profound gratitude to my family for their unfailing support and for always believing in me. I am especially grateful to Mirco, because his love, his esteem and his continuous encouragement have been indispensable in every stage of this thesis development.

A Coruña, May 2023.

Table of Contents

Abstract **xv**

Resumen **xvii**

Resumo **xix**

Abbreviations and notations **xxi**

Introduction **1**

1 Total Value Adjustment in a multi-currency setting with deterministic FX rates **9**

1.1 Introduction 9

1.2 Formulation in terms of partial differential equations 11

1.2.1 Replicating portfolio 16

1.2.2 Pricing partial differential equations 20

1.3 Formulation in terms of expectations 25

1.4 Numerical methods 27

1.4.1 Lagrange-Galerkin method 27

1.4.2 Monte Carlo method 39

1.4.3 Multilevel Picard iteration 43

1.5 Numerical results 45

1.5.1 Spread option 47

1.5.2 Exchange option 59

1.5.3 Sum of call options 64

1.6 Conclusions 75

2 Total Value Adjustment in a multi-currency setting with stochastic FX rates **77**

2.1 Introduction 77

2.2 Formulation in terms of partial differential equations 78
2.2.1 Replicating portfolio 83
2.2.2 Pricing partial differential equations 87
2.3 Formulation in terms of expectations 92
2.4 Numerical methods 93
2.4.1 Monte Carlo method 93
2.4.2 Multilevel Picard iteration 97
2.5 Numerical results 98
2.5.1 Spread option 100
2.5.2 Option on the maximum 101
2.5.3 Best of put/put option 106
2.5.4 Basket option 113
2.6 Conclusions 118

Conclusions **119**

A A stochastic Asset Liability Management model for life insurance companies **123**
A.1 Introduction 123
A.2 The model 128
A.3 Liability model 133
A.3.1 The surrender and new production model 138
A.3.2 The mortality model 140
A.3.3 Approximation of future cash flows 141
A.3.4 Interest rate model associated to the term structure of interest rates 146
A.4 Asset model 149
A.5 First stage of portfolio rebalancing 151
A.6 Second stage of portfolio optimization 153
A.7 Market data 154
A.8 Numerical results 156
A.9 Conclusions 166

Resumen extenso **169**

Resumo extenso **181**

Bibliography **192**

List of Tables

1.1 Analysis of boundary conditions [41] 33

1.2 Analysis of boundary conditions [41] 34

1.3 Financial data 46

1.4 Counterparty's credit spread data. Values are in basis points (bps) . . 46

1.5 Spread option. Comparison of Monte Carlo method and Lagrange-Galerkin (LG). Risk-free value (Test 1) 49

1.6 Spread option, nonlinear problem and deterministic exponential Vasicek credit spread. Comparison of Monte Carlo (with simple rectangular (SimpR) and trapezoidal (SimpT) quadrature formulae), multilevel Picard iteration (MPI) and Lagrange-Galerkin (LG) methods. Total value adjustment (Test 2) 50

1.7 Spread option, nonlinear problem and deterministic CIR credit spread. Comparison of Monte Carlo (with simple rectangular (SimpR) and trapezoidal (SimpT) quadrature formulae), multilevel Picard iteration (MPI) and Lagrange Galerkin (LG) methods. Total value adjustment (Test 2) 51

1.8 Spread option, linear problem and deterministic exponential Vasicek credit spread. Comparison of Monte Carlo (with composite rectangular (CompR) and trapezoidal (CompT) quadrature formulae) and Lagrange-Galerkin (LG) methods. Total value adjustment (Test 3) . . 52

1.9 Spread option, linear problem and deterministic CIR credit spread. Comparison of Monte Carlo (with composite rectangular (CompR) and trapezoidal (CompT) quadrature formulae) and Lagrange-Galerkin (LG) methods. Total value adjustment (Test 3) 52

1.10 Spread option, linear problem and deterministic exponential Vasicek credit spread. Comparison of Monte Carlo (with composite rectangular (CompR) and trapezoidal (CompT) quadrature formulae) and Lagrange-Galerkin (LG) methods. Risky value (Test 3) 53

1.11 Spread option, nonlinear problem and stochastic exponential Vasicek credit spread. Comparison of Monte Carlo (with simple rectangular (SimpR) and trapezoidal (SimpT) quadrature formulae) and multilevel Picard iteration (MPI). Total value adjustment (Test 4) 54

1.12 Spread option, nonlinear problem and stochastic CIR credit spread. Comparison of Monte Carlo (with simple rectangular (SimpR) and trapezoidal (SimpT) quadrature formulae) and multilevel Picard iteration (MPI). Total value adjustment (Test 4) 55

1.13 Spread option, linear problem and stochastic exponential Vasicek credit spread. Comparison of Monte Carlo with simple rectangular (SimpR), simple trapezoidal (SimT), composite rectangular (CompR) and trapezoidal (CompT) quadrature formulae. Total value adjustment (Test 5) 57

1.14 Spread option, linear problem and stochastic CIR credit spread. Comparison of Monte Carlo with simple rectangular (SimpR), simple trapezoidal (SimT), composite rectangular (CompR) and trapezoidal (CompT) quadrature formulae. Total value adjustment (Test 5) 57

1.15 Exchange option, nonlinear problem and deterministic exponential Vasicek credit spread. Comparison of Monte Carlo (with simple rectangular (SimpR) and trapezoidal (SimpT) quadrature formulae), multilevel Picard iteration (MPI) and Lagrange-Galerkin (LG) methods. Total value adjustment (Test 6) 60

1.16 Exchange option, nonlinear problem and deterministic CIR credit spread. Comparison of Monte Carlo (with simple rectangular (SimpR) and trapezoidal (SimpT) quadrature formulae), multilevel Picard iteration (MPI) and Lagrange-Galerkin (LG) methods. Total value adjustment (Test 6) 60

1.17 Exchange option, linear problem and deterministic exponential Vasicek credit spread. Comparison of Monte Carlo (with composite rectangular (CompR) and trapezoidal (CompT) quadrature formulae) and Lagrange-Galerkin (LG) methods. Total value adjustment (Test 7) . . 62

1.18 Exchange option, linear problem and deterministic CIR credit spread. Comparison of Monte Carlo (with composite rectangular (CompR) and trapezoidal (CompT) quadrature formulae) and Lagrange Galerkin (LG) methods. Total value adjustment (Test 7) 63

1.19 Exchange option, nonlinear problem and stochastic exponential Vasicek credit spread. Comparison of Monte Carlo (with simple rectangular (SimpR) and trapezoidal (SimpT) quadrature formulae) and multilevel Picard iteration (MPI) methods. Total value adjustment (Test 8) 64

1.20 Exchange option, nonlinear problem and stochastic CIR credit spread. Comparison of Monte Carlo (with simple rectangular (SimpR) and trapezoidal (SimpT) quadrature formulae) and multilevel Picard iteration (MPI) methods. Total value adjustment (Test 8) 65

1.21 Exchange option, linear problem and stochastic exponential Vasicek credit spread. Comparison of Monte Carlo with simple rectangular (SimpR), simple trapezoidal (SimpT), composite rectangular (CompR) and trapezoidal (CompT) quadrature formulae. Total value adjustment (Test 9) 66

1.22 Exchange option, linear problem and stochastic CIR credit spread. Comparison of Monte Carlo with simple rectangular (SimpR), simple trapezoidal (SimpT), composite rectangular (CompR) and trapezoidal (CompT) quadrature formulae. Total value adjustment (Test 9) . . . 66

1.23 Sum of call options, nonlinear problem and deterministic exponential Vasicek credit spread. Comparison of Monte Carlo (with simple rectangular (SimpR) and trapezoidal (SimpT) quadrature formulae), multilevel Picard iteration (MPI) and Lagrange-Galerkin (LG) methods. Total value adjustment (Test 10) 68

1.24 Sum of call options, nonlinear problem and deterministic CIR credit spread. Comparison of Monte Carlo (with simple rectangular (SimpR) and trapezoidal (SimpT) quadrature formulae), multilevel Picard iteration (MPI) and Lagrange Galerkin (LG) methods. Total value adjustment (Test 10) 69

1.25 Sum of call options, linear problem and deterministic exponential Vasicek credit spread. Comparison of Monte Carlo (with composite rectangular (CompR) and trapezoidal (CompT) quadrature formulae) and Lagrange-Galerkin (LG) methods. Total value adjustment (Test 11) . 71

1.26 Sum of call options, linear problem and deterministic CIR credit spread. Comparison of Monte Carlo (with composite rectangular (CompR) and trapezoidal (CompT) quadrature formulae) and Lagrange-Galerkin (LG) methods. Total value adjustment (Test 11) 71

1.27 Data for the sum of call options. For $N = 2, 4, 8, 16, 32$ we respectively consider the rows of the table from 1 to $2, 4, 8, 16, 32$. 72

1.28 Sum of call options. Monte Carlo confidence intervals. Risk-free value 72

1.29 Sum of call options, nonlinear problem and stochastic exponential Vasicek credit spread. Multilevel Picard iteration (MPI) results. Total value adjustment and elapsed time in seconds (Test 12) 73

1.30 Sum of call options, nonlinear problem and stochastic CIR credit spread. Multilevel Picard iteration (MPI) results. Total value adjustment and elapsed time in seconds (Test 12) 74

1.31 Sum of call options, linear problem and stochastic exponential Vasicek credit spread. Monte Carlo with composite rectangular (CompR) and trapezoidal (CompT) quadrature formulae results. Total value adjustment and elapsed time (Test 13) 75

1.32 Sum of call options, linear problem and stochastic CIR credit spread. Monte Carlo with composite rectangular (CompR) and trapezoidal (CompT) quadrature formulae results. Total value adjustment and elapsed time (Test 13) 75

2.1 Financial data 100

2.2 Counterparty's credit spread data. Values are in basis points (bps) . . 100

2.3 Spread option, nonlinear problem and exponential Vasicek credit spread. Multilevel Picard iteration (MPI) results. Total value adjustment (Test 1) 101

2.4 Spread option, nonlinear problem and CIR credit spread. Multilevel Picard iteration (MPI) results. Total value adjustment (Test 1) . . . 102

2.5 Spread option, linear problem and exponential Vasicek credit spread. Monte Carlo with composite trapezoidal quadrature formula results. Total value adjustment (Test 1) 102

2.6 Spread option, linear problem and CIR credit spread. Monte Carlo with composite trapezoidal quadrature formula results. Total value adjustment (Test 1) 103

2.7 Option on the maximum. Monte Carlo confidence intervals. Risk-free value 105

2.8 Option on the maximum, nonlinear problem and exponential Vasicek credit spread. Comparison of Monte Carlo (with simple rectangular (SimpR) and trapezoidal (SimpT) quadrature formulae) and multilevel Picard iteration (MPI). Total value adjustment (Test 2) 105

2.9 Option on the maximum, nonlinear problem and CIR credit spread. Comparison of Monte Carlo (with simple rectangular (SimpR) and trapezoidal (SimpT) quadrature formulae) and multilevel Picard iteration (MPI). Total value adjustment (Test 2) 105

2.10 Option on the maximum, linear problem and exponential Vasicek credit spread. Comparison of Monte Carlo with simple rectangular (SimpR), simple trapezoidal (SimT), composite rectangular (CompR) and trapezoidal (CompT) quadrature formulae. Total value adjustment (Test 3) 107

2.11 Option on the maximum, linear problem and CIR credit spread. Comparison of Monte Carlo with simple rectangular (SimpR), simple trapezoidal (SimT), composite rectangular (CompR) and trapezoidal (CompT) quadrature formulae. Total value adjustment (Test 3) 107

2.12 Best of put/put option, nonlinear problem and exponential Vasicek credit spread. Comparison of Monte Carlo (with simple rectangular (SimpR) and trapezoidal (SimpT) quadrature formulae) and multilevel Picard iteration (MPI). Total value adjustment (Test 4) 110

2.13 Best of put/put option, nonlinear problem and CIR credit spread. Comparison of Monte Carlo (with simple rectangular (SimpR) and trapezoidal (SimpT) quadrature formulae) and multilevel Picard iteration (MPI). Total value adjustment (Test 4) 110

2.14 Best of put/put option, linear problem and exponential Vasicek credit spread. Comparison of Monte Carlo with simple rectangular (SimpR), simple trapezoidal (SimT), composite rectangular (CompR) and trapezoidal (CompT) quadrature formulae. Total value adjustment (Test 5) 112

2.15 Best of put/put option, linear problem and CIR credit spread. Comparison of Monte Carlo with simple rectangular (SimpR), simple trapezoidal (SimT), composite rectangular (CompR) and trapezoidal (CompT) quadrature formulae. Total value adjustment (Test 5) 112

2.16 Data for the basket option. For $N = 2, 4, 8, 16$ we respectively consider the first $3, 5, 9, 17$ rows of the table on the left and the corresponding column of the table on the right for the vector of weights α. 114

2.17 Basket option. Monte Carlo confidence intervals. Risk-free value . . . 115

2.18 Basket option, nonlinear problem and exponential Vasicek credit spread. Multilevel Picard iteration (MPI) results. Total value adjustment and elapsed time in seconds (Test 7) 115

2.19 Basket option, nonlinear problem and CIR credit spread. Multilevel Picard iteration (MPI) results. Total value adjustment and elapsed time in seconds (Test 7) 116

2.20 Basket option, linear problem and exponential Vasicek credit spread. Monte Carlo with composite rectangular (CompR) and trapezoidal (CompT) quadrature formulae results. Total value adjustment and elapsed time (Test 8) 117

2.21 Basket option, linear problem and CIR credit spread. Monte Carlo with composite rectangular (CompR) and trapezoidal (CompT) quadrature formulae results. Total value adjustment and elapsed time (Test 8) 117

A.1 Simplified life insurance company's balance sheet 129

A.2 ALM model 131

A.3 Example of representative contracts (model points) for different policyholders' ages and different minimum guaranteed rates of return. All contracts have the same time-to-maturity, so that a model point is a couple $(\bar{A}, g)$, where $\bar{A}$ and g are the representative age and the minimum guaranteed rate of return, respectively 132

A.4 Surrender ($p^S_{q,k}$) and new production ($p^P_{q,k}$) probabilities depending on the threshold interval I^q and on the period k 139
A.5 2019 period life table: death probabilities in percentage for men ($\mathcal{M}$) and women ($\mathcal{F}$) for given age intervals. Source: ISTAT (Italian National Institute of Statistics) 141
A.6 Swaption prices observed on September 30, 2020. Source: Bloomberg 148
A.7 Constraints imposed in the optimization problem of the first stage of portfolio rebalancing 152
A.8 Asset classes representative indexes, short rate representative index and benchmark index. Duration, annualized mean and annualized standard deviation for daily log-returns are reported 155
A.9 Correlation matrix between the asset classes, the short rate and the benchmark index 156
A.10 Initial portfolio composition in the numerical tests 156
A.11 Initial number of policyholders in each model point 158
A.12 Probability of default for different values of the participation rate β . 163
A.13 2020 period life table: death probabilities in percentage for men ($\mathcal{M}$) and women ($\mathcal{F}$) for given age intervals. Source: ISTAT (Italian National Institute of Statistics) 164

List of Figures

1.1 Transactions occurring with the treasury and the FX market to fund the trade. Straight lines refer to initial transactions, that take place at time t, while curved lines to final transactions taking place at time $t+dt$. Blue lines indicate amounts denominated in currency D, whereas red ones represent cash denominated in currency C_0. 18

1.2 Transactions occurring when trading a fully collateralized foreign derivative. Straight lines refer to initial transactions, that take place at time t, while curved lines to final transactions taking place at time $t + dt$. Blue lines indicate amounts denominated in the domestic currency D, whereas red ones represent cash denominated in the foreign currency F. 20

1.3 Spread option with deterministic credit spread. Convergence of MPI with exponential Vasicek dynamics for credit spread on the left and CIR dynamics on the right (Test 2) 51

1.4 Spread option with stochastic credit spread. Convergence of MPI with exponential Vasicek dynamics for credit spread on the left and CIR dynamics on the right (Test 4) 55

1.5 Spread option in the nonlinear case. Total value adjustment with exponential Vasicek credit spread on the left and with CIR credit spread on the right (Test 4) 56

1.6 Spread option in the linear case. Exponential Vasicek credit spread on the top and CIR credit spread on the bottom. Risky value on the left and XVA on the right (Test 5) 58

1.7 Exchange option with deterministic credit spread. Convergence of the MPI with exponential Vasicek dynamics for credit spread on the left and CIR dynamics on the right. 61

1.8 Exchange option in the nonlinear case. Total value adjustment with both exponential Vasicek credit spread (on the left) and CIR credit spread (on the right) (Test 8) 65

1.9 Exchange option in the linear case. Exponential Vasicek credit spread on the top and CIR credit spread on the bottom. Risky value on the left and XVA on the right (Test 9) 67

1.10 Sum of call options with deterministic credit spread. Convergence of the MPI with exponential Vasicek dynamics for credit spread on the left and CIR dynamics on the right. 69

1.11 Sum of call options with stochastic credit spread. Convergence of the MPI with exponential Vasicek dynamics for credit spread on the left and CIR dynamics on the right. 74

2.1 Transactions occurring with the treasury, the FX market and the REPO market to fund the trade. Straight lines refer to initial transactions, that take place at time t, while curved lines to final transactions taking place at time $t + dt$. Continuous lines represent cash transactions whereas dashed ones represent asset transactions. Blue lines indicate amounts denominated in currency D, whereas red ones represent cash of asset transactions denominated in currency C_0. 85

2.2 Option on the maximum. Convergence of the MPI with exponential Vasicek dynamics for credit spread on the left and CIR dynamics on the right. 104

2.3 Option on the maximum in the nonlinear case. Total value adjustment with exponential Vasicek credit spread on the left and with CIR credit spread on the right (Test 2) 106

2.4 Option on the maximum in the linear case. Exponential Vasicek credit spread (top) and CIR credit spread (bottom). Risky value (left) and XVA (right) (Test 3) 108

2.5 Best of put/put option. Convergence of the MPI with exponential Vasicek dynamics for credit spread on the left and CIR dynamics on the right. 111

2.6 Best of put/put option. Price difference between the collateralized derivative and the uncollateralized derivative ($C^{\%} = 0$). 113

2.7 Basket option. Convergence of the MPI with exponential Vasicek dynamics for credit spread on the left and CIR dynamics on the right. . 116

A.1 Portfolio composition rebalancing 159

A.2 Model points weights on liabilities value at different times 159

A.3 Mean number of alive policies at each time. On the left the total number is plotted; on the right the distinction between males and females is taken into account 160

A.4 Mean number of alive policies with different starting time. The plot on the top displays the evolution of the number of alive contracts that started at time zero; lines in the plot on the bottom show the evolution of the numbers of alive policies that started at time $1, 2, \ldots, 9$, respectively 161

A.5 Evolution of the average actuarial reserves for different values of the participation rate β 162

A.6 Evolution of the average difference between asset value and liability value for different values of the participation rate β 162

A.7 Mean number of alive policies at each time for different values of the participation rate β 164

A.8 Mean number of alive policies at each time with 2019 period life table and 2020 period life table 165

A.9 Mean number of alive policies with 2019 period life table and 2020 period life table 165

Abstract

This thesis is devoted to the mathematical modelling and numerical solution of problems related to the valuation of financial options including total value adjustment (XVA) in a multicurrency setting.

In order to build the models, we assume European options with underlying assets written in different currencies, stochastic credit spread of the counterparty and, eventually, stochastic foreign exchange rates. Depending on the choice of the mark-to-market value, nonlinear or linear partial differential equations (PDEs) are derived. We also make use of the nonlinear and linear Feynman-Kac theorems to deduce the equivalent models in terms of expectations.

For each derived model, we propose numerical methods. When the number of stochastic factors is no greater than two, we propose a Lagrange-Galerkin scheme (based on the method of characteristics and the finite element method) for solving the PDEs, eventually combined with fixed point techniques for the nonlinear problems. For problems that include more than two underlying assets and/or stochastic FX rates, we propose the use of Monte Carlo simulations applied to the formulations based on expectations, combined with a Picard method and the more efficient multilevel Picard iteration (MPI) scheme for the nonlinear cases.

We apply these techniques to different options of European type that validate the performance of the models as well as the proposed numerical methods.

Resumen

Esta tesis está dedicada al modelado matemático y simulación numérica de problemas de valoración de opciones financieras que incluyen ajuste de valoración total (XVA) en un marco multi-divisa.

Con el fin de construir los modelos, suponemos opciones europeas sobre subyacentes escritos en diferentes monedas, un diferencial crediticio de la contraparte estocástico y, eventualmente, tasas de cambio también estocásticas. Dependiendo de la elección del valor de mercado del derivado en caso de incumplimiento (*mark to market*), deducimos ecuaciones en derivadas parciales lineales y no lineales. También hacemos uso de los teoremas (lineal y no lineal) de Feynman-Kac para deducir los modelos equivalentes en términos de esperanzas.

Para los modelos deducidos proponemos su resolución mediante distintos métodos numéricos. Cuando el número de variables estocásticas es inferior o igual a dos proponemos un esquema de Lagrange-Galerkin (basado en el método de las características y el método de elementos finitos), eventualmente combinado con una técnica de punto fijo para los problemas no lineales. Para los casos que involucran más de dos subyacentes y/o tasas de cambio estocásticas, proponemos simulaciones basadas en el método de Monte Carlo, combinadas con un método de Picard o el más eficiente esquema de iteración de Picard multinivel para los problemas no lineales.

Aplicamos todas estas técnicas para valorar diferentes opciones europeas, habiendo obtenido buenos resultados que validan tanto los modelos como los métodos numéricos propuestos.

Resumo

Esta tese está dedicada ao modelado matemático e simulación numérica de problemas de valoración de opcións financeiras que inclúen axuste de valoración total (XVA) nun marco multi-divisa.

Co fin de construír os modelos, supomos opcións europeas sobre subxacentes escritos en diferentes moedas, un diferencial crediticio da contraparte estocástico e, eventualmente, taxas de cambio tamén estocásticas. Dependendo da elección do valor de mercado do derivado en caso de incumprimento (*mark to market*), deducimos ecuacións en derivadas parciais lineais e non lineais. Tamén facemos uso dos teoremas (lineal e non lineal) de Feynman-Kac para deducir os modelos equivalentes en termos de esperanzas.

Para os modelos deducidos propomos a súa resolución mediante distintos métodos numéricos. Cando o número de variables estocásticas é inferior ou igual a dous propomos un esquema de Lagrange-Galerkin (baseado no método das características e o método de elementos finitos), eventualmente combinado cunha técnica de punto fixo para os problemas non lineais. Para os casos que involucran máis de dous subxacentes e/ou taxas de cambio estocásticas, propomos simulacións baseadas no método de Monte Carlo, combinadas cun método de Picard ou o máis eficiente esquema de iteración de Picard multinivel para os problemas non lineais.

Aplicamos todas estas técnicas para valorar diferentes opcións europeas, obtendo bos resultados que validan tanto os modelos como os métodos numéricos propostos.

Abbreviations and notations

XVA	Total Value Adjustment
CDS	Credit Default Swap
FX	Foreign Exchange
OIS	Overnight Index Swap
D	Domestic currency
C_j	j-th foreign currency
W^D	Risk-free derivative value in currency D
V^D	Risky derivative value in currency D
U	Total value adjustments in currency D
M^D	Mark–to–market close out in currency D
Π	Self-financing portfolio
X^{D,C_j}	FX rate between currencies D and C_j
h	Counterparty's credit spread
S^i	Price of the underlying asset denominated in currency C_i
$S^{i,D}$	Price in currency D of the underlying asset denominated in currency C_i
C^{C_0}	Value of the collateral denominated in currency C_0
C^D	Value of the collateral in currency D
β^D	Value of the collateral account in currency D
B^D	Funding account in currency D
r^D	OIS rate in currency D

r^{C_j}	OIS rate in currency C_j
$f^{C,D}$	Borrowing rate in currency D
$f^{B,D}$	Lending rate in currency D
f^{D}	Funding rate in currency D
r^{R}	REPO rate
b^{D,C_j}	Cross-currency basis between currencies D and C_j
sb^{D,C_j}	Cross-currency basis spread between currencies D and C_j

FEM	Finite Element Method
LG	Lagrange-Galerkin
MPI	Multilevel Picard Iteration
RAI	Relative Approximation Increments

ALM	Asset Liability Management

m_i	i-th model point
$\Pi_{k,i}$	Premium payments at period k for model point m_i
$P_{k,i}$	New production at period k for model point m_i
$D_{k,i}$	Death payments at period k for model point m_i
$\Gamma_{k,i}$	Surrender payments at period k for model point m_i
$M_{k,i}$	Maturity payments at period k for model point m_i
$cf_{k,i}$	Cash flows at period k for model point m_i
${}_sn_{k,i}$	Number of policyholders in the model point m_i that entered into the contract at time s and are still alive at period k
$n_{k,i}$	Total number of alive policyholders in model point m_i at the end of period k
${}_sn^D_{k,i}$	Numbers of policyholders in model point m_i that started the contract at time s and die at period k

${}_sn^S_{k,i}$	Numbers of policyholders in model point m_i that started the contract at time s and surrender at period k
${}_sn^M_{k,i}$	Numbers of policyholders in model point m_i that started the contract at time s and reach maturity at period k
$n^P_{k,i}$	Number of new policyholders in the i-th model point at period k
$g_{k,i}$	Minimum guaranteed rate of return at period k for model point m_i
$\beta_{k,i}$	Participation rate at period k for model point m_i
R^P_k	Asset portfolio return at period k
R^I_k	Benchmark index rate of return at period k
$L_{k,i}$	Liabilities value at period k for model point m_i
L^D_k	Liabilities duration at period k
A_k	Assets value at period k
A^D_k	Assets duration at period k
$\boldsymbol{\alpha}_k$	Asset classes weights at period k
$\boldsymbol{R}_k$	Vector of asset classes return at period k

Introduction

After the financial crisis started in 2007, it became clear that any pricing framework should take into account the possibility of default of any counterparty involved in the trade [28, 61], as well as aspects related to collateral posting, liquidity risk or funding costs [52, 85]. Therefore, different valuation adjustments due to these factors must be considered when pricing a derivative. The set of these adjustments is globally referred to as Total Value Adjustment or XVA, where "X" stands for the different letters that appear in the value adjustments associated to credit (CVA), debit (DVA), funding (FVA), collateral (CollVA), capital (KVA) or margin (MVA), for example. The initial and more classical adjustments were motivated by counterparty risks related to credit, funding and collateral. Later on, the adjustments related to capital and margin have been added. Among the classical and more general references on the topic, we address the readers to the books [21, 28, 52] and the references therein.

Most of the literature has addressed the modelling and computation of the different adjustments or the total value adjustment for a single currency setting. In this framework, three main methodologies have been developed. A first approach, following the seminal papers by Piterbarg [82] and Burgard and Kjaer [22] that obtain PDE formulations by hedging arguments on suitable portfolios and the application of Itô's lemma for jump-diffusion processes. This approach in terms of PDEs formulation has been followed in [43], where the problem is also equivalently written in terms of expectations. Moreover, it has been also addressed in [4] and [3], where PDE models with one and two stochastic factors have been mathematically analysed

and numerically solved for pricing European options with one and two stochastic factors. A second approach follows the initial ideas in [18] to obtain the CVA by means of formulations based on expectations, next extended to the collateralized, close-out and funding costs in [78]. Also this approach has been addressed in [5, 2] for American options and in [15] for Levy dynamics. A third approach is based on backward stochastic differential equations and it has been introduced in [26] and [27].

Recently, attention has been given to the extension of valuation adjustments from the single currency to the multi-currency setting [44]. Indeed, nowadays financial institutions may operate in different currencies, for example making investments on derivatives with underlying assets denominated in domestic currencies, and funding or posting collateral in foreign currencies. The three previously indicated methodologies that have been developed can be extended to the multi-currency setting.

In this thesis we mainly follow [8, 89], where we have focused on the formulations based on PDEs and expectations, and add some improvements. Therefore, we start building a multi-currency framework, following the ideas in [44], where the joint consideration of CVA, FVA, CollVA and repo adjustments are taken into account. For the additional inclusion of KVA or MVA in the XVA, the ideas in [51, 50] in the single currency case could be considered.

More precisely, in this work we address the European options pricing problem in a multi-currency setting when taking into account the valuation adjustments associated to counterparty risk. For this purpose, stochastic intensities of default are assumed and underlying assets denominated in different currencies are involved. Our approach is based on the same framework and assumptions as in [43], although extended to a multi-currency environment and with the additional hypothesis of a zero default intensity for the hedger. In particular, we take into consideration the following assumptions:

- The counterparty can default, but the hedger is default-free.
- Prices of the involved underlying assets are modelled by correlated diffusion processes.

- The events of investor default do not affect the evolution of the prices of the involved underlying assets.

- The stochastic credit spread of the counterparty is modelled as a positive mean reverting process, which is correlated with the processes followed by the prices of the underlying assets and, eventually, with the processes followed by the foreign exchange (FX) rates.

Following [44], we first obtain formulations of the XVA pricing problem in terms of partial differential equations (PDEs). For this purpose, we employ hedging, no arbitrage and self-financing arguments jointly with a choice for the mark-to-market value of the derivative at default. This choice leads either to a linear problem, if the mark-to-market value is equal to the price of the derivative when counterparty risk is not taken into account (risk-free derivative), or to a nonlinear problem if it is equal to the price of the derivative including the counterparty risk (risky derivative).

Note that the consideration of several stochastic underlying assets, of the stochastic counterparty's credit spread and, eventually, of the stochastic foreign exchange rates implies that the number of stochastic factors increases significantly, so that the so-called *curse of dimensionality* comes into place when deterministic numerical methods (as finite differences or finite element methods) are considered for the solution of the corresponding linear and nonlinear high dimensional PDEs models. Actually, these deterministic numerical methods involve an exponentially increasing computational cost in the dimension of the PDE.

Thus, we address the solution of the linear and nonlinear PDEs only in the case of a derivative written on two underlying assets in different currencies, with constant foreign exchange rates and deterministic time-dependent counterparty's credit spread. More precisely, we employ a semi-Lagrangian (also known as characteristics) method for the time discretization combined with the Finite Element Method (FEM) for the discretization of the spatial variables which are associated to the stochastic factors. The joint consideration of semi-Lagrangian methods with finite element methods is usually referred to as Lagrange-Galerkin methods. These techniques are specially

useful for the discretization of the so called convection dominated PDE problems, where the terms containing first order derivatives (convection terms) dominate the ones containing the second order derivatives (diffusion terms). In this setting, the proposed techniques avoid the presence of spurious oscillations that appear when more conventional time discretization techniques are considered. Additional fixed point techniques are used when nonlinear PDEs are involved.

Probabilistic methods based on Feynman-Kac formula to obtain an equivalent formulation of the PDE problems in terms of expectations seem an appropriate alternative to avoid the *curse of dimensionality*, that arises when using other numerical approaches to solve multidimensional PDE problems. Therefore, in a second step, we deduce the corresponding formulations of the pricing problem in terms of expectations with the goal of applying a Monte Carlo method for computing the total value adjustment.

In the nonlinear case, a general nonlinear Feynman-Kac formula has been proposed in the seminal work [79]. Among the possible probabilistic methods, the most *naive* comes from the consideration of the so called "Monte Carlo of Monte Carlo" (also known as nested Monte Carlo simulation or straight-forward Monte Carlo method), which would give rise to an at least exponentially growing computational cost of the approximation method in the inverse of the prescribed approximation accuracy. In the nonlinear case, among the recent advanced nonlinear Monte Carlo techniques to solve the semilinear PDEs formulations, we point out three of them: branching diffusion methods (see, for example, [72, 57, 58]), deep learning based methods (see, for example, [54, 1, 64]) and multilevel Picard iterations (see, for example, [37, 62, 38]).

Picard iteration techniques are approximation methods for solving a fixed-point equation. These methods can be applied to solve nonlinear models formulated in terms of expectations that have been obtained from the corresponding nonlinear PDEs by means of a nonlinear Feynman-Kac formula. Once the Picard iteration method has been posed, it must be discretized by means of quadrature formulae. In this article, we propose Picard iteration methods to solve the nonlinear formulations arising in

XVA computation by using rectangular and trapezoidal quadrature formulae.

Recently, in [37], [62], and [38], the authors propose a family of multilevel Picard iteration methods, which mainly combine the multilevel Monte Carlo techniques from [55, 56] and [46] with Picard iteration methods. More precisely, in [38] the authors develop the theoretical analysis under suitable smoothness conditions while in [37] they address simulation studies including applications to financial pricing problems. As indicated in [37], the computational complexity increases at most linearly in the dimension of the PDE and quartically in the inverse of the prescribed accuracy. In this thesis, in the nonlinear problem case we also apply the numerical multilevel Picard iteration methods proposed in [37].

Finally, it is important to point out that this thesis has been developed in the frame of the European Industrial Doctorate ABC-EU-XVA, which involves a research stay in an industrial partner, in this case the insurance company Unipol Gruppo S.p.A. During the stay, the author of this thesis has carried out a relevant research work related to the development of a new stochastic Asset Liability Management (ALM) model for a life insurance company, dealing with both an asset portfolio and a liability portfolio.

The developments and achievements of this research work appear in the article [35] and are also contained in the Annexe of the thesis.

The outline of this thesis is as follows.

In Chapter 1 we model the price of a European option written on different underlying assets denominated in foreign currencies under the assumption of deterministic foreign exchange rates. Also, we assume that the derivative is partially collateralized in cash in a foreign currency and that the counterparty has a stochastic intensity of default. By using a hedging strategy to build a self-financing portfolio, we derive either nonlinear or linear PDE models for the price of the derivative and for the total

value adjustment. Then, we use the Feynmam-Kac theorem to write the XVA as an expectation. From the numerical point of view, we address the solution of the pricing PDE using a Finite Element Method under the assumption that the credit spread is a deterministic time-dependent function and the derivative depends on two stochastic underlying assets so that we consider a two-dimensional problem. Instead, the formulation based on expectations allows the use of Monte Carlo techniques to approximate the total value adjustment in a higher dimensional setting. In the case of nonlinear problems, the Monte Carlo method requires the Picard iteration or multilevel Picard iteration techniques.

In Chapter 2 we follow the same methodologies as in the previous chapter and extend the deterministic exchange rates model to the case of stochastic foreign exchange rates. Moreover, we assume the collateral is made up of bonds in a foreign currency. New models are formulated both in terms of linear and nonlinear PDEs and expectations, the hedging arguments requiring the additional consideration of the exposure to foreign exchange risk. In this high-dimensional setting, we do not address the solution of the pricing PDEs, but focus on the expectation formulation of the total value adjustment and, therefore, on the Monte Carlo approximation. In the numerical results section, we present some examples to illustrate the performance of the proposed numerical techniques. In particular, we analyse the impact of introducing stochasticity in the foreign exchange rates dynamics and of using the collateral made up of bonds instead of cash.

In Appendix A we build a stochastic Asset Liability Management (ALM) model for a life insurance company, dealing with both an asset portfolio, made up of bonds, equity and cash, and a liability portfolio, comprising with-profit life insurance policies. We define a mortality model and a surrender model, as well as a new production model. First, with the purpose of ensuring the solvency of the company and the

achievement of a competitive return, in the interest of both shareholders and policyholders, the insurer's portfolio is periodically rebalanced according to the solution of a nonlinearly constrained optimization problem, that aims to match asset and liability durations, subject to the attainment of a target return. In addition, several real world constraints are imposed. When computing the company balance sheet projections, we consider not only future maturity and death payments, but also future surrender payments and all the cash flows due to new production, in order to obtain estimates that are as reliable as possible. The estimation of the timing and of the numbers of future surrenders and of future new policyholders requires the approximation of conditional expectations: to this end, we employ the Least Squares Monte Carlo technique. Secondly, for each bonds asset class and for equity asset class we propose a sectorial optimization problem with the aim of maximizing the expected value of a chosen utility function, subject to the results obtained from the first stage of portfolio rebalancing. Finally, we analyse a case study.

Chapter 1

Total Value Adjustment in a multi-currency setting with deterministic FX rates

1.1 Introduction

In this first chapter, we address the European options pricing problem in a multi-currency setting when taking into account the valuation adjustments associated to counterparty risk. In particular, we consider a derivative written on different underlying assets that are denominated in different currencies. We also assume that the derivative is partially collateralized in cash in a foreign currency. First, we assume foreign exchange (FX) rates are time dependent deterministic processes, whereas the model with stochastic FX rates will be posed in Chapter 2. We consider a zero default intensity for the hedger and a stochastic default intensity for the counterparty, which is equivalent to stochastic credit spread of the counterparty.

Note that in our previous closely related work [8] we have chosen a Gaussian dynamics for the credit spread of the counterparty, but this approach suffers from the possibility of reaching negative credit spread values with positive probability.

Therefore, in this thesis we want to consider a more realistic assumption on the credit spread dynamics given by choosing a positive mean-reversion process.

We follow an approach based on hedging arguments and, by applying Itô's formula for jump diffusion processes, we obtain partial differential equation (PDE) formulations of the derivative pricing problem. In order to pose the PDE formulation for the XVA price, we note that the risky derivative value is obtained by summing the total value adjustment to the derivative risk-free value, i.e., the value that the derivative would have in absence of counterparty risk. Therefore, the XVA can be seen as the difference between the risky derivative value and the risk-free derivative value, that satisfies the classical multidimensional Black-Scholes equation. This allows to obtain a PDE problem for the total value adjustment. Depending on the choice of the mark-to-market value of the derivative at default, different kinds of XVA pricing PDEs arise: if the mark-to-market value is equal to the risky derivative value, then a nonlinear PDE is obtained; if the mark-to-market value is equal to the risk-free derivative value, then a linear PDE that involves the risk-free value of the derivative is obtained.

The presence of many stochastic factors makes the deterministic numerical methods commonly used to solve PDEs to be affected by the *curse of dimensionality*, so we address the solution of the pricing PDEs for both assumptions on the mark-to-market value at default in the case where the derivative only depends on two underlying assets and the counterparty's credit spread is a deterministic function of time. In particular, we address the solution of the PDEs problems by using a Lagrange-Galerkin method.

In order to avoid the *curse of dimensionality* when considering the general case with more than two underlying assets and with stochastic counterparty's credit spread, the Feynman-Kac formula can be applied to formulate the XVA problems in terms of expectations, so that Monte Carlo method can be employed. In particular, in the nonlinear case Picard iteration methods are needed to compute the value adjustment. We use both the simple fixed-point method and the multilevel Picard iteration method proposed in [37] and also recalled in this thesis. The results obtained with the

formulation in terms of expectations of the XVA pricing problems are compared with the results obtained with a Lagrange-Galerkin method for the PDEs discretization.

The chapter is structured as follows. In Section 1.2 we obtain the mathematical model for XVA based either on nonlinear or linear PDEs. In Section 1.3 we write the problem in terms of expectations with the purpose of applying Monte Carlo techniques. In Section 1.4 we describe the proposed numerical methods to compute the total value adjustment. In particular, in Subsection 1.4.1 we describe the proposed Lagrange-Galerkin method to solve both the nonlinear and the linear PDEs when the counterparty's credit spread is a deterministic function of time; in Subsection 1.4.2 we describe the Monte Carlo method and the quadrature formulae used to approximate the integral in the XVA formulae; in Subsection 1.4.3 we introduce the multilevel Picard iteration method. In Section 1.5 we present and analyse the numerical results related to some examples for different choices of the derivative payoff. More precisely, we consider a *spread option*, an *exchange option* and a *sum of call options*. Finally, in Section 1.6 we point out several main conclusions.

1.2 Formulation in terms of partial differential equations

In this section, following [43, 44] the value of a derivative is modelled by taking into account the valuation adjustments that have to be considered in case of a possible default of the counterparties involved in the deal.

We consider a trade between a non-defaultable hedger and a defaultable counterparty in a multi-currency framework, where a domestic currency D and foreign currencies $C_0, \dots, C_N$ are involved. For $j = 0, \dots, N$, let X_t^{D,C_j} be the FX rate between currencies D and C_j at time t, namely the domestic price at time t of one unit of the foreign currency C_j.

We denote by Q^D the risk neutral probability measure of the domestic market. In

the next chapter we will show that the dynamics of X_t^{D,C_j} under Q^D is described by

$$dX_t^{D,C_j} = (r^D - r^{C_j})X_t^{D,C_j}dt + \sigma^{X^j} X_t^{D,C_j} dW^{X^j}, \quad j = 0, \ldots, N\,,$$

where r^D and r^{C_j} are the short-term rates in the domestic market and in the $j-$foreign market, respectively. Moreover, σ^{X^j} is the volatility of X_t^{D,C_j} and W^{X^j} is a Q^D-Brownian motion. Nevertheless, throughout this chapter we consider $\sigma^{X^j} = 0$ in order to have deterministic FX rates:

$$dX_t^{D,C_j} = (r^D - r^{C_j})X_t^{D,C_j}dt, \quad j = 0, \ldots, N\,,$$

while the consideration of stochastic rates will be addressed in the next chapter. Furthermore, in the numerical examples we consider constant values for X_t^{D,C_j}, so that subindex t will be removed in that part of the present chapter.

We denote by $S_t = (S_t^1, \ldots, S_t^N)$ the vector of the prices of the underlying assets S^i at time t, each one of them being denominated in its corresponding currency C_i, and by h_t the counterparty's credit spread at time t. The credit spread of an entity is typically calculated as the difference between the rate of return on a bond issued by the risky entity and the risk-free rate. Therefore, the credit spread gives an indication of the market's view of the riskiness of that bond and of the probability of default of an entity. In fact, the intensity of default λ can be modelled [43] as

$$\lambda \approx \frac{h}{1 - R_C}\,,$$

where R_C is the entity's recovery rate.

We assume that under the real world measure P the evolution of the prices of the underlying assets in each currency and of the counterparty's credit spread are governed by the following SDEs:

$$dS_t^i = \mu^{S^i} S_t^i\, dt + \sigma^{S^i} S_t^i\, dW_t^{S^i,P}, \quad \text{for } i = 1, \ldots, N\,, \tag{1.1}$$

$$dh_t = \mu^{h,P}(t, h_t)\, dt + \sigma^{h,P}(t, h_t)\, dW_t^{h,P}\,, \tag{1.2}$$

where μ^{S^i} and $\mu^{h,P}$ are the real world drifts of the processes S_t^i and h_t, respectively. Moreover, σ^{S^i} and $\sigma^{h,P}$ are their respective volatility functions, while $W^{S^i,P}$ and $W^{h,P}$

are Brownian motions under the real world measure P. Moreover, we assume that the assets prices and spread processes in (1.1) and (1.2) are correlated. Thus, we consider the $(N+1)\times(N+1)$ correlation matrix given by

$$\operatorname{corr}(S^1,\dots,S^N,h)=\begin{pmatrix} 1 & \rho^{S^1S^2} & \cdots & \rho^{S^1S^N} & \rho^{S^1h} \\ \rho^{S^1S^2} & 1 & \cdots & \rho^{S^2S^N} & \rho^{S^2h} \\ \vdots & \vdots & \ddots & \vdots & \vdots \\ \rho^{S^1S^N} & \rho^{S^2S^N} & \cdots & 1 & \rho^{S^Nh} \\ \rho^{S^1h} & \rho^{S^2h} & \cdots & \rho^{S^Nh} & 1 \end{pmatrix}, \tag{1.3}$$

where the $N\times N$ submatrix contains the correlations between assets ($\rho^{S^iS^j}$) and the last row (column) contains the correlations between each asset and the spread (ρ^{S^ih}). We consider constant values for correlations.

By changing the probability measure from P to the risk-neutral measure in the domestic currency, Q^D, in (1.1) we have that the dynamics of S^i, for $i=1,\dots,N$, is given by

$$dS_t^i=(r^i-q^i)S_t^i\,dt+\sigma^{S^i}S_t^i\,dW_t^{S^i,Q^D}, \tag{1.4}$$

where r^i and q^i represent the short-term rate in currency C_i and the dividend paid by S^i, respectively, and W^{S^i,Q^D} is a standard Brownian motion under Q^D. Although in the numerical examples we consider constant values for r^i, q^i and for the volatility σ^i, time dependent functions can be assumed in all the developments.

By changing the probability measure from P to Q^D in (1.2), the drift of h is given by $\mu^{h,P}-M^h\sigma^{h,P}$, where M^h is the counterparty's market price of credit risk.

As indicated in [19], the study of historical credit spreads time series suggests that credit spreads exhibit mean reverting and fat tails properties. Therefore, under the risk-neutral measure Q^D, we model the counterparty's credit spread by an exponential Vasicek process, i.e., we assume that the logarithm of h follows a Vasicek dynamics. More precisely, we denote by $\tilde{h}$ the logarithm of h and assume

$$d\tilde{h}_t=\alpha\,(\theta-\tilde{h}_t)\,dt+\sigma^h\,dW^{h,Q^D},$$

where α, θ and σ^h are positive constant and W^{h,Q^D} is a Brownian motion under the risk-neutral measure Q^D. In particular, α is the mean reversion rate, θ is the mean reversion level and σ^h is the volatility of the mean reversion process. Therefore, by applying Itô's formula (see, for example, [81]) to $h_t = \exp(\tilde{h})$, we get

$$dh_t = \alpha\, h_t\, (m - \log(h_t))\, dt + \sigma^h\, h_t\, dW^{h,Q}\ ,\ \text{with}\ \ m = \theta + \frac{(\sigma^h)^2}{2\alpha}\,. \tag{1.5}$$

The exponential transformation of the Vasicek model ensures the positivity of h.

However, in the literature the credit spread is often assumed to follow a Cox-Ingersoll-Ross (CIR) process, so that the dynamics of h is given by the following mean reverting SDE:

$$dh_t = \alpha\, (\theta - h_t)\, dt + \sigma^h \sqrt{h_t}\, dW^{h,Q^D}\,, \tag{1.6}$$

where α, θ and σ^h are positive constants and if the Feller condition is fulfilled, i.e., $2\,\alpha\,\theta\ >\ (\sigma^h)^2$, then h remains strictly positive. In Section 1.5, where numerical results are presented, we also report results with CIR dynamics for the credit spread. However, in the development of the thesis we only show the mathematical models obtained with exponential Vasicek dynamics, since it would be redundant to repeat the same steps with only a different dynamics for the credit spread. Note that in [8] we have considered a Normal dynamics for the counterparty's credit spread, but we now consider a more realistic hypothesis by assuming it is modelled by a positive mean-reversion process.

Next, we denote by J_t the counterparty's default state at time t, that is to say:

$$\begin{cases} J_t\ =\ 1\,, & \text{if the counterparty defaults before or at time } t\,, \\ J_t\ =\ 0\,, & \text{otherwise.} \end{cases} \tag{1.7}$$

The derivative value in the domestic currency D at time t is given by $V_t^D = V^D(t, S_t, h_t, J_t)$. The price in currency D of the same derivative traded between two non-defaultable counterparties is referred to as risk-free derivative price and it is denoted by $W_t^D = W^D(t, S_t)$. We assume the derivative is partially collateralized in

cash in the foreign currency C_0. We denote by $C_t^{C_0}$ the collateral account value at time t in currency C_0.

The close-out procedure in case of default event is described in ISDA (International Swaps and Derivatives Association) documentation: if the surviving party is a net debtor, then she must pay the whole close-out value to the defaulting party; if the surviving party is a net creditor, then she is able to recover only a fraction of her credits. We assume that the derivative is traded under the presence of a collateral account. Collateralized contracts are regulated by the Credit Support Annex (CSA) to the ISDA Master Agreement. Therefore, taking into account the presence of the collateral, that has the role to reduce the exposure, the expression of the risky derivative value at default is given by:

$$\begin{aligned} V^D(t, S_t, h_t, 1) = C^D(t) + R_C \left(M^D(t, S_t, h_t) - C^D(t) \right)^+ \\ + \left(M^D(t, S_t, h_t) - C^D(t) \right)^- , \end{aligned} \tag{1.8}$$

with $M^D(t, S_t, h_t)$ representing the mark-to-market derivative price and $C^D(t)$ denoting the collateral account value in domestic currency D. Moreover, we have used the notation $x^+ = \max(x, 0)$ and $x^- = \min(x, 0)$. Equation (1.8) means that, in case of counterparty's default:

- if the hedger is a net debtor, i.e., $M^D - C^D \leq 0$, then the hedger has to pay the whole mark-to-market derivative value to the counterparty;
- if the hedger is a net creditor, i.e., $M^D - C^D > 0$, then the hedger is able to recover a fraction of her credits, given by $C^D + R_C(M^D - C^D)$.

Note that, since the recovery rate R_C is between 0 and 1, the default payment $C^D + R_C(M^D - C^D)$ is always greater than the default payment it would happen in absence of collateral, that is just given by $R_C M^D$. Therefore, the collateralization improves the recovery in case of counterparty's default.

By using Equation (1.8), we can define the variation of V^D at default as:

$$\Delta V^D = C^D + R_C(M^D - C^D)^+ + (M^D - C^D)^- - V^D , \tag{1.9}$$

where we have suppressed the dependence on time t, on the underlying assets S_t and on the counterparty's credit spread h_t to ease the notation.

1.2.1 Replicating portfolio

In order to price the derivative, we consider a self-financing portfolio Π that hedges all the risk factors, which are:

- the market risk due to changes in S^1, $S^2, \ldots,$ S^N;
- the counterparty's spread risk due to changes in h;
- the counterparty's default risk.

More precisely:

- the market risk due to changes in S^i, for $i = 1, \ldots, N$, is hedged by trading in fully cash collateralized derivatives on the same underlying assets. For $i = 1, \ldots, N$, the net present value in currency C_i of the derivative written on the underlying asset S^i is denoted by H^i, so that $H^{i,D} = H^i X^{D,C_i}$ represents the net present value of H^i in the currency D;
- in order to hedge the spread risk due to changes in counterparty's credit spread h and the counterparty's default risk, the hedger has to trade in two credit default swaps with different maturities written on the counterparty:
  - a short term credit default swap, $CDS^D(t, t+dt)$, that is an overnight credit default swap with unit notional. The protection buyer pays a premium at time t equal to $h_t dt$ and receives $(1 - R_C)$ at time $t + dt$ if the counterparty defaults between t and $t+dt$. We assume that $h_t dt$ is such that $CDS^D(t, t+dt) = 0$;
  - a long term credit default swap, $CDS^D(t, T)$, that is a cash collateralized credit default swap maturing on T. In general, $CDS^D(t, T)$ is not null.

We now assume that the hedger buys the derivative from the counterparty, with $V_t^D > 0$, and we describe the operations she would enact in a generic small time interval $[t, t+dt]$ with the treasury and the FX market to fund the trade. The transactions are represented in Figure 1.1.

- At time t, the hedger borrows V_t^D cash from her bank treasury to buy the derivative from the counterparty and receives the collateral amount $C_t^{C_0}$ in currency C_0.
- The hedger exchanges the cash $C_t^{C_0}$ in the FX spot market, obtaining $C_t^D = C_t^{C_0} X_t^{D,C_0}$, that she gives to the treasury. Therefore, the outstanding debt to the treasury is $V_t^D - C_t^D$, that will grow at the borrowing rate in currency D, denoted by $f_t^{B,D}$.
- At time $t+dt$, the hedger has to pay back the collateral plus interest, given by the OIS rate in currency C_0, denoted by $r_t^{C_0}$. So, according to a forward contract agreed at time t, she sells forward the amount $C_t^{C_0}(1 + r^{C_0} dt)$ in currency C_0 multiplied by the forward FX rate $X_t^{D,C_0} \frac{1+r^D dt}{1+(r^{C_0}+b^{C_0,D})dt}$ and receives $C_t^{C_0}(1 + r^{C_0} dt)$ in currency C_0. The rate r^D is the OIS rate in the domestic currency D, whereas $b^{C_0,D}$ denotes the short term cross-currency basis between currencies C_0 and D, which is an adjustment that needs to be made in the C_0 rate. The hedger pays the amount $C_t^{C_0}(1 + r^{C_0} dt)$ to the counterparty.
- At time $t+dt$ the debt to treasury is

$$\left(V_t^D - C_t^D\right)\left(1 + f_t^D dt\right) + C_t^D \left(1 + (r^D + b^{D,C_0})dt\right).$$

Note that in the case $V_t < 0$, the trades would be right the opposite.

We denote by B_t^D the value of the funding account in the domestic currency D at time t and by Ω_t the number of shares of the funding account at time t. Thus, in order to ensure that the self financing condition holds, we have the following funding constraint condition:

$$\Omega_t B_t^D = -\left(V_t^D - C_t^{C_0} X_t^{D,C_0}\right). \tag{1.10}$$

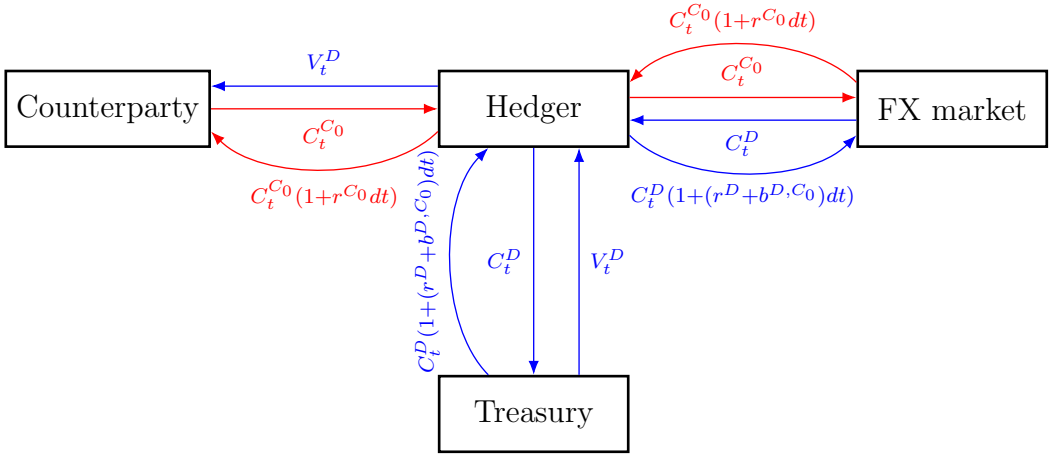

Figure 1.1: Transactions occurring with the treasury and the FX market to fund the trade. Straight lines refer to initial transactions, that take place at time t, while curved lines to final transactions taking place at time $t + dt$. Blue lines indicate amounts denominated in currency D, whereas red ones represent cash denominated in currency C_0.

Note that if $\Omega_t > 0$, then the hedger has to finance her position by borrowing from the treasury and she will pay an interest rate $f_t^{D,C}$, where C stands for cost. Vice versa, if the hedger's position is positive, she will invest money by lending to the treasury and earning at the rate $f_t^{D,B}$, where B stands for benefit. Therefore, if we define the funding rate in currency D as

$$f_t^D = f_t^{D,C}\mathbb{1}_{\Omega_t>0} + f_t^{D,B}\mathbb{1}_{\Omega_t<0}\,, \tag{1.11}$$

we have that

$$B_t^D = \exp\left(\int_0^t f_t^D ds\right)\,. \tag{1.12}$$

Hence, we consider a replicating portfolio Π that is an extension to the multi-currency framework of the portfolio in [3] and such that:

- α_t^i is the weight of the fully collateralized derivative H_t^i, for $i = 1, \ldots, N$, in the portfolio composition at time t;
- γ_t and ϵ_t are the weights of the long term CDS and short term CDS, respectively, in the portfolio composition at time t;

- Ω_t represents the number of shares of the funding account at time t;
- β_t^D denotes the cash in the collateral accounts of the portfolio at time t.

Thus, the portfolio at time t is given by:

$$\Pi_t = \sum_{i=1}^{N} \alpha_t^i H_t^{i,D} + \gamma_t CDS^D(t,T) + \epsilon_t CDS^D(t,t+dt) + \Omega_t B_t^D + \beta_t^D \,. \tag{1.13}$$

The composition of the collateral account β^D is given by

$$\beta_t^D = -\sum_{i=1}^{N} \alpha_t^i H_t^{i,D} - \gamma_t CDS^D(t,T) - C_t^{C_0} X_t^{D,C_0} \,.$$

In order to infer the variation of the collateral account in the time interval $[t, t+dt]$, we analyse the transactions occurring when trading a generic fully collateralized derivative in a foreign currency F. We denoted the value of the foreign derivative by H^F and we again assume the hedger buys the derivative, with $H_t^F > 0$.

- At time t, the hedger borrows $H_t^D = H_t^F X^{D,F}$ cash from her bank treasury, that exchanges in the FX market receiving H_t^F in currency F. Thus, the hedger buys the derivative.
- The hedger receives the collateral with value H_t^F and exchanges this amount in the FX market, getting H_t^D, that she gives back to the treasury.
- At time $t+dt$ the hedger has to give back the collateral plus interest, given by the OIS rate in currency F, r_t^F. Therefore, at time t the hedger agrees to exchange forward in the FX market the amount $H_t^F(1+r^F dt)$ in currency F multiplied by the forward FX rate $X_t^{D,F} \frac{1+r^D dt}{1+(r^F+b^{F,D})dt}$, where $b^{F,D}$ is the cross-currency basis between currency F and currency D, and receives $H_t^F(1+r^F dt)$ in currency F. The hedger pays this amount to the counterparty. The variation in the collateral account is given by

$$H_t^D \Big(1 + (r^D + b^{D,F})dt\Big) \,.$$

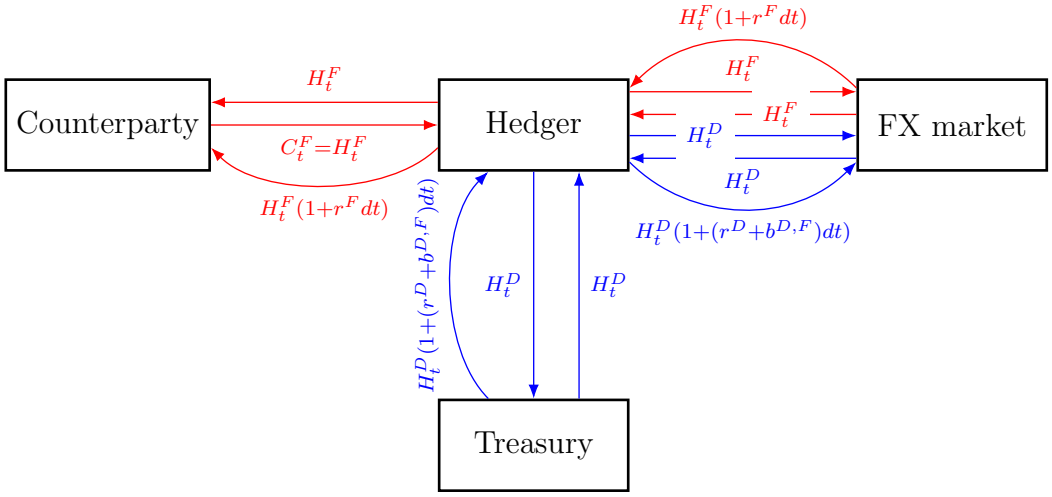

Figure 1.2: Transactions occurring when trading a fully collateralized foreign derivative. Straight lines refer to initial transactions, that take place at time t, while curved lines to final transactions taking place at time $t+dt$. Blue lines indicate amounts denominated in the domestic currency D, whereas red ones represent cash denominated in the foreign currency F.

Therefore, from Figure 1.1 and Figure 1.2 we infer that the variation of the collateral account in the time interval $[t, t+dt]$ is given by:

$$d\bar{\beta}_t^D = \left[-\sum_{i=1}^{N} \alpha_t^i (r^D + b^{D,C_j}) H_t^{i,D} - \gamma_t r^D CDS^D(t,T) - \left(r^D + b^{D,C_0} \right) C_t^{C_0} X_t^{D,C_0} \right] dt\,,$$

where b^{D,C_j}, for $j = 0, \ldots, N$, is the cross-currency basis between the domestic currency D and the foreign currency C_j.

1.2.2 Pricing partial differential equations

Once we have built our replicating portfolio, we consider the no arbitrage and the self-financing conditions to infer the pricing PDEs. Therefore, we have

$$\Pi(t) + V^D(t, S_t, h_t, J_t) = 0,$$

thus:

$$\begin{aligned} -dV_t^D &= d\Pi_t \\ &= \sum_{i=1}^{N} \alpha_t^i dH_t^{i,D} + \gamma_t dCDS^D(t,T) + \epsilon_t dCDS^D(t,t+dt) \\ &\qquad + \Omega_t dB^D + d\bar{\beta}_t^D \,. \end{aligned} \tag{1.14}$$

As $V_t^D = V^D(t, S_t, h_t, J_t)$ depends on diffusion and jump processes, we apply Itô's formula for jump-diffusion processes [81] to obtain that the variation of V^D in the time interval $[t, t+dt]$ is given by:

$$\begin{aligned} dV_t^D = &\frac{\partial V^D}{\partial t} dt + \sum_{i=1}^{N} \frac{\partial V^D}{\partial S^i} dS_t^i + \frac{\partial V^D}{\partial h} dh_t + \Delta V_t^D dJ_t \\ &+ \left[\frac{1}{2} \sum_{i,k=1}^{N} \rho^{S^i S^k} \sigma^{S^i} \sigma^{S^k} S_t^i S_t^k \frac{\partial^2 V^D}{\partial S^i \partial S^k} \right. \\ &\qquad \left. + \frac{1}{2} (\sigma^h h_t)^2 \frac{\partial^2 V^D}{\partial h} + \sum_{i=1}^{N} \rho^{S^i h} \sigma^{S^i} \sigma^h S_t^i h_t \frac{\partial^2 V^D}{\partial S^i \partial h} \right] dt \,, \end{aligned}$$

where $\Delta V_t^D = V^D(t, S_t, h_t, 1) - V^D(t, S_t, h_t, 0)$ represents the jump of V_t^D in case of default at time t, which is given by (1.9).

The dynamics of the short term credit default swap, $CDS^D(t, t+dt)$, and of the funding account, B_t^D, are respectively given by:

$$dCDS^D(t,t+dt) = h_t \, dt - (1 - R_C) \, dJ_t \,, \tag{1.15}$$

$$dB_t^D = f^D B_t^D \, dt \,. \tag{1.16}$$

From the funding condition on our strategy, stated in (1.10), we obtain

$$\Omega_t = -\frac{V_t^D - C_t^D}{B_t^D} \,.$$

Thus, the change in Π_t from t to $t+dt$ is given by:

$$\begin{aligned}
d\Pi_t &= \sum_{i=1}^{N} \alpha_t^i dH_t^{i,D} + \gamma_t dCDS^D(t,T) + \epsilon_t dCDS^D(t,t+dt) \\
&\quad - \frac{V_t^D - C_t^{C_0} X_t^{D,C_0}}{B_t^D} dB_t^D + d\bar{\beta}_t^D \\
&= \sum_{i=1}^{N} \alpha_t^i \left(\frac{\partial H^{i,D}}{\partial t} dt + \frac{\partial H^{i,D}}{\partial S^i} dS_t^i + \frac{1}{2} (\sigma^{S^i} S_t^i)^2 \frac{\partial^2 H^{i,D}}{\partial (S^i)^2} dt \right) \\
&\quad + \gamma_t \left[\frac{\partial CDS^D(t,T)}{\partial t} dt + \frac{\partial CDS^D(t,T)}{\partial h} dh_t + \frac{1}{2} (\sigma^h h)^2 \frac{\partial^2 CDS^D(t,T)}{\partial h^2} dt \right] \\
&\quad + \gamma_t \Delta CDS^D(t,T) dJ_t + \epsilon_t \left[h_t dt - (1-R_C) dJ_t \right] - (V^D - C_t^{C_0} X_t^{D,C_0}) f^D dt \\
&\quad - \sum_{i=1}^{N} \alpha_t^i (r^D + b^{D,C_i}) H_t^i dt - r^D CDS^D(t,T) dt - (r^D + b^{D,C_0}) C_t^{C_0} X_t^{D,C_0} dt \,.
\end{aligned}$$

In order to hedge the risk of the portfolio Π, we choose:

$$\begin{aligned}
\alpha_t^i &= -\frac{\partial V^D / \partial S^i}{\partial H^{i,D} / \partial S^i}, \quad \text{for } i = 1, \ldots, N, \\
\gamma_t &= -\frac{\partial V^D / \partial h}{\partial CDS^D(t,T) / \partial h}, \\
\epsilon_t &= \frac{1}{1-R_C} \left(\gamma_t \Delta CDS^D(t,T) + \Delta V^D \right) .
\end{aligned}$$

Next, we take into account the Black-Scholes equations that model H^i and $CDS^D(t,T)$, namely

$$\begin{aligned}
\frac{\partial H^{i,D}}{\partial t} + \frac{1}{2} (\sigma^{S^i} S^i)^2 \frac{\partial^2 H^{i,D}}{\partial (S^i)^2} + (r^i - q^i) S^i \frac{\partial H^{i,D}}{\partial S^i} &= (r^D + b^{D,C_i}) H^{i,D}, \\
\frac{\partial CDS^D(t,T)}{\partial t} + \frac{1}{2} (\sigma^h h)^2 \frac{\partial CDS^D(t,T)}{\partial h^2} + (\mu^{h,P} - M^h \sigma^{h,P}) \frac{\partial CDS^D(t,T)}{\partial h} & \\
+ \frac{h}{1-R_C} \Delta CDS^D(t,T) &= r^D CDS^D(t,T) \,.
\end{aligned}$$

Thus, (1.14) turns into:

$$\begin{aligned}
&\frac{\partial V^D}{\partial t} + \sum_{i=1}^{N} \frac{\partial V^D}{\partial S^i}(r^i - q^i)S^i + \frac{\partial V^D}{\partial h}(\mu^h - M^h\sigma^h) \\
&\qquad + \frac{1}{2}\sum_{i,k=1}^{N} \rho^{S^iS^k}\sigma^{S^i}\sigma^{S^k}S^iS^k\frac{\partial^2 V^D}{\partial S^i \partial S^k} + \frac{1}{2}(\sigma^h h)^2\frac{\partial^2 V^D}{\partial h^2} + \sum_{i=1}^{N}\rho^{S^ih}\sigma^{S^i}\sigma^h S^i\frac{\partial^2 V^D}{\partial S^i\partial h} \\
&= -\frac{h}{1-R_C}\Delta V^D + f^D V^D + (r^D + b^{D,C_0} - f^D)C^{C_0}X^{D,C_0}\,.
\end{aligned}$$

Therefore, we obtain the following pricing PDE:

$$\frac{\partial V^D}{\partial t} + \mathcal{L}_{Sh}V^D - f^D V^D + \frac{h}{1-R_C}\Delta V^D = (r^D + b^{D,C_0} - f^D)C^{C_0}X^{D,C_0}\,, \tag{1.17}$$

where the second order differential operator $\mathcal{L}_{Sh}$ is given by

$$\begin{aligned}
\mathcal{L}_{Sh} &= \frac{1}{2}\sum_{i,k=1}^{N}\rho^{S^iS^k}\sigma^{S^i}\sigma^{S^k}S^iS^k\frac{\partial^2}{\partial S^i\partial S^k} + \frac{1}{2}(\sigma^h h)^2\frac{\partial^2}{\partial h^2} \\
&\quad + \sum_{i=1}^{N}\rho^{S^ih}\sigma^{S^i}\sigma^h S^i\frac{\partial^2}{\partial S^i\partial h} + \sum_{i=1}^{N}(r^i - q^i)S^i\frac{\partial}{\partial S^i} + (\mu^h - M^h\sigma^h)\frac{\partial}{\partial h}\,.
\end{aligned} \tag{1.18}$$

Finally, we use the Q-drift of h given in (1.5) to write the differential operator (1.18) as follows:

$$\begin{aligned}
\mathcal{L}_{Sh} &= \frac{1}{2}\sum_{i,k=1}^{N}\rho^{S^iS^k}\sigma^{S^i}\sigma^{S^k}S^iS^k\frac{\partial^2}{\partial S^i\partial S^k} + \frac{1}{2}(\sigma^h h)^2\frac{\partial^2}{\partial h^2} \\
&\quad + \sum_{i=1}^{N}\rho^{S^ih}\sigma^{S^i}\sigma^h S^i\frac{\partial^2}{\partial S^i\partial h} + \sum_{i=1}^{N}(r^i - q^i)S^i\frac{\partial}{\partial S^i} + \alpha h(m - \log(h))\frac{\partial}{\partial h}\,.
\end{aligned} \tag{1.19}$$

In the pricing equation (1.17) the variation of V^D upon default is involved and is given by (see (1.9)):

$$\Delta V_t^D = C_t^D + R_C(M_t^D - C_t^D)^+ + (M_t^D - C_t^D)^- - V_t^D\,.$$

Following the seminal article [22], in the literature two possible values for the mark-to-market at default, M^D, can be chosen: either equal to the risky value or to the risk-free value of the derivative. Thus, we derive the following PDEs for both cases.

- If $M^D = V^D$, the variation of V^D upon default is given by:

$$\begin{aligned}\Delta V^D &= C^D + R_C(V^D - C^D)^+ + (V^D - C^D)^- - V^D \\ &= -(1 - R_C)(V_t^D - C_t^D)^+ ,\end{aligned}$$

  thus Equation (1.17) turns into

$$\frac{\partial V^D}{\partial t} + \mathcal{L}_{Sh} V^D - f^D V^D = h(V^D - C^D)^+ + (c^D + b^{D,C_0} - f^D)C^D . \tag{1.20}$$

- If $M^D = W^D$, the variation of V^D upon default is given by:

$$\begin{aligned}\Delta V^D &= C^D + R_C(W^D - C^D)^+ + (W^D - C^D)^- - V^D \\ &= W^D - V^D - (1 - R_C)(W^D - C^D)^+ ,\end{aligned}$$

  so that Equation (1.17) becomes

$$\begin{aligned}&\frac{\partial V^D}{\partial t} + \mathcal{L}_{Sh} V^D - \left(\frac{h}{1 - R_C} + f^D\right) V^D \\ &\quad = h(W^D - C^D)^+ - \frac{h}{1 - R_C} W^D + (r^D + b^{D,C_0} - f^D)C^D .\end{aligned} \tag{1.21}$$

Next, in order to pose the PDEs formulation for the XVA price, the risky derivative value can be split up into $V^D = W^D + U$, where W^D and U represent the risk-free derivative price and the XVA price, respectively.

Note that the risk-free derivative price W^D satisfies the classical multidimensional Black-Scholes equation:

$$\begin{cases} \partial_t W^D + \mathcal{L}_S W^D - f^D W^D = 0 , \\ W^D(T, S) = G(S) , \end{cases} \tag{1.22}$$

where $G = G(S)$ is the payoff function and

$$\mathcal{L}_S = \frac{1}{2} \sum_{i,k=1}^{N} \rho^{S^i S^k} \sigma^{S^i} \sigma^{S^k} S^i S^k \frac{\partial^2}{\partial S^i \partial S^k} + \sum_{i=1}^{N} (r^i - q^i) S^i \frac{\partial}{\partial S^i} . \tag{1.23}$$

Moreover, since the final conditions for V^D and for W^D coincide, i.e.,

$$W^D(T, S) = V^D(T, S, h) = G(S) ,$$

the final condition for U is given by $U(T,S,h)=0$.

Therefore, depending on the choice of the mark-to-market value at default we obtain two possible PDE problems satisfied by the XVA.

- Nonlinear final value problem (case $M=V^D$):

$$\begin{cases} \dfrac{\partial U}{\partial t}+\mathcal{L}_{Sh}U-f^DU \\ \qquad\qquad =h(W^D+U-C^D)^+ +(r^D+b^{D,C_0}-f^D)C^D\,, \\ U(T,S,h)=0\,. \end{cases} \tag{1.24}$$

- Linear final value problem (case $M=W^D$):

$$\begin{cases} \dfrac{\partial U}{\partial t}+\mathcal{L}_{Sh}U-\left(\frac{h}{1-R_C}+f^D\right)U \\ \qquad\qquad =h(W^D-C^D)^+ +(r^D+b^{D,C_0}-f^D)C^D\,, \\ U(T,S,h)=0\,. \end{cases} \tag{1.25}$$

In both cases, $(t,S,h)\in[0,T)\times(0,+\infty)^N\times(0,+\infty)$.

Note that the spatial dimension of problems (1.24) and (1.25) depends on the number of underlying assets, so that the PDE easily becomes high dimensional in space and the numerical solution requires specific discretization techniques to overcome the *curse of dimensionality* (see [70] or [69], as examples using sparse grids with recombination technique for solving high-dimensional PDEs for derivatives pricing). Therefore, alternative formulations in terms of expectations are obtained in the next section, so that appropriate numerical Monte Carlo techniques could be efficiently applied.

1.3 Formulation in terms of expectations

In order to compute the total value adjustment when more than two stochastic factors are involved, a first approach could be made by using the Monte Carlo method,

which is suitable to approximate expectations in a multidimensional framework, thus allowing to manage problems that involve more than two stochastic factors.

First, in order to compute the values of U by using the Monte Carlo method in the nonlinear model (1.24), we apply the nonlinear Feynman-Kac theorem, that relates the solution of nonlinear PDEs with the solution of BSDEs. The statement of the nonlinear Feynman-Kac theorem dates back from the seminal paper [80]. As the nonlinear term in (1.24) appears in the unknown U and not in the first order derivatives, Theorem 1.1 in the recent work by Beck et al. [14] can be applied to formulate the nonlinear problem (1.24) in terms of a nonlinear integral equation. Note that in [14] a large number of previous references on the nonlinear Feynman-Kac theorem are indicated, probably the here treated nonlinear PDE could be framed in many of them. Secondly, the linear Feynman-Kac theorem (see [81], for example) can be applied to the linear problem (1.25).

- If $M^D = V^D$, the total value adjustment at time t satisfies the equation

$$U(t,S_t,h_t) = E_t^{Q^D}\Bigg[-\int_t^T e^{-f^D(u-t)}\cdot\Big(h_u\Big(W^D(u,S_u)+U(u,S_u,h_u)-C^D(u)\Big)^+ + \Big(r^D+b^{D,C_0}-f^D\Big)C^D(u)\Big)du\Bigg]. \tag{1.26}$$

  Note that (1.26) is an integral equation as the unknown U appears also at the right hand side in the integral. We are interested in the XVA at the current time $t=0$, when the derivative is priced, that is to say

$$U(0,S_0,h_0) = E_0^{Q^D}\Bigg[-\int_0^T e^{-f^D u}\cdot\Big(h_u\Big(W^D(u,S_u)+U(u,S_u,h_u)-C^D(u)\Big)^+ + \Big(r^D+b^{D,C_0}-f^D\Big)C^D(u)\Big)du\Bigg]. \tag{1.27}$$

- If $M^D = W^D$, the total value adjustment at time t is given by

$$U(t,S_t,h_t) = E_t^{Q^D}\Bigg[-\int_t^T \exp\left(-\int_t^u \left(\frac{h_r}{1-R_C}+f^D\right)dr\right) \cdot \left(h_u\left(W^D(u,S_u)-C^D(u)\right)^+ + \left(r^D+b^{D,C_0}-f^D\right)C^D(u)\right)du\Bigg]. \tag{1.28}$$

Note that (1.28) gives an explicit formula for XVA. In particular, at time $t=0$ we have

$$U(0,S_0,h_0) = E_0^{Q^D}\Bigg[-\int_0^T \exp\left(-\int_0^u \left(\frac{h_r}{1-R_C}+f^D\right)dr\right) \cdot \left(h_u\left(W^D(u,S_u)-C^D(u)\right)^+ + \left(r^D+b^{D,C_0}-f^D\right)C^D(u)\right)du\Bigg]. \tag{1.29}$$

1.4 Numerical methods

In the previous section, two multidimensional problems for pricing the total valuation adjustment have been posed either in the event that $M^D = W^D$ (linear case) or in the event that $M^D = V^D$ (nonlinear case). In this section, we propose different numerical methods to compute the total value adjustment in both cases.

1.4.1 Lagrange-Galerkin method

Problems governed by partial differential equations can be numerically solved by classical finite differences or finite element methods when the number of spatial-like variables is less or equal to three. Otherwise, these deterministic numerical methods based on geometrical discretizations become highly computational demanding to solve the problems and we have to make use of other methodologies.

In this work we will consider the solution of PDEs problems for obtaining the XVA where only two spatial variables are involved. We will compare the results obtained with the proposed methods to solve these PDEs problems with alternative techniques we propose for the case of a higher number of stochastic factors.

Therefore, we first assume that the derivative is written on two underlying assets and the credit spread is a time dependent deterministic function. Moreover, we build this deterministic function as an approximation of the case with stochastic credit spread, indeed it results to be a particular limit of the corresponding stochastic models.

Thus, we set $\sigma^h = 0$ both in the case of the exponential Vasicek dynamics (1.5) and of the CIR dynamics (1.6). In the first case, the credit spread is the solution of the following deterministic Initial Value Problem (IVP)

$$\begin{cases} dh(t) = \alpha h(t) \left(\theta - \log\left(h(t)\right)\right) dt\,, \\ h(0) = h_0\,, \end{cases} \tag{1.30}$$

so that

$$h(t) = \exp\left(\theta - e^{-\alpha t + \log\left(\theta - \log(h_0)\right)}\right)\,. \tag{1.31}$$

In the case of CIR dynamics, the deterministic credit spread h is the solution of the following IVP

$$\begin{cases} dh(t) = \alpha h(t) \left(\theta - h(t)\right) dt\,, \\ h(0) = h_0\,, \end{cases} \tag{1.32}$$

so that

$$h(t) = \theta - (\theta - h_0)\, e^{\alpha t}\,. \tag{1.33}$$

In this framework, we propose a semi-Lagrangian time discretization technique combined with a finite element method for the spatial-like variables. This combination is usually referred to as Lagrange-Galerkin (LG) technique.

This discretization technique (as those based on finite difference methods) needs the truncation of the possibly unbounded spatial domain to a bounded domain and the

imposition of appropriate boundary conditions at certain boundaries of the bounded domain.

First of all, in order to pose more classical initial value problems instead of final value problems, we introduce the time-to-maturity, $\tau = T - t$. In this way, the problem (1.22) satisfied by the risk-free derivative, can be written as

$$\begin{cases} \partial_\tau W^D - \mathcal{L}_S W^D + f^D W^D = 0\,, \\ W^D(0,S) = G(S)\,. \end{cases} \tag{1.34}$$

Moreover, the nonlinear XVA problem (1.24) can be written as the following initial value problem:

$$\begin{cases} \partial_\tau U - \mathcal{L}_S U + f^D U \\ \qquad = -h\left(W^D + U - C^D\right)^+ - \left(r^D + b^{D,C_0} - f^D\right) C^D\,, \\ U(0,S^1,S^2) = 0\,, \end{cases} \tag{1.35}$$

whereas the linear problem (1.25) is given by

$$\begin{cases} \partial_\tau U - \mathcal{L}_S U + \left(\dfrac{h}{1-R_C} + f^D\right) U \\ \qquad = -h\left(W^D - C^D\right)^+ - \left(r^D + b^{D,C_0} - f^D\right) C^D\,, \\ U(0,S^1,S^2) = 0\,, \end{cases} \tag{1.36}$$

where $\tau \in (0,T)$ and $(S^1,S^2) \in (0,S^1_\infty \times (0,S^2_\infty)$. Moreover, S^1_∞ and S^2_∞ are large enough numbers so that the value at the financial region of interest is not affected by the choice of the boundary conditions at the truncated domain. Typically, this truncation argument is used in most PDEs models arising in financial problems.

Taking into account that the problem (1.34) for the risk free derivative price, the nonlinear problem (1.35) for the XVA and the linear problem (1.36) for the XVA involve the same differential operator $\mathcal{L}_S$, the partial differential equations of the

three problems can be equivalently written as:

$$\partial_\tau W^D - \operatorname{div}(A\nabla W^D) + \mathbf{b}\cdot\nabla W^D + f^D W^D = 0\,, \tag{1.37}$$

$$\partial_\tau U^D - \operatorname{div}(A\nabla U^D) + \mathbf{b}\cdot\nabla U^D + f^D U = g_1(U^D, W^D)\,, \tag{1.38}$$

$$\partial_\tau U^D - \operatorname{div}(A\nabla U^D) + \mathbf{b}\cdot\nabla U^D + \left(\frac{h}{1-R_C} + f^D\right) U = g_2(W^D)\,, \tag{1.39}$$

respectively, where the matrix A and the vector $\mathbf{b}$ are given by

$$A = \frac{1}{2}\begin{pmatrix} (\sigma^{S^1})^2 (S^1)^2 & \sigma^{S^1}\sigma^{S^2}\rho^{S^1S^2} S^1 S^2 \\ \sigma^{S^1}\sigma^{S^2}\rho^{S^1S^2} S^1 S^2 & (\sigma^{S^2})^2 (S^2)^2 \end{pmatrix},$$

$$\mathbf{b} = \begin{pmatrix} \left((\sigma^{S^1})^2 + \frac{1}{2}\sigma^{S^1}\sigma^{S^2}\rho^{S^1S^2} - r^1 + q^1\right) S^1 \\ \left((\sigma^{S^2})^2 + \frac{1}{2}\sigma^{S^1}\sigma^{S^2}\rho^{S^1S^2} - r^2 + q^2\right) S^2 \end{pmatrix}, \tag{1.40}$$

while g_1 and g_2 denote the right hand side term of the nonlinear and the linear problems for the XVA, respectively.

In the following, we will focus on the linear risky problem, since the risk-free and nonlinear risky problems can be treated in a similar way. We will also omit the superscript D in the variables, as all of them are always written in the domestic currency.

Time discretization with semi-Lagrangian method

For the time discretization we use the semi-Lagrangian method. For this purpose, we introduce the material derivative of U given by

$$\frac{DU}{D\tau} = \frac{\partial U}{\partial \tau} + \mathbf{b}\cdot\nabla U = \frac{\partial U}{\partial \tau} + b_1\frac{\partial U}{\partial S^1} + b_2\frac{\partial U}{\partial S^2}\,,$$

which represents the derivative along the characteristic curves associated to the vector field $\mathbf{b}$. In terms of the material derivative, the XVA linear equation in (1.39) turns into

$$\frac{DU}{D\tau} - \operatorname{div}(A\nabla U) + \left(\frac{h}{1-R_C} + f^D\right) U = g_2(W^D)\,. \tag{1.41}$$

For the time discretization we consider a uniform mesh with a constant time step, $\Delta\tau = T/N_T > 0$, and the time mesh points $\tau^n = n\Delta\tau$, for $n = 0, 1, \ldots, N_T$, with $N_T > 1$ being a natural number, so that we have $N_T + 1$ time mesh points in the time interval $[0, T]$.

At each time mesh point τ^{n+1}, we approximate the material derivative by the upwinded finite differences scheme along the characteristics:

$$\frac{DU}{D\tau}(\tau^{n+1}, .) \approx \frac{U^{n+1} - U^n \circ \chi^n}{\Delta\tau}, \tag{1.42}$$

where $\chi^n(S^1, S^2) = \chi((S^1, S^2), \tau^{n+1}; \tau_n)$, with χ being the solution of the ODE problem associated to the characteristic curve:

$$\begin{cases} \dfrac{d\chi_1}{d\tau} = b_1(\chi_1) = \left((\sigma^{S^1})^2 + \dfrac{1}{2}\sigma^{S^1}\sigma^{S^2}\rho^{S^1S^2} - r^1 + q^1 \right) \chi_1 \,, \\ \chi_1(\tau^{n+1}) = S^1 \,, \end{cases}$$

$$\begin{cases} \dfrac{d\chi_2}{d\tau} = b_2(\chi_2) = \left((\sigma^{S^2})^2 + \dfrac{1}{2}\sigma^{S^1}\sigma^{S^2}\rho^{S^1S^2} - r^2 + q^2 \right) \chi_2 \,, \\ \chi_2(\tau^{n+1}) = S^2 \,. \end{cases}$$

Note that $\chi(\tau) = \chi((S^1, S^2), \tau^{n+1}; \tau)$ represents the characteristic curve associated to the velocity field $\mathbf{b}$ passing through (S^1, S^2) at instant τ^{n+1}.

In the method of characteristics (also known as semi-Lagrangian method) that we propose for the time discretization, we approximate the material derivative by expression (1.42) and replace it in (1.41) to pose the semi-discretized in time problem:

$$\begin{cases} \dfrac{U^{n+1} - U^n \circ \chi^n}{\Delta\tau} - \operatorname{div}(A\nabla U^{n+1}) + \left(\dfrac{h}{1 - R_C} + f^D \right) U^{n+1} = g_2(W^{n+1}) \\ U^0(S^1, S^2) = 0 \,, \end{cases}$$

where $U^n \approx U(\tau^n, \cdot)$. It is easy to check that the components of χ^n are given by:

$$\chi_1^n = S^1 \exp\left(- \left((\sigma^{S^1})^2 + \frac{1}{2}\sigma^{S^1}\sigma^{S^2}\rho^{S^1S^2} - r^1 + q^1 \right) \Delta\tau \right) \,,$$

$$\chi_2^n = S^2 \exp\left(- \left((\sigma^{S^2})^2 + \frac{1}{2}\sigma^{S^1}\sigma^{S^2}\rho^{S^1S^2} - r^2 + q^2 \right) \Delta\tau \right) \,.$$

Analysis of boundary conditions

In order to apply the finite element method to approximate the total value adjustment, we need to truncate the unbounded domain and we consider the bounded domain $\Omega^* = (0,T)\times(0,S^1_\infty)\times(0,S^2_\infty)$. We will follow Fichera's theory [41, 76] to determine which boundaries of the domain need an imposed condition.

Let us consider points $(x_0,x_1,x_2) = (\tau,S^1,S^2) \in \Omega^* = (0,T)\times(0,S^1_\infty)\times(0,S^2_\infty)$, and introduce the notation

$$\Gamma_i^{*,-} = \left\{(x_0,x_1,x_2) \in \partial\Omega^* \,/\, x_i = 0\right\} ,$$
$$\Gamma_i^{*,+} = \left\{(x_0,x_1,x_2) \in \partial\Omega^* \,/\, x_i = x_i^\infty\right\} .$$

We now introduce the matrix function A^* and the vector function $\mathbf{b}^*$ such that

$$A^* = \frac{1}{2}\begin{pmatrix} 0 & 0 & 0 \\ 0 & (\sigma^{S^1})^2 x_1^2 & \rho^{S^1S^2}\sigma^{S^1}\sigma^{S^2}x_1x_2 \\ 0 & \rho^{S^1S^2}\sigma^{S^1}\sigma^{S^2}x_1x_2 & (\sigma^{S^2})^2x_2^2 \end{pmatrix} , \quad \mathbf{b}^* = \begin{pmatrix} -1 \\ (r^1-q^1)x_1 \\ (r^2-q^2)x_2 \end{pmatrix} ,$$

and the scalar function $c^* = -f^D$, so that equation (1.36) can be written as:

$$\sum_{i,j=0}^{2} a^*_{ij}\frac{\partial^2 U}{\partial x_i \partial x_j} + \sum_{i=0}^{2} b^*_i \frac{\partial U}{\partial x_i} + c^* U = 0\,.$$

Following [76], we introduce the following subsets of $\partial\Omega^*$ in terms of the vector $\mathbf{m}$, orthogonal to the boundary and pointing inwards Ω^*:

$$\Sigma^0 = \left\{ x \in \partial\Omega^* \,:\, \sum_{i,j=0}^{2} a^*_{ij} m_i m_j = 0 \right\} ,$$
$$\Sigma^1 = \partial\Omega^* - \Sigma^0\,,$$
$$\Sigma^2 = \left\{ x \in \Sigma^0 \,:\, \sum_{i=0}^{2}\left(b^*_i - \sum_{j=0}^{2}\frac{\partial a^*_{ij}}{\partial x_j}\right) m_i < 0 \right\} .$$

We need to impose boundary conditions on $\Sigma^1 \cup \Sigma^2$.

	Γ_0^-	Γ_0^+
$\mathbf{m}$	$(1,0,0)$	$(-1,0,0)$
$a^*_{00}m_0m_0$	0	0
$a^*_{01}m_0m_1$	0	0
$a^*_{02}m_0m_2$	0	0
$a^*_{10}m_1m_0$	0	0
$a^*_{11}m_1m_1$	0	0
$a^*_{12}m_1m_2$	0	0
$a^*_{20}m_2m_0$	0	0
$a^*_{21}m_2m_1$	0	0
$a^*_{22}m_2m_2$	0	0
$\sum_{i,j=0}^{1} a^*_{ij}m_im_j$	0	0
$a^*_{00,0}$	0	0
$a^*_{01,1}$	0	0
$a^*_{02,2}$	0	0
$a^*_{10,0}$	0	0
$a^*_{11,1}$	$(\sigma^{S^1})^2x_1$	$(\sigma^{S^1})^2x_1$
$a^*_{12,2}$	$\frac{1}{2}\rho^{S^1S^2}\sigma^{S^1}\sigma^{S^2}x_1$	$\frac{1}{2}\rho^{S^1S^2}\sigma^{S^1}\sigma^{S^2}x_1$
$a^*_{20,0}$	0	0
$a^*_{21,1}$	$\frac{1}{2}\rho^{S^1S^2}\sigma^{S^1}\sigma^{S^2}x_2$	$\frac{1}{2}\rho^{S^1S^2}\sigma^{S^1}\sigma^{S^2}x_2$
$a^*_{22,2}$	$(\sigma^{S^2})^2x_2$	$(\sigma^{S^2})^2x_2$
b^*_0	-1	-1
b^*_1	$(r^1-q^1)x_1$	$(r^1-q^1)x_1$
b^*_2	$(r^2-q^2)x_2$	$(r^2-q^2)x_2$
$(b^*_0-a^*_{0j,j})m_0$	-1	1
$(b^*_1-a^*_{1j,j})m_1$	0	0
$(b^*_2-a^*_{2j,j})m_2$	0	0
$\sum_{i=0}^{2}(b^*_i-a^*_{ij,j})m_i$	-1	1

Table 1.1: Analysis of boundary conditions [41]

	Γ_1^-	Γ_1^+	Γ_2^-	Γ_2^+
$\mathbf{m}$	$(0,1,0)$	$(0,-1,0)$	$(0,0,1)$	$(0,0,-1)$
$a^*_{00}m_0m_0$	0	0	0	0
$a^*_{01}m_0m_1$	0	0	0	0
$a^*_{02}m_0m_2$	0	0	0	0
$a^*_{10}m_1m_0$	0	0	0	0
$a^*_{11}m_1m_1$	0	$\frac{1}{2}(\sigma^{S^1})^2(x_1^\infty)^2$	0	0
$a^*_{12}m_1m_2$	0	0	0	0
$a^*_{20}m_2m_0$	0	0	0	0
$a^*_{21}m_2m_1$	0	0	0	0
$a^*_{22}m_2m_2$	0	0	0	$\frac{1}{2}(\sigma^{S^2})^2(x_2^\infty)^2$
$\sum_{i,j=0}^{1} a^*_{ij}m_im_j$	0	$\frac{1}{2}(\sigma^{S^1})^2(x_1^\infty)^2$	0	$\frac{1}{2}(\sigma^{S^2})^2(x_2^\infty)^2$
$a^*_{00,0}$	0	0	0	0
$a^*_{01,1}$	0	0	0	0
$a^*_{02,2}$	0	0	0	0
$a^*_{10,0}$	0	0	0	0
$a^*_{11,1}$	0	$(\sigma^{S^1})^2x_1^\infty$	$(\sigma^{S^1})^2x_1$	$(\sigma^{S^1})^2x_1$
$a^*_{12,2}$	0	$\frac{1}{2}\rho^{S^1S^2}\sigma^{S^1}\sigma^{S^2}x_1^\infty$	$\frac{1}{2}\rho^{S^1S^2}\sigma^{S^1}\sigma^{S^2}x_1$	$\frac{1}{2}\rho^{S^1S^2}\sigma^{S^1}\sigma^{S^2}x_1$
$a^*_{20,0}$	0	0	0	0
$a^*_{21,1}$	$\frac{1}{2}\rho^{S^1S^2}\sigma^{S^1}\sigma^{S^2}x_2$	$\frac{1}{2}\rho^{S^1S^2}\sigma^{S^1}\sigma^{S^2}x_2$	0	$\frac{1}{2}\rho^{S^1S^2}\sigma^{S^1}\sigma^{S^2}x_2^\infty$
$a^*_{22,2}$	$(\sigma^{S^2})^2x_2$	$(\sigma^{S^2})^2x_2$	0	$(\sigma^{S^2})^2x_2^\infty$
b^*_0	-1	-1	-1	-1
b^*_1	0	$(r^1-q^1)x_1^\infty$	$(r^1-q^1)x_1$	$(r^1-q^1)x_1$
b^*_2	$(r^2-q^2)x_2$	$(r^2-q^2)x_2$	0	$(r^2-q^2)x_2^\infty$
$(b^*_0-a^*_{0j,j})m_0$	0	0	0	0
$(b^*_1-a^*_{1j,j})m_1$	0	z_1	0	0
$(b^*_2-a^*_{2j,j})m_2$	0	0	0	z_2
$\sum_{i=0}^{2}(b^*_i-a^*_{ij,j})m_i$	0	z_1	0	z_2

$$z_1 = ((\sigma^{S^1})^2 - r^1 + q^1 + \tfrac{1}{2}\rho^{S^1S^2}\sigma^{S^1}\sigma^{S^2})x_1^\infty$$
$$z_2 = ((\sigma^{S^2})^2 - r^2 + q^2 + \tfrac{1}{2}\rho^{S^1S^2}\sigma^{S^1}\sigma^{S^2})x_2^\infty$$

Table 1.2: Analysis of boundary conditions [41]

Tables 1.1 and 1.2 summarize the values we need to identify the sets Σ^0, Σ^1 and Σ^2. Note that $y_{,j}$ denotes a partial derivative of y with respect to x_j and Euler summation on repeated indices is used. We will assume $r^i - q^i > 0$ for $i = 1, 2$. We deduce:

$$\Sigma^0 = \Gamma_0^- \cup \Gamma_0^+ \cup \Gamma_1^- \cup \Gamma_2^- \,, \qquad \Sigma^1 = \Gamma_1^+ \cup \Gamma_2^+ \,, \qquad \Sigma^2 = \Gamma_0^- \,,$$

and, following [41, 76], we have to impose conditions on $\Sigma^1 \cup \Sigma^2 = \Gamma_0^- \cup \Gamma_1^+ \cup \Gamma_2^+$. According to the stated notation, $x_0 = \tau$ and Γ_0^- corresponds to the initial condition; thus, we need to impose boundary conditions on the right ($S^1 = S^1_\infty$) and upper ($S^2 = S^2_\infty$) boundaries of Ω.

Proposed boundary conditions on $S^1 = S^1_\infty$. In order to deduce the conditions to impose on the right boundary of the domain, we make use of a previous methodology [33, 24, 6]. We consider equation (1.36), divide by $(S^1)^2$ and make S^1 tend to infinity, thus obtaining

$$\frac{1}{2}(\sigma^{S^1})^2 \frac{\partial^2 U}{\partial (S^1)^2} = 0 \,,$$

so that we can write U as:

$$U(\tau, S^1, S^2) = H_0(\tau) + H_1(\tau) S^1 + H_2(\tau) S^2 + H_3(\tau) S^1 S^2 + H_4(\tau)(S^2)^2 \,.$$

Equation (1.36) can be written, in this particular case, as

$$\partial_\tau U - \operatorname{div}(\widehat{A} \nabla U) + \widehat{\mathbf{b}} \cdot \nabla U + \left(\frac{h}{1 - R_C} + f^D \right) U = g_2(W) \,,$$

where

$$\widehat{A} = \frac{1}{2} \begin{pmatrix} 0 & \sigma^{S^1} \sigma^{S^2} \rho^{S^1 S^2} S^1 S^2 \\ \sigma^{S^1} \sigma^{S^2} \rho^{S^1 S^2} S^1 S^2 & (\sigma^{S^2})^2 (S^2)^2 \end{pmatrix} ,$$

and the time discretization by the characteristics method leads to

$$U^{n+1} - \Delta\tau \operatorname{div}(\widehat{A} \nabla U^{n+1}) + \left(\frac{h}{1 - R_C} + f^D \right) \Delta\tau \, U^{n+1} = \Delta\tau \, g_2(W^{n+1}) + U^n \circ \widehat{\chi}^n \,,$$

where $\widehat{\chi}^n$ (related to the velocity field $\widehat{\mathbf{b}}$) is given by

$$\begin{cases} \widehat{\chi}_1^n(S^1,S^2) = S^1 \exp\left(-\left(\frac{1}{2}\sigma^{S^1}\sigma^{S^2}\rho^{S^1S^2} - r^1 + q^1\right)\Delta\tau\right), \\ \widehat{\chi}_2^n(S^1,S^2) = S^2 \exp\left(-\left((\sigma^{S^2})^2 + \frac{1}{2}\sigma^{S^1}\sigma^{S^2}\rho^{S^1S^2} - r^2 + q^2\right)\Delta\tau\right). \end{cases}$$

Thus,

$$\left(1 + \left(\frac{h}{1-R_C} + f^D\right)\Delta\tau\right) U^{n+1} - \Delta\tau \,\mathrm{div}\,(\widehat{A}\nabla U^{n+1}) = \Delta\tau\, g_2(W^{n+1}) + U^n \circ \widehat{\chi}^n$$

or, equivalently,

$$\begin{aligned} &\left(1 + \left(\frac{h}{1-R_C} + f^D\right)\Delta\tau\right)\left[H_0(\tau) + H_1(\tau)S^1 + H_2(\tau)S^2 + H_3(\tau)S^1S^2 + H_4(\tau)(S^2)^2\right] \\ &\quad - \frac{\Delta\tau}{2}\frac{\partial}{\partial S^1}\Big[0 + \sigma^{S^1}\sigma^{S^2}\rho^{S^1S^2}S^1S^2\Big(H_2(\tau) + H_3(\tau)S^1 + 2H_4(\tau)S^2\Big)\Big] \\ &\quad - \frac{\Delta\tau}{2}\frac{\partial}{\partial S^2}\Big[\sigma^{S^1}\sigma^{S^2}\rho^{S^1S^2}S^1S^2\Big(H_1(\tau) + H_3(\tau)S^2\Big) \\ &\quad + (\sigma^{S^2})^2(S^2)^2\left(H_2(\tau) + H_3(\tau)S^1 + 2H_4(\tau)S^2\right)\Big] \\ &\quad = \Delta\tau\, g_2(W^{n+1}) + U^n \circ \widehat{\chi}^n\,. \end{aligned}$$

If we choose $H_1(\tau) = H_2(\tau) = H_3(\tau) = H_4(\tau) = 0$, then

$$U^{n+1}(S^1_\infty, S^2) = H_0^{n+1} = \frac{\Delta\tau\, g_2(W^{n+1}) + U^n \circ \widehat{\chi}^n}{1 + \left(\frac{h}{1-R_C} + f^D\right)\Delta\tau}\,.$$

Thus, a non homogeneous Dirichlet boundary condition is derived on the right boundary of the truncated domain.

In the risk-free problem, the derived Dirichlet boundary condition is given by:

$$U^{n+1}(S^1_\infty, S^2) = \frac{U^n \circ \widehat{\chi}^n}{1 + f^D\Delta\tau}\,,$$

while the analogous condition in the nonlinear risky problem is

$$U^{n+1}(S^1_\infty, S^2) = \frac{\Delta\tau\, g_1(U^n, W^{n+1}) + U^n \circ \widehat{\chi}^n}{1 + f^D\Delta\tau}\,.$$

Proposed boundary conditions on $S^2 = S^2_\infty$. Similarly to what we did in the previous paragraph, on the upper boundary we can deduce an analogous Dirichlet boundary condition:

$$U^{n+1}(S^1, S^2_\infty) = \widetilde{H_0}^{n+1} = \frac{\Delta\tau\, g_2(W^{n+1}) + U^n \circ \widetilde{\xi}^n}{1 + \left(\dfrac{h}{1-R_C} + f^D\right)\Delta\tau}\,,$$

where $\widetilde{\xi}^n$ is given by:

$$\begin{cases} \widetilde{\xi}^n_1(S^1, S^2) = S^1 \exp\left(-\left((\sigma^{S^1})^2 + \dfrac{1}{2}\sigma^{S^1}\sigma^{S^2}\rho^{S^1S^2} - r^1 + q^1\right)\Delta\tau\right) \\ \widetilde{\xi}^n_2(S^1, S^2) = S^2 \exp\left(-\left(\dfrac{1}{2}\sigma^{S^1}\sigma^{S^2}\rho^{S^1S^2} - r^2 + q^2\right)\Delta\tau\right)\,. \end{cases}$$

In the risk-free problem, the Dirichlet boundary condition is

$$U^{n+1}(S^1, S^2_\infty) = \frac{U^n \circ \widetilde{\xi}^n}{1 + f^D\Delta\tau}\,,$$

while in the nonlinear problem it is given by

$$U^{n+1}(S^1, S^2_\infty) = \frac{\Delta\tau\, g_1(U^n, W^{n+1}) + U^n \circ \widetilde{\xi}^n}{1 + f^D\Delta\tau}\,.$$

Finite element method

We now consider a triangular mesh of the domain and the finite element space of piecewise linear Lagrange polynomials. At each time step, τ^n, we can use Green's formula and pose the variational formulation corresponding to the risky linear problem:

Find $U^{n+1} \in \left\{\varphi \in H^1(\Omega)/\varphi = H_5^{n+1} \text{ on } \Gamma_1^+, \varphi = \widetilde{H_5}^{n+1} \text{ on } \Gamma_2^+\right\}$ such that

$$\begin{aligned} &\int_\Omega U^{n+1}\varphi\, dS^1\, dS^2 + \Delta\tau \int_\Omega A\nabla U^{n+1}\nabla\varphi\, dS^1\, dS^2 \\ &\quad + \Delta\tau\left(\frac{h(T-\tau^{n+1})}{1-R_C} + f^D\right)\int_\Omega U^{n+1}\varphi\, dS^1\, dS^2 \\ &\quad = \int_\Omega (U^n \circ \chi^n)\varphi\, dS^1\, dS^2 + \Delta\tau \int_\Omega g_2(U^n)\varphi\, dS^1\, dS^2\,, \qquad \forall\varphi \in H^1_*(\Omega)\,, \end{aligned}$$

where $H^1_*(\Omega) = \left\{\varphi \in H^1(\Omega) \,/\, \varphi = 0 \text{ on } \Gamma_1^+ \cup \Gamma_2^-\right\}$.

Next, for fixed natural numbers $M > 0$ and $L > 0$, we consider a uniform mesh of the computational domain Ω, the nodes of which are (S_i^1, S_j^2), with:

$$S_i^1 = i\Delta S^1 \,(i = 0, 1, \ldots, M+1)\,, \quad \Delta S^1 = \frac{S_\infty^1}{M+1}\,,$$
$$S_j^2 = j\Delta S^2 \,(j = 0, 1, \ldots, L+1)\,, \quad \Delta S^2 = \frac{S_\infty^2}{L+1}\,.$$

Let us remark that a non uniform mesh can also be considered. We introduce the finite element spaces

$$Y_h = \left\{\varphi_h \in \mathcal{C}(\Omega) \,/\, \varphi_h|_{T_k} \in \mathcal{P}_1\,, \forall T_k \in \mathcal{T}\right\}$$
$$Y_h^* = \left\{\varphi_h \in Y_h \,/\, \varphi_h = 0 \text{ on } \Gamma_1 \cup \Gamma_2\right\}$$

and search U_h^{n+1} satisfying the boundary conditions and such that

$$\int_\Omega U_h^{n+1}\varphi_h \, dS^1\, dS^2 + \Delta\tau \int_\Omega A\nabla U_h^{n+1}\nabla\varphi_h \, dS^1\, dS^2 \tag{1.43}$$
$$+ \Delta\tau \left(\frac{h(T-\tau^{n+1})}{1-R_C} + f^D\right)\int_\Omega U_h^{n+1}\varphi_h \, dS^1\, dS^2$$
$$= \int_\Omega (U_h^n \circ \chi^n)\varphi \, dS^1\, dS^2 + \Delta\tau \int_\Omega g_2(U_h^n)\varphi_h \, dS^1\, dS^2\,, \qquad \forall\varphi_h \in Y_h^*\,. \tag{1.44}$$

The different integrals that take part in (1.44) are approximated by adequate quadrature formulae, and the system of linear equations is solved by a LU factorization method.

The risk-free problem is solved in a similar way; the differences with respect to the described risky linear problem concern the right hand side member and the coefficient of the unknown, W, in the PDE. Thus, the risk-free price is the solution of the following variational problem:
Find W_h such that:

$$\left(1 + \Delta\tau\, f^D\right)\int_\Omega W_h^{n+1}\varphi_h \, dS^1\, dS^2 + \Delta\tau \int_\Omega A\nabla W_h^{n+1}\nabla\varphi_h \, dS^1\, dS^2$$
$$= \int_\Omega (W_h^n \circ \chi^n)\varphi \, dS^1\, dS^2\,, \qquad \forall\varphi_h \in Y_h^*\,.$$

Fixed point iteration

In the nonlinear problem (1.35), an additional fixed point iteration method is implemented to approximate the solution. The scheme, in terms of the strong formulation, is described in Algorithm 1.

Algorithm 1 Fixed-point algorithm

Let $N > 1$, $n = 0$, $\varepsilon > 0$, $U^0 = 0$
while $n \leq N$ **do**
  Let $U^{n+1,0} = U^n$, $\ell = 0$, $e = \varepsilon + 1$
  while $e \geq \varepsilon$ **do**
    Find $U^{n+1,\ell+1}$ solution of

$$U^{n+1,\ell+1} - \Delta\tau \,\mathrm{div}\,(A\nabla U^{n+1,\ell+1}) + f^D \Delta\tau\, U^{n+1,\ell+1} = \Delta\tau\, g_1(U^{n+1,\ell}, W^{n+1}) + U^n \circ \chi^n$$

    $e = \frac{\|U^{\ell+1} - U^\ell\|}{\|U^\ell\|}$
    $\ell = \ell + 1$
  end while
  $n = n + 1$
end while

1.4.2 Monte Carlo method

In the numerical examples in Section 1.5 we assume constant FX rates. We need a time discretization in order to discretize the dynamics of the underlying assets S^i $(i = 1, \ldots, N)$ and of the credit spread h by using Euler-Maruyama scheme [65]. Thus, we choose a uniform mesh with Z nodes, $0 = t_0 < t_1 < \cdots < t_{Z-1} = T$, and we denote by $\Delta t = t_z - t_{z-1}$ the distance between two consecutive nodes. Hence, we denote by $S^i_z = S^i(t_z)$, $\tilde{h}_z = \tilde{h}(t_z) = \log(h(t_z))$ and $h_z = h(t_z)$, and by $\Delta W^{S^i}_z = W^{S^i}_z - W^{S^i}_{z-1}$, for $i = 1, \ldots, N$, and $\Delta W^h_z = W^h_z - W^h_{z-1}$ correlated Brownian increments, according to

the correlation matrix (1.3). Thus, these correlated Brownian motions can be built by Cholesky factorization. Therefore, for the underlying assets $S^1, \ldots, S^N$ we have

$$S^i_{z+1} = S^i_z + (r^i - q^i) S^i_z \, \Delta t + \sigma^{S^i} S^i_z \, \Delta W^{S^i}_z$$

and for the credit spread in the case of the exponential Vasicek dynamics we have

$$h_{z+1} = e^{\tilde{h}_{z+1}}, \quad \text{with} \quad \tilde{h}_{z+1} = \tilde{h}_z + \alpha(\theta - \tilde{h}_z)\Delta t + \sigma^h \Delta W^h_z \, .$$

In the case of the CIR model for the credit spread, the Euler-Maruyama scheme

$$h_{z+1} = h_z + \alpha(\theta - h_z)\Delta t + \sigma^h \sqrt{h_z} \Delta W^h_z$$

can lead to negative values since the Gaussian increment is not bounded from below, even if the Feller condition is satisfied and, thus, the continuous version of the process is positive. Therefore, we use the "full truncation" scheme proposed in [30], given by

$$h_{z+1} = h_z + \alpha(\theta - h^+_z)\Delta t + \sigma^h \sqrt{h^+_z} \Delta W^h_z \, .$$

Nonlinear case ($M = V^D$)

When $M = V^D$, a fixed-point method, or Picard iteration method, is implemented to compute the XVA price, given by the integral equation (1.27). More precisely, we start from $U^0 = 0$ and recursively compute:

$$\begin{aligned} U^{\ell+1}(0,S,h) = & E^{Q^D}_0 \Bigg[- \int_0^T e^{-f^D u} \Bigg(h_u \left(W^D(u, S_u) + U^\ell(u, S_u, h_u) - C^D(u) \right)^+ \\ & + \left(r^D + b^{D,C_0} - f^D \right) C^D(u) \Bigg) du \, \Bigg| \, S_0 = S, h_0 = h \Bigg] \end{aligned} \tag{1.45}$$

for $\ell = 0, 1, 2, \ldots$ until convergence is attained.

At each iteration (1.45) of the fixed-point algorithm of the nonlinear model the computation of an integral term is required. We consider either a simple rectangular or simple trapezoidal quadrature formula. Therefore, if we denote by $I^{NL,\ell}$ the integral

in the right hand side of (1.45), thus

$$I^{NL,\ell} = \int_0^T e^{-f^D u} \Big(h_u \left(W^D(u, S_u) + U^\ell(u, S_u, h_u) - C^D(u) \right)^+ + \left(r^D + b^{D,C_0} - f^D \right) C^D(u) \Big) du \,, \tag{1.46}$$

then we approximate the integral as follows:

$$I^{NL,\ell} \simeq T \Big[h_u \left(W^D(0, S_0) + U^\ell(0, S_0, h_0) - C^D(0) \right)^+ + \left(r^D + b^{D,C_0} - f^D \right) C^D(0) \Big] \tag{1.47}$$

or

$$I^{NL,\ell} \simeq \frac{T}{2} \Big[e^{-f^D T} \Big(h_T \left(W^D(T, S_T) - C^D(T) \right)^+ + \left(r^D + b^{D,C_0} - f^D \right) C^D(T) \Big) + \Big(h_0 \left(W^D(0, S_0) + U^\ell(0, S_0, h_0) - C^D(0) \right)^+ + \left(r^D + b^{D,C_0} - f^D \right) C^D(0) \Big) \Big] . \tag{1.48}$$

In the nonlinear case we use only simple quadrature formulae, because we just know the final value of U, that is $U_T = 0$, while composite formulae require to know the values of U at internal nodes of our time discretization. One could approximate the value of U at each node going backwards from the last node, although in this way a nested Monte Carlo problem arises. However, in order to improve our estimates we also implement the multilevel Picard iterations method proposed in [37] and [62], and recalled in the Subsection 1.4.3, that allows to consider the values at the internal nodes of our time discretization.

Linear case ($M = W^D$)

When $M = W^D$, Equation (1.29) gives an explicit expression for the XVA price that is computed with the help of numerical formulae for the approximation of the integral that use the time discretization stated above. As in the case of the nonlinear

model, we use either a rectangular or a trapezoidal formula, but in the linear case also composite formulae can be implemented. Therefore, if we denote by I^L the integral in the right hand side of (1.29), thus

$$\begin{aligned} I^L = &\int_0^T \exp\left(-\int_0^u \left(\frac{h_r}{1-R_C} + f^D\right) dr\right) \\ &\cdot \left(h_u \left(W^D(u, S_u) - C^D(u)\right)^+ + \left(r^D + b^{D,C_0} - f^D\right) C^D(u)\right) du\,, \end{aligned} \tag{1.49}$$

then we approximate the integral either with a simple rectangular or a simple trapezoidal formula, respectively given by

$$\begin{aligned} I^L \simeq &T\left[\exp\left(-T\left(\frac{h_T}{1-R_C} + f\right)\right)\right. \\ &\left.\cdot \left(h_T \left(W^D(T, S_T) - C^D(T)\right)^+ + \left(r^D + b^{D,C_0} - f^D\right) C^D(T)\right)\right] \end{aligned} \tag{1.50}$$

and

$$\begin{aligned} I^L \simeq &\frac{T}{2}\left[\exp\left(-\frac{T}{2}\left(\frac{h_T + h_0}{1-R_C} + 2f^D\right)\right)\right. \\ &\cdot \left(h_T \left(W^D(T, S_T) - C^D(T)\right)^+ + \left(r^D + b^{D,C_0} - f^D\right) C^D(T)\right) \\ &\left. + \left(h_0 \left(W^D(0, S_0) - C^D(0)\right)^+ + \left(r^D + b^{D,C_0} - f^D\right) C^D(0)\right)\right]. \end{aligned} \tag{1.51}$$

Moreover, we approximate the integral (1.49) with the rectangular and the trapezoidal composite formulae given by

$$\begin{aligned} I^L \simeq &\Delta t \sum_{z_1=0}^{Z-2} \exp\left(-\Delta t \sum_{z_2=0}^{z_1-1}\left(\frac{h_{t_{z_2}}}{1-R_C} + f\right)\right) \\ &\cdot \left(h_{z_1} \left(W^D(t_{z_1}, S_{z_1}) - C^D(t_{z_1})\right)^+ + \left(r^D + b^{D,C_0} - f^D\right) C^D(t_{z_1})\right) \end{aligned} \tag{1.52}$$

and

$$
\begin{aligned}
I^L \simeq \frac{\Delta t}{2} \sum_{z_1=0}^{Z-2} \Bigg[& \exp\left(-\frac{\Delta t}{2} \sum_{z_2=0}^{z_1-1} \left(\frac{h_{t_{z_2}} + h_{t_{z_2+1}}}{1 - R_C} + 2 f^D \right) \right) \\
& \cdot \left(h_{z_1} \left(W^D(t_{z_1}, S_{z_1}) - C^D(t_{z_1}) \right)^+ + \left(r^D + b^{D,C_0} - f^D \right) C^D(t_{z_1}) \right) \\
& + \exp\left(-\frac{\Delta t}{2} \sum_{z_2=0}^{z_1} \left(\frac{h_{t_{z_2}} + h_{t_{z_2+1}}}{1 - R_C} + 2 f^D \right) \right) \\
& \cdot \Bigg(h_{z_1+1} \left(W^D(t_{z_1+1}, S_{z_1+1}) - C^D(t_{z_1+1}) \right)^+ \\
& + \left(r^D + b^{D,C_0} - f^D \right) C^D(t_{z_1+1}) \Bigg) \Bigg] .
\end{aligned} \tag{1.53}
$$

1.4.3 Multilevel Picard iteration

In this subsection we briefly describe the main idea in the Multilevel Picard Iteration (MPI) method. For further details about the method, we address the reader to [37], for example.

The multilevel Picard iteration method is based in the adaptation of the multilevel Monte Carlo approach of Heinrich [55, 56] and Giles [46] to the Picard approximation method. The multilevel Monte Carlo path simulations are based on the multigrid ideas, that facilitates the reduction of the computational complexity when estimating an expected value derived from a stochastic differential equation via Monte Carlo path simulations.

In order to apply the multilevel Picard iteration, we define a function Φ as

$$
\begin{aligned}
\left(\Phi(\mathtt{u}) \right)(s,x) = \mathrm{E}_s^Q \Bigg[& - \int_s^T e^{-f^D(t-s)} \\
& \left(h_t \left(W^D(t, S_t) + \mathtt{u} - C^D(t) \right)^+ \right. \\
& \left. + \left(r^D + b^{D,C_0} - f^D \right) C^D(t) \right) dt \,\Big|\, x = (S_s, h_s) \Bigg]
\end{aligned} \tag{1.54}
$$

and a sequence of Picard approximations $(\mathtt{u}_n)_{n \in \mathbb{N}_0}$ such that $\mathtt{u}_{n+1} = \Phi(\mathtt{u}_n)$ for all $n \in \mathbb{N}_0$. By using the Banach fixed-point theorem, it can be proved that the sequence

$(\mathfrak{u}_n)_{n\in\mathbb{N}_0}$ converges at least exponentially fast to the solution of $u = \Phi(u)$. Therefore, for all sufficiently large $n \in \mathbb{N}$, we have

$$\begin{aligned} u \approx \mathfrak{u}_n &= \mathfrak{u}_1 + \sum_{l=1}^{n-1}(\mathfrak{u}_{l+1} - \mathfrak{u}_l) = \Phi(\mathfrak{u}_0) + \sum_{l=1}^{n-1}(\Phi(\mathfrak{u}_l) - \Phi(\mathfrak{u}_{l-1})) \\ &\approx \Psi_{n,\rho}(\mathfrak{u}_0) + \sum_{l=1}^{n-1}(\Psi_{n-l,\rho}(\mathfrak{u}_l) - \Psi_{n-l,\rho}(\mathfrak{u}_{l-1})), \end{aligned} \tag{1.55}$$

where $\Psi_{n,\rho}(\mathfrak{u}_l)$ is a discrete approximation of $\Phi(\mathfrak{u}_l)$ with $m_{n,l,\rho}$ Monte Carlo paths. More precisely,

$$\begin{aligned} \left(\Psi_{n,\rho}\left(\mathfrak{u}_l\right)\right)(s,x) = -\frac{1}{m_{n,l,\rho}} &\sum_{i=1}^{m_{n,l,\rho}} \sum_{t\in]s,T]} q_s^{n,l,\rho}(t) \\ \cdot e^{-f^D(t-s)} &\left(h_t^{i,n,x}\left(W^D(t, S_t^{i,n,x}) + \mathfrak{u}_l - C^D(t)\right)^+ \right. \\ &\left. + \left(r^D + b^{D,C_0} - f^D\right) C^D(t) \right), \end{aligned} \tag{1.56}$$

where $(q^{n,l,\rho})_{n,l,\rho\in\mathbb{N}_0,l<n}$ denotes the family of quadrature rules for the approximation of the integral and the superscripts i, n, x refer to the i-th Monte Carlo path with initial point x in the n-th Picard iteration. In particular, in our numerical examples we have chosen $m_{n,l,\rho} = \rho^{n-l}$, as also proposed in [37].

Note that the quadrature rules $q^{n,l,\rho}$ are just functions on $[0,T]$ which have non-zero values only on a finite subset of $[0,T]$. In our numerical examples, we have chosen the left-rectangle rule with ρ^{n-l} rectangles, so that, for $s \in]0,T]$,

$$q_s^{n,l,\rho} = \frac{T-s}{\rho^{n-l}}\, \mathbb{1}_{s+i\frac{T-s}{\rho^{n-l}}, i\in\mathbb{N}_0}(t), \quad t \in]s,T]. \tag{1.57}$$

Since the XVA price in (1.27) can be seen as solution of $\mathfrak{u} = \Phi(\mathfrak{u})$, from (1.55) we obtain our multilevel Picard iteration scheme:

$$\begin{cases} U_{0,\rho} = u_0, \\ U_{n,\rho} = \Psi_{n,\rho}\left(U_{0,\rho}\right) + \sum_{l=1}^{n-1}\left(\Psi_{n-l,\rho}\left(U_{l,\rho}\right) - \Psi_{n-l,\rho}\left(U_{l-1,\rho}\right)\right). \end{cases} \tag{1.58}$$

This recursive approximation scheme keeps the computational cost moderate compared to the desired approximation precision (see, for example, [37]).

Note that in the original multilevel Monte Carlo approach the different levels correspond to approximations with different step sizes in time or space, while in the multilevel Picard iterations method different levels correspond to different stages of the Picard iteration. Therefore, the approximations (1.58) are "full history recursive" in the sense that for every $n, \rho \in \mathbb{N}$ the "full history" of approximations, i.e., $U_{0,\rho}, U_{1,\rho}, \ldots, U_{n-1,\rho}$, needs to be computed recursively in order to compute $U_{n,\rho}$.

Relative Approximation Increments

In Section 1.5 and Section 2.5 the empirical convergence of the algorithm is tested. More precisely, we compute

$$U^i_{\rho,\rho}, \text{ for } (\rho, i) \in \{1, \ldots, \rho_{max}\} \times \{1, \ldots, N_{runs}\}, \tag{1.59}$$

for fixed values of maximum ρ, ρ_{max} and number of runs, N_{runs}. Then, we define the Relative Approximation Increments (RAI) of parameters ρ_{max} and N_{runs} as

$$RAI\left(\rho; \rho_{max}, N_{runs}\right) = \frac{\frac{1}{N_{runs}} \sum_{i=1}^{10} \left| U^i_{\rho+1,\rho+1} - U^i_{\rho,\rho} \right|}{\frac{1}{N_{runs}} \sum_{i=1}^{10} \left| U^i_{\rho_{max},\rho_{max}} \right|}, \tag{1.60}$$

for $\rho = 1, \ldots, \rho_{max} - 1$. The empirical convergence is shown by plotting the Relative Approximation Increments $RAI\left(\rho; \rho_{max}, N_{runs}\right)$, for $\rho = 1, \ldots, \rho_{max} - 1$, against ρ. In particular, in our numerical tests we have chosen $\rho_{max} = 5$ and $N_{runs} = 10$, as in one of the examples proposed in [37].

1.5 Numerical results

In this section we report some tests that illustrate the behaviour of the previously describe numerical methods when they are used for the evaluation of different multiasset options [83] in the presence of counterparty risk.

$r = (0.05, 0.03)$	$f^D = 0.06$	$R_C = 0.30$
$q = (0.03, 0.02)$	$r^D = 0.04$	
$\sigma^S = (0.30, 0.20)$	$b^{D,C_0} = 0.01$	

Table 1.3: Financial data

Exp Vasicek	$h_0 = 200$	$\alpha = 4.97$	$\theta = 3.83$	$\sigma^h = 1.41$
CIR	$h_0 = 200$	$\alpha = 1.29$	$\theta = 51.79$	$\sigma^h = 4.50$

Table 1.4: Counterparty's credit spread data. Values are in basis points (bps)

Our aim is to analyse how the choice of the mark-to-market, the initial values of the underlying assets and of the counterparty's credit spread, as well as its dynamics, affect the total valuation adjustment and, therefore, the price of the financial derivative.

In all examples we consider constant FX rates, so that we have dropped subindex t to use the notation X^{D,C_j} instead of X_t^{D,C_j} throughout this section.

The elapsed computational time depends on the number of the underlying assets and on the value assigned to the mark-to-market value M^D, as well as on the choice of the parameters associated to the numerical methods (such as, N_P, Z and those involved in the discretization of PDEs).

Unless otherwise stated, we have used data listed in Table 1.3 and Table 1.4. We have denoted by $r = (r^1, r^2)$ the vector of the short-term rates in the foreign markets, $q = (q^1, q^2)$ the vector of the dividends paid by the corresponding underlying assets and $\sigma^S = (\sigma^{S^1}, \sigma^{S^2})$ the vector of the assets volatilities.

It is important to point out that the parameters for the dynamics of the credit spread are borrowed from [19], where the credit spread is calibrated on market data. So, they are calibrated parameters.

Moreover, the maturities of the options are set to $T = 1$ year. Finally, we have chosen the collateral account C^D to be a percentage $C^{\%} = 0.25$ of the risk-free derivative value.

Concerning the parameters of the numerical methods, for the Monte Carlo method

we have used $N_P = 10^4$ paths and $Z = 252$ time nodes. For the Lagrange-Galerkin method, different meshes have been used and the number of nodes are indicated in the different tables containing the results. Moreover, for the fixed point iteration methods that have been additionally applied in the nonlinear PDEs, the tolerance of the stopping test in the error between two consecutive iterations has been set to 10^{-16}.

In the following, we present and analyse numerical results related to a *spread option*, an *exchange option* and a *sum of call options*. Other examples can be found in [7]. For each product, we first assume the counterparty credit spread is a time dependent deterministic function and the derivative is written on two stochastic underlying assets. In this case, we compare the Lagrange-Galerkin results with the Monte Carlo 99% confidence intervals. In the nonlinear case, we also show that the Multilevel Picard Iteration values are in agreement with the ones obtained with the Lagrange-Galerkin method. In a more general case, when the credit spread is stochastic and, eventually, the derivative depends on more than two stochastic underlying assets, we do not address the solution of the PDE formulation.

In all tables we use LG for the results obtained with the proposed Lagrange-Galerkin method for PDEs and MPI for the computed results with the Multilevel Picard Iteration method.

All tests corresponding to Monte Carlo and MPI methods have been performed by using Matlab on an Intel(R) Core(TM) i7-8550U, 1.99 GHz, 16 GB (RAM), x64-based processor. The tests corresponding to Lagrange-Galerkin method have been developed by using C++ on an AMD Ryzen7(R) 5700X, 64GB (RAM) processor.

1.5.1 Spread option

We first assume the hedger buys from a counterparty a *spread option*, written on two underlying assets, each of them being denominated in a different currency. The payoff function is given by

$$G(t, S^1, S^2) = \left(X^{D,C_2} S^2 - X^{D,C_1} S^1 - K \right)^+, \tag{1.61}$$

where K is the strike value in the domestic currency D.

In our numerical tests, we have set the value of the strike to $K = 15$ and we have selected nodes that are in the proximity of the at the money line, i.e., $X^{D,C_2}S^2 - X^{D,C_1}S^1 - K = 0$.

Test 1: Risk-free value.

We first compute the risk-free price of the spread option for different initial values of the underlying assets both with the Monte Carlo and the Lagrange-Galerkin methods. Note that the risk-free value obviously depends only on two stochastic factors, that are the two underlying assets, being independent of the credit spread.

Table 1.5 shows the computed risk-free prices. The table header indicates the used method and the number of nodes (in both directions) and time steps in the Lagrange-Galerkin method. We use the notation $S^{i,D} = X^{D,C_i}S^i$, for $i = 1, 2$, so that we can display all the prices in the same currency D. For each considered initial point $(S^{1,D}, S^{2,D})$, the risk-free value computed with Lagrange-Galerkin falls inside the Monte Carlo 99% confidence intervals, also in the case of the coarser mesh.

Test 2: Nonlinear problem, deterministic time dependent credit spread.

We now consider the deterministic exponential Vasicek (1.31) and CIR (1.33) dynamics for the credit spread and compute the total value adjustment in the nonlinear case, when the PDE formulation is given by (1.24) and the formulation in terms of expectation is reported in (1.27). Note that in the case of deterministic counterparty's credit spread, only two stochastic factors are considered when pricing a spread option.

Table 1.6 and Table 1.7 show the computed total value adjustment. The tables headers indicate the used quadrature formulae in Monte Carlo simulations, the value of parameter ρ in the multilevel Picard iteration method, and the number of nodes and time steps in the Lagrange-Galerkin method. From both tables we can deduce that the multilevel Picard iteration and the Lagrange-Galerkin results are in agreement and they are closer to each other when setting $\rho = 5$ in the MPI method and taking

a finer mesh in the LG one. However, MPI and LG values do not belong to the confidence intervals computed with Monte Carlo method, the results with trapezoidal formula being the closest ones to the MPI and LG results, especially in the case of CIR dynamics that are shown in Table 1.7.

The convergence of the multilevel Picard iteration method has been tested by computing the Relative Approximation Increments (RAI) defined in Subsection 1.4.3. We recall that in (1.60) we have set $\rho_{max} = 5$, $N_{runs} = 10$, and we have computed $RAI(\rho, \rho_{max}, N_{runs})$ for $\rho = 1, \ldots, 4$. Figure 1.3 shows the empirical convergence of the method.

Test 3: Linear problem, deterministic time dependent credit spread.

Still considering the deterministic exponential Vasicek and CIR dynamics for the credit spread, we compute the XVA in the linear case, when the PDE formulation is given by (2.32) and the formulation in terms of expectation is reported in (2.36).

Table 1.8 and Table 1.9 show the Monte Carlo confidence intervals computed with

Risk-free value			
	Monte Carlo	LG	
$(S^{1,D}, S^{2,D})$		$21\times21, 100$	$41\times41, 200$
$(9, 21)$	$[0.7784, 0.8782]$	0.7899	0.8122
$(9, 24)$	$[2.0457, 2.2119]$	2.0893	2.1063
$(9, 27)$	$[3.9481, 4.1775]$	4.0258	4.0434
$(12, 24)$	$[1.0582, 1.1827]$	1.0933	1.1058
$(12, 27)$	$[2.3745, 2.5654]$	2.4400	2.4494
$(12, 30)$	$[4.2351, 4.4894]$	4.3342	4.3451
$(15, 27)$	$[1.3606, 1.5105]$	1.4168	1.4214
$(15, 30)$	$[2.7155, 2.9316]$	2.8016	2.8041
$(15, 33)$	$[4.5435, 4.8233]$	4.6633	4.6678
$(18, 30)$	$[1.6789, 1.8546]$	1.7536	1.7521
$(18, 33)$	$[3.0645, 3.3064]$	3.1684	3.1655
$(18, 36)$	$[4.8677, 5.1733]$	5.0042	5.0030
$(21, 33)$	$[2.0091, 2.2111]$	2.0997	2.0933
$(21, 36)$	$[3.4188, 3.6868]$	3.5380	3.5302
$(21, 39)$	$[5.2017, 5.5334]$	5.3507	5.3440

Table 1.5: Spread option. Comparison of Monte Carlo method and Lagrange-Galerkin (LG). Risk-free value (Test 1)

the composite rectangular and trapezoidal quadrature formulae and the Lagrange-Galerkin method values. The Monte Carlo confidence intervals coincide in the three or four decimal figures when using both composite formulae. We have also used simple quadrature formulae to deduce the confidence intervals, although we do not report these results, because they do not agree with the confidence intervals computed with the composite quadrature formulae and the XVA values computed with the Lagrange-Galerkin method. Instead, from tables 1.8 and 1.9 we can see that the LG results belong to the reported Monte Carlo confidence intervals.

We also show in Table 1.10 the risky price of the spread option with an exponential Vasicek credit spread. Again, we can see that the results computed with the Lagrange-Galerkin method belong to the Monte Carlo 99% confidence intervals obtained with composite quadrature formulae.

Total value adjustment

	Monte Carlo		MPI		LG	
$(S^{1,D}, S^{2,D})$	SimpR	SimpT	$\rho = 4$	$\rho = 5$	$21\times21, 100$	$41\times41, 200$
$(9, 21)$	$[-0.0109, -0.0097]$	$[-0.0059, -0.0052]$	-0.0019	-0.0020	-0.0021	-0.0021
$(9, 24)$	$[-0.0274, -0.0253]$	$[-0.0148, -0.0137]$	-0.0049	-0.0053	-0.0054	-0.0053
$(9, 27)$	$[-0.0515, -0.0487]$	$[-0.0280, -0.0264]$	-0.0100	-0.0102	-0.0103	-0.0102
$(12, 24)$	$[-0.0147, -0.0131]$	$[-0.0080, -0.0071]$	-0.0026	-0.0028	-0.0028	-0.0028
$(12, 27)$	$[-0.0318, -0.0294]$	$[-0.0172, -0.0159]$	-0.0059	-0.0062	-0.0063	-0.0062
$(12, 30)$	$[-0.0554, -0.0522]$	$[-0.0301, -0.0284]$	-0.0106	-0.0109	-0.0111	-0.0110
$(15, 27)$	$[-0.0188, -0.0169]$	$[-0.0102, -0.0091]$	-0.0035	-0.0036	-0.0037	-0.0036
$(15, 30)$	$[-0.0363, -0.0336]$	$[-0.0197, -0.0182]$	-0.0069	-0.0070	-0.0072	-0.0071
$(15, 33)$	$[-0.0595, -0.0560]$	$[-0.0323, -0.0304]$	-0.0113	-0.0117	-0.0120	-0.0118
$(18, 30)$	$[-0.0230, -0.0208]$	$[-0.0125, -0.0113]$	-0.0045	-0.0043	-0.0045	-0.0045
$(18, 33)$	$[-0.0409, -0.0379]$	$[-0.0222, -0.0206]$	-0.0076	-0.0079	-0.0081	-0.0080
$(18, 36)$	$[-0.0639, -0.0601]$	$[-0.0347, -0.0326]$	-0.0124	-0.0126	-0.0128	-0.0127
$(21, 33)$	$[-0.0274, -0.0249]$	$[-0.0149, -0.0135]$	-0.0052	-0.0052	-0.0054	-0.0053
$(21, 36)$	$[-0.0456, -0.0423]$	$[-0.0247, -0.0229]$	-0.0087	-0.0088	-0.0091	-0.0090
$(21, 39)$	$[-0.0683, -0.0642]$	$[-0.0371, -0.0349]$	-0.0132	-0.0135	-0.0137	-0.0135

Table 1.6: Spread option, nonlinear problem and deterministic exponential Vasicek credit spread. Comparison of Monte Carlo (with simple rectangular (SimpR) and trapezoidal (SimpT) quadrature formulae), multilevel Picard iteration (MPI) and Lagrange-Galerkin (LG) methods. Total value adjustment (Test 2)

Total value adjustment

$(S^{1,D}, S^{2,D})$	Monte Carlo SimpR	Monte Carlo SimpT	MPI $\rho = 4$	MPI $\rho = 5$	LG $21\times21, 100$	LG $41\times41, 200$
$(9, 21)$	$[-0.0109, -0.0097]$	$[-0.0074, -0.0066]$	-0.0057	-0.0062	-0.0061	-0.0062
$(9, 24)$	$[-0.0274, -0.0253]$	$[-0.0186, -0.0172]$	-0.0152	-0.0161	-0.0160	-0.0160
$(9, 27)$	$[-0.0515, -0.0487]$	$[-0.0351, -0.0332]$	-0.0309	-0.0310	-0.0308	-0.0308
$(12, 24)$	$[-0.0147, -0.0131]$	$[-0.0100, -0.0089]$	-0.0081	-0.0084	-0.0084	-0.0084
$(12, 27)$	$[-0.0318, -0.0294]$	$[-0.0216, -0.0200]$	-0.0180	-0.0188	-0.0187	-0.0187
$(12, 30)$	$[-0.0554, -0.0522]$	$[-0.0378, -0.0356]$	-0.0325	-0.0332	-0.0331	-0.0331
$(15, 27)$	$[-0.0188, -0.0169]$	$[-0.0127, -0.0115]$	-0.0107	-0.0108	-0.0109	-0.0108
$(15, 30)$	$[-0.0363, -0.0336]$	$[-0.0247, -0.0229]$	-0.0214	-0.0214	-0.0214	-0.0214
$(15, 33)$	$[-0.0595, -0.0560]$	$[-0.0406, -0.0382]$	-0.0346	-0.0356	-0.0356	-0.0355
$(18, 30)$	$[-0.0230, -0.0208]$	$[-0.0156, -0.0142]$	-0.0138	-0.0134	-0.0135	-0.0134
$(18, 33)$	$[-0.0409, -0.0379]$	$[-0.0279, -0.0258]$	-0.0233	-0.0239	-0.0242	-0.0241
$(18, 36)$	$[-0.0639, -0.0601]$	$[-0.0435, -0.0409]$	-0.0383	-0.0381	-0.0382	-0.0381
$(21, 33)$	$[-0.0274, -0.0249]$	$[-0.0187, -0.0169]$	-0.0161	-0.0158	-0.0161	-0.0160
$(21, 36)$	$[-0.0456, -0.0423]$	$[-0.0311, -0.0288]$	-0.0268	-0.0269	-0.0271	-0.0269
$(21, 39)$	$[-0.0683, -0.0642]$	$[-0.0466, -0.0438]$	-0.0405	-0.0409	-0.0409	-0.0407

Table 1.7: Spread option, nonlinear problem and deterministic CIR credit spread. Comparison of Monte Carlo (with simple rectangular (SimpR) and trapezoidal (SimpT) quadrature formulae), multilevel Picard iteration (MPI) and Lagrange Galerkin (LG) methods. Total value adjustment (Test 2)

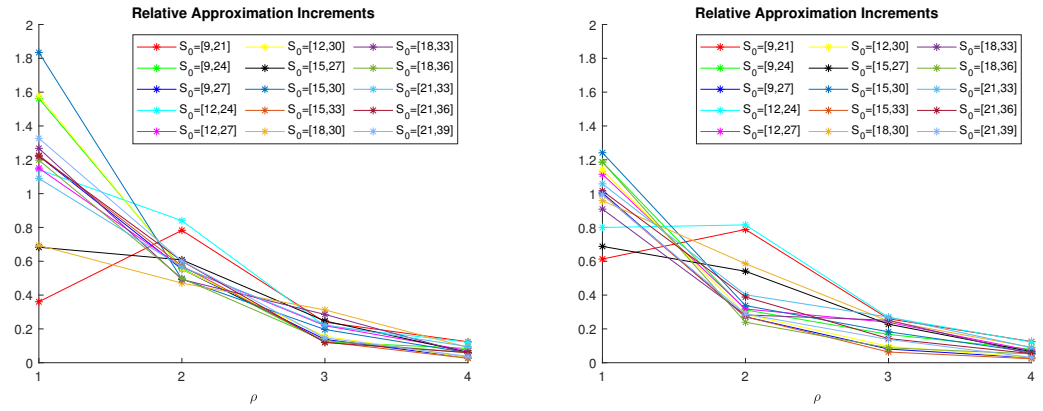

Figure 1.3: Spread option with deterministic credit spread. Convergence of MPI with exponential Vasicek dynamics for credit spread on the left and CIR dynamics on the right (Test 2)

Total value adjustment

$(S^{1,D}, S^{2,D})$	Monte Carlo CompR	Monte Carlo CompT	LG $21\times21,100$	LG $41\times41,200$
$(9, 21)$	$[-0.0022, -0.0020]$	$[-0.0022, -0.0019]$	-0.0021	-0.0021
$(9, 24)$	$[-0.0055, -0.0051]$	$[-0.0055, -0.0051]$	-0.0054	-0.0053
$(9, 27)$	$[-0.0105, -0.0099]$	$[-0.0104, -0.0098]$	-0.0103	-0.0102
$(12, 24)$	$[-0.0030, -0.0027]$	$[-0.0029, -0.0026]$	-0.0028	-0.0028
$(12, 27)$	$[-0.0064, -0.0060]$	$[-0.0064, -0.0059]$	-0.0063	-0.0062
$(12, 30)$	$[-0.0113, -0.0106]$	$[-0.0112, -0.0105]$	-0.0111	-0.0110
$(15, 27)$	$[-0.0038, -0.0034]$	$[-0.0038, -0.0034]$	-0.0037	-0.0036
$(15, 30)$	$[-0.0074, -0.0068]$	$[-0.0073, -0.0067]$	-0.0072	-0.0071
$(15, 33)$	$[-0.0121, -0.0114]$	$[-0.0120, -0.0113]$	-0.0120	-0.0118
$(18, 30)$	$[-0.0047, -0.0042]$	$[-0.0046, -0.0042]$	-0.0045	-0.0044
$(18, 33)$	$[-0.0083, -0.0077]$	$[-0.0082, -0.0076]$	-0.0081	-0.0080
$(18, 36)$	$[-0.0130, -0.0122]$	$[-0.0129, -0.0121]$	-0.0128	-0.0127
$(21, 33)$	$[-0.0055, -0.0050]$	$[-0.0055, -0.0050]$	-0.0054	-0.0053
$(21, 36)$	$[-0.0092, -0.0086]$	$[-0.0092, -0.0085]$	-0.0091	-0.0089
$(21, 39)$	$[-0.0139, -0.0130]$	$[-0.0137, -0.0129]$	-0.0137	-0.0135

Table 1.8: Spread option, linear problem and deterministic exponential Vasicek credit spread. Comparison of Monte Carlo (with composite rectangular (CompR) and trapezoidal (CompT) quadrature formulae) and Lagrange-Galerkin (LG) methods. Total value adjustment (Test 3)

Total value adjustment

$(S^{1,D}, S^{2,D})$	Monte Carlo CompR	Monte Carlo CompT	LG $21\times21,100$	LG $41\times41,200$
$(9, 21)$	$[-0.0066, -0.0059]$	$[-0.0066, -0.0059]$	-0.0061	-0.0062
$(9, 24)$	$[-0.0167, -0.0155]$	$[-0.0167, -0.0154]$	-0.0160	-0.0160
$(9, 27)$	$[-0.0316, -0.0299]$	$[-0.0315, -0.0298]$	-0.0307	-0.0307
$(12, 24)$	$[-0.0089, -0.0080]$	$[-0.0089, -0.0080]$	-0.0084	-0.0084
$(12, 27)$	$[-0.0194, -0.0180]$	$[-0.0194, -0.0179]$	-0.0186	-0.0186
$(12, 30)$	$[-0.0340, -0.0320]$	$[-0.0339, -0.0320]$	-0.0330	-0.0330
$(15, 27)$	$[-0.0114, -0.0103]$	$[-0.0114, -0.0103]$	-0.0109	-0.0108
$(15, 30)$	$[-0.0222, -0.0205]$	$[-0.0221, -0.0205]$	-0.0214	-0.0213
$(15, 33)$	$[-0.0365, -0.0344]$	$[-0.0364, -0.0343]$	-0.0355	-0.0354
$(18, 30)$	$[-0.0140, -0.0127]$	$[-0.0140, -0.0127]$	-0.0134	-0.0133
$(18, 33)$	$[-0.0250, -0.0232]$	$[-0.0250, -0.0231]$	-0.0242	-0.0240
$(18, 36)$	$[-0.0391, -0.0368]$	$[-0.0391, -0.0368]$	-0.0381	-0.0380
$(21, 33)$	$[-0.0167, -0.0152]$	$[-0.0167, -0.0152]$	-0.0161	-0.0159
$(21, 36)$	$[-0.0279, -0.0259]$	$[-0.0278, -0.0258]$	-0.0270	-0.0268
$(21, 39)$	$[-0.0419, -0.0394]$	$[-0.0418, -0.0393]$	-0.0408	-0.0406

Table 1.9: Spread option, linear problem and deterministic CIR credit spread. Comparison of Monte Carlo (with composite rectangular (CompR) and trapezoidal (CompT) quadrature formulae) and Lagrange-Galerkin (LG) methods. Total value adjustment (Test 3)

Risky value				
	Monte Carlo		LG	
$(S^{1,D}, S^{2,D})$	CompR	CompT	$21\times21, 100$	$41\times41, 200$
$(9, 21)$	$[0.7784, 0.8782]$	$[0.7784, 0.8782]$	0.7879	0.8101
$(9, 24)$	$[2.0457, 2.2119]$	$[2.0457, 2.2119]$	2.0839	2.1009
$(9, 27)$	$[3.9481, 4.1775]$	$[3.9481, 4.1775]$	4.0155	4.0332
$(12, 24)$	$[1.0582, 1.1827]$	$[1.0582, 1.1827]$	1.0905	1.1029
$(12, 27)$	$[2.3745, 2.5654]$	$[2.3745, 2.5654]$	2.4337	2.4432
$(12, 30)$	$[4.2351, 4.4894]$	$[4.2351, 4.4894]$	4.3231	4.3341
$(15, 27)$	$[1.3606, 1.5105]$	$[1.3606, 1.5105]$	1.4132	1.4178
$(15, 30)$	$[2.7155, 2.9316]$	$[2.7155, 2.9316]$	2.7944	2.7970
$(15, 33)$	$[4.5435, 4.8233]$	$[4.5435, 4.8233]$	4.6514	4.6560
$(18, 30)$	$[1.6789, 1.8546]$	$[1.6789, 1.8546]$	1.7491	1.7476
$(18, 33)$	$[3.0645, 3.3064]$	$[3.0645, 3.3064]$	3.1603	3.1575
$(18, 36)$	$[4.8677, 5.1733]$	$[4.8677, 5.1733]$	4.9914	4.9904
$(21, 33)$	$[2.0091, 2.2111]$	$[2.0091, 2.2111]$	2.0943	2.0880
$(21, 36)$	$[3.4188, 3.6868]$	$[3.4188, 3.6868]$	3.5289	3.5213
$(21, 39)$	$[5.2017, 5.5334]$	$[5.2017, 5.5334]$	5.3369	5.3304

Table 1.10: Spread option, linear problem and deterministic exponential Vasicek credit spread. Comparison of Monte Carlo (with composite rectangular (CompR) and trapezoidal (CompT) quadrature formulae) and Lagrange-Galerkin (LG) methods. Risky value (Test 3)

Test 4: Nonlinear problem, stochastic credit spread.

We now consider the more general case when the credit spread is a stochastic process following either an exponential Vasicek (1.5) or a CIR (1.6) dynamics and the mark-to-market value is equal to the risky derivative value (nonlinear case). Note that in the case of stochastic credit spread of the counterparty, three stochastic factors are involved in the pricing of the spread option.

Table 1.11 and Table 1.12 illustrate the computed XVA for some fixed initial values of the underlying assets. For each fixed value of $S^{1,D}$ we analyse three different possibilities: out of the money option, at the money option and in the money option, respectively. When considering a stochastic credit spread, we do not address the solution of the XVA pricing PDE with Lagrange-Galerkin method and we take MPI values as reference values. Indeed, we have seen in the case of the deterministic time dependent credit spread that MPI and LG results are very close, but not inside the Monte Carlo confidence intervals. The multilevel Picard iteration method is tested either with $\rho = 4$ or with $\rho = 5$. Moreover, we have tested the convergence of the MPI

Total value adjustment

$(S^{1,D}, S^{2,D})$	Monte Carlo SimpR	Monte Carlo SimpT	MPI $\rho = 4$	MPI $\rho = 5$
$(9, 21)$	$[-0.0109, -0.0097]$	$[-0.0058, -0.0051]$	-0.0018	-0.0019
$(9, 24)$	$[-0.0274, -0.0253]$	$[-0.0147, -0.0136]$	-0.0050	-0.0051
$(9, 27)$	$[-0.0515, -0.0487]$	$[-0.0279, -0.0263]$	-0.0105	-0.0104
$(12, 24)$	$[-0.0147, -0.0131]$	$[-0.0078, -0.0070]$	-0.0025	-0.0025
$(12, 27)$	$[-0.0318, -0.0294]$	$[-0.0170, -0.0157]$	-0.0056	-0.0060
$(12, 30)$	$[-0.0554, -0.0522]$	$[-0.0299, -0.0282]$	-0.0110	-0.0109
$(15, 27)$	$[-0.0188, -0.0169]$	$[-0.0099, -0.0089]$	-0.0035	-0.0033
$(15, 30)$	$[-0.0363, -0.0336]$	$[-0.0194, -0.0180]$	-0.0066	-0.0067
$(15, 33)$	$[-0.0595, -0.0560]$	$[-0.0321, -0.0302]$	-0.0116	-0.0116
$(18, 30)$	$[-0.0230, -0.0208]$	$[-0.0122, -0.0110]$	-0.0039	-0.0040
$(18, 33)$	$[-0.0409, -0.0379]$	$[-0.0218, -0.0202]$	-0.0074	-0.0076
$(18, 36)$	$[-0.0639, -0.0601]$	$[-0.0343, -0.0323]$	-0.0121	-0.0124
$(21, 33)$	$[-0.0274, -0.0249]$	$[-0.0145, -0.0132]$	-0.0046	-0.0048
$(21, 36)$	$[-0.0456, -0.0423]$	$[-0.0243, -0.0226]$	-0.0082	-0.0084
$(21, 39)$	$[-0.0683, -0.0642]$	$[-0.0367, -0.0345]$	-0.0131	-0.0132

Table 1.11: Spread option, nonlinear problem and stochastic exponential Vasicek credit spread. Comparison of Monte Carlo (with simple rectangular (SimpR) and trapezoidal (SimpT) quadrature formulae) and multilevel Picard iteration (MPI). Total value adjustment (Test 4)

method for all the initial underlying assets values considered in the tables by plotting the relative approximation increments in Figure 1.4. As for the deterministic credit spread case, the Monte Carlo confidence intervals, obtained with a simple Picard iteration, do not contain the multilevel Picard iteration results. As expected, the total value adjustment is negative because, when buying the derivative, the hedger will ask the counterparty for a reduction in the price due to the possibility of the counterparty's default. Also, we can see that the total value adjustment becomes more negative when the option is in the money and less negative when it is out of the money, indeed in the former case the hedger would be worst affected by the counterparty's default, because the option is more valuable.

Figure 1.5 shows the total value adjustment for different underlying assets initial values computed with the multilevel Picard iteration method. In particular, each point of the plot shows the average MPI value on $N_{runs} = 10$ runs with the parameter ρ fixed to 4. The choice of the ρ value is due to the fact that from Table 1.11 and Table 1.12 we infer that results with $\rho = 4$ and $\rho = 5$ are very close to each others and it is not worth to produce plots by using $\rho = 5$, that is more time consuming. In

Total value adjustment

$(S^{1,D}, S^{2,D})$	Monte Carlo SimpR	Monte Carlo SimpT	MPI $\rho = 4$	MPI $\rho = 5$
$(9, 21)$	$[-0.0109, -0.0097]$	$[-0.0069, -0.0061]$	-0.0055	-0.0055
$(9, 24)$	$[-0.0274, -0.0253]$	$[-0.0175, -0.0162]$	-0.0142	-0.0146
$(9, 27)$	$[-0.0515, -0.0487]$	$[-0.0335, -0.0317]$	-0.0291	-0.0290
$(12, 24)$	$[-0.0147, -0.0131]$	$[-0.0092, -0.0083]$	-0.0076	-0.0075
$(12, 27)$	$[-0.0318, -0.0294]$	$[-0.0203, -0.0188]$	-0.0164	-0.0171
$(12, 30)$	$[-0.0554, -0.0522]$	$[-0.0359, -0.0339]$	-0.0311	-0.0378
$(15, 27)$	$[-0.0188, -0.0169]$	$[-0.0118, -0.0106]$	-0.0102	-0.0197
$(15, 30)$	$[-0.0363, -0.0336]$	$[-0.0231, -0.0214]$	-0.0192	-0.0193
$(15, 33)$	$[-0.0595, -0.0560]$	$[-0.0384, -0.0362]$	-0.0330	-0.0328
$(18, 30)$	$[-0.0230, -0.0208]$	$[-0.0145, -0.0131]$	-0.0115	-0.0117
$(18, 33)$	$[-0.0409, -0.0379]$	$[-0.0260, -0.0242]$	-0.0215	-0.0219
$(18, 36)$	$[-0.0639, -0.0601]$	$[-0.0411, -0.0387]$	-0.0347	-0.0352
$(21, 33)$	$[-0.0274, -0.0249]$	$[-0.0172, -0.0157]$	-0.0137	-0.0141
$(21, 36)$	$[-0.0456, -0.0423]$	$[-0.0290, -0.0269]$	-0.0239	-0.0243
$(21, 39)$	$[-0.0683, -0.0642]$	$[-0.0439, -0.0413]$	-0.0374	-0.0377

Table 1.12: Spread option, nonlinear problem and stochastic CIR credit spread. Comparison of Monte Carlo (with simple rectangular (SimpR) and trapezoidal (SimpT) quadrature formulae) and multilevel Picard iteration (MPI). Total value adjustment (Test 4)

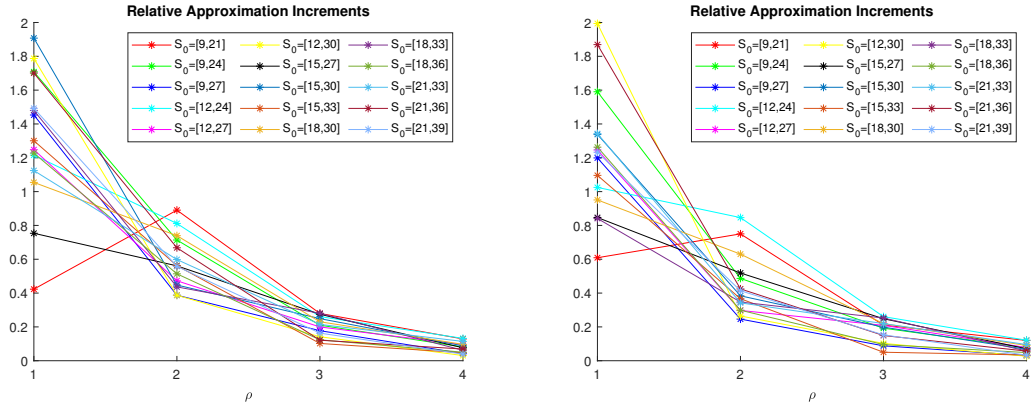

Figure 1.4: Spread option with stochastic credit spread. Convergence of MPI with exponential Vasicek dynamics for credit spread on the left and CIR dynamics on the right (Test 4)

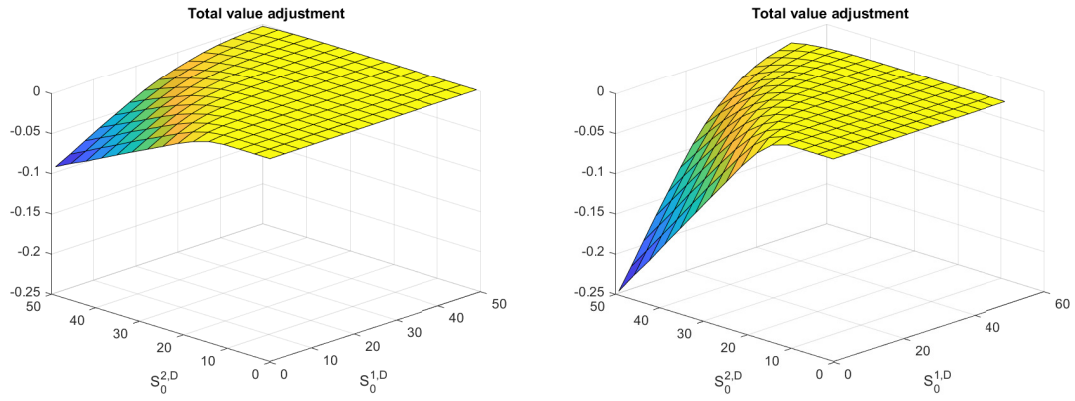

Figure 1.5: Spread option in the nonlinear case. Total value adjustment with exponential Vasicek credit spread on the left and with CIR credit spread on the right (Test 4)

fact, one run of MPI with $\rho = 4$ takes slightly more than 1 second, but with $\rho = 5$ it takes about 340 seconds. From the figure it is evident that the XVA is more negative under the assumption of CIR credit spread than under the assumption of exponential Vasicek credit spread.

Test 5: Linear problem, stochastic credit spread.

We move to the linear problem with stochastic credit spread.

Table 1.13 and Table 1.14 show the Monte Carlo confidence intervals for the total value adjustment with exponential Vasicek and CIR credit spread, respectively. The confidence intervals coincide in the three or four decimal figures when using both composite formulae, that we take as reference values, while the simple formulae give results that are a bit far from the composite formulae results.

Figure 1.6 shows the risky price and the total value adjustment. For each point of the plots we consider the average Monte Carlo value obtained by approximating the integral in the XVA formula with composite trapezoidal formula. As for the nonlinear case, the XVA is more negative when the credit spread is modelled as a CIR process. However, the difference between the plotted risky prices under the two

Total value adjustment

$(S^{1,D}, S^{2,D})$	Monte Carlo SimpR	SimpT	CompR	CompT
$(9, 21)$	$[-0.0007, -0.0006]$	$[-0.0058, -0.0052]$	$[-0.0021, -0.0018]$	$[-0.0021, -0.0018]$
$(9, 24)$	$[-0.0020, -0.0017]$	$[-0.0148, -0.0137]$	$[-0.0055, -0.0050]$	$[-0.0054, -0.0050]$
$(9, 27)$	$[-0.0042, -0.0037]$	$[-0.0281, -0.0266]$	$[-0.0108, -0.0101]$	$[-0.0107, -0.0100]$
$(12, 24)$	$[-0.0010, -0.0007]$	$[-0.0078, -0.0070]$	$[-0.0028, -0.0025]$	$[-0.0028, -0.0025]$
$(12, 27)$	$[-0.0023, -0.0019]$	$[-0.0171, -0.0158]$	$[-0.0063, -0.0058]$	$[-0.0062, -0.0057]$
$(12, 30)$	$[-0.0044, -0.0038]$	$[-0.0301, -0.0284]$	$[-0.0114, -0.0107]$	$[-0.0113, -0.0106]$
$(15, 27)$	$[-0.0012, -0.0010]$	$[-0.0100, -0.0090]$	$[-0.0036, -0.0032]$	$[-0.0035, -0.0031]$
$(15, 30)$	$[-0.0026, -0.0022]$	$[-0.0195, -0.0181]$	$[-0.0072, -0.0066]$	$[-0.0071, -0.0065]$
$(15, 33)$	$[-0.0046, -0.0040]$	$[-0.0323, -0.0305]$	$[-0.0122, -0.0114]$	$[-0.0120, -0.0113]$
$(18, 30)$	$[-0.0015, -0.0012]$	$[-0.0123, -0.0111]$	$[-0.0044, -0.0039]$	$[-0.0043, -0.0039]$
$(18, 33)$	$[-0.0029, -0.0024]$	$[-0.0220, -0.0204]$	$[-0.0080, -0.0074]$	$[-0.0080, -0.0073]$
$(18, 36)$	$[-0.0048, -0.0042]$	$[-0.0346, -0.0326]$	$[-0.0129, -0.0121]$	$[-0.0128, -0.0120]$
$(21, 33)$	$[-0.0018, -0.0014]$	$[-0.0146, -0.0133]$	$[-0.0052, -0.0047]$	$[-0.0051, -0.0046]$
$(21, 36)$	$[-0.0032, -0.0027]$	$[-0.0246, -0.0228]$	$[-0.0089, -0.0082]$	$[-0.0088, -0.0082]$
$(21, 39)$	$[-0.0051, -0.0044]$	$[-0.0370, -0.0348]$	$[-0.0138, -0.0129]$	$[-0.0136, -0.0128]$

Table 1.13: Spread option, linear problem and stochastic exponential Vasicek credit spread. Comparison of Monte Carlo with simple rectangular (SimpR), simple trapezoidal (SimT), composite rectangular (CompR) and trapezoidal (CompT) quadrature formulae. Total value adjustment (Test 5)

Total value adjustment

$(S^{1,D}, S^{2,D})$	Monte Carlo SimpR	SimpT	CompR	CompT
$(9, 21)$	$[-0.0029, -0.0025]$	$[-0.0069, -0.0061]$	$[-0.0060, -0.0053]$	$[-0.0060, -0.0053]$
$(9, 24)$	$[-0.0077, -0.0071]$	$[-0.0176, -0.0163]$	$[-0.0154, -0.0142]$	$[-0.0154, -0.0142]$
$(9, 27)$	$[-0.0153, -0.0144]$	$[-0.0337, -0.0318]$	$[-0.0296, -0.0280]$	$[-0.0296, -0.0279]$
$(12, 24)$	$[-0.0038, -0.0034]$	$[-0.0093, -0.0083]$	$[-0.0080, -0.0072]$	$[-0.0080, -0.0072]$
$(12, 27)$	$[-0.0088, -0.0081]$	$[-0.0204, -0.0189]$	$[-0.0178, -0.0165]$	$[-0.0177, -0.0164]$
$(12, 30)$	$[-0.0162, -0.0152]$	$[-0.0361, -0.0340]$	$[-0.0316, -0.0298]$	$[-0.0316, -0.0298]$
$(15, 27)$	$[-0.0049, -0.0043]$	$[-0.0118, -0.0107]$	$[-0.0103, -0.0092]$	$[-0.0102, -0.0092]$
$(15, 30)$	$[-0.0100, -0.0092]$	$[-0.0233, -0.0216]$	$[-0.0203, -0.0188]$	$[-0.0202, -0.0187]$
$(15, 33)$	$[-0.0172, -0.0161]$	$[-0.0386, -0.0364]$	$[-0.0338, -0.0319]$	$[-0.0338, -0.0318]$
$(18, 30)$	$[-0.0060, -0.0054]$	$[-0.0145, -0.0132]$	$[-0.0126, -0.0114]$	$[-0.0125, -0.0113]$
$(18, 33)$	$[-0.0112, -0.0103]$	$[-0.0262, -0.0243]$	$[-0.0228, -0.0211]$	$[-0.0227, -0.0211]$
$(18, 36)$	$[-0.0183, -0.0170]$	$[-0.0413, -0.0389]$	$[-0.0362, -0.0340]$	$[-0.0361, -0.0339]$
$(21, 33)$	$[-0.0071, -0.0064]$	$[-0.0173, -0.0158]$	$[-0.0150, -0.0136]$	$[-0.0150, -0.0136]$
$(21, 36)$	$[-0.0124, -0.0114]$	$[-0.0292, -0.0271]$	$[-0.0254, -0.0235]$	$[-0.0253, -0.0235]$
$(21, 39)$	$[-0.0194, -0.0181]$	$[-0.0442, -0.0415]$	$[-0.0386, -0.0363]$	$[-0.0385, -0.0362]$

Table 1.14: Spread option, linear problem and stochastic CIR credit spread. Comparison of Monte Carlo with simple rectangular (SimpR), simple trapezoidal (SimT), composite rectangular (CompR) and trapezoidal (CompT) quadrature formulae. Total value adjustment (Test 5)

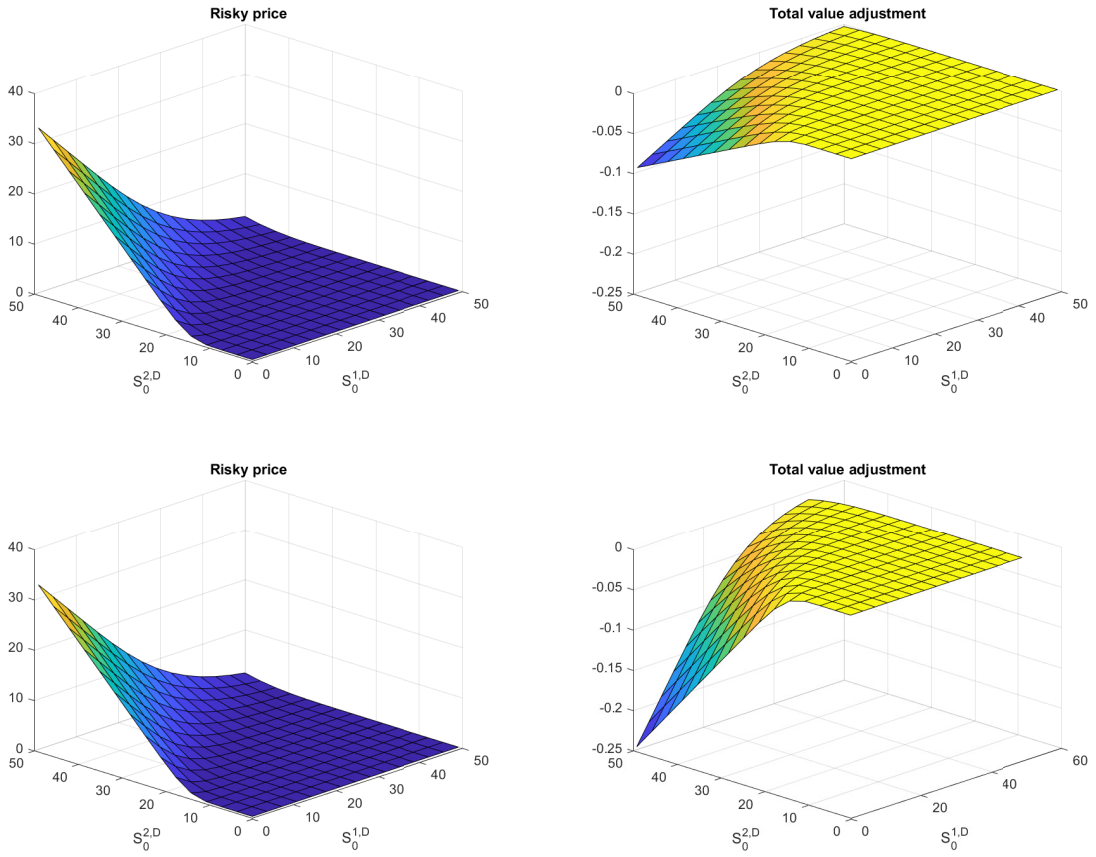

Figure 1.6: Spread option in the linear case. Exponential Vasicek credit spread on the top and CIR credit spread on the bottom. Risky value on the left and XVA on the right (Test 5)

alternative assumptions for the dynamics of the credit spread is not evident, because the difference between the total value adjustments is negligible with respect to the derivative prices.

From Table 1.13 and Table 1.14 and from Figure 1.6 we can take out the same conclusions to those drawn in the nonlinear case: the XVA becomes more negative when the price of the asset S^2 increases, namely when the option is in the money and the XVA approaches to zero when the S^2 price decreases, namely when the option is out of the money.

1.5.2 Exchange option

In this subsection, we assume that the default-free hedger buys from the defaultable counterparty an *exchange option*, written on an underlying asset S^1, denominated in the domestic currency, and an underlying asset S^2, denominated in a foreign currency C_2. Hence, the payoff function of the option is given by

$$G(t, S^1, S^2) = (S^1 - X^{D,C_2} S^2)^+. \tag{1.62}$$

Test 6: Nonlinear problem, deterministic time dependent credit spread.

First, we compare the XVA computed with different numerical methods in the case of the nonlinear problem with a deterministic credit spread. Note that in the setting of deterministic credit spread of the counterparty, only two stochastic factors are involved in the pricing of exchange options.

The points where we show the different values are close to the at the money line, $S^1 - X^{D,C_2} S^2 = 0$.

Table 1.15 and Table 1.16 show the results for the XVA. The multilevel Picard iteration and the Lagrange-Galerkin methods values are quite far from the Monte Carlo confidence intervals obtained with a fixed-point method and simple quadrature formulae for the approximation of the integral in the XVA expression in (2.34). The MPI and the LG results are closer to each other if we take $\rho = 5$ in the MPI method and a mesh of 41×41 nodes with 200 time steps in the LG method, except for the last two points when we assume an exponential Vasicek dynamics for the credit spread and in the last three points under the assumption of a CIR credit spread. This is due to the fact that the Lagrange-Galerkin results are not reliable near the fixed right and upper boundaries of the computational domain, in our case located at $S^1_\infty = 60$ and $S^2_\infty = 60$, respectively.

We show the empirical convergence of the multilevel Picard iteration method by plotting the relative approximations increments in Figure 1.7.

Total value adjustment

$(S^{1,D}, S^{2,D})$	Monte Carlo SimpR	Monte Carlo SimpT	MPI $\rho = 4$	MPI $\rho = 5$	LG $21\times21, 100$	LG $41\times41, 200$
$(12, 9)$	$[-0.0410, -0.0389]$	$[-0.0222, -0.0211]$	-0.0078	-0.0081	-0.0084	-0.0083
$(12, 12)$	$[-0.0200, -0.0184]$	$[-0.0108, -0.0099]$	-0.0037	-0.0039	-0.0041	-0.0040
$(12, 15)$	$[-0.0087, -0.0076]$	$[-0.0047, -0.0041]$	-0.0015	-0.0016	-0.0017	-0.0017
$(21, 18)$	$[-0.0537, -0.0503]$	$[-0.0290, -0.0272]$	-0.0103	-0.0105	-0.0109	-0.0107
$(21, 21)$	$[-0.0350, -0.0322]$	$[-0.0189, -0.0174]$	-0.0065	-0.0068	-0.0071	-0.0069
$(21, 24)$	$[-0.0220, -0.0197]$	$[-0.0118, -0.0106]$	-0.0040	-0.0042	-0.0044	-0.0043
$(30, 27)$	$[-0.0677, -0.0632]$	$[-0.0366, -0.0342]$	-0.0134	-0.0133	-0.0137	-0.0134
$(30, 30)$	$[-0.0500, -0.0460]$	$[-0.0270, -0.0248]$	-0.0093	-0.0096	-0.0100	-0.0098
$(30, 33)$	$[-0.0362, -0.0327]$	$[-0.0195, -0.0176]$	-0.0067	-0.0069	-0.0072	-0.0070
$(42, 39)$	$[-0.0871, -0.0810]$	$[-0.0471, -0.0437]$	-0.0170	-0.0169	-0.0172	-0.0169
$(42, 42)$	$[-0.0700, -0.0644]$	$[-0.0377, -0.0347]$	-0.0131	-0.0134	-0.0135	-0.0132
$(42, 45)$	$[-0.0557, -0.0506]$	$[-0.0300, -0.0273]$	-0.0103	-0.0107	-0.0103	-0.0101

Table 1.15: Exchange option, nonlinear problem and deterministic exponential Vasicek credit spread. Comparison of Monte Carlo (with simple rectangular (SimpR) and trapezoidal (SimpT) quadrature formulae), multilevel Picard iteration (MPI) and Lagrange-Galerkin (LG) methods. Total value adjustment (Test 6)

Total value adjustment

$(S^{1,D}, S^{2,D})$	Monte Carlo SimpR	Monte Carlo SimpT	MPI $\rho = 4$	MPI $\rho = 5$	LG $21\times21, 100$	LG $41\times41, 200$
$(12, 9)$	$[-0.0410, -0.0389]$	$[-0.0279, -0.0265]$	-0.0241	-0.0247	-0.0250	-0.0248
$(12, 12)$	$[-0.0200, -0.0184]$	$[-0.0135, -0.0125]$	-0.0115	-0.0118	-0.0121	-0.0119
$(12, 15)$	$[-0.0087, -0.0076]$	$[-0.0058, -0.0051]$	-0.0045	-0.0048	-0.0051	-0.0051
$(21, 18)$	$[-0.0537, -0.0503]$	$[-0.0364, -0.0342]$	-0.0318	-0.0320	-0.0325	-0.0321
$(21, 21)$	$[-0.0350, -0.0322]$	$[-0.0237, -0.0218]$	-0.0199	-0.0207	-0.0210	-0.0207
$(21, 24)$	$[-0.0220, -0.0197]$	$[-0.0148, -0.0133]$	-0.0124	-0.0127	-0.0131	-0.0129
$(30, 27)$	$[-0.0677, -0.0632]$	$[-0.0460, -0.0429]$	-0.0411	-0.0405	-0.0407	-0.0403
$(30, 30)$	$[-0.0500, -0.0460]$	$[-0.0338, -0.0311]$	-0.0288	-0.0292	-0.0299	-0.0295
$(30, 33)$	$[-0.0362, -0.0327]$	$[-0.0245, -0.0221]$	-0.0206	-0.0209	-0.0215	-0.0212
$(42, 39)$	$[-0.0871, -0.0810]$	$[-0.0591, -0.0549]$	-0.0525	-0.0515	-0.0512	-0.0506
$(42, 42)$	$[-0.0700, -0.0644]$	$[-0.0474, -0.0436]$	-0.0404	-0.0407	-0.0401	-0.0397
$(42, 45)$	$[-0.0557, -0.0506]$	$[-0.0376, -0.0342]$	-0.0317	-0.0324	-0.0307	-0.0303

Table 1.16: Exchange option, nonlinear problem and deterministic CIR credit spread. Comparison of Monte Carlo (with simple rectangular (SimpR) and trapezoidal (SimpT) quadrature formulae), multilevel Picard iteration (MPI) and Lagrange-Galerkin (LG) methods. Total value adjustment (Test 6)

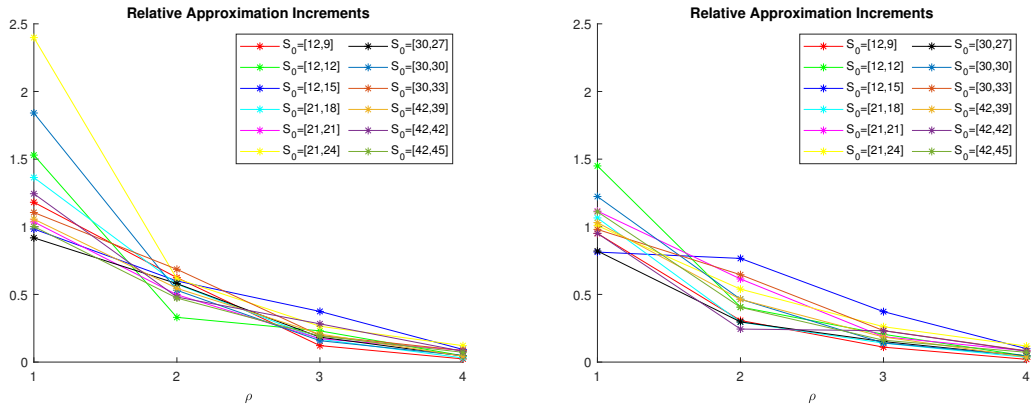

Figure 1.7: Exchange option with deterministic credit spread. Convergence of the MPI with exponential Vasicek dynamics for credit spread on the left and CIR dynamics on the right.

Test 7: Linear problem, deterministic time dependent credit spread.

The results in the linear case with deterministic credit spread are reported in Table 1.17 and in Table 1.18.

The Lagrange-Galerkin method values with the finer mesh of 41×41 nodes and 200 time steps are not inside the Monte Carlo confidence intervals obtained with simple formulae, that are not reported, but are inside the confidence intervals obtained with composite formulae, except for the last considered point. In particular, the LG value in the last point, i.e., when $S^{1,D} = 42$ and $S^{2,D} = 45$, is slightly outside the Monte Carlo confidence interval with composite rectangular quadrature formula in the case of the exponential Vasicek credit spread, and is not in both confidence intervals in the case of the CIR credit spread. As pointed out when discussing about the results in the nonlinear case, this is due to the fact that the last point is too close to the spatial boundaries chosen in the LG method. Also, we can observe that each LG value is very close to the lower bound of the corresponding Monte Carlo confidence interval and that by refining the spatial and time meshes in the LG method the values become less negative. Therefore, we can expect that by using a finer mesh in the Lagrange-Galerkin method we can obtain values that are closer to the centres of the Monte

Total value adjustment

$(S^{1,D}, S^{2,D})$	Monte Carlo CompR	Monte Carlo CompT	LG $21\times21, 100$	LG $41\times41, 200$
$(12, 9)$	$[-0.0084, -0.0079]$	$[-0.0083, -0.0079]$	-0.0084	-0.0083
$(12, 12)$	$[-0.0040, -0.0037]$	$[-0.0040, -0.0037]$	-0.0041	-0.0040
$(12, 15)$	$[-0.0017, -0.0015]$	$[-0.0017, -0.0015]$	-0.0017	-0.0017
$(21, 18)$	$[-0.0109, -0.0102]$	$[-0.0108, -0.0101]$	-0.0109	-0.0107
$(21, 21)$	$[-0.0071, -0.0065]$	$[-0.0070, -0.0065]$	-0.0071	-0.0069
$(21, 24)$	$[-0.0044, -0.0040]$	$[-0.0044, -0.0039]$	-0.0044	-0.0043
$(30, 27)$	$[-0.0137, -0.0128]$	$[-0.0136, -0.0127]$	-0.0137	-0.0134
$(30, 30)$	$[-0.0101, -0.0093]$	$[-0.0100, -0.0092]$	-0.0100	-0.0098
$(30, 33)$	$[-0.0073, -0.0066]$	$[-0.0072, -0.0066]$	-0.0072	-0.0070
$(42, 39)$	$[-0.0177, -0.0164]$	$[-0.0175, -0.0163]$	-0.0172	-0.0168
$(42, 42)$	$[-0.0142, -0.0130]$	$[-0.0140, -0.0129]$	-0.0135	-0.0132
$(42, 45)$	$[-0.0113, -0.0102]$	$[-0.0112, -0.0101]$	-0.0103	-0.0101

Table 1.17: Exchange option, linear problem and deterministic exponential Vasicek credit spread. Comparison of Monte Carlo (with composite rectangular (CompR) and trapezoidal (CompT) quadrature formulae) and Lagrange-Galerkin (LG) methods. Total value adjustment (Test 7)

Carlo confidence intervals.

Test 8: Nonlinear problem, stochastic credit spread.

We now consider the nonlinear case with stochastic credit spread and analyse how different initial values of the counterparty's credit spread affect the total value adjustment. In the case of stochastic spread of the counterparty, three stochastic factors are involved in the pricing of exchange options.

We fix the initial value of the first underlying asset to $S^{1,D} = 30$ and choose the values of $S^{2,D}$ equal to 27, 30, 33, so that to consider the in the money, at the money and out of the money cases, respectively. The results are shown in Table 1.19 for the exponential Vasicek credit spread and in Table 1.20 for the CIR credit spread. The Monte Carlo method with simple quadrature formulae does not approximate well enough the total value adjustment, overestimating, in absolute terms, the XVA with respect the multilevel Picard iterations results, that we take as reference values.

Total value adjustment

$(S^{1,D}, S^{2,D})$	Monte Carlo CompR	Monte Carlo CompT	LG $21\times21, 100$	LG $41\times41, 200$
$(12, 9)$	$[-0.0252, -0.0239]$	$[-0.0252, -0.0239]$	-0.0249	-0.0248
$(12, 12)$	$[-0.0122, -0.0112]$	$[-0.0122, -0.0112]$	-0.0121	-0.0119
$(12, 15)$	$[-0.0053, -0.0046]$	$[-0.0053, -0.0046]$	-0.0051	-0.0051
$(21, 18)$	$[-0.0329, -0.0309]$	$[-0.0328, -0.0308]$	-0.0324	-0.0321
$(21, 21)$	$[-0.0214, -0.0197]$	$[-0.0213, -0.0196]$	-0.0210	-0.0207
$(21, 24)$	$[-0.0134, -0.0120]$	$[-0.0133, -0.0120]$	-0.0131	-0.0128
$(30, 27)$	$[-0.0415, -0.0387]$	$[-0.0414, -0.0386]$	-0.0406	-0.0402
$(30, 30)$	$[-0.0305, -0.0281]$	$[-0.0305, -0.0280]$	-0.0298	-0.0294
$(30, 33)$	$[-0.0221, -0.0200]$	$[-0.0220, -0.0199]$	-0.0214	-0.0211
$(42, 39)$	$[-0.0533, -0.0496]$	$[-0.0532, -0.0495]$	-0.0510	-0.0505
$(42, 42)$	$[-0.0428, -0.0393]$	$[-0.0427, -0.0393]$	-0.0400	-0.0396
$(42, 45)$	$[-0.0340, -0.0309]$	$[-0.0339, -0.0308]$	-0.0306	-0.0302

Table 1.18: Exchange option, linear problem and deterministic CIR credit spread. Comparison of Monte Carlo (with composite rectangular (CompR) and trapezoidal (CompT) quadrature formulae) and Lagrange Galerkin (LG) methods. Total value adjustment (Test 7)

As expected, the XVA is affected by the increasing of the probability of the counterparty's default: it becomes more negative when it is more likely that the counterparty defaults. Also, we can see that the total value adjustment is more negative under the assumption of a CIR credit spread. This is evident also in Figure 1.8 especially for low initial values of $S^{2,D}$ and large values of the counterparty's intensity of default.

Test 9: Linear problem, stochastic credit spread.

When considering the linear problem (results in Table 1.21 for the exponential Vasicek credit spread and in Table 1.22 for the CIR credit spread) we can draw the same conclusions as for the nonlinear problem.

Figure 1.9 shows the risky price and the XVA. Under the assumption of a CIR credit spread, it can be seen that when the option is out of the money the total value adjustment remains small, even increasing the probability of the counterparty's default, although when the option is in the money the total value adjustment decays quickly when increasing the counterparty's credit spread h. This is less clear in the

case of an exponential Vasicek credit spread, because XVA is smaller, in absolute terms.

1.5.3 Sum of call options

Finally, we assume the hedger buys from the counterparty a portfolio of European call options in different currencies, so that the portfolio payoff function is the sum of the payoff functions of the involved call options, i.e.

$$G(t, S^1, \dots, S^N) = \sum_{i=1}^{N} (X^{D,C_i} S^i - K^i)^+ , \tag{1.63}$$

where $S^1, \dots, S^N$ are the N assets respectively denominated in currencies $C_1, \dots, C_N$, and $K^1, \dots, K^N$ are the strike values given in the domestic currency D.

In our numerical tests we first assume the derivative is written on two underlying assets, i.e. $N = 2$, and we use data reported listed in Table 1.3. The strike values are set to $K^1 = 15$ and $K^2 = 12$. When considering more than two underlying assets, the values of S_0^i, r^i, q^i, σ^{S^i}, K^i, for $i = 1, \dots, N$, are taken form Table 1.27.

Total value adjustment

	Monte Carlo		MPI	
$(S^{2,D}, h)$	SimpR	SimpT	$\rho = 4$	$\rho = 5$
$(27, 0.010)$	$[-0.0273, -0.0254]$	$[-0.0191, -0.0176]$	-0.0130	-0.0133
$(27, 0.015)$	$[-0.0476, -0.0444]$	$[-0.0292, -0.0272]$	-0.0160	-0.0166
$(27, 0.020)$	$[-0.0677, -0.0632]$	$[-0.0393, -0.0366]$	-0.0183	-0.0185
$(27, 0.025)$	$[-0.0878, -0.0819]$	$[-0.0494, -0.0460]$	-0.0222	-0.0209
$(30, 0.010)$	$[-0.0201, -0.0185]$	$[-0.0142, -0.0130]$	-0.0103	-0.0103
$(30, 0.015)$	$[-0.0351, -0.0323]$	$[-0.0217, -0.0199]$	-0.0113	-0.0123
$(30, 0.020)$	$[-0.0500, -0.0460]$	$[-0.0292, -0.0268]$	-0.0141	-0.0142
$(30, 0.025)$	$[-0.0648, -0.0596]$	$[-0.0366, -0.0336]$	-0.0155	-0.0156
$(33, 0.010)$	$[-0.0145, -0.0131]$	$[-0.0104, -0.0094]$	-0.0072	-0.0075
$(33, 0.015)$	$[-0.0254, -0.0230]$	$[-0.0159, -0.0143]$	-0.0090	-0.0090
$(33, 0.020)$	$[-0.0362, -0.0327]$	$[-0.0212, -0.0191]$	-0.0101	-0.0102
$(33, 0.025)$	$[-0.0470, -0.0425]$	$[-0.0266, -0.0240]$	-0.0117	-0.0116

Table 1.19: Exchange option, nonlinear problem and stochastic exponential Vasicek credit spread. Comparison of Monte Carlo (with simple rectangular (SimpR) and trapezoidal (SimpT) quadrature formulae) and multilevel Picard iteration (MPI) methods. Total value adjustment (Test 8)

Total value adjustment

$(\bar{S}^2, h)$	Monte Carlo SimpR	Monte Carlo SimpT	MPI $\rho = 4$	MPI $\rho = 5$
$(27, 0.010)$	$[-0.0273, -0.0254]$	$[-0.0227, -0.0211]$	-0.0206	-0.0210
$(27, 0.015)$	$[-0.0476, -0.0444]$	$[-0.0361, -0.0335]$	-0.0324	-0.0332
$(27, 0.020)$	$[-0.0677, -0.0632]$	$[-0.0493, -0.0458]$	-0.0439	-0.0439
$(27, 0.025)$	$[-0.0878, -0.0819]$	$[-0.0624, -0.0581]$	-0.0584	-0.0558
$(30, 0.010)$	$[-0.0201, -0.0185]$	$[-0.0170, -0.0156]$	-0.0160	-0.0160
$(30, 0.015)$	$[-0.0351, -0.0323]$	$[-0.0269, -0.0246]$	-0.0227	-0.0245
$(30, 0.020)$	$[-0.0500, -0.0460]$	$[-0.0366, -0.0336]$	-0.0333	-0.0331
$(30, 0.025)$	$[-0.0648, -0.0596]$	$[-0.0463, -0.0425]$	-0.0410	-0.0411
$(33, 0.010)$	$[-0.0145, -0.0131]$	$[-0.0125, -0.0112]$	-0.0112	-0.0115
$(33, 0.015)$	$[-0.0254, -0.0230]$	$[-0.0197, -0.0177]$	-0.0176	-0.0177
$(33, 0.020)$	$[-0.0362, -0.0327]$	$[-0.0267, -0.0241]$	-0.0234	-0.0236
$(33, 0.025)$	$[-0.0470, -0.0425]$	$[-0.0338, -0.0304]$	-0.0303	-0.0301

Table 1.20: Exchange option, nonlinear problem and stochastic CIR credit spread. Comparison of Monte Carlo (with simple rectangular (SimpR) and trapezoidal (SimpT) quadrature formulae) and multilevel Picard iteration (MPI) methods. Total value adjustment (Test 8)

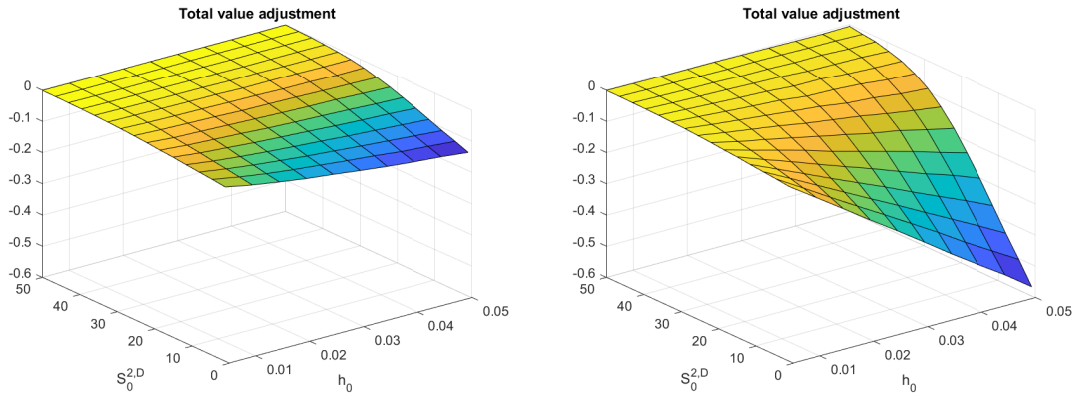

Figure 1.8: Exchange option in the nonlinear case. Total value adjustment with both exponential Vasicek credit spread (on the left) and CIR credit spread (on the right) (Test 8)

Total value adjustment

$(S^{2,D}, h)$	Monte Carlo SimpR	SimpT	CompR	CompT
$(27, 0.010)$	$[-0.0109, -0.0096]$	$[-0.0191, -0.0177]$	$[-0.0140, -0.0129]$	$[-0.0140, -0.0128]$
$(27, 0.015)$	$[-0.0109, -0.0097]$	$[-0.0294, -0.0273]$	$[-0.0170, -0.0156]$	$[-0.0169, -0.0156]$
$(27, 0.020)$	$[-0.0110, -0.0097]$	$[-0.0396, -0.0369]$	$[-0.0196, -0.0180]$	$[-0.0195, -0.0179]$
$(27, 0.025)$	$[-0.0110, -0.0097]$	$[-0.0499, -0.0465]$	$[-0.0219, -0.0202]$	$[-0.0217, -0.0201]$
$(30, 0.010)$	$[-0.0084, -0.0073]$	$[-0.0142, -0.0130]$	$[-0.0107, -0.0096]$	$[-0.0107, -0.0096]$
$(30, 0.015)$	$[-0.0085, -0.0074]$	$[-0.0218, -0.0200]$	$[-0.0129, -0.0117]$	$[-0.0128, -0.0116]$
$(30, 0.020)$	$[-0.0085, -0.0074]$	$[-0.0294, -0.0269]$	$[-0.0148, -0.0134]$	$[-0.0147, -0.0133]$
$(30, 0.025)$	$[-0.0085, -0.0074]$	$[-0.0369, -0.0339]$	$[-0.0165, -0.0150]$	$[-0.0164, -0.0149]$
$(33, 0.010)$	$[-0.0064, -0.0054]$	$[-0.0104, -0.0094]$	$[-0.0080, -0.0071]$	$[-0.0079, -0.0070]$
$(33, 0.015)$	$[-0.0064, -0.0055]$	$[-0.0159, -0.0143]$	$[-0.0096, -0.0085]$	$[-0.0095, -0.0085]$
$(33, 0.020)$	$[-0.0065, -0.0055]$	$[-0.0214, -0.0193]$	$[-0.0110, -0.0098]$	$[-0.0109, -0.0097]$
$(33, 0.025)$	$[-0.0065, -0.0055]$	$[-0.0269, -0.0242]$	$[-0.0122, -0.0109]$	$[-0.0121, -0.0108]$

Table 1.21: Exchange option, linear problem and stochastic exponential Vasicek credit spread. Comparison of Monte Carlo with simple rectangular (SimpR), simple trapezoidal (SimpT), composite rectangular (CompR) and trapezoidal (CompT) quadrature formulae. Total value adjustment (Test 9)

Total value adjustment

$(S^{2,D}, h)$	Monte Carlo SimpR	SimpT	CompR	CompT
$(27, 0.010)$	$[-0.0181, -0.0165]$	$[-0.0227, -0.0211]$	$[-0.0220, -0.0203]$	$[-0.0220, -0.0203]$
$(27, 0.015)$	$[-0.0244, -0.0224]$	$[-0.0361, -0.0336]$	$[-0.0340, -0.0315]$	$[-0.0339, -0.0315]$
$(27, 0.020)$	$[-0.0306, -0.0281]$	$[-0.0494, -0.0460]$	$[-0.0459, -0.0426]$	$[-0.0458, -0.0425]$
$(27, 0.025)$	$[-0.0366, -0.0337]$	$[-0.0627, -0.0583]$	$[-0.0576, -0.0536]$	$[-0.0575, -0.0535]$
$(30, 0.010)$	$[-0.0139, -0.0125]$	$[-0.0170, -0.0155]$	$[-0.0165, -0.0151]$	$[-0.0165, -0.0150]$
$(30, 0.015)$	$[-0.0186, -0.0168]$	$[-0.0269, -0.0246]$	$[-0.0254, -0.0232]$	$[-0.0254, -0.0232]$
$(30, 0.020)$	$[-0.0232, -0.0210]$	$[-0.0367, -0.0337]$	$[-0.0342, -0.0313]$	$[-0.0342, -0.0313]$
$(30, 0.025)$	$[-0.0277, -0.0252]$	$[-0.0465, -0.0427]$	$[-0.0429, -0.0393]$	$[-0.0429, -0.0392]$
$(33, 0.010)$	$[-0.0105, -0.0092]$	$[-0.0125, -0.0112]$	$[-0.0122, -0.0109]$	$[-0.0122, -0.0109]$
$(33, 0.015)$	$[-0.0139, -0.0123]$	$[-0.0197, -0.0177]$	$[-0.0187, -0.0168]$	$[-0.0186, -0.0167]$
$(33, 0.020)$	$[-0.0173, -0.0154]$	$[-0.0268, -0.0242]$	$[-0.0251, -0.0225]$	$[-0.0250, -0.0225]$
$(33, 0.025)$	$[-0.0206, -0.0184]$	$[-0.0339, -0.0306]$	$[-0.0314, -0.0282]$	$[-0.0313, -0.0282]$

Table 1.22: Exchange option, linear problem and stochastic CIR credit spread. Comparison of Monte Carlo with simple rectangular (SimpR), simple trapezoidal (SimpT), composite rectangular (CompR) and trapezoidal (CompT) quadrature formulae. Total value adjustment (Test 9)

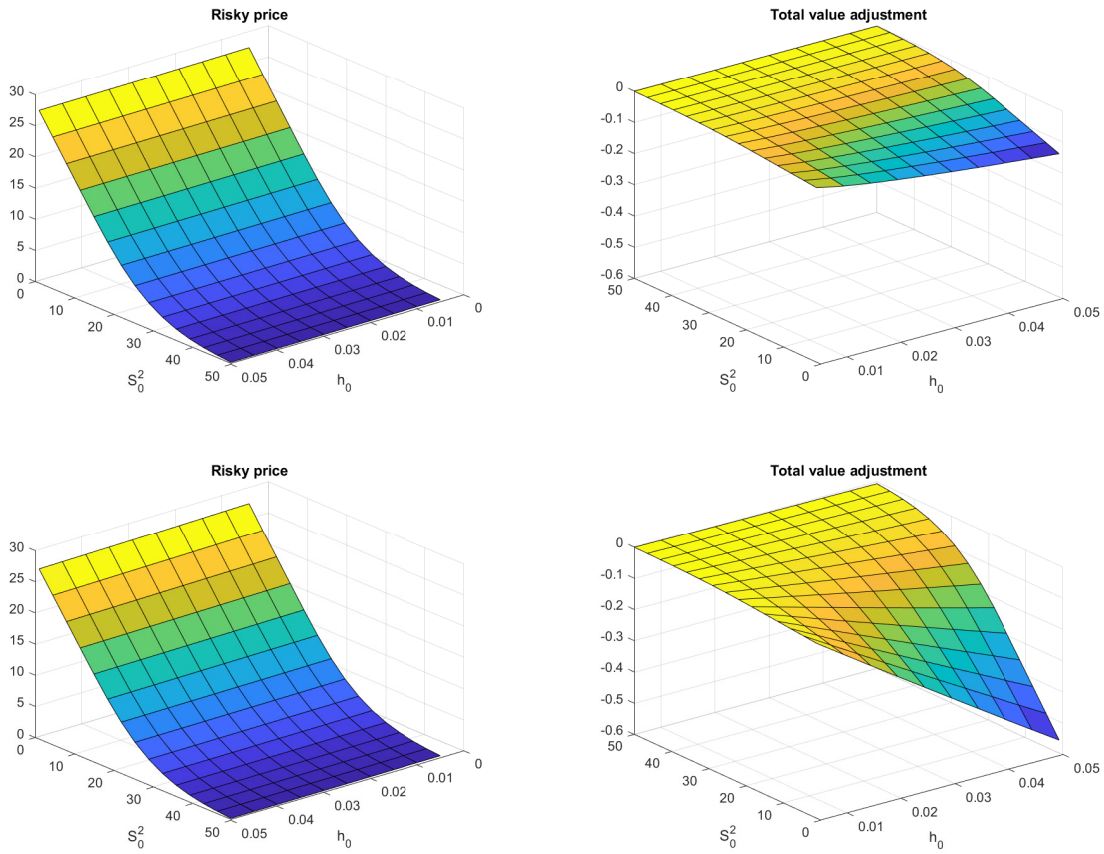

Figure 1.9: Exchange option in the linear case. Exponential Vasicek credit spread on the top and CIR credit spread on the bottom. Risky value on the left and XVA on the right (Test 9)

Total value adjustment

$(S^{1,D}, S^{2,D})$	Monte Carlo SimpR	Monte Carlo SimpT	MPI $\rho = 4$	MPI $\rho = 5$	LG $21\times21, 100$	LG $41\times41, 200$
$(12, 9)$	$[-0.0087, -0.0076]$	$[-0.0047, -0.0041]$	-0.0015	-0.0016	-0.0016	-0.0017
$(12, 12)$	$[-0.0206, -0.0191]$	$[-0.0111, -0.0103]$	-0.0037	-0.0040	-0.0042	-0.0042
$(12, 15)$	$[-0.0480, -0.0459]$	$[-0.0261, -0.0250]$	-0.0095	-0.0095	-0.0099	-0.0098
$(15, 9)$	$[-0.0251, -0.0231]$	$[-0.0135, -0.0125]$	-0.0050	-0.0048	-0.0050	-0.0050
$(15, 12)$	$[-0.0368, -0.0345]$	$[-0.0200, -0.0187]$	-0.0071	-0.0073	-0.0077	-0.0075
$(15, 15)$	$[-0.0642, -0.0614]$	$[-0.0349, -0.0334]$	-0.0125	-0.0128	-0.0134	-0.0131
$(18, 9)$	$[-0.0503, -0.0474]$	$[-0.0273, -0.0257]$	-0.0098	-0.0099	-0.0102	-0.0101
$(18, 12)$	$[-0.0620, -0.0588]$	$[-0.0337, -0.0319]$	-0.0121	-0.0122	-0.0128	-0.0126
$(18, 15)$	$[-0.0893, -0.0857]$	$[-0.0486, -0.0467]$	-0.0175	-0.0179	-0.0185	-0.0182

Table 1.23: Sum of call options, nonlinear problem and deterministic exponential Vasicek credit spread. Comparison of Monte Carlo (with simple rectangular (SimpR) and trapezoidal (SimpT) quadrature formulae), multilevel Picard iteration (MPI) and Lagrange-Galerkin (LG) methods. Total value adjustment (Test 10)

As in the previous examples, we assume that the counterparty is defaultable, while the hedger is default-free. Hence, only the hedger will charge the counterparty an adjustment on the trade, thus reducing the value of the derivative with respect to the risk-free setting.

Test 10: Nonlinear problem, deterministic time dependent credit spread.

We first consider a sum of two call options in the nonlinear case with the deterministic time dependent credit spread and show the numerical results in Table 1.23 and in Table 1.24, whereas the convergence of the multilevel Picard iteration method is shown in Figure 1.10. We have chosen the initial value of the underlying assets so that for each of the two call options we consider the in the money, the at the money and the out of the money cases and test all the possible combinations. As in the previously analysed products, we can see that multilevel Picard iteration method results are close to the ones obtained with Lagrange-Galerkin method, especially when taking $\rho = 5$ in the MPI and a finer mesh in the LG.

Total value adjustment

$(S^{1,D}, S^{2,D})$	Monte Carlo SimpR	Monte Carlo SimpT	MPI $\rho = 4$	MPI $\rho = 5$	LG $21\times21, 100$	LG $41\times41, 200$
$(12, 9)$	$[-0.0087, -0.0076]$	$[-0.0059, -0.0051]$	-0.0047	-0.0049	-0.0048	-0.0051
$(12, 12)$	$[-0.0206, -0.0191]$	$[-0.0140, -0.0129]$	-0.0114	-0.0121	-0.0125	-0.0126
$(12, 15)$	$[-0.0480, -0.0459]$	$[-0.0328, -0.0314]$	-0.0292	-0.0290	-0.0295	-0.0294
$(15, 9)$	$[-0.0251, -0.0231]$	$[-0.0170, -0.0156]$	-0.0155	-0.0147	-0.0150	-0.0151
$(15, 12)$	$[-0.0368, -0.0345]$	$[-0.0251, -0.0235]$	-0.0219	-0.0221	-0.0228	-0.0225
$(15, 15)$	$[-0.0642, -0.0614]$	$[-0.0438, -0.0419]$	-0.0385	-0.0390	-0.0398	-0.0393
$(18, 9)$	$[-0.0503, -0.0474]$	$[-0.0342, -0.0322]$	-0.0301	-0.0302	-0.0303	-0.0303
$(18, 12)$	$[-0.0620, -0.0588]$	$[-0.0422, -0.0401]$	-0.0371	-0.0372	-0.0382	-0.0378
$(18, 15)$	$[-0.0893, -0.0857]$	$[-0.0610, -0.0586]$	-0.0540	-0.0544	-0.0551	-0.0546

Table 1.24: Sum of call options, nonlinear problem and deterministic CIR credit spread. Comparison of Monte Carlo (with simple rectangular (SimpR) and trapezoidal (SimpT) quadrature formulae), multilevel Picard iteration (MPI) and Lagrange Galerkin (LG) methods. Total value adjustment (Test 10)

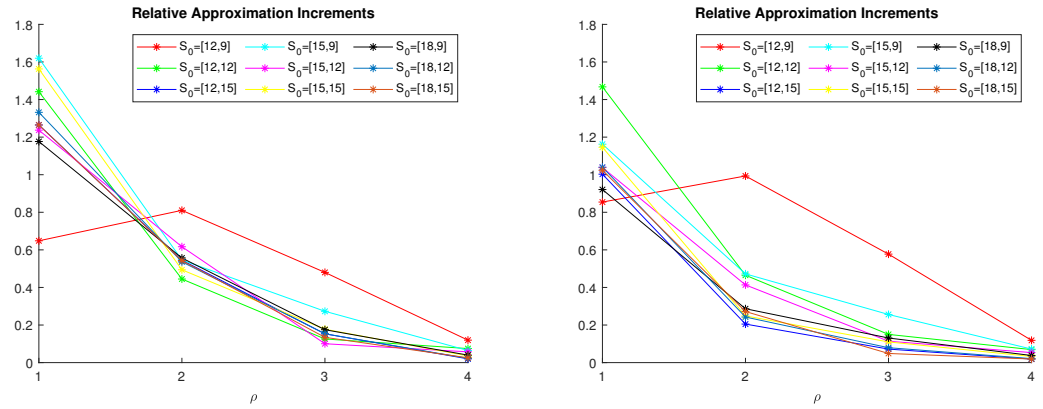

Figure 1.10: Sum of call options with deterministic credit spread. Convergence of the MPI with exponential Vasicek dynamics for credit spread on the left and CIR dynamics on the right.

Test 11: Linear problem, deterministic time dependent credit spread.

For the linear case with deterministic credit spread, XVA numerical results are shown in Table 1.25 for the exponential Vasicek dynamics and in Table 1.26 for the CIR dynamics. In the first case, when taking a mesh of 21×21 nodes and 100 time steps in the Lagrange-Galerkin method, there are some values outside the corresponding Monte Carlo confidence intervals. However, when taking a finer mesh, the resulting XVA values are inside or on the lower bound of Monte Carlo confidence intervals obtained with the rectangular composite formula. When considering the trapezoidal composite formula, there are some LG values that are slightly outside the corresponding Monte Carlo confidence intervals. As already pointed out in the case of the exchange option, the use of an even more refined mesh probably makes the Lagrange-Galerkin values less negative and, therefore, closer to the centres of the confidence intervals. In the case of the CIR dynamics, the Lagrange-Galerkin results with both the considered discretization meshes are inside the Monte Carlo confidence intervals, except for the point $(S^{1,D}, S^{1,D}) = (15, 15)$, where the XVA obtained with the coarser mesh is slightly outside the confidence intervals.

We now consider the sum of call options on different numbers N of assets in their corresponding currencies. Table 1.27 shows data for the case of $N = 32$ assets. Note that when considering a number of assets lower than 32, we use the data of rows $i = 1, \ldots, N$ appearing in Table 1.27 (i.e., for the case of 2 assets we consider the rows $i = 1, 2$, and so on for 4, 8, 16 and 32 assets).

Table 1.28 shows the risk-free prices, that are obviously independent of the counterparty's credit spread and of the choice of the mark-to-market value. With the chosen data, the risk-free price increases by increasing the number of the underlying assets, so we expect that the XVA becomes more negative. The total value adjustment is analysed in the next two tests both in the nonlinear case and in the linear case.

Total value adjustment

	Monte Carlo		LG	
$(S^{1,D}, S^{2,D})$	CompR	CompT	$21\times21, 100$	$41\times41, 200$
$(12, 9)$	$[-0.0018, -0.0015]$	$[-0.0017, -0.0015]$	-0.0016	-0.0017
$(12, 12)$	$[-0.0042, -0.0039]$	$[-0.0041, -0.0038]$	-0.0042	-0.0042
$(12, 15)$	$[-0.0098, -0.0094]$	$[-0.0097, -0.0093]$	-0.0099	-0.0098
$(15, 9)$	$[-0.0051, -0.0047]$	$[-0.0050, -0.0046]$	-0.0050	-0.0050
$(15, 12)$	$[-0.0075, -0.0070]$	$[-0.0074, -0.0070]$	-0.0077	-0.0075
$(15, 15)$	$[-0.0131, -0.0125]$	$[-0.0130, -0.0124]$	-0.0133	-0.0131
$(18, 9)$	$[-0.0102, -0.0096]$	$[-0.0101, -0.0096]$	-0.0102	-0.0101
$(18, 12)$	$[-0.0126, -0.0120]$	$[-0.0125, -0.0119]$	-0.0128	-0.0126
$(18, 15)$	$[-0.0182, -0.0175]$	$[-0.0181, -0.0174]$	-0.0185	-0.0182

Table 1.25: Sum of call options, linear problem and deterministic exponential Vasicek credit spread. Comparison of Monte Carlo (with composite rectangular (CompR) and trapezoidal (CompT) quadrature formulae) and Lagrange-Galerkin (LG) methods. Total value adjustment (Test 11)

Total value adjustment

	Monte Carlo		LG	
$(S^{1,D}, S^{2,D})$	CompR	CompT	$21\times21, 100$	$41\times41, 200$
$(12, 9)$	$[-0.0053, -0.0046]$	$[-0.0053, -0.0046]$	-0.0047	-0.0051
$(12, 12)$	$[-0.0126, -0.0117]$	$[-0.0126, -0.0117]$	-0.0125	-0.0125
$(12, 15)$	$[-0.0296, -0.0283]$	$[-0.0295, -0.0282]$	-0.0294	-0.0293
$(15, 9)$	$[-0.0153, -0.0141]$	$[-0.0153, -0.0141]$	-0.0149	-0.0150
$(15, 12)$	$[-0.0226, -0.0212]$	$[-0.0226, -0.0212]$	-0.0227	-0.0225
$(15, 15)$	$[-0.0396, -0.0379]$	$[-0.0395, -0.0378]$	-0.0397	-0.0392
$(18, 9)$	$[-0.0309, -0.0291]$	$[-0.0308, -0.0290]$	-0.0302	-0.0302
$(18, 12)$	$[-0.0381, -0.0362]$	$[-0.0381, -0.0361]$	-0.0380	-0.0377
$(18, 15)$	$[-0.0551, -0.0529]$	$[-0.0549, -0.0528]$	-0.0550	-0.0545

Table 1.26: Sum of call options, linear problem and deterministic CIR credit spread. Comparison of Monte Carlo (with composite rectangular (CompR) and trapezoidal (CompT) quadrature formulae) and Lagrange-Galerkin (LG) methods. Total value adjustment (Test 11)

i	$S^{i,D}$	r^i	q^i	σ^{S^i}	K^i	i	$S^{i,D}$	r^i	q^i	σ^{S^i}	K^i
1	11	0.020	0.030	0.300	15	17	11	0.018	0.025	0.324	10
2	13	0.020	0.010	0.200	12	18	13	0.006	0.032	0.288	11
3	13	0.037	0.011	0.289	15	19	15	0.001	0.035	0.306	13
4	14	0.026	0.024	0.299	10	20	14	0.017	0.033	0.277	13
5	14	0.024	0.024	0.277	13	21	10	0.026	0.011	0.325	13
6	11	0.008	0.033	0.271	13	22	13	0.014	0.020	0.308	11
7	10	0.002	0.032	0.201	10	23	12	0.018	0.013	0.330	15
8	13	0.014	0.016	0.210	10	24	10	0.015	0.035	0.230	15
9	10	0.017	0.022	0.265	13	25	15	0.018	0.014	0.245	12
10	14	0.021	0.017	0.265	15	26	15	0.023	0.013	0.271	14
11	13	0.006	0.034	0.228	10	27	11	0.010	0.021	0.274	14
12	15	0.011	0.029	0.279	12	28	13	0.022	0.012	0.291	12
13	15	0.029	0.012	0.290	15	29	12	0.008	0.030	0.323	11
14	11	0.013	0.028	0.308	12	30	12	0.003	0.045	0.279	11
15	15	0.008	0.037	0.246	12	31	13	0.002	0.035	0.341	11
16	14	0.033	0.011	0.261	11	32	13	0.026	0.024	0.309	12

Table 1.27: Data for the sum of call options. For $N = 2, 4, 8, 16, 32$ we respectively consider the rows of the table from 1 to $2, 4, 8, 16, 32$.

Risk-free value	
N	Monte Carlo
2	$[1.9330, 2.0468]$
4	$[7.1207, 7.3713]$
8	$[13.5861, 13.9660]$
16	$[30.8413, 31.4230]$
32	$[60.2779, 61.1494]$

Table 1.28: Sum of call options. Monte Carlo confidence intervals. Risk-free value

Total value adjustment			Elapsed time		
	MPI			MPI	
N	$\rho = 4$	$\rho = 5$	N	$\rho = 4$	$\rho = 5$
2	−0.0057	−0.0058	2	11.1905	3816.6932
4	−0.0216	−0.0215	4	16.7175	4775.5968
8	−0.0400	−0.0409	8	26.4006	7375.3050
16	−0.0912	−0.0913	16	42.3238	12573.8821
32	−0.1778	−0.1795	32	75.8329	22500.3082

Table 1.29: Sum of call options, nonlinear problem and stochastic exponential Vasicek credit spread. Multilevel Picard iteration (MPI) results. Total value adjustment and elapsed time in seconds (Test 12)

Test 12: Nonlinear problem, stochastic credit spread.

We assume the counterparty's credit spread is stochastic and that the mark-to-market value is equal to the risky derivative value (nonlinear case).

Table 1.29 and Table 1.30 show the total value adjustment for different numbers of underlying assets. In particular, we show the average value of XVA on $N_{runs} = 10$ runs of the multilevel Picard iteration method. Also, the tables report the elapsed computational time for $N_{runs} = 10$ runs of the MPI. The elapsed computational time does not depend on the dynamics chosen for the credit spread, but increases by increasing the value of the parameter ρ. In fact, we recall that the number of simulations is fixed to $m_{n,l,\rho} = \rho^{n-l}$ and the number of rectangles is chosen to be ρ^{n-l}, so that larger values of ρ correspond to larger numbers of simulations and of discretization nodes.

Figure 1.11 shows that the empirical convergence of the multilevel Picard iteration for different numbers of assets.

Test 13: Linear problem, stochastic credit spread.

Finally, we consider the sum of up to $N = 32$ call options in the linear case and report the computed total value adjustment and the elapsed time in Table 1.31 and in Table 1.32. Results are obtained by using the Monte Carlo method with composite

Total value adjustment			Elapsed time		
	MPI			MPI	
N	$\rho = 4$	$\rho = 5$	N	$\rho = 4$	$\rho = 5$
2	−0.0150	−0.0151	2	12.1386	3596.6193
4	−0.0561	−0.0556	4	15.8039	4988.5962
8	−0.1048	−0.1059	8	27.1096	7512.3959
16	−0.2391	−0.2379	16	41.6914	12348.0835
32	−0.4649	−0.4661	32	75.2775	21826.0707

Table 1.30: Sum of call options, nonlinear problem and stochastic CIR credit spread. Multilevel Picard iteration (MPI) results. Total value adjustment and elapsed time in seconds (Test 12)

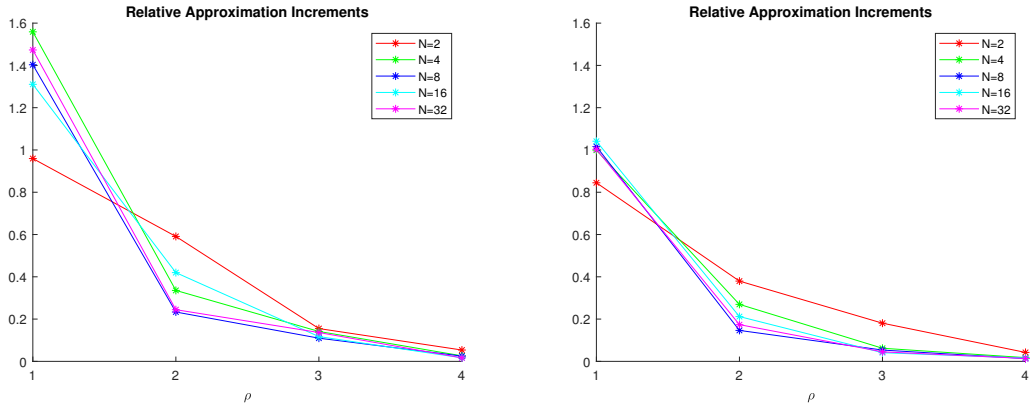

Figure 1.11: Sum of call options with stochastic credit spread. Convergence of the MPI with exponential Vasicek dynamics for credit spread on the left and CIR dynamics on the right.

Total value adjustment			Elapsed time		
	Monte Carlo			Monte Carlo	
N	CompR	CompT	N	CompR	CompT
2	$[-0.0061, -0.0057]$	$[-0.0060, -0.0056]$	2	0.5384	0.5389
4	$[-0.0222, -0.0212]$	$[-0.0220, -0.0211]$	4	0.6200	0.6814
8	$[-0.0415, -0.0399]$	$[-0.0411, -0.0396]$	8	0.8646	0.8936
16	$[-0.0922, -0.0896]$	$[-0.0915, -0.0889]$	16	2.6761	2.6853
32	$[-0.1809, -0.1762]$	$[-0.1796, -0.1748]$	32	3.4442	3.5099

Table 1.31: Sum of call options, linear problem and stochastic exponential Vasicek credit spread. Monte Carlo with composite rectangular (CompR) and trapezoidal (CompT) quadrature formulae results. Total value adjustment and elapsed time (Test 13)

Total value adjustment			Elapsed time		
	Monte Carlo			Monte Carlo	
N	CompR	CompT	N	CompR	CompT
2	$[-0.0156, -0.0147]$	$[-0.0155, -0.0146]$	2	0.5177	0.5528
4	$[-0.0564, -0.0544]$	$[-0.0563, -0.0542]$	4	0.6640	0.6759
8	$[-0.1063, -0.1031]$	$[-0.1061, -0.1029]$	8	0.8809	0.9064
16	$[-0.2380, -0.2328]$	$[-0.2375, -0.2323]$	16	2.5279	2.5478
32	$[-0.4647, -0.4562]$	$[-0.4637, -0.4552]$	32	3.7823	3.7983

Table 1.32: Sum of call options, linear problem and stochastic CIR credit spread. Monte Carlo with composite rectangular (CompR) and trapezoidal (CompT) quadrature formulae results. Total value adjustment and elapsed time (Test 13)

quadrature formulae and the 99% confidence intervals are reported. As in the non-linear case, the XVA is more negative for larger values of N. The elapsed time does not depend on the choice of the credit spread dynamics and the trapezoidal formula is a little more time-consuming than the rectangular formula.

1.6 Conclusions

In this chapter, we have addressed the modelling and the computation of the total value adjustment in a multi-currency setting by considering a derivative written on

assets denominated in foreign currencies. We have assumed that the foreign exchange rates are deterministic, the derivative is collateralized in cash in a foreign currency and the counterparty's intensity of default is an exponential Vasicek or a CIR process.

The portfolio replication and the dynamic hedging methodologies have provided the formulation of the total value adjustment pricing problem in terms of nonlinear and linear PDEs. Then, the use of Feynman-Kac formulae has provided the equivalent formulations in terms of expectations that allow to apply Monte Carlo simulation techniques to the corresponding nonlinear and linear models.

First, we have numerically solved the total value adjustment pricing PDEs by applying the Lagrange-Galerkin method under the assumption that the counterparty's credit spread is a deterministic function of time and the derivative is written on two underlying assets. Then, from the comparison with Lagrange-Galerkin method results, we have deduced that in the nonlinear case the multilevel Picard iteration method results can be taken as reference values, whereas in the linear case we can consider the Monte Carlo confidence intervals obtained by using composite quadrature formulae for the approximation of the integral in the total value adjustment formulae.

Briefly, we have seen that the total value adjustment is more negative when the derivative is more valuable and that it becomes more and more negative by increasing the counterparty's probability of default.

In the next chapter, we extend the model and the methodologies proposed in this chapter to the more realistic and complex setting of stochastic foreign exchange rates.

Chapter 2

Total Value Adjustment in a multi-currency setting with stochastic FX rates

2.1 Introduction

In Chapter 1 we have addressed the computation of the XVA in a multicurrency setting for different European vanilla options by means of appropriate proposed models that are formulated in terms of expectations. Moreover, the XVA pricing problem has been also formulated in terms of nonlinear and linear PDEs, although their numerical solution has been addressed in the particular case of deterministic counterparty's credit spread with a Lagrange-Galerkin method. The statement of the models in the multicurrency setting has been obtained by means of appropriate replicating portfolios and it was assumed that the foreign exchange rates between the involved currencies are constant.

The main objective objective of this chapter is the extension of the methodology developed in Chapter 1 to the more realistic and complex modelling approach that considers stochastic foreign exchange rates. For this purpose, we mainly follow the

ideas developed in [89].

First, this extension requires the introduction of appropriate stochastic dynamics for FX rates and for the underlying assets prices.

As a first approach, we will consider that the stochastic dynamics of each FX rate follows a geometric Brownian motion process, although in the future other more general dynamics could be considered.

Also, in this chapter we assume that the derivative is partially collateralized and the collateral is a portfolio of bonds denominated in a foreign currency, which is a difference with respect to [89].

As in Chapter 1, we assume a positive mean-reversion dynamics for the credit spread, a more realistic assumption with respect to the Gaussian process used in [89].

The chapter is organized as follows. In Section 2.2 we deduce mathematical models for XVA formulated in terms of nonlinear or linear PDEs problems, depending on the choice of the mark-to-market derivative value. In Section 2.3 we formulate the problems in terms of expectations. In Section 2.4 we introduce the proposed numerical methods to approximate XVA price. In particular, Subsection 2.4.1 and Subsection 2.4.2 deal with Monte Carlo and multilevel Picard iteration methods, respectively. In Section 2.5 we show and discuss numerical results that correspond to different examples of European options: *spread option*, *option on the maximum*, *best of put/put option*, *basket option*. Finally, in Section 2.6 we summarize the main conclusions.

2.2 Formulation in terms of partial differential equations

In this section, we deduce a PDE formulation for the value of a derivative which is traded between a default-free hedger and a defaultable counterparty in a multi-currency setting. Therefore, we take into account the valuation adjustment due to the fact that the counterparty may default (counterparty risk). More precisely, we extend the models in Chapter 1 by assuming that the FX rates have stochastic dynamics.

We denote by D the domestic currency and by $C_0, \ldots, C_N$ the foreign currencies. For $j = 0, \ldots, N$, let X_t^{D,C_j} be the FX rate between currencies D and C_j at time t, i.e., the value in domestic currency D of one unit of the foreign currency C_j at time t. The dynamics of the stochastic FX rate X_t^{D,C_j} under the real world measure P is described by the SDEs:

$$dX_t^{D,C_j} = \mu^{X^j} X_t^{D,C_j} dt + \sigma^{X^j} X_t^{D,C_j} dW_t^{X^j,P}, \tag{2.1}$$

where μ^{X^j} and σ^{X^j} are respectively the real world drift and the volatility of X^{D,C_j}, while $W^{X^j,P}$ is a standard P-Brownian process. Obviously, if $C_j = D$ for a certain j, then $X_t^{D,C_j} = 1$ at any time t. We denote by $X_t = (X_t^{D,C_0}, \ldots, X_t^{D,C_N})$ the vector of the FX rates values at time t and by $\bar{X}_t = (X_t^{D,C_1}, \ldots, X_t^{D,C_N})$ the vector of the FX rates values, except the value of X^{D,C_0}, at time t. Indeed, this notation will be useful in the following, since we will consider derivatives written on N underlying assets denominated in currencies $C_1, \ldots, C_N$, respectively, while C_0 will be the currency of the collateral account.

Alternative more complex models to the geometric Brownian motion defined by (2.1) are proposed in the literature (see [67, 49], for example). The additional consideration of local, stochastic or local/stochastic volatilities leads to increasing the complexity and the number of stochastic factors, although the same methodology could be applied.

For $i = 1, \ldots, N$, let S_t^i denote the price of a foreign asset in units of the foreign currency C_i at time t and let $S_t = (S_t^1, \ldots, S_t^N)$ be the vector of the assets prices at time t. Moreover, let h_t be the counterparty's credit spread at time t. We assume that under the real world measure P the evolution of the prices of the foreign assets and of the counterparty's credit spread are respectively governed by the SDEs:

$$dS_t^i = \mu^{S^i} S_t^i \, dt + \sigma^{S^i} S_t^i \, dW_t^{S^i,P}, \qquad \text{for } i = 1, \ldots, N, \tag{2.2}$$

$$dh_t = \mu^{h,P}(t, h_t) \, dt + \sigma^{h,P}(t, h_t) \, dW_t^{h,P}, \tag{2.3}$$

where $\mu^{S^i,P}$ and $\mu^{h,P}$ are the real world drifts of the processes, while σ^{S_i} and $\sigma^{h,P}$ are

their volatilities. Moreover, $W^{S^i,P}$ and $W^{h,P}$ are Brownian processes under the real world measure P.

We assume that all the processes are correlated with constant correlations. The correlation matrix is given by:

$$\text{corr}(S,X,h) = \begin{bmatrix} 1 & \rho^{S^1,S^2} & \cdots & \rho^{S^1,S^N} & \rho^{S^1,X^0} & \rho^{S^1,X^1} & \cdots & \rho^{S^1,X^N} & \rho^{S^1,h} \\ \rho^{S^1,S^2} & 1 & \cdots & \rho^{S^2,S^N} & \rho^{S^2,X^0} & \rho^{S^2,X^1} & \cdots & \rho^{S^2,X^N} & \rho^{S^2,h} \\ \vdots & \vdots & \vdots & \vdots & \vdots & \vdots & \vdots & \vdots & \vdots \\ \rho^{S^1,S^N} & \rho^{S^2,S^N} & \cdots & 1 & \rho^{S^N,X^0} & \rho^{S^N,X^1} & \cdots & \rho^{S^N,X^N} & \rho^{S^N,h} \\ \rho^{S^1,X^0} & \rho^{S^2,X^0} & \cdots & \rho^{S^N,X^0} & 1 & \rho^{X^0,X^1} & \cdots & \rho^{X^0,X^N} & \rho^{X^0,h} \\ \rho^{S^1,X^1} & \rho^{S^2,X^1} & \cdots & \rho^{S^N,X^1} & \rho^{X^0,X^1} & \rho^{X^0,X^1} & \cdots & \rho^{X^1,X^N} & \rho^{X^1,h} \\ \vdots & \vdots & \vdots & \vdots & \vdots & \vdots & \vdots & \vdots & \vdots \\ \rho^{S^1,X^N} & \rho^{S^2,X^N} & \cdots & \rho^{S^N,X^N} & \rho^{X^0,X^N} & \rho^{X^1,X^N} & \cdots & 1 & \rho^{X^N,h} \\ \rho^{S^1,h} & \rho^{S^2,h} & \cdots & \rho^{S^N,h} & \rho^{X^0,h} & \rho^{X^1,h} & \cdots & \rho^{X^N,h} & 1 \end{bmatrix} \tag{2.4}$$

In order to infer the dynamics of X^{D,C_j}, for $j = 0,\ldots,N$, under the risk neutral probability measure of the domestic market, denoted by Q^D, we consider two bonds with maturity T in the domestic market and in the j-th foreign market, for $j = 0,\ldots,N$, the prices of which at time t are denoted by B_t^D and $B_t^{C_j}$, respectively.

By using equation (2.1), the discounted price of the foreign bond in the domestic currency D is given by

$$\begin{aligned} \hat{B}_t^{j,D} &= (B_t^D)^{-1} B_t^{C_j} X_t^{D,C_j} \\ &= \hat{B}_0^{j,D} \exp\left(\left(r^j - r^D + \mu^{X^j} - \frac{(\sigma^{X^j})^2}{2} \right) t + \sigma^{X^j} W_t^{X^j,P} \right), \end{aligned} \tag{2.5}$$

where r^D and r^j, $j = 0,\ldots,N$, are the short-term rates in the domestic market and in the j-th foreign market, respectively. Thus, we are assuming that interest rates r^D and r^j are constant. Note that the consideration of stochastic evolution of these interest rates would increase the number of stochastic factors in a significant way. The idea is to address this step in a future work.

Thus, the dynamics of $\hat{B}_t^{j,D}$ under the real measure P is given by

$$d\hat{B}_t^{j,D} = (\mu^{X^j} + r^j - r^D)\hat{B}_t^{j,D}dt + \sigma^{X^j}\hat{B}_t^{j,D}dW_t^{X^j,P}. \tag{2.6}$$

From Girsanov's Theorem [47], there exists an equivalent measure Q^D, such that we can build a Brownian motion W^{X^j,Q^D} under the measure Q^D, which is defined as:

$$W_t^{X^j,Q^D} = W_t^{X^j,P} + \int_0^t m_s^j ds,$$

or equivalently, W^{X^j,Q^D} satisfies the relation $dW_t^{X^j,Q^D} = dW_t^{X^j,P} + m_t^j dt$, where m_t is the process associated to the change of measure.

Therefore, the dynamics of $\hat{B}_t^{j,D}$ under the measure Q^D is given by

$$d\hat{B}_t^{j,D} = (\mu^{X^j} + r^j - r^D - m_t^j\,\sigma^{X^j})\hat{B}_t^{j,D}dt + \sigma^{X^j}\hat{B}_t^{j,D}dW_t^{X^j,Q^D}. \tag{2.7}$$

Since $\hat{B}_t^{j,D}$ must be a martingale under Q^D, we get

$$r^D - r^j = \mu^{X^j} - m_t^j\,\sigma^{X^j}, \tag{2.8}$$

that leads to

$$X_t^{D,C_j} = X_0^{D,C_j}\exp\left(\left(r^D - r^j - \frac{(\sigma^{X^j})^2}{2}\right)t + \sigma^{X^j}W_t^{X^j,Q^D}\right), \tag{2.9}$$

or equivalently,

$$dX_t^{D,C_j} = (r^D - r^j)X_t^{D,C_j}dt + \sigma^{X^j}X_t^{D,C_j}dW_t^{X^j,Q^D}. \tag{2.10}$$

Also, we need to infer the dynamics of S_t^i under the risk neutral measure of the domestic market Q^D. For this purpose, we assume that the dynamics of S_t^i under the risk neutral measure of the domestic market and under the risk neutral measure of the foreign market, denoted by Q^{C_i}, are respectively given by the SDEs:

$$dS_t^i = \mu^{S^i,Q^D}S_t^i dt + \sigma^{S^i}S_t^i dW_t^{S^i,Q^D}, \tag{2.11}$$

$$dS_t^i = (r^i - q^i)S_t^i dt + \sigma^{S^i}S_t^i dW_t^{S^i,Q^{C_i}}, \tag{2.12}$$

where μ^{S^i,Q^D} is the drift of S^i_t under the measure Q^D, σ^{S^i} is its volatility, r^i is the short-term rate of the i-th foreign market and q^i is the continuous dividend yield paid by S^i_t. Moreover, W^{S^i,Q^D}_t and $W^{S^i,Q^{C_i}}_t$ are a Q^D-Brownian motion and a Q^{C_i}-Brownian motion, respectively.

We denote by $S^{i,D}_t$ the price of the foreign underlying asset S^i in the domestic currency D, that is to say, $S^{i,D}_t = S^i_t X^{D,C_i}_t$. From (2.10) and (2.11), by applying the classical Itô's formula we obtain that the dynamics of $S^{i,D}$ follows the SDE:

$$\begin{aligned} dS^{i,D}_t &= d(S^i_t X^{D,C_i}_t) \\ &= (r^D - r^i + \mu^{S^i,Q^D} + \rho^{S^iX^i}\sigma^{S^i}\sigma^{X^i})S^i_t X^{D,C_i}_t dt \\ &\quad + (\sigma^{S^i} dW^{S^i,Q^D} + \sigma^{X^i} dW^{X^i,Q^D})S^i_t X^{D,C_i}_t. \end{aligned} \tag{2.13}$$

Since the drift of $S^{i,D}$ under the risk neutral measure of the domestic market is given by $(r^D - q^i)$, we obtain

$$\mu^{S^i,Q^D} = r^i - q^i - \rho^{S^iX^i}\sigma^{S^i}\sigma^{X^i}.$$

Therefore, from (2.11) we get that the dynamics of S^i_t under the risk neutral measure of the domestic market follows the SDE:

$$dS^i_t = (r^i - q^i - \rho^{S^iX^i}\sigma^{S^i}\sigma^{X^i})S^i_t dt + \sigma^{S^i} S^i_t dW^{S^i,Q^D}_t. \tag{2.14}$$

As in Chapter 1, we assume that under the risk-neutral measure Q^D, the counterparty's credit spread follows an exponential Vasicek process, so that

$$dh_t = \alpha\, h_t\, (m - \log(h_t))\, dt + \sigma^h\, h_t\, dW^{h,Q}\ , \text{ with } \ m = \theta + \frac{(\sigma^h)^2}{2\alpha}\,, \tag{2.15}$$

where α, θ and σ^h are positive constant and W^{h,Q^D} is a Brownian motion under the risk-neutral measure Q^D. In Section 2.5, where we report numerical examples, we also show results obtained with the assumption of the CIR dynamics for the credit spread.

Finally, the derivative value in the domestic currency D at time t is given by $V^D_t = V^D(t, S_t, X_t, h_t, J_t)$, where J_t is the counterparty's default state at time t,

i.e., $J_t = 1$ in case of default before or at time t, otherwise $J_t = 0$, and the risk-free derivative value in currency D is denoted by $W_t^D = W^D(t, S_t, X_t)$. In this chapter, we assume the derivative is traded under a collateralization agreement and the collateral is composed of a portfolio of bonds denominated in currency C_0. We denote by $C_t^{C_0}$ and C_t^D the values of the collateral account at time t in currencies C_0 and D, respectively, i.e., $C_t^D = C_t^{C_0} X^{D,C_0}$.

2.2.1 Replicating portfolio

Once we have deduced the dynamics of the processes involved in the model under the domestic risk neutral measure Q^D, in order to compute the derivative value, we implement a self-financing strategy by building a portfolio Π which hedges all the risk factors, which are:

- the market risk due to changes in S^i, for $i = 1, \dots, N$;
- the FX risk due to changes in X^{D,C_j}, for $j = 0, \dots, N$;
- the counterparty's spread risk due to changes in h;
- the counterparty's default risk.

More precisely, we extend the portfolio in Chapter 1, where FX rates were supposed to be deterministic, in order to take into account also the exposure to the FX risk due to changes in the FX rates. The FX risk is hedged by trading in $N + 1$ fully collateralized FX derivatives: for $j = 0, \dots, N$, E^j denotes the net present value in currency D of the derivative written on the FX rate X^{D,C_j}.

As in Chapter 1, we assume the hedger buys the derivative from the counterparty and we describe the transactions occurring with her treasury, the FX market and the REPO market. This transactions are represented in Figure 2.1.

- At time t, the hedger borrows V_t^D cash from her treasury to buy the derivative and receives bonds denominated in currency C_0 from the counterparty as collateral.

- The hedger sells the bonds got as collateral in the repo market and receives the cash amount, in currency C_0, corresponding to the bonds spot price $C_t^{C_0}$.

- The hedger exchanges the cash received from the repo market in the FX market, obtaining $C_t^D = C_t^{C_0} X_t^{D,C_0}$ in the domestic currency D, that she gives to the treasury. Therefore, the outstanding debt to the treasury is $V_t^D - C_t^D$, that will grow at the funding rate f_t^D.

- At time $t + dt$ the repo position has to be closed. The hedger buys back the bonds, that she gives to the counterparty, by paying the cash $C_t^{C_0}$ plus interest $C_t^{C_0} r_t^R$, where r^R is the instantaneous repo rate. In order to pay the repo market, according to a forward contract agreed at time t, the hedger sells forward the amount $C_t^{C_0}(1 + r_t^R dt)$ multiplied by the forward FX rate $X_t^{D,C_0} \frac{1+r^D dt}{1+(r^{C_0}+b^{C_0,D})dt}$ and receives $C_t^{C_0}(1 + r_t^R dt)$ in currency C_0.

- At time $t + dt$ the debt to the treasury is

$$\begin{aligned} &\left(V_t^D - C_t^D\right)\left(1 + f_t^D dt\right) + C_t^D \left(1 + \left(r^D + r^R - r^{C_0} - b^{C_0,D}\right) dt\right) \\ &= \left(V_t^D - C_t^D\right)\left(1 + f_t^D dt\right) + C_t^D \left(1 + \left(r^D + r^R + sb^{D,C_0}\right) dt\right), \end{aligned} \tag{2.16}$$

  where $sb^{D,C_0} = b^{D,C_0} - r^{C_0}$ is the cross currency basis spread.

As in Chapter 1, we denote by B_t^D and Ω_t the value in currency D and the number of shares of the funding account at time t. Thus, according to the self-financing condition of the replicating strategy:

$$\Omega_t B_t^D = -\left(V_t^D - C_t^{C_0} X_t^{D,C_0}\right), \tag{2.17}$$

so that the number of shares of the funding account in the portfolio Π_t at time t is given by:

$$\Omega_t = -\frac{V_t^D - C_t^{C_0} X_t^{D,C_0}}{B_t^D}. \tag{2.18}$$

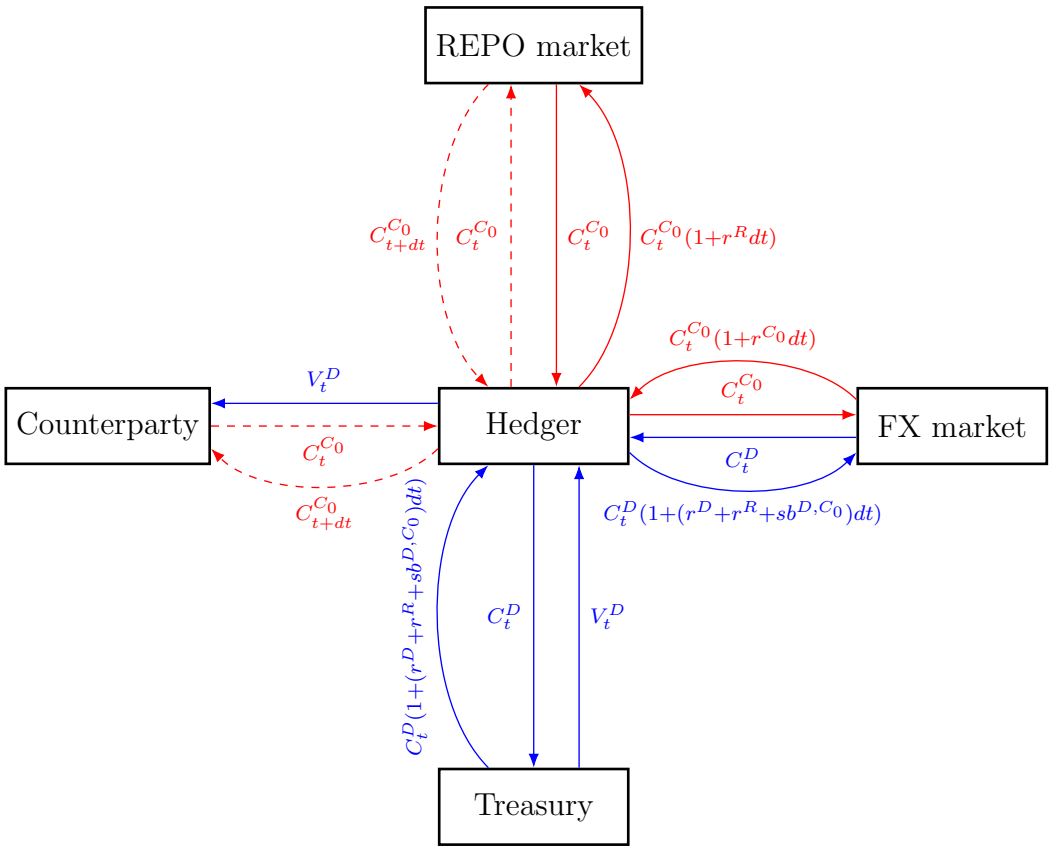

Figure 2.1: Transactions occurring with the treasury, the FX market and the REPO market to fund the trade. Straight lines refer to initial transactions, that take place at time t, while curved lines to final transactions taking place at time $t+dt$. Continuous lines represent cash transactions whereas dashed ones represent asset transactions. Blue lines indicate amounts denominated in currency D, whereas red ones represent cash of asset transactions denominated in currency C_0.

Therefore, the replicating portfolio Π_t at time t is made as follows:

$$\begin{aligned}\Pi_t = &\sum_{i=1}^{N} \alpha_t^i H_t^{i,D} + \sum_{j=0}^{N} \eta_t^j E_t^j + \gamma_t CDS^D(t,T) + \epsilon_t CDS^D(t,t+dt) \\ &+ \Omega_t B_t^D + \beta_t^D,\end{aligned} \tag{2.19}$$

where

- α_t^i represents the weight of the derivative $H_t^{i,D}$, for $i = 1, \ldots, N$, in the portfolio composition at time t;
- η_t^j denotes the weight of the derivative E_t^j, for $j = 0, \ldots, N$, in the portfolio composition at time t;
- γ_t and ϵ_t are the units of the long term credit default swap and of the short term credit default swap, respectively, in the portfolio composition at time t;
- Ω_t represents the number of shares of the funding account in the portfolio composition at time t;
- β_t^D denotes the amount of cash in the collateral account at time t, which is composed of

$$\beta_t^D = -\sum_{i=1}^{N} \alpha_t^i H_t^{i,D} - \sum_{j=0}^{N} \eta_t^j E_t^j - \gamma_t CDS^D(t,T) + C_t^{C_0} X_t^{D,C_0}. \tag{2.20}$$

The variation of the collateral account in the time interval from t to $t+dt$ is given by

$$\begin{aligned}d\bar{\beta}_t^D = -\Bigg[&\sum_{i=1}^{N} \alpha_t^i (r^D + b^{D,C_j}) H_t^{i,D} + \sum_{j=0}^{N} \eta_t^j r^D E_t^j + \gamma_t r^D CDS^D(t,T) \\ &- \left(r^D + r^R + sb^{D,C_0}\right) C_t^{C_0} X_t^{D,C_0}\Bigg] dt\,.\end{aligned} \tag{2.21}$$

2.2.2 Pricing partial differential equations

Next, we deduce the pricing PDEs. As a consequence of the no arbitrage condition, we have

$$\Pi_t(t, S_t, X_t, h_t, J_t) + V^D(t, S_t, X_t, h_t, J_t) = 0,$$

so that the self-financing condition leads to $-dV_t^D = d\Pi_t$, thus

$$\begin{aligned} -dV_t^D = &\sum_{i=1}^{N} \alpha_t^i dH_t^{i,D} + \sum_{j=0}^{N} \eta_t^j dE_t^j + \gamma_t dCDS^D(t,T) + \epsilon_t dCDS^D(t,t+dt) \\ &+ \Omega_t dB_t + d\bar{\beta}_t^D. \end{aligned} \tag{2.22}$$

From Itô's formula for jump-diffusion processes [81] we obtain the variation of V^D from t to $t+dt$:

$$\begin{aligned} dV_t^D = &\frac{\partial V^D}{\partial t}dt + \sum_{i=1}^{N} \frac{\partial V^D}{\partial S^i} dS_t^i + \sum_{j=0}^{N} \frac{\partial V^D}{\partial X^j} dX_t^j + \frac{\partial V^D}{\partial h} dh_t + \Delta V^D dJ_t \\ &+ \left[\frac{1}{2} \sum_{i,k=1}^{N} \rho^{S^i S^k} \sigma^{S^i} \sigma^{S^k} S_t^i S_t^k \frac{\partial^2 V^D}{\partial S^i S^k} + \frac{1}{2} \sum_{j,l=0}^{N} \rho^{X^j X^l} \sigma^{X^j} \sigma^{X^l} X_t^j X_t^l \frac{\partial^2 V^D}{\partial X^j X^l} \right. \\ &+ \frac{1}{2} (\sigma^h h_t)^2 \frac{\partial^2 V^D}{\partial h^2} + \sum_{i=1}^{N} \sum_{j=0}^{N} \rho^{S^i X^j} \sigma^{S^i} \sigma^{X^j} S_t^i X_t^j \frac{\partial^2 V^D}{\partial S^i \partial X^j} \\ &\left. + \sum_{i=1}^{N} \rho^{S^i h} \sigma^{S^i} \sigma^h S_t^i h_t \frac{\partial^2 V^D}{\partial S^i \partial h} + \sum_{j=0}^{N} \rho^{X^j h} \sigma^{X^j} \sigma^h X_t^j h_t \frac{\partial^2 V^D}{\partial X^j \partial h} \right] dt, \end{aligned}$$

where ΔV^D is the variation of V_t^D at default, defined as

$$\Delta V^D = V^D(t, S_t, X_t, h_t, 1) - V^D(t, S_t, X_t, h_t, 0). \tag{2.23}$$

Note that if the counterparty defaults at time t the value of the risky derivative at time t is given by

$$\begin{aligned} V^D(t, S_t, X_t, h_t, 1) = &C^{C_0}(t) X_t^{D,C_0} + R_C \left(M^D(t, S_t, X_t, h_t) - C^{C_0}(t) X_t^{D,C_0} \right)^+ \\ &+ \left(M^D(t, S_t, X_t, h_t) - C^{C_0}(t) X_t^{D,C_0} \right)^-, \end{aligned} \tag{2.24}$$

where $M(t, S_t, X_t, h_t)$ denotes the mark-to-market price and R_C the counterparty's recovery rate. Therefore, the variation of V^D at default can be written as

$$\begin{aligned}\Delta V^D = C^{C_0} X^{D,C_0} + R_C (M^D - C^{C_0} X^{D,C_0})^+ \\ + (M^D - C^{C_0} X^{D,C_0})^- - V^D.\end{aligned} \tag{2.25}$$

Thus, by also taking into account the dynamics of the short term CDS in (1.15) and of the funding account in (1.16), we obtain that the change in Π_t in the infinitesimal interval $[t, t + dt]$ is given by

$$\begin{aligned}
d\Pi_t = &\sum_{i=1}^{N} \alpha_t^i \Bigg(\frac{\partial H^{i,D}}{\partial t} + (r^i - q^i - \rho^{S^i X^i} \sigma^{S^i} \sigma^{X^i}) S_t^i \frac{\partial H^{i,D}}{\partial S^i} + (r^D - r^i) X_t^i \frac{\partial H^{i,D}}{\partial X^i} \\
&\quad + \frac{1}{2} (S_t^i \sigma^{S^i})^2 \frac{\partial^2 H^{i,D}}{\partial (S_t^i)^2} + \frac{1}{2} (X_t^i \sigma^{X^i})^2 \frac{\partial^2 H^{i,D}}{\partial (X^i)^2} \\
&\quad + \rho^{S^i X^i} \sigma^{S^i} \sigma^{X^i} S_t^i X_t^i \frac{\partial^2 H^{i,D}}{\partial S^i \partial X^i} - (r^D + b^{D,C_j}) H^{i,D} \Bigg) dt \\
&+ \sum_{j=0}^{N} \eta^j \left[\frac{\partial E^j}{\partial t} + (r^D - r^j) X_t^j \frac{\partial E^j}{\partial X^j} + \frac{1}{2} (X_t^j \sigma^{X^j})^2 \frac{\partial^2 E^j}{\partial (X^j)^2} - r^D E^j \right] dt \\
&+ \sum_{i=1}^{N} \alpha_t^i \sigma^{S^i} S_t^i \frac{\partial H^{i,D}}{\partial S^i} dW_t^{S^i} \\
&+ \sum_{i=1}^{N} \alpha_t^i \sigma^{X^i} X_t^i \frac{\partial H^{i,D}}{\partial X^i} dW_t^{X^i} + \sum_{j=0}^{N} \eta_t^j \sigma^{X^j} X_t^j \frac{\partial E^j}{\partial X^j} dW_t^{X^j} \\
&+ \gamma_t \left[\frac{\partial CDS^D(t,T)}{\partial t} dt + \frac{\partial CDS^D(t,T)}{\partial h} dh + \frac{1}{2} (\sigma^h h)^2 \frac{\partial^2 CDS^D(t,T)}{\partial h^2} dt \right] \\
&- \gamma_t r^D CDS^D(t,T) dt + \gamma_t \Delta CDS^D(t,T) dJ_t + \epsilon_t \left[h_t dt - (1 - R_C) dJ \right] \\
&- (V_t^D - C_t^{C_0} X^0) f^D dt - (r^D + r^R + s b^{D,C_0}) C_t^{C_0} X_t^{D,C_0} dt.
\end{aligned}$$

Therefore, in order to hedge the risks in the portfolio Π, we choose:

$$\begin{aligned}
\alpha_t^i &= -\frac{\frac{\partial V^D}{\partial S^i}}{\frac{\partial H^{i,D}}{\partial S^i}}, \quad i = 1, \dots, N, \\
\eta_t^0 &= -\frac{\frac{\partial V^D}{\partial X^0}}{\frac{\partial E^0}{\partial X^0}}, \qquad\qquad \eta_t^i = -\frac{\frac{\partial V^D}{\partial X^i} + \alpha_t^i \frac{\partial H^{i,D}}{\partial X^i}}{\frac{\partial E^i}{\partial X^i}}, \quad i = 1, \dots, N, \\
\gamma_t &= \frac{\frac{\partial V^D}{\partial h}}{\frac{\partial CDS^D(t,T)}{\partial h}}, \\
\epsilon_t &= \frac{1}{1-R}\left(\gamma_t \Delta CDS^D(t,T) - \Delta V^D\right).
\end{aligned}$$

Next, we take into account the equations satisfied by $H^{i,D}$, E^j and $CDS^D(t,T)$, which are respectively given by:

$$\begin{aligned}
&\frac{\partial H^{i,D}}{\partial t} + \frac{(S^i\sigma^{S^i})^2}{2}\frac{\partial^2 H^{i,D}}{\partial (S^i)^2} + \frac{(X^i\sigma^{X^i})^2}{2}\frac{\partial^2 H^{i,D}}{\partial (X^i)^2} \\
&\qquad + \rho^{S^iX^i}\sigma^{S^i}\sigma^{X^i}S^iX^i\frac{\partial^2 H^{i,D}}{\partial S^i \partial X^i} + (r^i - q^i - \rho^{S^iX^i}\sigma^{S^i}\sigma^{X^i})S^i\frac{\partial H^{i,D}}{\partial S^i} \\
&\qquad + (r^D - r^i)X^i\frac{\partial H^{i,D}}{\partial X^i} = (r^D + b^{D,C_i})H^{i,D}, \\
&\frac{\partial E^j}{\partial t} + \frac{1}{2}(X^j\sigma^{X^j})^2\frac{\partial^2 E^j}{\partial (X^j)^2} + (r^D - r^j)X^j\frac{\partial E^j}{\partial X^j} = r^D E^j, \\
&\frac{\partial CDS^D(t,T)}{\partial t} + \frac{1}{2}(\sigma^h h)^2\frac{\partial^2 CDS^D(t,T)}{\partial h^2} + (\mu^{h,P} - M^h\sigma^{h,P})\frac{\partial CDS^D(t,T)}{\partial h} \\
&\qquad + \frac{h}{1-R}\Delta CDS^D(t,T) = r^D CDS^D(t,T).
\end{aligned}$$

Finally, from the previous arguments, equation (2.22) turns into

$$\begin{aligned}
&\frac{\partial V^D}{\partial t} + \mathcal{L}_{SXh}V^D \\
&\quad = -\frac{h}{1-R}\Delta V^D + f^D V^D + (r^D + r^R + sb^{D,C_0} - f^D)C^{C_0}X^{D,C_0},
\end{aligned} \tag{2.26}$$

where the differential operator $\mathcal{L}_{SXh}$ is given by

$$\begin{aligned}\mathcal{L}_{SXh} = &\frac{1}{2}\sum_{i,k=1}^{N}\rho^{S^iS^k}\sigma^{S^i}\sigma^{S^k}S^iS^k\frac{\partial^2}{\partial S^i\partial S^k} + \frac{1}{2}\sum_{j,l=0}^{N}\rho^{X^jX^l}\sigma^{X^j}\sigma^{X^l}X^jX^l\frac{\partial^2}{\partial X^j\partial X^l}\\ &+\sum_{i=1}^{N}\sum_{j=0}^{N}\rho^{S^iX^j}\sigma^{S^i}\sigma^{X^j}S^iX^j\frac{\partial^2}{\partial S^i\partial X^j} + \frac{1}{2}(\sigma^h h)^2\frac{\partial^2}{\partial h^2}\\ &+\sum_{i=1}^{N}\rho^{S^ih}\sigma^{S^i}\sigma^h S^ih\frac{\partial^2}{\partial S^i\partial h} + \sum_{j=0}^{N}\rho^{X^jh}\sigma^{X^j}\sigma^h X^jh\frac{\partial^2}{\partial X^j\partial h}\\ &+\sum_{i=1}^{N}(r^i - q^i - \rho^{S^iX^i}\sigma^{S^i}\sigma^{X^i})S^i\frac{\partial}{\partial S^i}\\ &+\sum_{j=0}^{N}(r^D - r^j)X^j\frac{\partial}{\partial X^j} + (\mu^{h,P} - M^h\sigma^{h,P})\frac{\partial}{\partial h}.\end{aligned} \tag{2.27}$$

As in Chapter 1, we choose two possible values for the mark-to-market value M^D in (2.25), either equal to the risky derivative value or equal to the value of the risky-free derivative in terms of counterparty risk. Therefore, from these two possibilities, we get two alternative PDEs models.

- If $M^D = V^D$, the PDE (2.26) turns into:

$$\begin{aligned}&\frac{\partial V^D}{\partial t} + \mathcal{L}_{SXh}V^D - f^DV^D\\ &\qquad = h(V^D - C^{C_0}X^{D,C_0})^+\\ &\qquad\quad + (r^D + r^R + sb^{D,C_0} - f^D)C^{C_0}X^{D,C_0}\,.\end{aligned} \tag{2.28}$$

- If $M^D = W^D$, the PDE (2.26) turns into:

$$\begin{aligned}&\frac{\partial V^D}{\partial t} + \mathcal{L}_{SXh}V^D - \left(\frac{h}{1-R} + f^D\right)V^D\\ &\qquad = h(W^D - C^{C_0}X^{D,C_0})^+ - \frac{h}{1-R_C}W^D\\ &\qquad\quad + (r^D + r^R + sb^{D,C_0} - f^D)C^{C_0}X^{D,C_0}\,.\end{aligned} \tag{2.29}$$

Note that the value of the risk-free derivative, W^D, satisfies the PDE:

$$\frac{\partial W^D}{\partial t} + \mathcal{L}_{S\bar{X}}W^D - f^DW^D = 0,$$

where

$$\begin{aligned}\mathcal{L}_{S\bar{X}} =&\frac{1}{2}\sum_{i,k=1}^{N}\rho^{S^iS^k}\sigma^{S^i}\sigma^{S^k}S^iS^k\frac{\partial^2}{\partial S^i\partial S^k}+\frac{1}{2}\sum_{j,l=1}^{N}\rho^{X^jX^l}\sigma^{X^j}\sigma^{X^l}X^jX^l\frac{\partial^2}{\partial X^j\partial X^l}\\&+\sum_{i,j=1}^{N}\rho^{S^iX^j}\sigma^{S^i}\sigma^{X^j}S^iX^j\frac{\partial^2}{\partial S^i\partial X^j}\\&+\sum_{i=1}^{N}(r^i-q^i-\rho^{S^iX^i}\sigma^{S^i}\sigma^{X^i})S^i\frac{\partial}{\partial S^i}+\sum_{j=1}^{N}(r^D-r^j)X^j\frac{\partial}{\partial X^j}.\end{aligned}\tag{2.30}$$

As both the risky derivative and the risk-free derivative at time T are equal to the payoff G, i.e.,

$$W^D(T,S,\bar{X})=V^D(T,S,X,h)=G(S,X),$$

then the total value adjustment U at maturity T is zero.

Therefore, by taking into account the equations satisfied by the risky and risk-free derivatives, we obtain the following alternative PDE problems satisfied by the total value adjustment.

- If $M^D=V^D$ the XVA is the solution of the nonlinear PDE problem:

$$\begin{cases}\frac{\partial U}{\partial t}+\mathcal{L}_{SXh}U-f^DU\\\qquad=h(W^D+U-C^{C_0}X^{D,C_0})^+\\\qquad\quad+(r^D+r^R+sb^{D,C_0}-f^D)C^{C_0}X^{D,C_0},\\U(T,S,X,h)=0.\end{cases}\tag{2.31}$$

- If $M^D=W^D$ the XVA is the solution of the linear PDE problem:

$$\begin{cases}\frac{\partial U}{\partial t}+\mathcal{L}_{SXh}U-\left(\frac{h}{1-R}+f^D\right)U\\\qquad=h(W^D-C^{C_0}X^{D,C_0})^+\\\qquad\quad+(r^D+r^R+sb^{D,C_0}-f^D)C^{C_0}X^{D,C_0},\\U(T,S,X,h)=0.\end{cases}\tag{2.32}$$

In both cases, the PDEs are posed in the unbounded domain

$$D = \{(t, S, X, h) \in [0, T) \times (0, +\infty)^N \times (0, +\infty)^{(N+1)} \times (0, +\infty)\}.$$

Note that the PDE model inferred in this section has the same structure as the one in Chapter 1. The difference between the two models lies in the fact that here we have $N + 1$ extra stochastic factors, namely $X^{D,C_0}, X^{D,C_1}, \ldots, X^{D,C_N}$, which are assumed to be constant in Chapter 1. Thus, the new model that incorporates the more realistic approach by considering stochastic foreign exchange rates also involves much higher spatial dimension in the PDEs problems. Therefore, when trying to solve these PDEs formulations by means of standard finite differences or finite element methods, the *curse of dimensionality* comes into place in a more relevant way. Thus, in the next section, we formulate the XVA problems in terms of expectations and then apply Monte Carlo techniques to approximate the XVA. In the nonlinear case we use Picard iteration or multilevel Picard iteration methods.

2.3 Formulation in terms of expectations

In order to apply Picard iteration methods based on Monte Carlo simulation techniques, we follow the same approach as in Chapter 1 and we first apply appropriate Feynman-Kac formulae for the nonlinear [14] and linear [81] PDEs to obtain their equivalent formulations in terms of expectations.

Thus, after applying the previously indicated Feynman-Kac formulae, we get two alternative integral equations.

- If $M^D = V^D$, the total value adjustment at time t is given by:

$$\begin{aligned} U(t, S_t, X_t, h_t) = \mathrm{E}_t^Q \Bigg[& - \int_t^T e^{-f^D(u-t)} \\ & \cdot \Big(h_u \left(W^D(u, S_u, \bar{X}_u) + U(u, S_u, X_u, h_u) - C^{C_0}(u) X_u^{D,C_0} \right)^+ \\ & + \left(r^D + r^R + s b^{D,C_0} - f^D \right) C^{C_0}(u) X_u^{D,C_0} \Big) du \Bigg], \end{aligned} \tag{2.33}$$

so that the XVA value at time $t = 0$ (also referred to as XVA price), is:

$$U(0, S_0, X_0, h_0) = \mathrm{E}_0^Q \Bigg[- \int_0^T e^{-f^D u} \cdot \Big(h_u \Big(W^D(u, S_u, \bar{X}_u) + U(u, S_u, X_u, h_u) - C^{C_0}(u) X_u^{D,C_0} \Big)^+ + \Big(r^D + r^R + sb^{D,C_0} - f^D \Big) C^{C_0}(u) X_u^{D,C_0} \Big) du \Bigg]. \tag{2.34}$$

- If $M^D = W^D$, the total value adjustment at time t is given by:

$$U(t, S_t, X_t, h_t) = \mathrm{E}_t^Q \Bigg[- \int_t^T \exp\left(- \int_t^u \left(\frac{h_r}{1-R} + f^D \right) dr \right) \cdot \Big(h_u \Big(W^D(u, S_u, \bar{X}_u) - C^{C_0}(u) X_u^{D,C_0} \Big)^+ + \Big(r^D + r^R + sb^{D,C_0} - f^D \Big) C^{C_0}(u) X_u^{D,C_0} \Big) du \Bigg]. \tag{2.35}$$

Therefore, the XVA price is:

$$U(0, S_0, X_0, h_0) = \mathrm{E}_0^Q \Bigg[- \int_0^T \exp\left(- \int_0^u \left(\frac{h_r}{1-R} + f^D \right) dr \right) \cdot \Big(h_u \Big(W^D(u, S_u, \bar{X}_u) - C^{C_0}(u) X_u^{D,C_0} \Big)^+ + \Big(r^D + r^R + sb^{D,C_0} - f^D \Big) C^{C_0}(u) X_u^{D,C_0} \Big) du \Bigg]. \tag{2.36}$$

2.4 Numerical methods

In this section, we introduce the numerical methods proposed to compute the total value adjustment both in the nonlinear and in the linear case. In particular, we adapt the Monte Carlo and multilevel Picard iteration methodologies introduced in Chapter 1 to the model with stochastic FX rates.

2.4.1 Monte Carlo method

In order to numerically approximate the XVA value in both the nonlinear case (2.34) and the linear case (2.36), we first introduce a time discretization based on a uniform

mesh with Z time nodes $t_Z = z\Delta t,\ z = 0, \ldots, Z-1$, the constant $\Delta t = T/(Z-1)$ being the time step.

Taking into account the previous time mesh, we can discretize the dynamics of the underlying assets S^i (for $i = 1, \ldots, N$), the FX rates X^j (for $j = 0, \ldots, N$) and the investor's credit spread h by using the Euler-Maruyama scheme [65]. Thus, for $z = 0, \ldots, Z-2$, we consider the iterative procedure:

$$\begin{aligned} S^i_{z+1} &= S^i_z + (r^i - q^i - \rho^{S^i X^i}\sigma^{S^i}\sigma^{X^i})S^i_z\Delta t + \sigma^{S^i} S^i_z \Delta W^{S^i}_{z+1}\,, \\ X^j_{z+1} &= X^j_z + (r^D - r^j)X^j_z\Delta t + \sigma^{X^j} X^j_z \Delta W^{X^j}_{z+1}\,. \end{aligned}$$

As already stated in Chapter 1, in the case of the exponential Vasicek dynamics the credit spread dynamics is approximated by the Euler-Maruyama scheme given by

$$h_{z+1} = e^{\tilde{h}_{z+1}}\,, \quad \text{with} \quad \tilde{h}_{z+1} = \tilde{h}_z + \alpha(\theta - \tilde{h}_z)\Delta t + \sigma^h \Delta W^h_z\,,$$

whereas in the case of the CIR model the credit spread is approximated by the "full truncation" scheme proposed in [30] and given by

$$h_{z+1} = h_z + \alpha(\theta - h^+_z)\Delta t + \sigma^h \sqrt{h^+_z}\Delta W^h_z\,.$$

The quantities $\Delta W^{S^i}_{z+1} = W^{S^i}_{z+1} - W^{S^i}_z$, for $i = 1, \ldots, N$, $\Delta W^{X^j}_{z+1} = W^{X^j}_{z+1} - W^{X^j}_z$, for $j = 0, \ldots, N$, and $\Delta W^h_{z+1} = W^h_{z+1} - W^h_z$ are increments of the corresponding Brownian motions, which are correlated according to the correlation matrix (2.4).

In both cases (2.34) and (2.36), the computation of XVA value requires integral approximation techniques by numerical quadrature formulae. In next paragraphs we describe the different methods we have used in the nonlinear and linear cases.

Nonlinear case ($M^D = V^D$)

We denote by I^{NL} the integral in the right hand side of (2.34), i.e.,

$$\begin{aligned} I^{NL} = \int_0^T e^{-f^D u} \Bigg(& h_u \left(W^D(u, S_u, \bar{X}_u) + U(u, S_u, X_u, h_u) - C^{C_0}(u) X^{D,C_0}_u \right)^+ \\ & + \left(r^D + r^R + s b^{D,C_0} - f^D \right) C^{C_0}(u) X^{D,C_0}_u \Bigg) du. \end{aligned} \tag{2.37}$$

We will approximate the integral by using the simple rectangular formula, as follows:

$$\begin{aligned} I^{NL} \simeq & T\Bigg(h_0\left(W_0^D + U_0 - C_0^{C_0} X_0^{D,C_0}\right)^+ \\ & + \left(r^D + r^R + sb^{D,C_0} - f^D\right) C_0^{C_0} X_0^{D,C_0}\Bigg), \end{aligned} \tag{2.38}$$

or the simple trapezoidal formula:

$$\begin{aligned} I^{NL} \simeq & \frac{T}{2}\Bigg(e^{-f^D T}\Bigg(h_T\left(W_T^D - C_T^{C_0} X_T^{D,C_0}\right)^+ \\ & + \left(r^D + r^R + sb^{D,C_0} - f^D\right) C_T^{C_0} X_T^{D,C_0}\Bigg) \\ & + h_0\left(W_0^D + U_0 - C_0^{C_0} X_0^{D,C_0}\right)^+ \\ & + \left(r^D + r^R + sb^{D,C_0} - f^D\right) C_0^{C_0} X_0^{D,C_0}\Bigg). \end{aligned} \tag{2.39}$$

Since (2.34) is an integral equation, the implementation of a fixed-point method (Picard iteration method) is required to compute the XVA price. Thus, starting from $U^0 = 0$, both in the case of the simple rectangular formula or the simple trapezoidal formula we respectively consider the iteration procedure:

$$\begin{aligned} U^{l+1}(0, S_0, X_0, h_0) = & TE_0^{Q^D}\Bigg[h_0\left(W_0^D + U_0^l - C_0^{C_0} X_0^{D,C_0}\right)^+ \\ & + \left(r^D + r^R + sb^{D,C_0} - f^D\right) C_0^{C_0} X_0^{D,C_0}\Bigg], \end{aligned} \tag{2.40}$$

or

$$\begin{aligned} U^{l+1}(0, S_0, X_0, h_0) = & \frac{T}{2} E_0^{Q^D}\Bigg[e^{-f^D T}\Bigg(h_T\left(W^D(T, S_T, \bar{X}_T) - C_T^{C_0} X_T^{D,C_0}\right)^+ \\ & + \left(r^D + r^R + sb^{D,C_0} - f^D\right) C_T^{C_0} X_T^{D,C_0}\Bigg) \\ & + h_0\left(W_0^D + U_0^l - C_0^{C_0} X_0^{D,C_0}\right)^+ \\ & + \left(r^D + r^R + sb^{D,C_0} - f^D\right) C_0^{C_0} X_0^{D,C_0}\Bigg], \end{aligned} \tag{2.41}$$

for $l = 0, 1, 2, \ldots$, until a convergence test with a prescribed tolerance is fulfilled.

Note that in the nonlinear case we consider only simple rectangular and simple trapezoidal formulae due to the fact that the use of composite formulae requires to know the values of U at intermediate time nodes, but we only know the final value of U, that is, U is null at the final node $t_{Z-1} = T$. Therefore, one could approximate the value of U at each node going backwards from the last node, although in this way a nested Monte Carlo problem arises.

Besides the previously described Picard iteration methods for the nonlinear model, we have also coded and applied to the nonlinear case the multilevel Picard iteration method proposed in [37] and recalled in Subsection 2.4.2. Note that this method is also applied in [37] to a special case of the model in [22] to obtain the CVA in a single currency setting. In Section 2.5 we will include the comparison between the results of the previously described Picard iteration methods and the multilevel Picard iteration.

Linear case ($M^D = W^D$)

In this case, we denote by I^L the integral in the right hand side of (2.36), i.e.,

$$\begin{aligned} I^L = \int_0^T & e^{-\int_0^u \left(\frac{h_r}{1-R} + f^D\right) dr} \\ & \cdot \left(h_u \left(W^D(u, S_u, \bar{X}_u) - C^{C_0}(u) X_u^{D,C_0} \right)^+ \right. \\ & \left. + \left(r^D + r^R + sb^{D,C_0} - f^D \right) C^{C_0}(u) X_u^{D,C_0} \right) du, \end{aligned} \tag{2.42}$$

and approximate the integral by using either the rectangular or the trapezoidal formulae. The simple and the composite rectangular formulae are respectively given by:

$$\begin{aligned} I^L \simeq\ & T \exp\left(-T \left(\frac{h_T}{1-R} + f^D \right) \right) \\ & \cdot \left(h_T \left(W_T^D - C_T^{C_0} X_T^{D,C_0} \right)^+ + \left(r^D + r^R + sb^{D,C_0} - f^D \right) C_T^{C_0} X_T^{D,C_0} \right), \end{aligned} \tag{2.43}$$

and

$$
\begin{aligned}
I^L \simeq\ & \Delta t \sum_{z_1=0}^{Z-2} \exp\left(-\Delta t \sum_{z_2=0}^{z_1-1}\left(\frac{h_{t_{z_2}}}{1-R}+f^D\right)\right) \\
& \cdot \left(h_{t_{z_1}}\left(W^D_{t_{z_1}}-C^{C_0}_{t_{z_1}}X^{D,C_0}_{t_{z_1}}\right)^+ + \left(r^D+r^R+sb^{D,C_0}-f^D\right)C^{C_0}_{t_{z_1}}X^{D,C_0}_{t_{z_1}}\right).
\end{aligned}
\tag{2.44}
$$

Instead, the simple and the composite trapezoidal formulae are respectively given by:

$$
\begin{aligned}
I^L \simeq\ & \frac{T}{2}\left[\exp\left(-\frac{T}{2}\left(\frac{h_T+h_0}{1-R}+2f^D\right)\right)\right. \\
& \cdot \left(h_T\left(W^D_T-C^{C_0}_T X^{D,C_0}_T\right)^+ + \left(r^D+r^R+sb^{D,C_0}-f^D\right)C^{C_0}_T X^{D,C_0}_T\right) \\
& \left.+\left(h_0\left(W^D_0-C^{C_0}_0 X^{D,C_0}_0\right)^+ + \left(r^D+r^R+sb^{D,C_0}-f^D\right)C^{C_0}_0 X^{D,C_0}_0\right)\right]
\end{aligned}
\tag{2.45}
$$

and

$$
\begin{aligned}
I^L \simeq\ & \frac{\Delta t}{2}\sum_{z_1=0}^{Z-2}\left[\exp\left(-\frac{\Delta t}{2}\sum_{z_2=0}^{z_1-1}\left(\frac{h_{t_{z_2}}+h_{t_{z_2+1}}}{1-R}+2f^D\right)\right)\right. \\
& \cdot \left(h_{t_{z_1}}\left(W^D_{t_{z_1}}-C^{C_0}_{t_{z_1}}X^{D,C_0}_{t_{z_1}}\right)^+\right. \\
& \left.+\left(r^D+r^R+sb^{D,C_0}-f^D\right)C^{C_0}_{t_{z_1}}X^{D,C_0}_{t_{z_1}}\right) \\
& +\exp\left(-\frac{\Delta t}{2}\sum_{z_2=0}^{z_1}\left(\frac{h_{t_{z_2}}+h_{t_{z_2+1}}}{1-R}+2f^D\right)\right) \\
& \cdot \left(h_{t_{z_1+1}}\left(W^D_{t_{z_1+1}}-C^{C_0}_{t_{z_1+1}}X^{D,C_0}_{t_{z_1+1}}\right)^+\right. \\
& \left.\left.+\left(r^D+r^R+sb^{D,C_0}-f^D\right)C^{C_0}_{t_{z_1+1}}X^{D,C_0}_{t_{z_1+1}}\right)\right].
\end{aligned}
\tag{2.46}
$$

2.4.2 Multilevel Picard iteration

As in Chapter 1, we use multilevel Picard iteration method (MPI) to approximate the solution of the nonlinear model. Therefore, we extend the approach in Section 1.4.3 to the case of the model with stochastic FX rates, so that the function Φ is now

given by

$$
\begin{aligned}
(\Phi(\mathfrak{u}))(s,x) = \mathrm{E}_s^Q\Bigg[& -\int_s^T e^{-f^D(t-s)} \\
& \Big(h_t\left(W^D(t,S_t,\bar{X}_t) + \mathfrak{u} - C^{C_0}(t)X_t^{D,C_0}\right)^+ \\
& + \left(r^D + r^R + sb^{D,C_0} - f^D\right) C^{C_0}(t)X_t^{D,C_0}\Big)dt \,\Big|\, x = (S_s, X_s, h_s)\Bigg].
\end{aligned} \tag{2.47}
$$

Accordingly, the discrete approximation of $\Phi(\mathfrak{u}_l)$ with $m_{n,l,\rho}$ Monte Carlo paths is given by

$$
\begin{aligned}
(\Psi_{n,\rho}(\mathfrak{u}_l))(s,x) = & -\frac{1}{m_{n,l,\rho}} \sum_{i=1}^{m_{n,l,\rho}} \sum_{t\in[s,T]} q_s^{n,l,\rho}(t) \\
& \cdot e^{-f^D(t-s)}\Big(h_t^{i,n,x}\left(W^D(t,S_t^{i,n,x},\bar{X}_t^{i,n,x}) + \mathfrak{u}_l - C^{C_0}(t)X_t^{D,C_0}\right)^+ \\
& + \left(r^D + r^R + sb^{D,C_0} - f^D\right) C^{C_0}(t)\left(X_t^{D,C_0}\right)^{i,n,x}\Big),
\end{aligned} \tag{2.48}
$$

where $(q^{n,l,\rho})_{n,l,\rho\in\mathbb{N}_0,l<n}$ denotes the family of quadrature rules for the approximation of the integral and the superscripts i,n,x refer to the i-th Monte Carlo path with initial point x in the n-th Picard iteration. In particular, in our numerical examples we have chosen $m_{n,l,\rho} = \rho^{n-l}$ with $\rho_{max} = 4$ or $\rho_{max} = 5$ and we show the mean over $N_{runs} = 10$.

2.5 Numerical results

In this section we present some results obtained by using the Monte Carlo and multilevel Picard iteration techniques. More precisely, we consider the pricing of some multiasset derivatives written on underlying assets denominated in different currencies [83], taking into account counterparty risk. Moreover, we obtain the corresponding total valuation adjustment (XVA) associated to the derivatives.

In particular, when applying the Monte Carlo method, we use different quadrature formulae to approximate integrals involved in the expressions of XVA price (2.34) and

(2.36) and analyse how this affects the 99% confidence intervals for the total value adjustment, as well as the elapsed computational time. Moreover, we are interested in how different choices of the initial values of the underlying assets, of the mark-to-market value M^D, and of the FX rates volatilities, affect both the risky derivative and the XVA prices. Also, we choose the collateral value to be a percentage $C^{\%}$ of the risk-free derivative value and analyse how the choice of the value of $C^{\%}$ affects the risky derivative and the XVA prices. Unless otherwise specified, we set $C^{\%} = 0.25$.

As regards to the Monte Carlo method, for the linear case and the nonlinear case with Picard iteration method we have set the number of simulations equal to 10^4 and the number of time nodes in the discretized dynamics of the involved processes to $Z = 252$.

We have also applied to all forthcoming numerical examples the multilevel Picard iteration method to solve the nonlinear model. More precisely, for the numerical solution with multilevel Picard iteration we have considered the Picard parameter ρ either equal to 4 or 5 and the number of Picard iterations $k = \rho$. At each Picard iteration l, we consider a composite rectangular quadrature formula with ρ^{k-l} rectangles and a number of Monte Carlo paths $m_{k,l,\rho} = \rho^{k-l}$, for $l = 1, \ldots, k$. Moreover, as also suggested in [37], we consider 10 runs of the multilevel Picard iteration method with the previous configuration to obtain the mean values we report in the corresponding tables for each numerical example.

In all forthcoming numerical examples, we have fixed the maturity T to 1 year.

Unless otherwise stated, we have used data listed in Table 2.1 and in Table 2.2. We have denoted by $r = (r^0, r^1, r^2)$ the vector of the short-term rates in the foreign markets, $q = (q^1, q^2)$ the vector of the dividends paid by the corresponding underlying assets, $\sigma^S = (\sigma^{S^1}, \sigma^{S^2})$ the vector of the assets volatilities, $X_0 = (X_0^{D,C_0}, X_0^{D,C_1}, X_0^{D,C_2})$ the vector of initial FX rates values, and $\sigma^X = (\sigma^{X^0}, \sigma^{X^1}, \sigma^{X^2})$ the vector of the FX rates volatilities. In all forthcoming tables and plots we use the notation $S^{i,D} = X^{D,C_i} S^i$, for $i = 1, 2$, so that we can consider all the prices in the same currency D.

All the described numerical methods for the examples have been implemented

$r = (0.035, 0.05, 0.03)$	$X_0 = (0.13, 0.89, 1.12)$	$f^D = 0.060$	$R_C = 0.30$
$q = (0.03, 0.02)$	$\sigma^X = (0.38, 0.40, 0.35)$	$b^{D,C_0} = 0.010$	
$\sigma^S = (0.30, 0.20)$		$r^D = 0.040$	
		$r^R = 0.042$	

Table 2.1: Financial data

Exp Vasicek	$h_0 = 200$	$\alpha = 4.97$	$\theta = 3.83$	$\sigma^h = 1.41$
CIR	$h_0 = 200$	$\alpha = 1.29$	$\theta = 51.79$	$\sigma^h = 4.50$

Table 2.2: Counterparty's credit spread data. Values are in basis points (bps)

from scratch in Matlab codes on an Intel(R) Core(TM) i7-8550U, 1.99 GHz, 16 GB (RAM), x64-based processor.

2.5.1 Spread option

First, we consider the *spread option* as in Section 1.5 to analyse how the introduction of stochasticity in the FX rates affects the total value adjustment. In particular, we consider:

- the model in the Chapter 1 with constant FX rates and the collateral in cash in a foreign currency C_0;
- the extension of the model in Chapter 1 to stochastic FX rates, keeping the collateral in cash;
- the model in this chapter, where the FX rates are stochastic and the collateral is made up of bonds in currency C_0.

Test 1: Comparison between constant and stochastic FX rates models.

Tables 2.3 and 2.4 report the comparison between the different models for the non-linear case, whereas tables 2.5 and 2.6 show the confidence intervals for the linear case.

Total value adjustment			
	MPI with $\rho = 4$		
FX rates Collateral $(S^{1,D}, S^{2,D})$	constant cash	stochastic cash	stochastic bonds
$(9, 21)$	-0.0018	-0.0078	-0.0127
$(9, 24)$	-0.0050	-0.0124	-0.0202
$(9, 27)$	-0.0105	-0.0176	-0.0287
$(12, 24)$	-0.0025	-0.0102	-0.0166
$(12, 27)$	-0.0056	-0.0139	-0.0227
$(12, 30)$	-0.0110	-0.0199	-0.0323
$(15, 27)$	-0.0035	-0.0117	-0.0192
$(15, 30)$	-0.0066	-0.0167	-0.0274
$(15, 33)$	-0.0116	-0.0226	-0.0367
$(18, 30)$	-0.0039	-0.0133	-0.0216
$(18, 33)$	-0.0074	-0.0174	-0.0286
$(18, 36)$	-0.0121	-0.0237	-0.0385
$(21, 33)$	-0.0046	-0.0153	-0.0248
$(21, 36)$	-0.0082	-0.0205	-0.0332
$(21, 39)$	-0.0131	-0.0246	-0.0402

Table 2.3: Spread option, nonlinear problem and exponential Vasicek credit spread. Multilevel Picard iteration (MPI) results. Total value adjustment (Test 1)

In particular, for the nonlinear case we report the multilevel Picard iteration values with $\rho = 4$ and for the linear case we consider the 99% Monte Carlo confidence intervals with the composite trapezoidal quadrature formula.

As expected and observed in tables 2.3 to 2.4, when assuming constant FX rates (therefore, neglecting FX risk), the pricing models underestimates the total value adjustment with respect to the model with the more realistic assumption of stochastic FX rates, both in the nonlinear and in the linear cases.

Moreover, in this setting, we can see that the choice of the collateral made up of bonds makes the XVA more negative with respect to the alternative choice of the collateral in cash.

2.5.2 Option on the maximum

We now assume that the default-free hedger buys from the defaultable counterparty an *option on the maximum* of two underlying assets: the price of the first one, S^1, is denominated in the foreign currency C_1, while the price of the second one, S^2, is

Total value adjustment			
	MPI with $\rho = 4$		
FX rates Collateral $(S^{1,D}, S^{2,D})$	constant cash	stochastic cash	stochastic bonds
$(9, 21)$	-0.0055	-0.0209	-0.0257
$(9, 24)$	-0.0142	-0.0332	-0.0410
$(9, 27)$	-0.0291	-0.0474	-0.0585
$(12, 24)$	-0.0076	-0.0273	-0.0336
$(12, 27)$	-0.0164	-0.0373	-0.0461
$(12, 30)$	-0.0311	-0.0535	-0.0659
$(15, 27)$	-0.0102	-0.0316	-0.0390
$(15, 30)$	-0.0192	-0.0452	-0.0559
$(15, 33)$	-0.0330	-0.0601	-0.0741
$(18, 30)$	-0.0115	-0.0355	-0.0437
$(18, 33)$	-0.0215	-0.0474	-0.0586
$(18, 36)$	-0.0347	-0.0633	-0.0780
$(21, 33)$	-0.0137	-0.0408	-0.0503
$(21, 36)$	-0.0239	-0.0546	-0.0672
$(21, 39)$	-0.0374	-0.0664	-0.0820

Table 2.4: Spread option, nonlinear problem and CIR credit spread. Multilevel Picard iteration (MPI) results. Total value adjustment (Test 1)

Total value adjustment			
	Monte Carlo with CompT		
FX rates Collateral $(S^{1,D}, S^{2,D})$	constant cash	stochastic cash	stochastic bonds
$(9, 21)$	$[-0.0021, -0.0018]$	$[-0.0083, -0.0074]$	$[-0.0135, -0.0121]$
$(9, 24)$	$[-0.0054, -0.0050]$	$[-0.0130, -0.0118]$	$[-0.0211, -0.0192]$
$(9, 27)$	$[-0.0107, -0.0100]$	$[-0.0186, -0.0171]$	$[-0.0301, -0.0278]$
$(12, 24)$	$[-0.0028, -0.0025]$	$[-0.0102, -0.0091]$	$[-0.0166, -0.0149]$
$(12, 27)$	$[-0.0062, -0.0057]$	$[-0.0150, -0.0136]$	$[-0.0243, -0.0222]$
$(12, 30)$	$[-0.0113, -0.0106]$	$[-0.0205, -0.0188]$	$[-0.0333, -0.0307]$
$(15, 27)$	$[-0.0035, -0.0031]$	$[-0.0122, -0.0109]$	$[-0.0197, -0.0178]$
$(15, 30)$	$[-0.0071, -0.0065]$	$[-0.0170, -0.0155]$	$[-0.0276, -0.0252]$
$(15, 33)$	$[-0.0120, -0.0113]$	$[-0.0225, -0.0207]$	$[-0.0365, -0.0337]$
$(18, 30)$	$[-0.0043, -0.0039]$	$[-0.0142, -0.0127]$	$[-0.0230, -0.0208]$
$(18, 33)$	$[-0.0080, -0.0073]$	$[-0.0191, -0.0174]$	$[-0.0310, -0.0283]$
$(18, 36)$	$[-0.0128, -0.0120]$	$[-0.0246, -0.0226]$	$[-0.0398, -0.0367]$
$(21, 33)$	$[-0.0051, -0.0046]$	$[-0.0162, -0.0146]$	$[-0.0263, -0.0238]$
$(21, 36)$	$[-0.0088, -0.0082]$	$[-0.0212, -0.0193]$	$[-0.0344, -0.0314]$
$(21, 39)$	$[-0.0136, -0.0128]$	$[-0.0267, -0.0245]$	$[-0.0432, -0.0398]$

Table 2.5: Spread option, linear problem and exponential Vasicek credit spread. Monte Carlo with composite trapezoidal quadrature formula results. Total value adjustment (Test 1)

Total value adjustment			
	Monte Carlo with CompT		
FX rates Collateral $(S^{1,D}, S^{2,D})$	constant cash	stochastic cash	stochastic bonds
$(9, 21)$	$[-0.0069, -0.0061]$	$[-0.0221, -0.0197]$	$[-0.0272, -0.0244]$
$(9, 24)$	$[-0.0175, -0.0162]$	$[-0.0345, -0.0315]$	$[-0.0426, -0.0389]$
$(9, 27)$	$[-0.0335, -0.0317]$	$[-0.0492, -0.0454]$	$[-0.0607, -0.0560]$
$(12, 24)$	$[-0.0092, -0.0083]$	$[-0.0271, -0.0243]$	$[-0.0334, -0.0300]$
$(12, 27)$	$[-0.0203, -0.0188]$	$[-0.0397, -0.0363]$	$[-0.0490, -0.0448]$
$(12, 30)$	$[-0.0359, -0.0339]$	$[-0.0543, -0.0501]$	$[-0.0670, -0.0619]$
$(15, 27)$	$[-0.0118, -0.0106]$	$[-0.0322, -0.0291]$	$[-0.0398, -0.0359]$
$(15, 30)$	$[-0.0231, -0.0214]$	$[-0.0451, -0.0412]$	$[-0.0557, -0.0509]$
$(15, 33)$	$[-0.0384, -0.0362]$	$[-0.0596, -0.0550]$	$[-0.0735, -0.0679]$
$(18, 30)$	$[-0.0145, -0.0131]$	$[-0.0375, -0.0340]$	$[-0.0463, -0.0419]$
$(18, 33)$	$[-0.0260, -0.0242]$	$[-0.0506, -0.0463]$	$[-0.0624, -0.0571]$
$(18, 36)$	$[-0.0411, -0.0387]$	$[-0.0650, -0.0600]$	$[-0.0802, -0.0741]$
$(21, 33)$	$[-0.0172, -0.0157]$	$[-0.0430, -0.0390]$	$[-0.0530, -0.0481]$
$(21, 36)$	$[-0.0290, -0.0269]$	$[-0.0561, -0.0514]$	$[-0.0692, -0.0634]$
$(21, 39)$	$[-0.0439, -0.0413]$	$[-0.0705, -0.0651]$	$[-0.0870, -0.0803]$

Table 2.6: Spread option, linear problem and CIR credit spread. Monte Carlo with composite trapezoidal quadrature formula results. Total value adjustment (Test 1)

denominated in the foreign currency C_2. The payoff function is given by:

$$G\left(t, S_t^1, S_t^2, X_t^{D,C_1}, X_t^{D,C_2}\right) = \left(\max\left(S_t^1 X_t^{D,C_1}, S_t^2 X_t^{D,C_2}\right) - K\right)^+, \tag{2.49}$$

where K denotes the strike value in domestic currency D, which is set to $K = 15$ in the numerical tests.

First, we consider the risk-free value that is independent of the choice of the mark-to-market value and of the credit spread dynamics.

For a fixed initial value of the first underlying asset, namely $S^{1,D} = 20$, we choose different initial values for the second one. Table 2.7 shows the 99% Monte Carlo confidence intervals for the risk-free value, which increases by increasing $S^{2,D}$.

Test 2: Nonlinear problem.

As regard to the nonlinear case with both exponential Vasicek and CIR dynamics for the credit spread, results are respectively reported in Table 2.8 and Table 2.9. We show the 99% Monte Carlo confidence intervals with simple quadrature formulae for the approximation of the integral in the XVA formula (2.34) and the multilevel

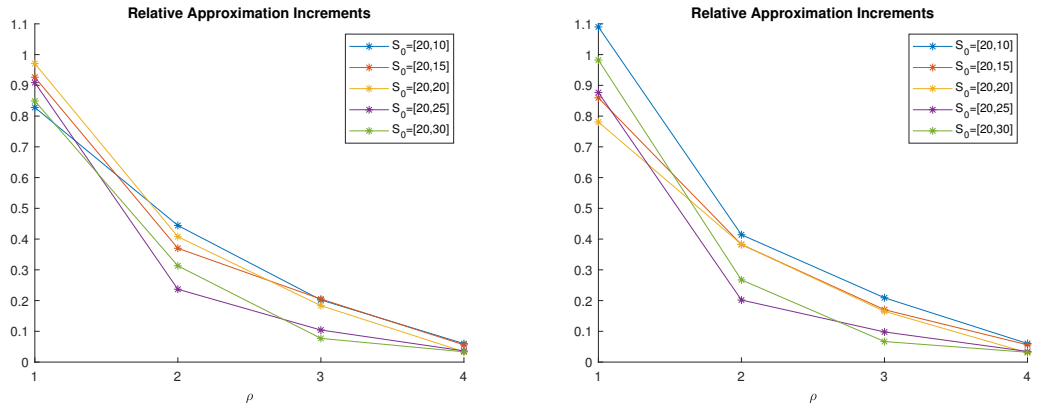

Figure 2.2: Option on the maximum. Convergence of the MPI with exponential Vasicek dynamics for credit spread on the left and CIR dynamics on the right.

Picard iteration values with $\rho = 4$ and $\rho = 5$, that we take as reference values. The relative approximation increments $RAI(\rho, \rho_{max}, N_{runs})$, for $\rho = 1, \ldots, 4$ and $\rho_{max} = 5$, are plotted in Figure 2.2. As already observed in the numerical results reported in Chapter 1, the simple quadrature formulae lead to an overestimation, in absolute terms, of the total value adjustment. Under both assumptions for the credit spread dynamics, we obviously obtain the same trend: the total value adjustment becomes more and more negative by increasing the initial price of S^2.

Figure 2.3 represents the total value adjustment with the exponential Vasicek and CIR dynamics for the credit spread for different initial values of the two underlying assets. Independently from the assets initial values, the XVA is negative, because the counterparty may default and, therefore, owes the hedger a reduction in the derivative price. Also, we can notice that under the assumption that the credit spread follows a CIR process the XVA is more negative.

Test 3: Linear problem.

We now assume the mark-to-market value is equal to the risk-free derivative value (linear problem).

Table 2.10 and Table 2.11 respectively show the Monte Carlo confidence intervals

Risk-free value	
$(S^{1,D}, S^{2,D})$	Monte Carlo
$(20, 10)$	$[6.5341, 7.0290]$
$(20, 15)$	$[7.7317, 8.2306]$
$(20, 20)$	$[10.0689, 10.6005]$
$(20, 25)$	$[13.2448, 13.8434]$
$(20, 30)$	$[16.9727, 17.6632]$

Table 2.7: Option on the maximum. Monte Carlo confidence intervals. Risk-free value

Total value adjustment				
	Monte Carlo		MPI	
$(S^{1,D}, S^{2,D})$	SimpR	SimpT	$\rho = 4$	$\rho = 5$
$(20, 10)$	$[-0.0989, -0.0919]$	$[-0.0603, -0.0560]$	-0.0314	-0.0310
$(20, 15)$	$[-0.1156, -0.1085]$	$[-0.0706, -0.0663]$	-0.0378	-0.0363
$(20, 20)$	$[-0.1486, -0.1410]$	$[-0.0908, -0.0862]$	-0.0464	-0.0476
$(20, 25)$	$[-0.1938, -0.1853]$	$[-0.1186, -0.1134]$	-0.0614	-0.0618
$(20, 30)$	$[-0.2471, -0.2372]$	$[-0.1513, -0.1453]$	-0.0781	-0.0800

Table 2.8: Option on the maximum, nonlinear problem and exponential Vasicek credit spread. Comparison of Monte Carlo (with simple rectangular (SimpR) and trapezoidal (SimpT) quadrature formulae) and multilevel Picard iteration (MPI). Total value adjustment (Test 2)

Total value adjustment				
	Monte Carlo		MPI	
$(S^{1,D}, S^{2,D})$	SimpR	SimpT	$\rho = 4$	$\rho = 5$
$(20, 10)$	$[-0.0989, -0.0919]$	$[-0.0708, -0.0658]$	-0.0638	-0.0624
$(20, 15)$	$[-0.1156, -0.1085]$	$[-0.0828, -0.0778]$	-0.0765	-0.0730
$(20, 20)$	$[-0.1486, -0.1410]$	$[-0.1066, -0.1012]$	-0.0939	-0.0960
$(20, 25)$	$[-0.1938, -0.1853]$	$[-0.1391, -0.1331]$	-0.1242	-0.1245
$(20, 30)$	$[-0.2471, -0.2372]$	$[-0.1775, -0.1706]$	-0.1583	-0.1611

Table 2.9: Option on the maximum, nonlinear problem and CIR credit spread. Comparison of Monte Carlo (with simple rectangular (SimpR) and trapezoidal (SimpT) quadrature formulae) and multilevel Picard iteration (MPI). Total value adjustment (Test 2)

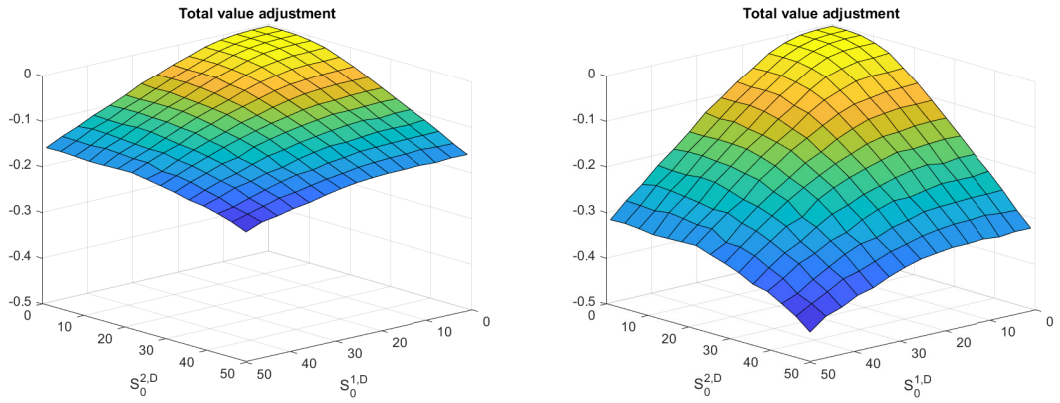

Figure 2.3: Option on the maximum in the nonlinear case. Total value adjustment with exponential Vasicek credit spread on the left and with CIR credit spread on the right (Test 2)

for the total value adjustment in case of exponential Vasicek and CIR credit spread. Again, the simple quadrature formulae do not approximate well the XVA compared to the composite ones. The composite rectangular and trapezoidal formulae provide closer results.

We also plot the risky price and the total value adjustment in Figure 2.4. We can see that the XVA tends to more negative values when increasing the initial values of one or both the underlying assets, namely when the option on the maximum is more valuable.

2.5.3 Best of put/put option

In this example, we assume that the hedger buys from the counterparty a *best of put/put option*, the payoff of which is given by:

$$G\left(t, S_t^1, S_t^2, X_t^{D,C_1}, X_t^{D,C_2}\right) = \max\left(\left(K^1 - S_t^1 X_t^{D,C_1}\right)^+, \left(K^2 - S_t^2 X_t^{D,C_2}\right)^+\right), \tag{2.50}$$

where S_t^1 and S_t^2 are the prices of the two underlying assets denominated in their respective foreign currencies C_1 and C_2. Moreover, we denote by $K = (K^1, K^2)$ the

Total value adjustment

$(S^{1,D}, S^{2,D})$	Monte Carlo SimpR	SimpT	CompR	CompT
$(20, 10)$	$[-0.0216, -0.0198]$	$[-0.0607, -0.0564]$	$[-0.0324, -0.0301]$	$[-0.0323, -0.0299]$
$(20, 15)$	$[-0.0252, -0.0233]$	$[-0.0710, -0.0667]$	$[-0.0379, -0.0355]$	$[-0.0377, -0.0353]$
$(20, 20)$	$[-0.0323, -0.0302]$	$[-0.0914, -0.0868]$	$[-0.0487, -0.0462]$	$[-0.0485, -0.0460]$
$(20, 25)$	$[-0.0421, -0.0397]$	$[-0.1193, -0.1141]$	$[-0.0636, -0.0607]$	$[-0.0633, -0.0604]$
$(20, 30)$	$[-0.0537, -0.0508]$	$[-0.1523, -0.1463]$	$[-0.0812, -0.0779]$	$[-0.0808, -0.0775]$

Table 2.10: Option on the maximum, linear problem and exponential Vasicek credit spread. Comparison of Monte Carlo with simple rectangular (SimpR), simple trapezoidal (SimT), composite rectangular (CompR) and trapezoidal (CompT) quadrature formulae. Total value adjustment (Test 3)

Total value adjustment

$(S^{1,D}, S^{2,D})$	Monte Carlo SimpR	SimpT	CompR	CompT
$(20, 10)$	$[-0.0424, -0.0392]$	$[-0.0711, -0.0661]$	$[-0.0649, -0.0602]$	$[-0.0647, -0.0601]$
$(20, 15)$	$[-0.0494, -0.0461]$	$[-0.0831, -0.0781]$	$[-0.0758, -0.0712]$	$[-0.0757, -0.0710]$
$(20, 20)$	$[-0.0634, -0.0599]$	$[-0.1070, -0.1016]$	$[-0.0976, -0.0926]$	$[-0.0974, -0.0924]$
$(20, 25)$	$[-0.0828, -0.0788]$	$[-0.1396, -0.1336]$	$[-0.1274, -0.1218]$	$[-0.1272, -0.1216]$
$(20, 30)$	$[-0.1056, -0.1010]$	$[-0.1782, -0.1712]$	$[-0.1626, -0.1561]$	$[-0.1623, -0.1558]$

Table 2.11: Option on the maximum, linear problem and CIR credit spread. Comparison of Monte Carlo with simple rectangular (SimpR), simple trapezoidal (SimT), composite rectangular (CompR) and trapezoidal (CompT) quadrature formulae. Total value adjustment (Test 3)

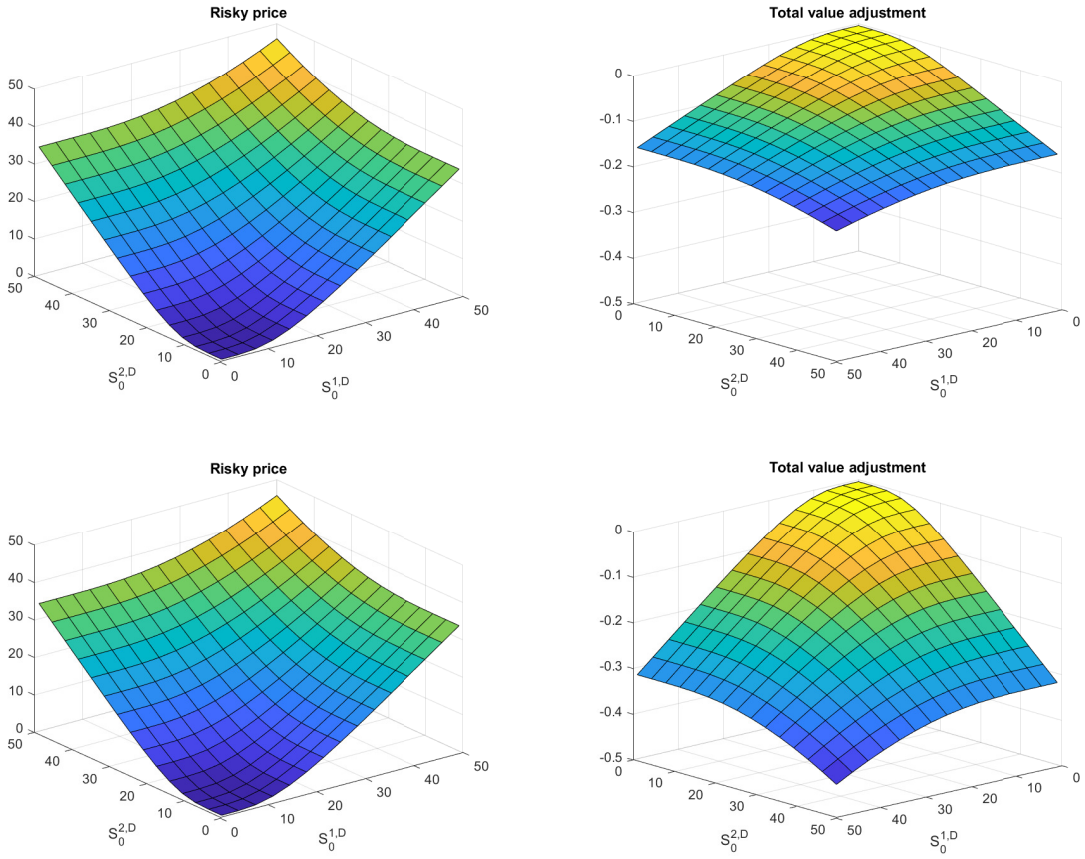

Figure 2.4: Option on the maximum in the linear case. Exponential Vasicek credit spread (top) and CIR credit spread (bottom). Risky value (left) and XVA (right) (Test 3)

vector of the strike values in the domestic currency D for the involved put options. In our numerical examples we have taken $S_0 = (12, 15)$ and $K = (12, 15)$.

We investigate how different values of the FX rates volatilities affect the XVA price and we analyse how the total value adjustment changes by increasing the collateral value, which is assumed to be a percentage $C^{\%}$ of the risk-free value.

Test 4: Nonlinear problem.

First, we keep fixed the volatility of X^{D,C_0}, say $\sigma^{X^0} = 0.275$, while for the volatilities of X^{D,C_1} and X^{D,C_2} we choose either a high volatility value, say 0.50, or a low volatility value, say 0.05. Moreover, we also consider the case of null FX rates volatilities, so that FX rates are deterministic time-dependent functions. In fact, by considering $\sigma^{X^j} \equiv 0$ in (2.10), we obtain $dX_t^{D,C_j} = (r^D - r^j)X_t^{D,C_j}dt$, so that

$$X_t^{D,C_j} = X_0^{D,C_j} \exp\left(\left(r^D - r^j\right)t\right). \tag{2.51}$$

Furthermore, we also consider the case of constant FX rates with $X_t^{D,C_j} = X_0^{D,C_j}$.

In tables 2.12 and 2.13 we show, for the nonlinear case, the total value adjustment confidence intervals and the multilevel Picard iteration values, that we take as reference values. Figure 2.5 shows that the multilevel Picard iteration method converges for all choices of σ^{X^0}. With reference to the cases with no null FX rates volatilities, XVA is, as expected, more negative when both X^{D,C_1} and X^{D,C_2} have higher volatility values, increases when only one of the two FX rates has a high volatility, and is greater when both the FX rates have lower volatility values. Indeed, higher volatilities correspond to higher levels of risk, therefore, in that case XVA becomes more negative, thus making the risky derivative price lower.

Note that when all volatilities are null we are considering time dependent deterministic FX rates that decrease with time from their initial value X_0^{D,C_j}, according to expression (2.51). In this case the XVA is less negative than any stochastic FX rates case.

In order to compare with the case of constant FX rates, we show in the last row

Total value adjustment

σ^X	Monte Carlo SimpR	Monte Carlo SimpT	MPI $\rho = 4$	MPI $\rho = 5$
$(0.275, 0.05, 0.05)$	$[-0.0252, -0.0239]$	$[-0.0155, -0.0147]$	-0.0082	-0.0083
$(0.275, 0.05, 0.50)$	$[-0.0529, -0.0506]$	$[-0.0326, -0.0312]$	-0.0175	-0.0176
$(0.275, 0.50, 0.05)$	$[-0.0436, -0.0416]$	$[-0.0267, -0.0255]$	-0.0138	-0.0142
$(0.275, 0.50, 0.50)$	$[-0.0649, -0.0626]$	$[-0.0399, -0.0385]$	-0.0214	-0.0214
$(0.000, 0.00, 0.00)$	$[-0.0232, -0.0219]$	$[-0.0143, -0.0135]$	-0.0075	-0.0076
$X^{D,C_j} \equiv X_0^{D,C_j}$	$[-0.0231, -0.0219]$	$[-0.0142, -0.0135]$	-0.0075	-0.0076

Table 2.12: Best of put/put option, nonlinear problem and exponential Vasicek credit spread. Comparison of Monte Carlo (with simple rectangular (SimpR) and trapezoidal (SimpT) quadrature formulae) and multilevel Picard iteration (MPI). Total value adjustment (Test 4)

Total value adjustment

σ^X	Monte Carlo SimpR	Monte Carlo SimpT	MPI $\rho = 4$	MPI $\rho = 5$
$(0.275, 0.05, 0.05)$	$[-0.0252, -0.0239]$	$[-0.0184, -0.0174]$	-0.0165	-0.0165
$(0.275, 0.05, 0.50)$	$[-0.0529, -0.0506]$	$[-0.0385, -0.0369]$	-0.0351	-0.0349
$(0.275, 0.50, 0.05)$	$[-0.0436, -0.0416]$	$[-0.0315, -0.0300]$	-0.0278	-0.0284
$(0.275, 0.50, 0.50)$	$[-0.0649, -0.0626]$	$[-0.0471, -0.0454]$	-0.0429	-0.0426
$(0.000, 0.00, 0.00)$	$[-0.0232, -0.0219]$	$[-0.0169, -0.0160]$	-0.0149	-0.0151
$X^{D,C_j} \equiv X_0^{D,C_j}$	$[-0.0231, -0.0219]$	$[-0.0169, -0.0160]$	-0.0150	-0.0152

Table 2.13: Best of put/put option, nonlinear problem and CIR credit spread. Comparison of Monte Carlo (with simple rectangular (SimpR) and trapezoidal (SimpT) quadrature formulae) and multilevel Picard iteration (MPI). Total value adjustment (Test 4)

of both tables the results for $X^{D,C_j} \equiv X_0^{D,C_j}$. These results coincide in the four decimal figures with the values of the deterministic time dependent case when the credit spread follows an exponential Vasicek dynamics and are a bit more negative than the deterministic case (where the FX rates values decrease with time) when assuming a CIR credit spread. Anyway, under the assumption of constant FX rates, the XVA is less neagative than in the stochastic FX rates case when certain level of volatility is assumed. The Monte Carlo confidence intervals seem to follow the same trend, but they underestimate the XVA.

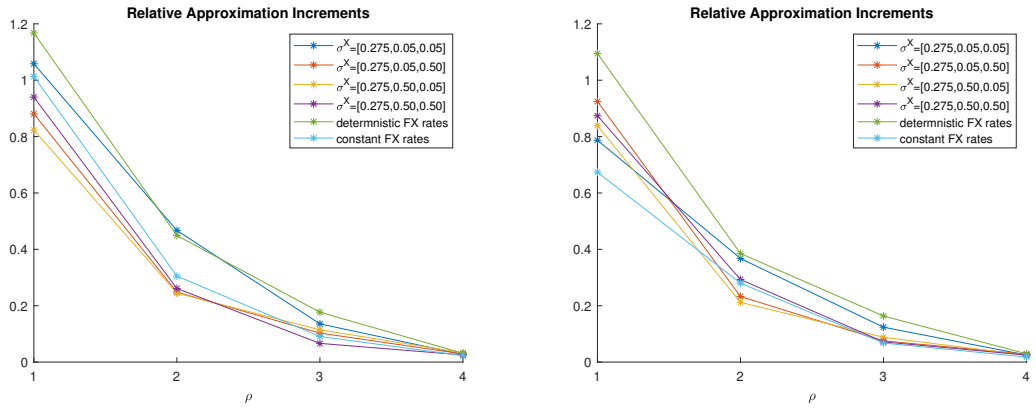

Figure 2.5: Best of put/put option. Convergence of the MPI with exponential Vasicek dynamics for credit spread on the left and CIR dynamics on the right.

Test 5: Linear problem.

In tables 2.14 and 2.15 we show the total value adjustment confidence intervals for the linear case with different values of the FX rates volatilities. We take the composite quadrature formulae results as reference values. We can draw conclusions similar to the previous nonlinear case.

Test 6: Collateralization.

In order to analyse the effect of collateralization, we now consider the data in Table 2.1 and Table 2.2 with $S^{1,D} = K^1 = 12$ and $S^{2,D} = K^2 = 15$, and let $C^{\%}$ assume increasing values. Note that if $C^{\%} = 0$, the derivative is not collateralized, whereas if $C^{\%} = 1$, the derivative is fully collateralized.

In Figure 2.6 we plot the difference between the prices of the best of put/put option for different levels $C^{\%}$ of collateralization and the price of the corresponding uncollateralized derivative. We consider both the nonlinear problem with exponential Vasicek credit spread (NL ExpVas) and with CIR credit spread (NL CIR) and the linear problem with exponential Vasicek credit spread (L ExpVas) and with CIR credit spread (L CIR).

Total value adjustment

σ^X	Monte Carlo SimpR	SimpT	CompR	CompT
$(0.275, 0.05, 0.05)$	$[-0.0058, -0.0054]$	$[-0.0156, -0.0148]$	$[-0.0086, -0.0081]$	$[-0.0086, -0.0081]$
$(0.275, 0.05, 0.50)$	$[-0.0121, -0.0114]$	$[-0.0328, -0.0314]$	$[-0.0180, -0.0172]$	$[-0.0179, -0.0171]$
$(0.275, 0.50, 0.05)$	$[-0.0097, -0.0091]$	$[-0.0269, -0.0256]$	$[-0.0146, -0.0139]$	$[-0.0145, -0.0138]$
$(0.275, 0.50, 0.50)$	$[-0.0146, -0.0138]$	$[-0.0402, -0.0387]$	$[-0.0219, -0.0210]$	$[-0.0218, -0.0209]$
$(0.000, 0.00, 0.00)$	$[-0.0053, -0.0050]$	$[-0.0144, -0.0136]$	$[-0.0079, -0.0075]$	$[-0.0079, -0.0075]$
$X^{D,C_j} \equiv X_0^{D,C_j}$	$[-0.0053, -0.0049]$	$[-0.0143, -0.0136]$	$[-0.0079, -0.0075]$	$[-0.0079, -0.0074]$

Table 2.14: Best of put/put option, linear problem and exponential Vasicek credit spread. Comparison of Monte Carlo with simple rectangular (SimpR), simple trapezoidal (SimT), composite rectangular (CompR) and trapezoidal (CompT) quadrature formulae. Total value adjustment (Test 5)

Total value adjustment

σ^X	Monte Carlo SimpR	SimpT	CompR	CompT
$(0.275, 0.05, 0.05)$	$[-0.0114, -0.0107]$	$[-0.0184, -0.0175]$	$[-0.0170, -0.0161]$	$[-0.0170, -0.0161]$
$(0.275, 0.05, 0.50)$	$[-0.0238, -0.0227]$	$[-0.0387, -0.0370]$	$[-0.0356, -0.0340]$	$[-0.0356, -0.0340]$
$(0.275, 0.50, 0.05)$	$[-0.0191, -0.0182]$	$[-0.0316, -0.0301]$	$[-0.0290, -0.0276]$	$[-0.0290, -0.0276]$
$(0.275, 0.50, 0.50)$	$[-0.0288, -0.0276]$	$[-0.0473, -0.0456]$	$[-0.0434, -0.0418]$	$[-0.0434, -0.0418]$
$(0.000, 0.00, 0.00)$	$[-0.0105, -0.0099]$	$[-0.0170, -0.0160]$	$[-0.0157, -0.0148]$	$[-0.0156, -0.0148]$
$X^{D,C_j} \equiv X_0^{D,C_j}$	$[-0.0105, -0.0099]$	$[-0.0169, -0.0160]$	$[-0.0156, -0.0148]$	$[-0.0156, -0.0147]$

Table 2.15: Best of put/put option, linear problem and CIR credit spread. Comparison of Monte Carlo with simple rectangular (SimpR), simple trapezoidal (SimT), composite rectangular (CompR) and trapezoidal (CompT) quadrature formulae. Total value adjustment (Test 5)

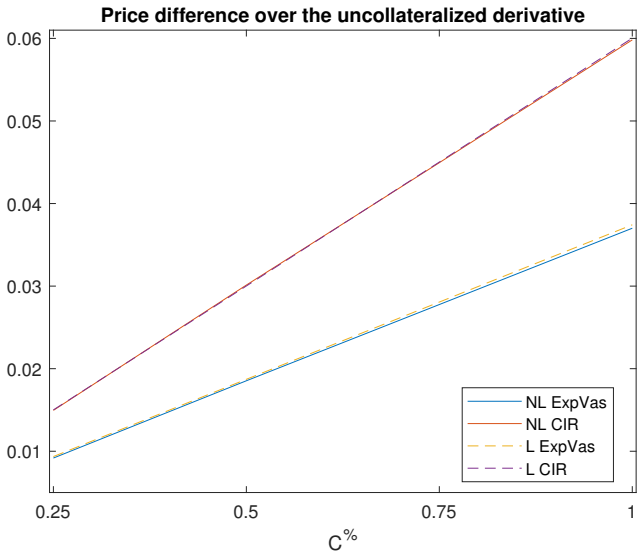

Figure 2.6: Best of put/put option. Price difference between the collateralized derivative and the uncollateralized derivative ($C^{\%} = 0$).

First, note that the plotted difference is positive, because the presence of collateral improves the recovery in case of the counterparty's default, thus increasing the price of the derivative with respect to the uncollateralized setting.

The additional amount that has to be paid for the presence of the collateral rises for larger values of the collateral, which leads to a lower exposure to counterparty's default.

Moreover, we can notice that the difference between nonlinear and linear cases is negligible in terms of price difference over the uncollateralized derivative. Finally, we can see that this difference is larger under the assumption of CIR credit spread, namely when the total value adjustment is more negative.

2.5.4 Basket option

Finally, in order to investigate how the elapsed computational time changes for the different mehods when increasing the number of the underlying assets, in this example we assume that the hedger buys from the counterparty a *basket call option* written

i	$S_0^{i,D}$	r^i	q^i	σ^{S^i}	X_0^{D,C_i}	σ^{X^i}	α			
							$N=2$	$N=4$	$N=8$	$N=16$
0	-	0.028	-	-	0.34	0.24				
1	14	0.047	0.046	0.315	0.18	0.27	0.46214	0.37471	0.10346	0.07302
2	12	0.050	0.023	0.341	0.62	0.29	0.53786	0.24501	0.10656	0.072656
3	16	0.046	0.017	0.248	0.62	0.29		0.12104	0.092846	0.062172
4	12	0.036	0.011	0.265	0.32	0.31		0.25924	0.14503	0.065838
5	11	0.027	0.026	0.240	0.74	0.33			0.14496	0.064
6	15	0.020	0.011	0.320	0.82	0.30			0.13598	0.074488
7	11	0.033	0.017	0.296	0.97	0.35			0.13061	0.063967
8	18	0.032	0.011	0.210	0.47	0.32			0.14056	0.046908
9	20	0.036	0.015	0.291	0.58	0.26				0.059024
10	20	0.034	0.019	0.320	1.09	0.31				0.056254
11	14	0.037	0.034	0.204	0.81	0.30				0.083855
12	16	0.036	0.018	0.268	0.95	0.33				0.065552
13	17	0.043	0.042	0.319	0.71	0.33				0.057539
14	15	0.042	0.010	0.349	1.10	0.27				0.060637
15	15	0.039	0.020	0.288	0.97	0.25				0.049381
16	10	0.033	0.018	0.205	1.14	0.31				0.04471

Table 2.16: Data for the basket option. For $N = 2, 4, 8, 16$ we respectively consider the first $3, 5, 9, 17$ rows of the table on the left and the corresponding column of the table on the right for the vector of weights α.

on N underlying assets $S^1, \dots, S^N$ with weights $\alpha^1, \dots, \alpha^N$. Therefore, the payoff function is given by:

$$G\left(t, S_t^1, S_t^2, X_t^{D,C_1}, X_t^{D,C_2}\right) = \left(\sum_{i=1}^{N} \alpha^i S_t^i X_t^{D,C^i} - K\right)^+. \tag{2.52}$$

In the numerical tests we have chosen $K = 5$, which represents the strike value in the domestic currency D.

In particular, we choose $N = 2, 4, 8, 16$ and for any chosen value of N we consider data in the first $N + 1$ rows of the left part in Table 2.16 and the corresponding column of the right part of the same table, where we have denoted by α the vector of the underlying assets weights, i.e., $\alpha = (\alpha^i, \dots, \alpha^N)$.

Table 2.17 shows the Monte Carlo confidence intervals for the risk-free value, which rises when increasing the number of the underlying assets, so that the total value adjustment will decrease.

Risk-free value	
N	Monte Carlo
2	$[7.4747, 7.6580]$
4	$[7.8330, 7.9872]$
8	$[8.2733, 8.3823]$
16	$[9.3117, 9.3842]$

Table 2.17: Basket option. Monte Carlo confidence intervals. Risk-free value

Total value adjustment			Elapsed time		
	MPI			MPI	
N	$\rho = 4$	$\rho = 5$	N	$\rho = 4$	$\rho = 5$
2	-0.0348	-0.0349	2	18.3053	5881.6020
4	-0.0367	-0.0369	4	27.3082	7665.0191
8	-0.0389	-0.0392	8	40.1646	11255.5800
16	-0.0433	-0.0438	16	62.2783	18503.2328

Table 2.18: Basket option, nonlinear problem and exponential Vasicek credit spread. Multilevel Picard iteration (MPI) results. Total value adjustment and elapsed time in seconds (Test 7)

Test 7: Nonlinear problem.

Table 2.18 and Table 2.19 show the total value adjustment in the nonlinear case. In particular, we report the average value of XVA and the elapsed time of $N_{runs} = 10$ runs of the multilevel Picard iteration method. Obviously, the elapsed time depends on the number of the underlying assets and on the value of the parameter ρ, that affects the number of simulations and of time nodes. However, the elapsed time is independent of the dynamics of the credit spread.

As shown in Figure 2.7, the multilevel Picard iteration method converges independently of the number of stochastic factors.

Total value adjustment			Elapsed time		
	MPI			MPI	
N	$\rho = 4$	$\rho = 5$	N	$\rho = 4$	$\rho = 5$
2	−0.0705	−0.0702	2	15.1060	5819.0015
4	−0.0740	−0.0740	4	25.7580	7755.2037
8	−0.0781	−0.0784	8	37.9215	11271.4253
16	−0.0873	−0.0877	16	61.9828	18643.6873

Table 2.19: Basket option, nonlinear problem and CIR credit spread. Multilevel Picard iteration (MPI) results. Total value adjustment and elapsed time in seconds (Test 7)

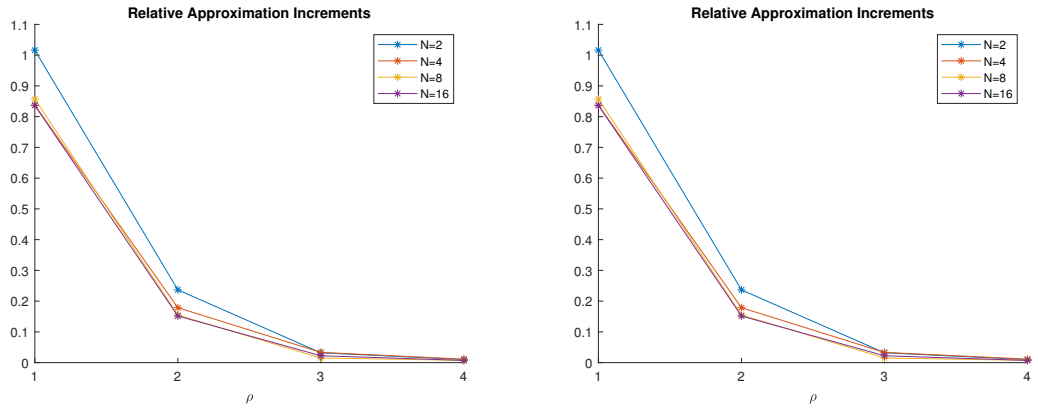

Figure 2.7: Basket option. Convergence of the MPI with exponential Vasicek dynamics for credit spread on the left and CIR dynamics on the right.

Total value adjustment			Elapsed time		
	Monte Carlo			Monte Carlo	
N	CompR	CompT	N	CompR	CompT
2	$[-0.0355, -0.0346]$	$[-0.0354, -0.0344]$	2	0.7369	0.7858
4	$[-0.0373, -0.0365]$	$[-0.0372, -0.0363]$	4	1.6829	2.0044
8	$[-0.0395, -0.0387]$	$[-0.0393, -0.0385]$	8	2.1968	2.2207
16	$[-0.0441, -0.0434]$	$[-0.0439, -0.0432]$	16	3.5992	3.6574

Table 2.20: Basket option, linear problem and exponential Vasicek credit spread. Monte Carlo with composite rectangular (CompR) and trapezoidal (CompT) quadrature formulae results. Total value adjustment and elapsed time (Test 8)

Total value adjustment			Elapsed time		
	Monte Carlo			Monte Carlo	
N	CompR	CompT	N	CompR	CompT
2	$[-0.0709, -0.0692]$	$[-0.0708, -0.0690]$	2	0.6807	0.7052
4	$[-0.0742, -0.0726]$	$[-0.0741, -0.0725]$	4	0.9841	0.9904
8	$[-0.0784, -0.0771]$	$[-0.0782, -0.0769]$	8	2.8884	2.9298
16	$[-0.0875, -0.0865]$	$[-0.0874, -0.0864]$	16	3.1174	3.4354

Table 2.21: Basket option, linear problem and CIR credit spread. Monte Carlo with composite rectangular (CompR) and trapezoidal (CompT) quadrature formulae results. Total value adjustment and elapsed time (Test 8)

Test 8: Linear problem.

Table 2.20 and Table 2.21 show the total value adjustment and the elapsed computation time in the linear case. The composite trapezoidal quadrature formula is slightly more time-consuming than the composite rectangular one, but the difference is negligible. Finally, in the linear case the computation of the total value adjustment with composite quadrature formulae is much less time-consuming than in the nonlinear case, where the use of composite quadrature formulae requires to apply the multilevel Picard iteration method.

2.6 Conclusions

In the previous chapter, the models and computations of the XVA for a multi-currency setting have been developed when deterministic exchange rates between the different currencies are considered. In order to pose a more realistic modelling approach, the main objective of the present chapter has been to extend the previous work to the consideration of stochastic models for the evolution of foreign exchange rates. Note that the consideration of stochastic exchange rates significantly increases the number of underlying risk factors. Thus, after proposing suitable dynamics for exchange rates evolution, the portfolio replication and the dynamic hedging methodologies have provided the formulation of the XVA pricing problem in terms of nonlinear and linear PDEs with larger dimensions than in the case of deterministic exchange rates. As in the previous chapter, we have applied Feynman-Kac formulae to obtain the expectations-based formulations of the total value adjustment problems.

In view of the comparison with the Lagrange-Galerkin method results reported in the previous chapter, in the nonlinear case we take as reference values for the total value adjustment the results obtained by using the multilevel Picard iteration method, whereas in the linear case we consider the confidence intervals obtained with Monte Carlo techniques and composite quadrature formulae for the approximation of the integrals involved in the total value adjustment formulae.

In this chapter, we have seen that the assumption of deterministic or constant foreign exchange rates causes an underestimation of the total value adjustment with respect to the more realistic assumption of stochastic foreign exchange rates. Also, the total value adjustment is more negative when the foreign exchange rates have higher levels of volatility with respect to when they have lower volatility values. Finally, we have noticed that the total value adjustment is more negative when the option price is higher, but becomes less negative when increasing the collateral value.

Conclusions

The objective of this work has been to contribute to the modelling and the computation of the total value adjustment in a multi-currency setting. Indeed, nowadays the consideration of the XVA when pricing a derivative has become relevant for financial institutions so that, in the literature, a lot of work has been recently developed in the framework of a single currency. Moreover, financial institutions may operate in different currencies. Therefore, in this thesis, we have extended some of the work in the single currency case to the multi-currency setting.

For this purpose, we have considered financial derivatives contracts that involve assets that are denominated in different foreign currencies as well as a stochastic spread for the counterparty, following either an exponential Vasicek or a CIR dynamics. Moreover, we have assumed the existence of a collateral account, also denominated in a foreign currency. In a first step, we have considered deterministic foreign exchange rates, and then we have assumed they follow stochastic Geometric Brownian motion dynamics. We have seen that the less realistic assumption of deterministic foreign exchange rates leads to an underestimation of the total value adjustment.

In this setting, an appropriate extension of the replicating portfolio to the multicurrency setting can be obtained. Thus, following analogous methodologies to the single currency case, we have built a self-financing portfolio, that hedges all the risk factors, including the foreign exchange risk when the foreign exchange rates are assumed to be stochastic. First, we have obtained a formulation based on nonlinear or linear PDEs, according to the choice of the mark–to–market value, for the price of different European options when including the total value adjustments. Secondly,

by using the Feynman-Kac theorem we have obtained formulations based on expectations that allow to approximate the total value adjustment by applying suitable Monte Carlo techniques, that are not affected by the *curse of dimensionality* arising when using deterministic numerical methods to solve high dimensional PDEs.

As regards the numerical approximation of the total value adjustment, we have first assumed that the foreign exchange rates are constant, the counterparty's credit spread is a deterministic time dependent function and the derivative depends on two underlying assets. Under these assumptions, we have proposed a Lagrange-Galerkin method, i.e., a semi-Lagrangian scheme for the time discretization combined with suitable finite element schemes for the spatial discretization, to solve the resulting two-dimensional pricing PDE. For the solution of the nonlinear PDE, a fixed point iteration is applied. In the linear case, the Lagrange-Galerkin method results have been compared to the results obtained with Monte Carlo techniques combined with suitable quadrature formulae for the approximation of the integral in the total value adjustment formula. In the linear case, Lagrange-Galerkin results are in agreement with Monte Carlo confidence intervals when composite quadrature formulae are employed.

In the nonlinear case, a Picard iteration is also needed when using the Monte Carlo method. From the comparison with the Lagrange-Galerkin method results, we conclude that simple quadrature formulae are not accurate enough. Therefore, we have introduced the multilevel Picard iteration method that allows to use composite quadrature formulae in an efficient way, by recursively computing the values of the unknown variable at intermediate nodes of the time discretization.

Therefore, when considering more than two stochastic factors, we have taken as reference values the multilevel Picard iteration method values in the nonlinear case and the Monte Carlo results with composite formulae in the linear one. Moreover, the computation of the total value adjustment in the nonlinear case is more time consuming than in the linear case, especially when considering a large number of underlying assets.

Overall, we have seen that the total value adjustment is more negative when the option is more valuable. Moreover, it becomes more negative when increasing the counterparty's intensity of default, namely when it is more likely the counterparty defaults. Also, the choice of larger values of volatilities for the foreign exchange rates makes the total value adjustment greater, in absolute terms. Moreover, we have noticed that the total value adjustment becomes less negative by increasing the collateral value. Finally, the assumption of a CIR dynamics for the credit spread leads to a more negative total value adjustment with respect to the alternative assumption of an exponential Vasicek credit spread.

As possible future extensions of the present work, a first step could be the extension of our methodologies for the incorporation of other valuation adjustments, such as capital value adjustment (KVA) and margin value adjustment (MVA). Moreover, we could consider more sophisticated models for the stochastic evolution of FX rates, by incorporating local, stochastic or local/stochastic volatility. Another extension could be the consideration of stochastic dynamics for the interest rates operating in each market in a multi-currency setting, thus additionally increasing the number of stochastic factors.

Concerning the type of options, for example the consideration of American options could be addressed in future works. As it happens in the single currency case, final-boundary value problems are replaced by complementarity problems associated to partial differential equations when addressing American options. In the context of formulations in terms of expectations, optimal stopping times come into place.

Appendix A

A stochastic Asset Liability Management model for life insurance companies

A.1 Introduction

Many financial decision problems involve the forecasting of future liability cash flows. For insurance products, the planning horizon extends beyond a decade: for example, pension funds have a planning horizon of more than 30 years. Thus, for an insurance company operating in life business, it is essential to build a model to forecast the evolution of cash inflows and outflows over time. All the techniques and the models used by a company to address financial risk due to the mismatching between assets and liabilities portfolios are part of the Asset and Liability Management (ALM). The traditional ALM programs focus on interest rate risk and liquidity risk, but, depending on the business model of the company, the specific definition of the underlying models for assets and liabilities may vary.

Historically, the first ALM methods were developed starting from the milestone works by Macaulay [71], Samuelson [86], Redington [84] and Fisher & Weil [42],

ordered according to the publication year. In these earlier models, the bond immunization, i.e., the matching between bond portfolio interest rate sensitivity and liability streams interest rate sensitivity, was the unique subject. These models are single stage models and do not take into account the stochastic evolution of interest rate since they use only the duration, or at most also the convexity, as risk measure. Nowadays, these techniques are unsuitable for an insurance company due to the complexity of both the asset portfolio and the liability portfolio. An insurance asset portfolio is not composed only of plain vanilla bonds and liquidity, but also of subordinated bonds which have embedded options (typically call options), structured bonds, no fixed income products, such as stocks, hedge funds, private equity, and real asset products (see [91]). However, when dealing with ALM models, the real challenge lies in the liability side. Due to the presence of surrender options, death benefits and other random features, an ALM model has to capture the stochastic dynamics and the uncertain characteristics inherent with insurance policies. The presence of these options with early exercise and asymmetric distribution makes essential the development of a suitable valuation functionality, not only to evaluate the company's balance sheet at current date, but also to simulate the firm's position at future dates.

So, a company needs to develop an ALM tool able to forecast its balance sheet evolution over time predicting future cash inflows and outflows, in order to ensure the solvency of the company, i.e., its capability to meet all its financial obligations. A correct forecasting of the evolution of the balance sheet, including cash flow generation, and the calculation of duration and convexity mismatching allow to manage the risk of future unexpected cash flows that could compromise the business of the firm.

But the aim of an ALM tool does not end here, because the purpose of ALM is to satisfy the interests of shareholders, policyholders and regulators in a common framework. Therefore, an ALM tool includes the allocation of assets to increase the profit of the company. The insurer invests in a portfolio the return of which is consistent with the offering of competitive products, in the shareholders' and policyholders' interest,

while satisfying the regulators. In this sense, ALM stands between risk management and strategic asset allocation, having the purpose of maximizing the investment returns, while minimizing the reinvestment risks. A complete guide on ALM models can be found in [92] and [93], and in the references therein.

It is clear that these models have a particular relevance in life insurance industry, even more after the introduction of the Solvency Capital Requirement computed under Solvency II Directive (see [87] and [90]), based on the computation of the 99.5% Value-at-Risk over one year of company's own funds, so that a proper joint estimation of both assets and liabilities values becomes essential.

The literature of ALM models for life insurance companies is very wide. We refer to [12], [13], [45] and [74], and the references therein. In the life insurance sector, the presence of embedded options in policies makes very difficult to correctly forecast the cash outflows (the problem of the pricing of embedded options has been widely treated in literature, see for example [10], [9], [11], [53] and [73]). The need of a more accurate approximation of the portfolio evolution over time, especially on liabilities side, jointly with the increase in computational power, makes feasible and suitable for an insurance firm the development of a stochastic scenario-based ALM model. In fact, significant resources have been invested into the development of such models, specially in insurance companies. Naturally, a trade off between complexity and practicality is always involved.

Starting from the seminal works by Bradley and Crane [16] and by Lane and Hutchinson [66], dynamic stochastic programming techniques have been applied to ALM models. In particular, Bradley and Crane were the first to use a dynamic recourse programming in a portfolio problem restricted to fixed interest securities. Stochastic programming in the form of a multistage recourse problem is a general formulation of a multistage ALM model in which the objective function is typically characterized in terms of the expected value of a linear or nonlinear utility function of wealth at the horizon (see [31]). This approach has become very popular in finance both among academics and practitioners. The literature on the application

of stochastic programming with recourse to ALM models is very wide. An interested reader could find some of these applications in [23], [25], [29], [32], [48] and [91]. Recently, Fernández et al in [40] have presented an ALM model for a life insurance company together with its numerical simulations performed in a new high performance computing architectures provided by GPUs technology. They consider a portfolio comprising with-profit life insurance policies with some innovations with respect to literature in the modelling of the surrenders of the policyholders. However, in the estimate of future supposed liabilities cash flows, they take into account neither possible future surrenders nor the so-called new production, i.e. the cash flows due to new policyholders which subscribe to the policy at future times.

In this appendix, based on [35], we build a two-stage stochastic ALM model for a life insurance company's portfolio. First, we propose a multistep reinvestment strategy using a scenario-based approach in which the assets and the liabilities are jointly simulated using appropriated stochastic models. On the asset side, we consider a portfolio composed of bonds, divided in buckets of duration, stocks and cash. On the liability side, we consider a portfolio comprising with-profit life insurance policies, such that policyholders' saving account earns a rate given by the maximum between a minimum guaranteed rate of return and a percentage, called participation rate, of the asset portfolio return. In order to keep track of the evolution of the liability portfolio, we take into account, in addition to the policyholders' saving account model, the biometric model and the surrender model. Also, we consider cash flows due to new production. The question of the issue of new policies has been investigated in previous works (see, for example, [39], [59] and [77]), but we propose, as far as we know, an innovative approach to this feature with respect to existing literature. At each time step k, we jointly simulate all the random variables of the model and, then, we compute asset duration and liability duration, estimating the projections of all future cash flows, made up of death, maturity and surrender payments, also related to new production. To the best of our knowledge, the fact that we consider also cash flows due to future surrenders and new production when computing balance sheet

projections constitutes an innovation with respect to literature and allows to better forecast the evolution of the balance sheet of an insurance company, therefore to compute more reliable estimates of actuarial reserves and of probabilities of default. From the technical point of view, it leads to the need to estimate conditional expectations with respect to the information available at time step k, so that we employ a Least Squares Monte Carlo technique. At each time step k, after having computed the duration of asset portfolio and of liability portfolio, we perform a rebalancing of the asset portfolio by solving a nonlinearly constrained optimization problem in which we minimize the distance between the asset duration and the liability duration, subject to the achievement of a target return and other constraints that are typical for an asset allocation problem. Indeed, we consider real world constraints, such as the so-called budget constraint, constraints that do not allow short sales, constraints on the upper and on the lower bounds for the size of a single asset class weight or of a combination of asset classes weights, constraints on single (on one asset class) and on portfolio turnover. This dynamic portfolio rebalancing strategy allows to simultaneously satisfy the interest of shareholders and policyholders. Indeed, the minimization of the distance between asset duration and liability duration permits to guarantee the solvency of the company, whereas the achievement of a target return allows to build a competitive portfolio. Since the decision rules previously described do not build an optimal dynamic reinvestment strategy, we propose a second stage of portfolio optimization in order to maximize the expected value of a chosen utility function, using the results obtained from the previous rebalancing strategy as investment constraints. However, we focus our analysis on the first stage of portfolio rebalancing strategy and we do not perform any tests on the second stage of the portfolio optimization, that requires standard stochastic programming techniques (see, for example, [31]), leaving the choice of a specific utility function and of the final wealth to the investment officer of the firm.

In order to test our ALM model, we firstly present our portfolio rebalancing strategy under certain market hypotheses and initial scenario assumptions. Moreover, we

focus on the evolution over time of the number of alive policies, that is affected by the mortality model as well as by the surrender and new production models. Finally, an analysis of the participation rate sensitivity is conducted by keeping track of the evolution over time of actuarial reserves, that is to say, the discounted value of all future cash flows on the liability side, and of own funds, and by investigating default probability.

The appendix is organized as follows. In Section A.2 we define our asset portfolio and liability portfolio, and we introduce the general features of our ALM model. In Section A.3 we focus on the liability model and on the computation of liability duration, that requires the estimation of future firm's cash flows, consisting of maturity, death and surrender payments, also related to new production, and entails the definition of a mortality model as well as a surrender and new production model. Moreover, we introduce the interest rate model associated to the term structure of interest rates. In Section A.4 we deal with the asset model, thus presenting bonds, equity and cash models. Then, in Section A.5, we introduce the nonlinearly constrained rebalancing rules to solve in order to dynamically restructure the asset portfolio. We consider several real world constraints. In Section A.6 we give an overview of the second stage of the portfolio optimization. In Section A.7 we describe market data and in Section A.8 we present and analyse some numerical results. Finally, in Section A.9, we point out the main conclusions.

A.2 The model

We build a stochastic ALM model with dynamic reinvestment strategy for a life insurance company's portfolio. Therefore, we deal with both a liability portfolio and an asset portfolio, that is regularly rebalanced in order to not only obtain a certain portfolio return, but also to be able to meet future financial obligations. In order to properly rebalance the company's portfolio, we need to forecast the balance sheet evolution over time, computing the joint projections of the future cash flows of both

liability and asset portfolios.

Assets	Liabilities and Shareholder's Equity
Capital invested in assets	Present value of life insurance policies Equity capital

Table A.1: Simplified life insurance company's balance sheet

A simplified balance sheet for a life insurance company is summarized in Table A.1. The last item, equity capital, consists of the surplus which is kept by the company's shareholders and is defined by:

$$\text{Equity capital} = \text{Assets} - \text{Present value of life insurance policies.} \tag{A.1}$$

On the assets side, we consider a portfolio composed of bonds, divided in buckets of duration, equity and cash. Bonds, equity and cash are simulated together over time according to stochastic models. The need of an insurance company to have a conservative investment strategy, as required by regulators [17], is reinforced in our model from the fact that in the case of with-profit life policies a more aggressive investment strategy would represent an advantage for policyholders, but an excessive risk for shareholders. In fact, policyholders would benefit from high returns and would not be hit by negative returns, since a minimum rate of return is guaranteed, while shareholders would be hit by negative returns and would barely benefit from positive returns, since only a small percentage of returns is kept by the company's shareholders. Therefore, the company refrains from following a more aggressive investment strategy. For these reasons, we hold larger positions in fixed-income assets, and we allocate a smaller percentage of the total in stocks. Moreover, we consider some real investment policy constraints on portfolio asset classes weights and on particular combinations of them.

On the liabilities side, we consider a portfolio only comprising the so-called with-profit life policies, a type of products that is very popular in life insurance business. In these contracts, on one hand, the policyholder pays a premium, that can be either

single, paid at the beginning of the contract, or periodic, paid with a certain frequency during the policy life. On the other hand, the insurer receives the premiums and invests this capital in the financial market. Moreover, the insurer pays both a periodic variable rate in a policyholder saving account and a benefit, that is disbursed at policy maturity date, if the policyholder is still alive, or before policy maturity date, if the contract ends before policy expiration, because the policyholder dies or decides to exercise the surrender option, if the contract entitles to abandon the policy before maturity. Our ALM model includes the surrender option. Also, we consider the possibility that policyholders do not enter into the policy all together, say at time 0, but there is the chance that a policyholder signs the contract in the following years, thus creating the so-called new production. In summary, we consider the most important features of a with-profit life policy:

- policyholders' saving account grows at a rate given by the maximum between a minimum guaranteed rate of return and a fraction of the asset portfolio return;
- a mortality model is taken into account to keep track of death occurrences;
- policyholders are entitled to surrender the contract at any time before the maturity date;
- cash flows due to the so-called new production are included.

In our model, the insurance company has to refund the beneficiaries of policies of policyholders that die before the maturity date, the policyholders that abandon the contract before policy expiration, as well as policyholders that are still alive when their policies expire. Except from the timing of payments due to the maturity of the policies, the timing of all the other payments is uncertain and depends on the market evolution and on the stochastic behaviour of policyholders' biometry. More precisely, the decision to abandon the contract before policy expiration and new production strongly depend on stochastic economic variables. Indeed, we infer the probability that a policyholder cancels the contract before maturity or that a new policyholder

subscribes to the policy comparing the earnings offered by the policy with the earnings offered by competing products in the market, represented by the return of a suitable benchmark index chosen from the market. This issue will be fully addressed in Section A.3.1. In contrast with surrender events and new production, death occurrences are actuarial events, that are usually assumed independent of economic variables. Therefore, in order to infer the number of policyholders that die before policy expiration, we follow a biometric model, based on a life table in which the survival probability of a policyholder is only dependent on age and gender. More details about the mortality model are given in Section A.3.2.

Our ALM model is summarized in Table A.2.

Asset Model	Liability Model
Bond with duration n_1 model	Policyholder account model
Bond with duration n_2 model	Surrender model
...	New production model
Equity model	Biometric model
Cash model	

Table A.2: ALM model

Since the set of contracts could be very copious and, also, each insurance contract could offer a different guaranteed rate of return, could be signed by policyholders of different ages and could expire at different dates, computing the joint projections of the future cash flows of both asset and liability portfolios for each contract can lead to a highly time-consuming task. In order to manage this issue, as in [40], we group policies with similar characteristics in buckets, called model points, thus reducing the computational cost of the calculus. More details on how to build the model points can be found in [63], for instance. Thus, our liability portfolio is given by the set of model points, $I = \{m_i / m_i \text{ is a model point}\}$, with cardinality $N_M := |I|$, so that we will work on a representative set of contracts. More precisely, in order to handle the heterogeneity of the plethora of different contracts in the liability portfolio, we gather together policies with similar minimum guaranteed rate of return, similar age

of the policyholder and same maturity date. For example, in Section A.8, where some numerical results are shown, we suppose that all the policies in our liability portfolio expire in 10 years, and that some of these contracts offer a minimum guaranteed rate of return of 0%, others of 1% and still others of 2%. Moreover, contracts are signed by policyholders aged from 38 to 67. We split the contracts in model points as shown in Table A.3.

		Minimum guaranteed rate of return		
		0%	1%	2%
Age	$[40, 44]$	$(40, 0\%)$	$(40, 1\%)$	$(40, 2\%)$
	$[45, 49]$	$(45, 0\%)$	$(45, 1\%)$	$(45, 2\%)$
	$[50, 54]$	$(50, 0\%)$	$(50, 1\%)$	$(50, 2\%)$
	$[55, 59]$	$(55, 0\%)$	$(55, 1\%)$	$(55, 2\%)$
	$[60, 64]$	$(60, 0\%)$	$(60, 1\%)$	$(60, 2\%)$
	$[65, 69]$	$(65, 0\%)$	$(65, 1\%)$	$(65, 2\%)$

Table A.3: Example of representative contracts (model points) for different policyholders' ages and different minimum guaranteed rates of return. All contracts have the same time-to-maturity, so that a model point is a couple $(\bar{A}, g)$, where $\bar{A}$ and g are the representative age and the minimum guaranteed rate of return, respectively

In conclusion of the general description of our ALM model, we introduce the possibility of default of the insurance company. Indeed, if a policyholder dies, abandons the contract, or is still alive at policy maturity date, the company has to pay a refund based on the value of the policyholder's saving account, that, as said before, earns an interest rate given by the maximum between a minimum guaranteed rate of return and a percentage of the return on the insurer's investment portfolio. Therefore, the company needs to use the capital that comes from new production if portfolio return is not sufficient to meet its liabilities, and, if there are not enough new policyholders, the company employs its own funds. If own funds become negative, the company is declared defaulted.

A.3 Liability model

In this section we describe how we model the cash flows connected to policyholders' benefits and premiums. Whereas some cash flows are scheduled, such as cash flows related to maturity payments, the timing of other cash flows is not known a priori and can depend either on the market situation, in the case of payments due to surrender option and in the case of cash inflows due to new production, or on actuarial events, in the case of payments due to death occurrences.

We consider a time discretization given by a mesh of equispaced time instants, $0 = t_0 < t_1 < \ldots < t_N = T$, and we define the period k as $[t_k, t_{k+1}]$, for $k = 0, \ldots, T-1$. In each period, we assume that premiums are paid at the beginning while benefits are disbursed at the end. Administrative costs are included in the premium.

At each period, we need to keep track not only of the number of alive policyholders, but also of the number of policyholders that die or exercise the surrender option, of the number of policies that expire, as well as of the number of new policyholders that subscribe to a contract. Therefore, we introduce the following notations:

- ${}_sn_{k,i}$ is the number of policyholders in the model point $m_i \in I$ that entered into the contract at time s and are still alive at the end of period k;

- $n_{k,i}$ is the total number of alive policyholders in model point $m_i \in I$ at the end of period k, independently from their starting times, so that

$$n_{k,i} = \sum_{s=0}^{T-1} {}_sn_{k,i};$$

- ${}_sn^D_{k,i}$, ${}_sn^S_{k,i}$, ${}_sn^M_{k,i}$ are the numbers of policyholders in model point $m_i \in I$ that started the contract at time s and die, surrender or reach maturity at period k, respectively;

- $\boldsymbol{n}^D_{k,i}$, $\boldsymbol{n}^S_{k,i}$ and $\boldsymbol{n}^M_{k,i}$ are the vectors defined as:

$$\boldsymbol{n}^X_{k,i} = ({}_0n^X_{k,i}, {}_1n^X_{k,i}, \ldots, {}_{k-1}n^X_{k,i}), \quad X = \{D, S, M\}; \tag{A.2}$$

- $n^P_{k,i}$ is the number of new policyholders in the i-th model point that enter into the contract at period k.

In the biometric model used to determine the policyholders' death rate, the distinction between men and women is taken into account. So, when the previous symbols present the superscript "$\mathcal{M}$" or "$\mathcal{F}$" they are referred only to the corresponding portion of male or female policyholders, respectively.

We denote by ${}_sl^D_{k,i}$, ${}_sl^S_{k,i}$ and ${}_sl^M_{k,i}$ the death, surrender and maturity benefits at period k for a policyholder in model point m_i that signed the contract at time s. They are the guaranteed payments in case of death of the policyholder, cancellation of the contract or policy expiration, respectively, and their sizes depend on policyholders' saving account. The saving account of policyholders in model point m_i at period k grows at a rate given by $\max(g_{k,i}, \beta_{k,i}R^P_k)$, where $g_{k,i}$ and $\beta_{k,i}$ are the minimum guaranteed rate of return and the participation rate at period k for the model point m_i, respectively, and R^P_k is the asset portfolio return at period k. Therefore, we assume death, surrender and maturity benefits at period k for a policyholder in model point m_i that entered into the contract at time s grow according to the recursive formula:

$$\begin{cases} {}_sl^X_{s,i} = l^P_{s,i}, \\ {}_sl^X_{k,i} = {}_sl^X_{k-1,i} \max(g_{k,i}, \beta_{k,i}R^P_k) + l^{\Pi}_{k,i}, \quad k > s, \end{cases} \tag{A.3}$$

where $l^P_{s,i}$ is the payment made by the policyholder when entering into the contract at period s, and $l^{\Pi}_{k,i}$ denotes the premium payment made by the policyholder at period k. In (A.3) X can be either D, S, or M.

Note that we have made the assumption that the benefits in case of death, survival at maturity or surrender evolve over time according to the same recursive formula, but, in general, they may have different structures. For example, there can be some penalties in case of surrender and the minimum guaranteed rate and the participation rate can depend on X.

Finally, we denote by $\boldsymbol{l}^D_{k,i}$, $\boldsymbol{l}^S_{k,i}$ and $\boldsymbol{l}^M_{k,i}$ the vectors given by:

$$\boldsymbol{l}^X_{k,i} = ({}_0l^X_{k,i}, {}_1l^X_{k,i}, \ldots, {}_{k-1}l^X_{k,i}), \quad X = \{D, S, M\}. \tag{A.4}$$

After having introduced the previous notations, we are able to list in the following the quantities we need to take into account to determine the cash flows at period k.

- **Premium payments**, Π_k. These are the payments made by policyholders at the beginning of period k, if still alive. At period k premium payments related to model point m_i are given by:

$$\Pi_{k,i} = n_{k-1,i} l^{\Pi}_{k,i}. \tag{A.5}$$

  Clearly, at period k the total amount of premium payments can be computed as follows:

$$\Pi_k = \sum_{i=1}^{N_M} \Pi_{k,i}. \tag{A.6}$$

- **New production**, P_k. It consists of payments made by new policyholders at the beginning of period k. New production at period k for the model point m_i is defined as:

$$P_{k,i} = n^P_{k,i} l^P_{k,i}, \tag{A.7}$$

  and the total amount of new production at period k is given by:

$$P_k = \sum_{i=1}^{N_M} P_{k,i}. \tag{A.8}$$

- **Death payments**, D_k. These are the rewards that the company has to give to the beneficiaries of policies of policyholders that die before maturity at period k. Death payments related to model point m_i are given by:

$$D_{k,i} = \boldsymbol{n}^D_{k,i} \cdot \boldsymbol{l}^D_{k,i}. \tag{A.9}$$

  Evidently, the total amount of death payments at period k is obtained as:

$$D_k = \sum_{i=1}^{N_M} D_{k,i}. \tag{A.10}$$

- **Surrender payments**, Γ_k. They are made up of the refunds that the company has to give to policyholders that abandon the policy before its contractual expiration date at period k. For model point m_i we have:

$$\Gamma_{k,i} = \boldsymbol{n}^S_{k,i} \cdot \boldsymbol{l}^S_{k,i}. \tag{A.11}$$

  The total amount of surrender payments at period k is given by:

$$\Gamma_k = \sum_{i=1}^{N_M} \Gamma_{k,i}. \tag{A.12}$$

- **Maturity payments**, M_k. These are the payments that the company has to make due to policies in model point m_i that reach maturity at time k. Maturity payments at period k for model point m_i are defined as:

$$M_{k,i} = \boldsymbol{n}^M_{k,i} \cdot \boldsymbol{l}^M_{k,i}, \tag{A.13}$$

  and the total amount of maturity payments at period k is obviously computed as:

$$M_k = \sum_{i=1}^{N_M} M_{k,i}. \tag{A.14}$$

Liability value

On the basis of previous definitions, we can write a formula to describe the evolution over time of the liability value. The value of liabilities related to model point m_i at time 0 is given by $L_{0,i} = \Pi_{0,i}$, and, for $k = 1, \ldots, T_i - 1$, it evolves according to:

$$L_{k,i} = L_{k-1,i}(1 + \max(g_{k,i}, \beta_{k,i} R^P_k)) + \Pi_{k,i} + P_{k,i} - D_{k,i} - \Gamma_{k,i}. \tag{A.15}$$

Since T_i denotes the maturity date of policies in model point m_i, $L_{k,i} = 0$ for $k \geq T_i$.

Cash flows

We can write the total amount of cash flows at period k as:

$$cf_k = \sum_{i=1}^{N_M} cf_{k,i}. \tag{A.16}$$

In the previous formula, $cf_{k,i}$ denotes the size of cash flows at period k for model point m_i, given by:

$$cf_{k,i} = \begin{cases} \Gamma_{k,i} + D_{k,i} & \text{if } t_k < T_i, \\ M_{k,i} + D_{k,i} & \text{if } t_k = T_i, \\ 0 & \text{otherwise,} \end{cases} \tag{A.17}$$

where T_i denotes the maturity date of policies in the i-th model point.

Liability duration

In the literature of ALM models, the most commonly used risk measure is duration. In order to compute the duration of our liabilities, using the Macaulay duration formula, we have to estimate the so-called actuarial reserves, that are the present value of the amount that the insurer needs at future periods to meet obligations associated to the policies. We denote by v_k the actuarial reserves at period k and we have that:

$$v_k = \sum_{i=1}^{N_M} v_{k,i}, \tag{A.18}$$

where $v_{k,i}$ denotes the reserves at period k connected to the i-th model point and is given by the sum of the discounted supposed cash flows at future periods $j > k$, that is to say:

$$v_{k,i} = \sum_{j>k} d_{j|k} cf_{j,i|k}. \tag{A.19}$$

In the previous formula, we have denoted by $d_{j|k}$ and $cf_{j,i|k}$ the discount factor at period j and the size of cash flows at period j for the model point m_i estimated at period k, respectively. More precisely, the discount factor $d_{j|k}$ is the price at time k of a zero-coupon bond with tenor j and is computed after having defined a model for the term structure of interest rates. Our choice for the interest rate model is described in Section A.3.4.

Once we have estimated the supposed liabilities cash flows, the liability duration

at period k, L_k^D, according to the Macaulay formula, is given by:

$$L_k^D = \frac{\sum_{j>k} j d_{j|k} cf_{j|k}}{\sum_{j>k} d_{j|k} cf_{j|k}}. \tag{A.20}$$

A.3.1 The surrender and new production model

In order to determine the timing and the size of surrender payments, as well as new production cash flows, we need to build a model for the probability of surrender and for the probability of new production, that is the probability that a contract is signed by a new client.

It makes sense that the exercise of surrender option is strongly dependent on market condition, since we can suppose that a policyholder abandons the policy if he finds in the market an analogous product which offers a higher rate of return with respect to the return rate offered by his policy at the same moment. Thus, following [40], the surrender probability is parametrized on the basis of the spread between the earnings offered by the insurance company, depending on the insurer's portfolio return, and the return offered by an analogous product in the market, represented by a benchmark index return. In this way, we can model the fact that if competing products return is greater than the rate of return offered by the policy, a policyholder is more motivated to surrender his investment.

In particular, for each period k and for each model point $m_i \in I$, we introduce the quantity $\delta r_{k,i}^S$ as:

$$\delta r_{k,i}^S = (R_k^I - \max(g_{k,i}, \beta_{k,i} R_k^P))^+, \tag{A.21}$$

where R_k^I is the benchmark index rate of return at period k. For the sake of brevity, we have used the notation $x^+ = \max(x, 0)$. Note that $\delta r_{k,i}^S$ does not depend on policyholder's gender or age, but only on the minimum guaranteed rate of return offered by the contract.

In order to size $\delta r_{k,i}^S$, we introduce the threshold intervals I^q, for $q = 1, \ldots, Q$. For example, in our numerical tests we choose $Q = 3$ and define $I^1 = [0, 0.01]$,

Interval	Period 0	1	2	...	$T-1$
I^1	p^S_{10}, p^P_{10}	p^S_{11}, p^P_{11}	p^S_{12}, p^P_{12}	...	p^S_{1T-1}, p^P_{1T-1}
I^2	p^S_{20}, p^P_{20}	p^S_{21}, p^P_{21}	p^S_{22}, p^P_{22}	...	p^S_{2T-1}, p^P_{2T-1}
$\vdots$	$\vdots$	$\vdots$	$\vdots$	...	$\vdots$
I^Q	p^S_{Q0}, p^P_{Q0}	p^S_{Q1}, p^P_{Q1}	p^S_{Q2}, p^P_{Q2}	...	p^S_{QT-1}, p^P_{QT-1}

Table A.4: Surrender ($p^S_{q,k}$) and new production ($p^P_{q,k}$) probabilities depending on the threshold interval I^q and on the period k

$I^2 = (0.01, 0.03]$, and $I^3 = (0.03, +\infty)$. We infer the surrender probability at period k for the model point m_i, $p^S_{k,i}$, from Table A.4, where surrender probabilities, depending only on the threshold interval I^q and on the period k, are denoted by p^S_{qk}, for $q = 1, 2, 3$ and $k = 0, \ldots, T-1$. In particular, if $\delta r^S_{k,i}$ falls in the interval I^q, then p^S_{qk} gives the surrender probability at period k for policies in model point m_i, i.e., $p^S_{k,i} = p^S_{qk}$.

After having inferred the probability of surrender at each period and for each model point, we model the number of policyholders that entered into the contract at period s and cancel it at period k by a Binomial distribution:

$$ {}_sn^S_{k,i} \sim Bin({}_sn_{k-1,i}, p^S_{k,i}). \tag{A.22} $$

Moreover, new production probability at period k for the model point m_i, denoted by $p^P_{k,i}$, is deduced in a similar way as the surrender probability, using Table A.4, where new production probabilities, p^P_{qk}, for $q = 1, 2, 3$ and $k = 0, \ldots, T-1$, depend only on the threshold interval I^q and on the period k. More precisely, we introduce the quantity

$$ \delta r^P_{k,i} = (\max(g_{k,i}, \beta_{k,i} R^P_k) - R^I_k)^+ \tag{A.23} $$

and assume that if $\delta r^P_{k,i}$ lies in the interval I^q, then new production probability at time k in the i-th model point is given by p^P_{qk}, i.e., $p^P_{k,i} = p^P_{qk}$.

Note that p^S_{qk} and p^P_{qk} in Table A.4 are chosen taking into account that surrender probability and new production probability increase with $\delta^S_{k,i}$ and $\delta^P_{k,i}$, respectively.

Once we have deduced the probability of new production from Table A.4 at each time for each model point, we can model the number of policyholders in the i-th model point that start the contract at time k, for $k > 0$, by a Binomial distribution:

$$n^P_{k,i} \sim Bin(n_{k-1,i}, p^P_{k,i}). \tag{A.24}$$

We point out that the use of $\delta r^S_{k,i}$ for surrender probability and $\delta r^P_{k,i}$ for new production probability is due to the fact that it is reasonable to assume that only if competing products in the market, represented by the benchmark return R^I, offer a rate of return greater than the rate of return offered by the insurance company, that is, $\max(g_{k,i}, \beta_{k,i} R^P_k)$, a private investor may be motivated to abandon the policy, so there may be surrenders, but there are not new policyholders signing the contract, vice versa, if $\max(g_{k,i}, \beta_{k,i} R^P_k)$ is greater than R^I_k, new clients may be motivated to put his savings in the policy, but there are not policyholders that exercise the surrender option.

A.3.2 The mortality model

Since the payments due to deaths of policyholders before maturity are not dependent on market condition, we use a biometric model in which the death probability is provided by a specific life table (Table A.5) depending on policyholders' age and gender. More precisely, since in numerical examples considered in Section A.8 we choose a time step of 1 year, that is to say, the distance between time k and time $k+1$ is 1 year, in Table A.5 we report the probabilities that individuals that have just had a birthday will not celebrate the next birthday.

We denote by $p^{D,\mathcal{M}}_i$ and $p^{D,\mathcal{F}}_i$ the death probabilities for the model point m_i for male and female policyholders, respectively. In particular, we model the number of male and female policyholders in model point m_i, that entered into the contract at time s and die at period k, ${}_s n^{D,\mathcal{M}}_{k,i}$ and ${}_s n^{D,\mathcal{F}}_{k,i}$, by a Binomial distribution, so that:

$${}_s n^{D,X}_{k,i} \sim Bin({}_s n^X_{k-1,i}, p^{D,X}_i), \quad X = \{\mathcal{M}, \mathcal{F}\}. \tag{A.25}$$

Age	$\mathcal{M}$ (%)	$\mathcal{F}$ (%)
$[40, 44]$	0.5740	0.3477
$[45, 49]$	0.8935	0.5512
$[50, 54]$	1.4243	0.8349
$[55, 59]$	2.2984	1.3452
$[60, 64]$	3.7245	2.1283
$[65, 69]$	6.0787	3.2981

Table A.5: 2019 period life table: death probabilities in percentage for men ($\mathcal{M}$) and women ($\mathcal{F}$) for given age intervals. Source: ISTAT (Italian National Institute of Statistics)

Obviously, the total number of deaths at period k for the model point m_i, denoted by $n^D_{k,i}$, is computed as:

$$n^D_{k,i} = \sum_{s=0}^{k-1} ({}_s n^{D,\mathcal{M}}_{k,i} + {}_s n^{D,\mathcal{F}}_{k,i}). \tag{A.26}$$

A.3.3 Approximation of future cash flows

In this section we deal with the estimation at period k of the projections of future cash flows, given by (A.16) and (A.17), at each period $j > k$, needed to compute the liability duration, according to (A.20). More precisely, we have to estimate the timing and the size of future death, surrender and maturity payments, taking into account that new policyholders can subscribe to a policy at future periods.

Future value of death, surrender and maturity benefits

The size of payments that the company has to make due to death of policyholders, abandons of the contract and policy contractual expiration depends on death, surrender and maturity benefits, that grow according to (A.3). Therefore, in order to measure the expected size of future payments at period k, we need to estimate:

$$\mathrm{E}[\max(g_{j,i}, \beta_{j,i} R^P_j)|\mathcal{F}_k], \quad \text{for } j > k, \tag{A.27}$$

where $\mathrm{E}[\cdot|\mathcal{F}_k]$ denotes the expectation with respect to the information available at period k, denoted by $\mathcal{F}_k$.

In order to estimate (A.27) we employ the Least Squares Monte Carlo Method [68]. More precisely, we can write the conditional expectation in (A.27) as linear combination of W basis functions $\{\psi^w\}_{w=1,\dots,W}$ as follows:

$$\mathrm{E}[\max(g_{j,i}, \beta_{j,i} R_j^P)|\mathcal{F}_k] \simeq \sum_{w=1}^{W} \bar{b}_{k,j,i}^w \psi^w(R_k^P) = \bar{b}_{k,j,i}^T \psi(R_k^P). \tag{A.28}$$

For example, we can choose the Laguerre polynomials as basis functions, being simple to implement, because they can be defined recursively:

$$\begin{cases} L_0(x) = 1, \\ L_1(x) = 1 - x, \\ L_k(x) = \frac{1}{k}((2(k-1) + 1 - x)L_{k-1}(x) - (k-1)L_{k-2}(x)), \quad k \geq 2. \end{cases} \tag{A.29}$$

We search for the regression coefficients $\bar{b}_{k,j,i}$ that are solution of the following problem:

$$\bar{b}_{k,j,i}^* = \underset{\bar{b}_{k,j,i}}{\operatorname{argmin}} \, \mathrm{E}_k \left[\left(\psi(R_k^P)^T \bar{b}_{k,j,i} - \mathrm{E}_k[\max(g_{j,i}, \beta_{j,i} R_j^P)] \right)^2 \right],$$

where we have used the notation $\mathrm{E}_k[\cdot] = \mathrm{E}[\cdot|\mathcal{F}_k]$.

We vanish the derivative with respect to $\bar{b}_{k,j,i}$ of the quantity to minimize and we get:

$$\mathrm{E}_k \left[\psi(R_k^P) \psi(R_k^P)^T \right] \bar{b}_{k,j,i}^* = \mathrm{E}_k \left[\psi(R_k^P) \max(g_{j,i}, \beta_{j,i} R_j^P) \right].$$

In order to compute the regression coefficients, we use Monte Carlo techniques. More precisely, we simulate N_P paths of R_k^P, for $k = 1, \dots, T$, and we denote by $R_k^{P,n}$ the value at time k in the n-th simulation. After having defined $\Psi_{k,i}$ as the $W \times W$ matrix with coefficients

$$(\Psi_{k,i})_{uv} = \frac{1}{N_P} \sum_{n=1}^{N_P} \psi^u(R_k^{P,n}) \psi^v(R_k^{P,n}),$$

and $d_{k,j,i}$ as the W-array with the v-th element given by

$$(d_{k,j,i})_v = \frac{1}{N_P} \sum_{n=1}^{N_P} \psi^v(R_k^{P,n}) \max(g_{j,i}, \beta_{j,i} R_j^{P,n}),$$

we reduce the problem of regression coefficients computation to the problem of solving the system $\Psi_{k,i} \bar{b}_{k,j,i} = d_{k,j,i}$.

Once we have obtained regression coefficients, we are able to compute

$$\mathrm{E}[\max(g_{j,i}, \beta_{j,i} R_j^P) | \mathcal{F}_k] \,, \qquad \text{for } j > k \,,$$

simply using (A.28). This means we need to simulate only the current value R_k^P.

Future death payments

Once we have estimated the value of the death benefit at future periods and predicted the number of policyholders who will die at each future period according to the biometric model described in Section A.3.2, we can compute the size of death payments according to (A.9) and (A.10).

Future surrender payments

In order to forecast the size and the timing of future surrender payments, we need to predict the number of policyholders that cancel the contract at each future period $j > k$ and, so, the probability of surrender at each period $j > k$. To do that, we compute:

$$\Delta R_i^S(j|k) = \mathrm{E}[\delta r_{j,i}^S | \mathcal{F}_k], \quad \text{for } j > k. \tag{A.30}$$

Indeed, the computation of (A.30) allows us to forecast the probability of surrender at future periods by using Table A.4 and, then, the number of abandons at each future periods according to (A.22). After having estimated the number of surrenders at future periods, we can use the estimation of the surrender benefit to compute the amount the company is expected to pay due to surrenders according to (A.11) and (A.12).

From the definition of $\delta r^S_{j,i}$ in (A.21), we get:

$$\Delta R^S_i(j|k) = \mathrm{E}_k[(R^I_j - \max(g_{j,i}, \beta_{j,i} R^P_j)^+], \quad \text{for } j > k. \tag{A.31}$$

Due to the nonlinearity of $\delta r^S_{j,i}$ we estimate the conditional expectations in (A.30) with a Least Squares approach [68], thus following the same procedure we have used to forecast future returns. Therefore, we write $\Delta R^S_i(j|k)$ as linear combination of basis functions $\{\psi^w\}_{w=1,\dots,W}$:

$$\Delta R^S_i(j|k) \simeq \sum_{w=1}^{W} \bar{\bar{b}}^w_{k,j,i} \psi^w(\hat{R}^P_{k,i}, R^I_k) = \bar{\bar{b}}^T_{k,j,i} \psi(\hat{R}^P_{k,i}, R^I_k), \tag{A.32}$$

where we have used the notation $\hat{R}^P_{k,i} = \max(g_{j,i}, \beta_{j,i} R^P_j)$.

This time, the basis functions are bidimensional functions. For example, we can choose the bidimensional Laguerre polynomials, given by the product of couples of unidimensional Laguerre polynomials, defined above.

We look for the regression coefficients $\bar{\bar{b}}^*_{k,j,i}$ such that:

$$\bar{\bar{b}}^*_{k,j,i} = \underset{\bar{\bar{b}}_{k,j,i}}{\operatorname{argmin}} \, \mathrm{E}_k \left[\left(\psi(\hat{R}^P_{k,i}, R^I_k)^T \bar{\bar{b}}_{k,j,i} - \mathrm{E}_k[\delta r_{j,i}] \right)^2 \right],$$

which leads to:

$$\mathrm{E}_k \left[\psi(\hat{R}^P_{k,i}, R^I_k) \psi(\hat{R}^P_{k,i}, R^I_k)^T \right] \bar{\bar{b}}^*_{k,j,i} = \mathrm{E}_k \left[\psi(\hat{R}^P_{k,i}, R^I_k) \delta r_{j,i} \right].$$

We use again Monte Carlo techniques to compute regression coefficients. More precisely, we simulate N_P paths of $\hat{R}^P_{k,i}$ and $\hat{R}^I_k$, for $k = 1, \dots, T$, and we denote by $\hat{R}^{P,n}_{k,i}$, $R^{I,n}_k$ their respective values at time k in the n-th simulation. This time, we have to solve the system $\Psi_{k,i} \bar{\bar{b}}_{k,j,i} = d_{k,j,i}$, where the $W \times W$ matrix $\Psi_{k,i}$ and the W-array $d_{k,j,i}$ are such that:

$$(\Psi_{k,i})_{uv} = \frac{1}{N_P} \sum_{n=1}^{N_P} \psi^u(\hat{R}^{P,n}_{k,i}, R^{I,n}_{k,i}) \psi^v(\hat{R}^{P,n}_{k,i}, R^{I,n}_{k,i}),$$

$$(d_{k,j,i})_v = \frac{1}{N_P} \sum_{n=1}^{N_P} \psi^v(\hat{R}^{P,n}_{k,i}, R^{I,n}_k)(R^{I,n}_j - \hat{R}^{P,n}_{j,i})^+.$$

After having computed regression coefficients, we obtain $R^S_i(j|k)$, for $j > k$, from (A.32), so that we need to simulate only the current values $\hat{R}^P_{k,i}$ and $\hat{R}^I_k$.

Future new production

Following the same procedure used for $\Delta R_i^S(j|k)$ in (A.30), we compute

$$\Delta R_i^P(j|k) = \mathrm{E}[\delta r_{j,i}^P | \mathcal{F}_k], \quad \text{for } j > k, \tag{A.33}$$

to predict the probability of new production at future periods by using Table A.4 with the aim to forecast the number of new policyholders signing a contract at the each future periods according to (A.24). New production cash flows are computed by (A.7) and (A.8).

Future maturity payments

As regard to maturity payments, they can be computed by (A.13) and (A.14), taking into account the estimation of maturity benefit and that the number of policyholders that are still alive at policy maturity date is given by the total number of policyholders that entered into the contract, at any time, minus the number of policyholders that died or surrendered the contract before policy expiration.

Benchmark index model

In conclusion of the section, we point out that in order to compute (A.30) we need to define both the dynamics of the benchmark return and the dynamics of the asset classes in the portfolio, to deduce the portfolio return, also needed to compute (A.27). To end the section, we describe the model for the benchmark return, whereas the dynamics of portfolio asset classes are described in Section A.4. We assume that the benchmark index price follows a geometric Brownian motion. Therefore, the price of the benchmark index, I_t, is governed by:

$$dI_t = \mu^I I_t dt + \sigma^I I_t dW_t^I, \tag{A.34}$$

where the constant parameters $\mu_I \in \mathbb{R}$ and $\sigma^I > 0$ are the drift and the volatility of the process I_t, respectively, and W_t^I is a Brownian motion. It is well known that the

solution of equation (A.34) at time t conditional to F_s, with $s < t$, is given by

$$I_t = I_s \exp\left(\left(\mu^I - \frac{(\sigma^I)^2}{2}\right)(t-s) + \sigma^I(W_t^I - W_s^I)\right). \tag{A.35}$$

A.3.4 Interest rate model associated to the term structure of interest rates

In order to compute the liability duration by using the Macaulay formula (A.20), we need to calculate the discount factors, that are prices of zero-coupon bonds, so that we need to evolve the term structure of interest rates. For this reason, we introduce a short rate model. The convenience in the use of a short rate model is that the term structure of interest rates is an affine term structure in the sense that, at time t, the zero rate with maturity T is an affine function of the instantaneous short rate process at time t. In particular, we choose the one factor Hull & White model in the version referred in the literature as $G1++$ model. For the equivalence between $G1++$ model and the original one factor Hull & White model see [20] and [60], for instance. The advantages in the use of the $G1++$ model with respect to its classical counterpart are well known. For example, the generation of forward paths is numerically more stable and the analytical formula for bond prices is more tractable.

In the $G1++$ model, the dynamics of the instantaneous short rate r_t under the risk neutral measure Q is given by

$$r_t = x_t + f_t, \tag{A.36}$$

with initial value r_0. We assume that the process x_t satisfies the following stochastic differential equation:

$$\begin{cases} x_0 = 0, \\ x_t = -a^x x_t dt + \sigma^x(t) dW_t^x, \end{cases} \tag{A.37}$$

where a^x is a positive constant, $\sigma^x(t)$ is a positive deterministic function, and W_t^x is a standard Brownian motion. The function f is deterministic and is given by an

exact fitting to the term structure of discount factors observed in the market. We choose to employ a piecewise constant functional specification for the volatility of the process x_t. More precisely, the volatility $\sigma^x(t)$ is constant in the intervals $[0,1]$, $(1,3]$, $(3,+\infty)$, so that:

$$\sigma^x(t) = \begin{cases} \sigma^1, & \text{if } t \in [0,1], \\ \sigma^2, & \text{if } t \in (1,3], \\ \sigma^3, & \text{if } t \in (3,+\infty). \end{cases} \tag{A.38}$$

The parameters a^x and σ^1, σ^2, σ^3 can be calibrated by using market swaption prices. In fact, [34] and [88], for example, present an approximated swaption pricing formula, effective in the setting of the $G1++$ model, in the case that the strike is at the money:

$$ES(0,T,t_k,K,N) = N\frac{VOL}{\sqrt{2\pi}}\sum_{i=1}^{k}\tau_i P(0,t_i) \equiv N\frac{VOL}{\sqrt{2\pi}}P_{t_1}^{t_k}, \tag{A.39}$$

where $ES(0,T,t_k,K,N)$ is the price at time 0 of a European call swaption with maturity T, strike K, and nominal value N, which gives the holder the right to enter at time $T = t_0$ into a swap in which the holder pays the fixed rate K and receives the Libor rate at dates $t_1,\ldots,t_k$, with $t_0 < t_1 < \ldots < t_k$. In (A.39) τ_i denotes the year fraction from t_{i-1} and t_i, $P(0,t_i)$ represents the price at time 0 of a zero-coupon bond with maturity t_i years, and

$$VOL = \sqrt{\int_0^T (\sigma(u)^x)^2 A^2 e^{2a^x u} du},$$

with

$$A = e^{-a^x T}\frac{P(0,T)}{a^x P_{t_1}^{t_k}} - e^{-a^x t_k}\frac{P(0,t_k)}{a^x P_{t_1}^{t_k}} - \frac{K}{a^x}\sum_{i=1}^{k} e^{-a^x t_i}\tau_i \frac{P(0,t_i)}{P_{t_1}^{t_k}}.$$

We have calibrated the $G1++$ model using the swaption prices observed on September 30, 2020, and reported in Table A.6, thus obtaining the following parameters values: $a^x = 0.0048$, and $\sigma^1 = 0.0018$, $\sigma^2 = 0.0042$, $\sigma^3 = 0.0065$.

Maturity	Tenor	Strike	Price
1	1	-0.00490	0.00074
2	2	-0.00423	0.00313
3	3	-0.00316	0.00792
5	4	-0.00081	0.01741
5	5	-0.00032	0.02221
7	7	0.00203	0.04046
10	10	0.00278	0.07113

Table A.6: Swaption prices observed on September 30, 2020. Source: Bloomberg

After having calibrated the parameters of the process x_t, in order to simulate the process r_t, we use its conditional distribution. More precisely, from (A.36) and (A.37), for $s < t$, we have that r_t, conditional to $\mathcal{F}_s$, is normally distributed with:

$$\begin{aligned}\mathrm{E}[r_t|\mathcal{F}_s] =& x_s e^{-a^x(t-s)} + f_t,\\ \mathrm{Var}[r_t|\mathcal{F}_s] =& (\sigma^x(t))^2 \frac{1-e^{-2a^x(t-s)}}{2a^x},\end{aligned}$$

where E and Var denote the mean and the variance under the measure Q, respectively.

In the framework of the $G1++$ model, the price of a zero coupon bond at time t with maturity at time T, $P(t,T)$, can be computed using the following formula:

$$P(t,T) = A(t,T)e^{-B(t,T)x_t}, \tag{A.40}$$

where

$$A(t,T) = \frac{P^M(0,T)}{P^M(0,t)} e^{\frac{1}{2}[V(t,T)-V(0,T)+V(0,t)]}, \tag{A.41}$$

$$B(t,T) = \frac{1-e^{-a^x(T-t)}}{a^x}, \tag{A.42}$$

$$V(t,T) = \frac{(\sigma^x(t))^2}{(a^x)^2}\left(T-t-2\frac{1-e^{-a^x(T-t)}}{a^x}+\frac{1-e^{-2a^x(T-t)}}{2a^x}\right). \tag{A.43}$$

In (A.41) $P^M(0,t)$ denotes the market price of a zero-coupon bond with maturity t years, observed at time 0, i.e., the initial term structure.

A.4 Asset model

Our asset portfolio is composed of bonds, equity and cash. We split the bonds into four classes with different maturities: a class for bonds with maturity less than 3 years; a class including all the bonds with maturity between 3 and 5 years; a class comprising bonds with maturity from 5 to 10 years; finally, a class consisting of bonds with maturity greater than 10 years.

Since an insurance company has a conservative investment strategy, the largest part of portfolio is composed of bonds. So, in our strategy, we consider a lower bound for the portion of portfolio invested in bonds. We also consider an upper bound for the part of portfolio invested in equity. The remaining part is invested in cash. Section A.5 deals with the question of constraints on portfolio weights with more details, whereas in the following we describe the stochastic models used to simulate the returns of portfolio asset classes.

Bonds and equity models

In order to simulate bonds and equity returns, we assume that the underlying indexes dynamics follow geometric Brownian motions. Therefore, denoting by S_t the price of equity index at time t and by B_t^τ the price at time t of bond index with duration τ, we have:

$$dS_t = \mu^S S_t dt + \sigma^S S_t dW_t^S, \tag{A.44}$$

$$dB_t^\tau = \mu^{B^\tau} B_t^\tau dt + \sigma^{B^\tau} B_t^\tau dW_t^{B^\tau}, \tag{A.45}$$

where $\mu^S, \mu^{B^\tau} \in \mathbb{R}$ are the drifts of the processes S_t and B_t^τ, respectively, and σ^S, σ^{B^τ} are strictly positive constant parameters representing their volatilities. Moreover, W_t^S and $W_t^{B^\tau}$ are correlated Brownian motions and, obviously, they are both correlated with the other sources of randomness in the model, i.e., W_t^I, that appears in (A.35), and W_t^x, that is involved in (A.37). It is well known that the solutions of equations

(A.44) and (A.45) at time t conditional to $\mathcal{F}_s$, with $s < t$, are respectively given by

$$S_t = S_s \exp\left(\left(\mu^S - \frac{(\sigma^S)^2}{2}\right)(t-s) + \sigma^S(W_t^S - W_s^S)\right), \tag{A.46}$$

$$B_t^\tau = B_s^\tau \exp\left(\left(\mu^{B^\tau} - \frac{(\sigma^{B^\tau})^2}{2}\right)(t-s) + \sigma^{B^\tau}(W_t^{B^\tau} - W_s^{B^\tau})\right). \tag{A.47}$$

We refer to the work by Doherty and Garven [36] as an early paper where the Geometric Brownian Motion has been used in modelling assets and liabilities. In the paper a discrete-time option pricing model is used to derive the "fair" rate of return of an insurance firm.

Cash model

The evolution of the dynamics of cash in the asset portfolio is deduced from the short rate model described in Section A.3, taking into account that (see [34], for instance):

$$e^{\int_0^t r(s)ds} = \frac{e^{\int_0^t x(s)ds}}{e^{-\int_0^t f(s)ds}} = \frac{e^{\int_0^t x(s)ds}}{P^M(0,t)e^{-\frac{1}{2}V(0,t)}}. \tag{A.48}$$

Note that the dynamics of the process x_t is given in (A.37), $P^M(0,t)$ denotes the market price of a zero-coupon bond with maturity t, and the value of $V(0,t)$ can be computed by (A.43).

We would like to point out that all the processes in the model are simulated according to their dynamics in the real world measure, P, but cash is simulated from r_t whose dynamics is in the risk neutral measure, Q. Indeed, in the case of cash we can assume that the dynamics in P coincides with the dynamics in Q, being the risk premium null.

Asset value

After having described the dynamics of portfolio asset classes, we are able to compute the asset portfolio return at each period k, R_k^P, so that we can write a formula for

the evolution of the asset value over time:

$$A_k = A_{k-1}(1 + R_k^P) + \Pi_k + P_k - D_k - \Gamma_k - M_k, \quad k > 0, \tag{A.49}$$

where A_0 is given by premiums collected from policyholders at period 0 plus the initial investment on the part of the company.

A.5 First stage of portfolio rebalancing

In our stochastic ALM model, we consider a dynamic reinvestment strategy in which the asset portfolio is restructured at each period k according to the evolution of the liability portfolio. We use a scenario-based simulation approach. For each scenario at each period k, the investment strategy decides which types of asset class must be sold or bought in order to guarantee that there is enough money to meet the obligations with policyholders and company's shareholders. In particular, for each simulation at each period k, we compute the duration of liabilities, the duration of asset portfolio and the asset portfolio return. Then, we rebalance our asset portfolio with the aim to accomplish two goals:

i. Matching between assets duration and liabilities duration. More precisely, we aspire to minimize the positive part of the difference between assets duration and liabilities duration, since liquidity problems can arise when the assets have a longer duration than liabilities, but not vice versa;

ii. Achievement of a certain target return. In particular, we ask that the portfolio return is not too much distant from the benchmark return.

In order to rebalance our portfolio composition, for each simulation at each period k, we solve a nonlinearly constrained optimization problem subject to several real world constraints. In particular, we consider the so-called budget constraint and no short selling constraint, and for each asset class we set upper and lower bounds and we fix a maximum turnover. In addition, we set a maximum portfolio turnover,

and we impose other linear constraints given by the investment policy. All these constraints are reasonable for an insurance company and we calibrate them on an EU-based life insurance company's portfolio. We summarize all these constraints in Table A.7, where we have denoted by $\boldsymbol{\alpha}_k = (\alpha_k^{B1}, \alpha_k^{B2}, \alpha_k^{B3}, \alpha_k^{B4}, \alpha_k^E, \alpha_k^C)$ the array of asset classes weights at period k. In particular, α_k^{Bn}, α_k^E, α_k^C are the weights in the portfolio composition at period k of the n-th class of bonds, equity and cash, respectively. We denote by $I_\alpha = \{B1, B2, B3, B4, E, C\}$. In Table A.7 m^B denotes the lower bound for the sum of the bonds weights in portfolio composition, M^E the upper bound for weight of equity, and TO and TO^{tot} are, respectively, the maximum turnover on each asset class and the maximum portfolio turnover.

Budget constraint	$\sum_{i\in I_\alpha} \alpha_k^i = 1$
No short selling constraint	$\alpha_k^i \geq 0, \quad \forall i \in I_\alpha$
Investment policy constraints	$\sum_{n=1}^4 \alpha_k^{Bn} \geq m^B$ $\alpha_k^E \leq M^E$
Turnover constraints	$\left\|\alpha_k^i - \alpha_{k-1}^i\right\| \leq TO, \quad \forall i \in I_\alpha$ $\sum_{i\in I_\alpha} \left\|\alpha_k^i - \alpha_{k-1}^i\right\| \leq TO^{tot}$

Table A.7: Constraints imposed in the optimization problem of the first stage of portfolio rebalancing

At period k the optimization problem consists of finding an optimal array of asset classes weights $\boldsymbol{\alpha}_k$ such that:

$$\begin{aligned} &\text{minimize} \quad (A^D(\boldsymbol{\alpha}_k) - L_k^D)^+; \\ &\text{subject to} \quad \begin{cases} \beta^L R_{k+1}^I \leq R_{k+1}^P \leq \beta^U R_{k+1}^I, \quad \text{with constant } \beta^L, \beta^U, \\ \text{constraints in Table A.7.} \end{cases} \end{aligned} \tag{A.50}$$

Note that assets duration, A^D, is a combination of durations of bonds in the asset portfolio.

In a general framework, we can include transaction costs, that arise when rebalancing the asset portfolio. In the case of no null transaction costs the portfolio return at period k is given by:

$$R_k^P = \boldsymbol{\alpha}_k \cdot \boldsymbol{R}_k - [\boldsymbol{c}^S \cdot (\boldsymbol{\alpha}_{k-1} - \boldsymbol{\alpha}_k)^+ + \boldsymbol{c}^B \cdot (\boldsymbol{\alpha}_k - \boldsymbol{\alpha}_{k-1})^+], \tag{A.51}$$

where $\boldsymbol{c}^S$ and $\boldsymbol{c}^B$ are the vectors of asset classes selling and buying costs, respectively, and $\boldsymbol{R}_k$ is the vector of asset classes returns at time k. In the numerical tests we assume null transaction costs, because the introduction of transaction costs different from zero substantially increases the elapsed computational time, but does not affect results in a significant way, in the sense that results with transaction costs are comparable to results without them.

A.6 Second stage of portfolio optimization

In the previous section we have chosen a portfolio rebalancing strategy that ensures the company will be solvable, and shareholders and policyholders will benefit from a competitive return. But the proposed strategy is not necessarily optimal. For this reason, we now introduce a second stage of portfolio optimization with the aim of maximizing the expected value of a chosen utility function, taking into account the results obtained from the first stage of portfolio rebalancing. Indeed, in the first step of portfolio rebalancing we consider only six asset classes, and in the second step for each bonds asset class and for equity asset class, taking into account several sub-sectors, we run a sectorial optimization problem that maximizes the expected utility function of terminal wealth over specified horizon (see [25]). We suggest to solve sectorial optimization problems in the second stage to refrain from managing an excessive number of asset classes. For instance, for each bond asset class sub-sectors could be government core and government peripheral bonds, financial and corporate bonds, financial investment grade and financial sub-investment grade bonds, etc. For equity asset class sub-sectors could be energy, healthcare, utilities, information technology, etc.

More precisely, chosen a utility function U, at each time step k we solve five sectorial optimization problems, so that we search for the optimal weights vectors $\boldsymbol{\omega}_k^i = (\omega_k^{i,1}, \ldots, \omega_k^{i,N_i})$, for $i \in I_\alpha \setminus \{C\}$, such that:

$$\begin{aligned} &\text{maximize} \quad \mathrm{E}_k \left[\max_{\boldsymbol{\varpi}_{k+1}^i} \mathrm{E}_{k+1} \left[\max_{\boldsymbol{\varpi}_{k+2}^i} \mathrm{E}_{k+2} \left[\ldots \max_{\boldsymbol{\varpi}_{T-1}^i} \mathrm{E}_{T-1} \left[U(\boldsymbol{\omega}_{T-1}^i \cdot \boldsymbol{R}_T^i) \right] \ldots \right] \right] \right]; \\ &\text{subject to} \quad \sum_{j=1}^{N_i} \omega_k^{i,j} = \alpha_k^i, \end{aligned} \tag{A.52}$$

where $\boldsymbol{R}_l^i$ and N_i are the vector of sub-sectors returns at period l and the number of sub-sectors for asset class i, respectively. In this way, an optimal portfolio strategy is proposed (see [75]).

However, in numerical results presented in Section A.8 we focus on the first step of the portfolio rebalancing strategy, because the second step can be performed by standard techniques of stochastic programming (see, for example, [31]).

A.7 Market data

In our portfolio optimization problem we assume the insurance company can invest in six specific asset classes, summarized in Table A.8. In order to simulate the dynamics of bonds and equity log-returns, respectively deduced from (A.44) and (A.45), we use the historical estimations of annualized mean and standard deviation of representative indexes daily log-returns, computed considering an annualization factor of 252. We do the same for the dynamics of log-returns of the benchmark index, used in the surrender and new production models. The dynamics of the benchmark return is inferred from (A.34). Indexes and their log-returns statistics are listed in Table A.8. We have considered daily observations from September 30, 2010 to September 30, 2020, for a total of 2614 observations. Data have been obtained from Bloomberg. Also, in Table A.8, for each representative index of the asset classes of the investable portfolio we

show the index duration, given by the average duration of the index components, weighted on the basis of their market prices. Finally, since cash log-returns are simulated by using the short rate model, in Table A.8, we report the representative index for the short rate, used only as proxy to estimate correlation between the dynamics of cash and the dynamics of all the other stochastic variables. Indeed, all the sources of randomness in the model are correlated. When simulating, the historical correlation of indexes is used as correlation between the Brownian motions in the model, i.e., W^I, involved in the dynamics of the benchmark index (A.34), W^x, included in the dynamics of the short rate (A.37), W^S, that is in the dynamics of equity (A.44), and W^{B^τ}, contained in the dynamics of bonds with duration τ (A.45).

Asset class		Index	Duration	Log-returns Mean	Log-returns Std
$B1$	bonds, maturity 1-3	EZ1X	1.883087	0.004453	0.006722
$B2$	bonds, maturity 3-5	EZ2X	3.814414	0.015954	0.016217
$B3$	bonds, maturity 5-10	EZ6X	6.859975	0.037001	0.033788
$B4$	bonds, maturity >10	EZ9X	16.48279	0.075430	0.080750
E	equity	MXEM	0	0.033442	0.183722
r	short rate	Eur003m	-	-	-
BI	benchmark	NCV0	-	0.028616	0.039320

Table A.8: Asset classes representative indexes, short rate representative index and benchmark index. Duration, annualized mean and annualized standard deviation for daily log-returns are reported

In Table A.9 we report the historical correlations.

Since the aim of an insurance company is not only to meet its financial obligations, but also to obtain a profit, we are interested in the changes in own funds value. Therefore, we keep track of the evolution over time of the difference between asset and liability values, so that we need to make an assumption on the relation between them at the initial time, say at time 0. In particular, we set the level of liabilities at the initial time to 90% of the value of the assets at the same time, that is to say, the

	$B1$	$B2$	$B3$	$B4$	E	r	BI
$B1$	1	0.9308	0.7422	0.5675	0.2288	0.0048	0.4078
$B2$	0.9308	1	0.9145	0.7588	0.1947	-0.0013	0.6187
$B3$	0.7422	0.9145	1	0.9310	0.1118	-0.0017	0.8263
$B4$	0.5675	0.7588	0.9310	1	-0.0086	0.0005	0.9121
E	0.2288	0.1947	0.1118	-0.0086	1	-0.0180	-0.1818
r	0.0048	0.0016	-0.0075	-0.0154	-0.0180	1	-0.0124
BI	0.4078	0.6187	0.8263	0.9121	-0.1818	-0.0124	1

Table A.9: Correlation matrix between the asset classes, the short rate and the benchmark index

following relation is satisfied:

$$L_0 = 0.887 A_0. \tag{A.53}$$

Another assumption we need to make concerns the initial portfolio composition, described in Table A.10. Portfolio is periodically rebalanced observing constraints on asset classes weights, as fully discussed in Section A.5. In particular, in Table A.7 we choose $m^B = 0.70$, $M^E = 0.20$, $TO = 0.05$, and $TO^{tot} = 30$.

Asset class		Weight
$B1$	bonds, maturity 1-3	21.09%
$B2$	bonds, maturity 3-5	22.91%
$B3$	bonds, maturity 5-10	35.79%
$B4$	bonds, maturity >10	15.38%
E	equity	3.74%
C	cash	1.09%

Table A.10: Initial portfolio composition in the numerical tests

A.8 Numerical results

In this section some numerical results are presented. In particular, we deduce how the portfolio has to be rebalanced according to the strategy illustrated in Section A.5. Also, we focus on the values of actuarial reserves and own funds. Moreover, we are

interested in the study of the impact of mortality model and of surrender and new production models on how the number of alive policies changes over time.

We have used 10^3 simulations for the phase of regression coefficients computation in the Least Squares Monte Carlo method and we have generated 10^4 different scenarios for the phase of portfolio composition optimization. All tests have been performed by using Matlab on an Intel(R) Core(TM) i7-8550U, 1.99 GHz, 16 GB (RAM), x64-based processor.

In the following, we make the assumptions listed below:

- all contracts have the same value, say €10 000, in the moment they are signed;
- all policies expire at the same future date, say at time $T = 10$ years;
- the initial number of policyholders in each model point is reported in Table A.11;
- at the initial time policies are equally distributed between male and female policyholders (gender equality);
- portfolio is rebalanced at each time step, that is one year;
- policyholders pay a single premium at the beginning of the contract;
- the participation rate β is the same for all model points, and is set to 95%, constant over time, unless otherwise stated.

In Figure A.1 we exhibit how the portfolio composition is rebalanced every year following the strategy described in Section A.5. In particular, we show the mean value of portfolio composition weights over all the scenarios. We infer that the weight of bonds with maturity less than 3 years has to increase significantly over time, while the weight of equity rises slightly. Moreover, the weights of cash and bonds with maturity between 3 and 5 years remain nearly constant over time, whereas we have to invest less and less in bonds with longer maturity. The portfolio composition evolution in Figure A.1 originates from the fact that all policies expire at time $T = 10$, so that

Age	Minimum guarantee 0%	1%	2%
40	50	5	1
45	55	5	3
50	55	10	3
55	60	25	15
60	70	80	23
65	60	100	50

Table A.11: Initial number of policyholders in each model point

liability duration approaches to zero with the passing of time. As a result, in order to match asset duration and liability duration, we need to invest more and more in asset classes with short duration, and less and less on asset classes with long duration.

In Figure A.2 we illustrate how much the liability value of each model point weighs on the total value of liabilities. We consider the interval $[0, 9]$, because at maturity date, i.e., $T = 10$, all policyholders have been refunded and the total liability value is zero. We note that the weights of model points related to younger policyholders increase over time, while the weights of model points associated with policyholders aged 60 or more decrease. In fact, young policyholders are less likely to die with respect to older policyholders (see Table A.5), so that death payments that the company has to make at each time are due especially to deaths of older policyholders. This means that the company has to refund before maturity more old policyholders than young policyholders, thus lightening the weight on the total value of liabilities of model points related to old policyholders.

As regard to the number of alive contracts, it decreases over time, as shown in Figure A.3. Evidently, at each time step new production is not enough to counterbalance deaths and surrenders. However, the evolution of the number of alive policies may be different if other assumptions are made on the model or another set of parameters is chosen. It is even possible that the number of alive contracts increases over time, since the number of new investors may exceed the number of policyholders who die or exercise the surrender option. The right plot in Figure A.3 considers separately

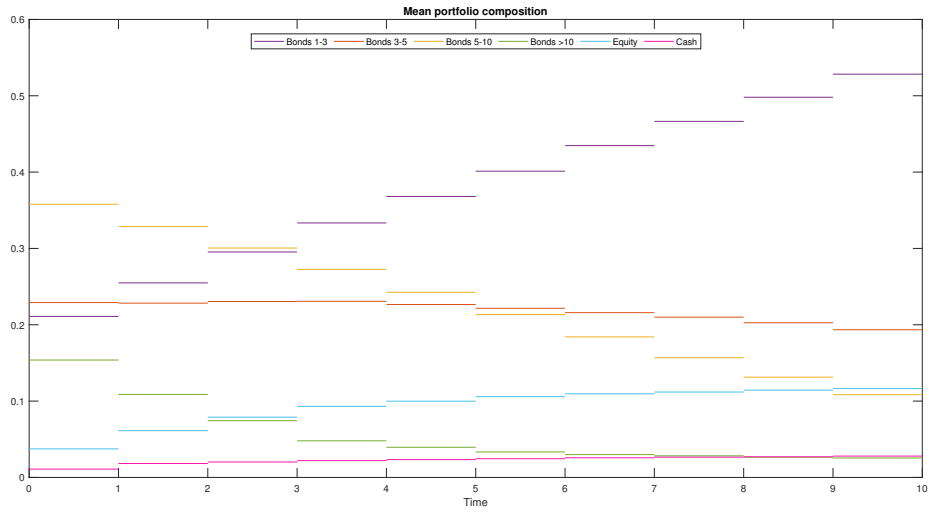

Figure A.1: Portfolio composition rebalancing

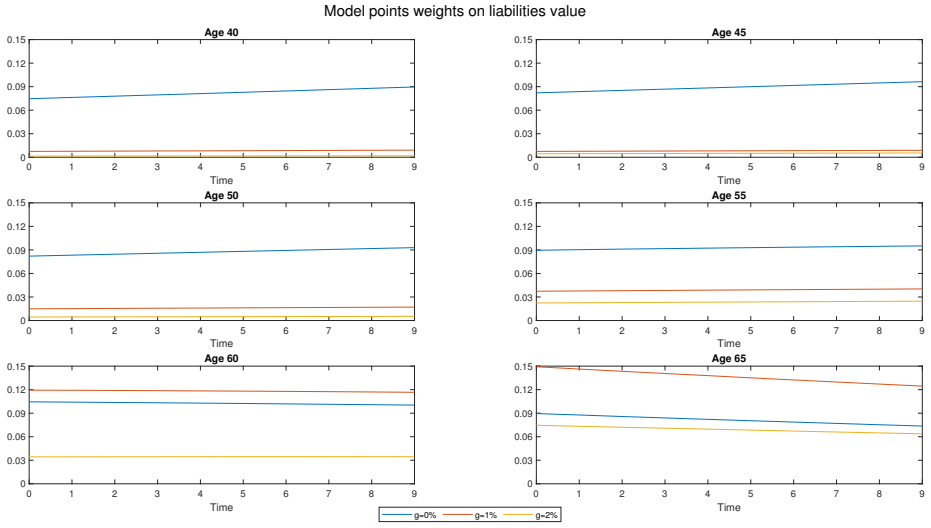

Figure A.2: Model points weights on liabilities value at different times

male and female policyholders, thus allowing us to evaluate the effect of mortality model on the changes of the alive policies number. In fact, since the surrender and the new production models do not depend on gender, the different rate of decrease

for men and women is only due to the fact that women mortality rate is lower than men mortality rate (see Table A.5).

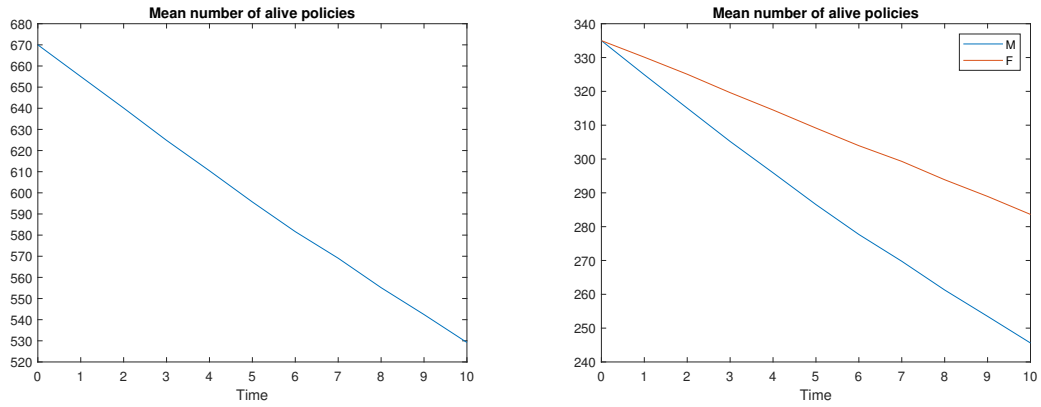

Figure A.3: Mean number of alive policies at each time. On the left the total number is plotted; on the right the distinction between males and females is taken into account

In order to better analyse the issue of new production, in Figure A.4 we plot the mean number over all the scenarios of alive policyholders considering separately policies with different starting time. So, on the top we show the number of policies that started at time 0, on the bottom the numbers of policies that started after time 0. As expected, the major decrease can be observed in the population that entered into the contract at time 0, meaning that at each time it is more likely that a policyholder who started the contract at time 0 dies or abandons the policy rather than a policyholder who started the contract after time 0. In fact, the set of policyholders that entered at time 0 is more numerous.

Participation rate sensitivity

So far we have considered a fixed participation rate, but it is interesting to study how different values for β influence actuarial reserves and own funds, as well as the number of abandons and new production.

In Figure A.5 we plot actuarial reserves for different values of β. As expected, if β grows, the payments that the company has to make due to policyholders who die,

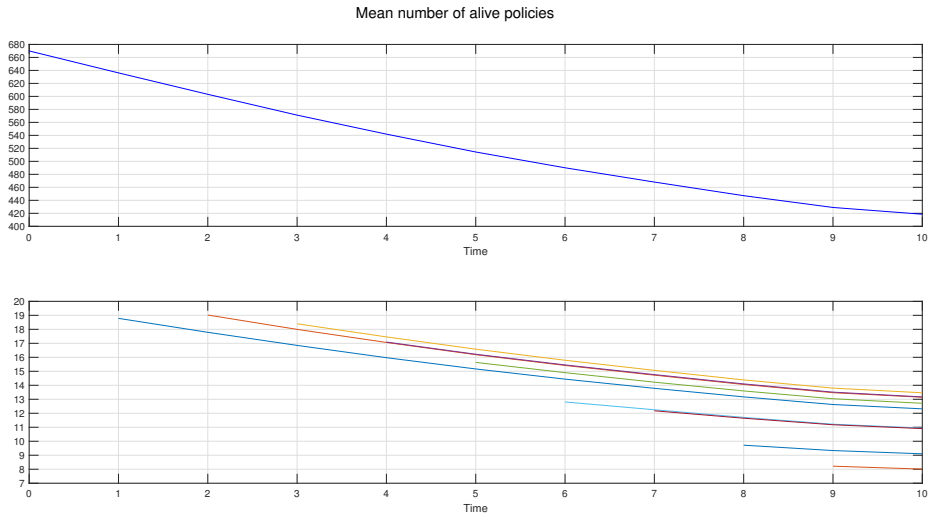

Figure A.4: Mean number of alive policies with different starting time. The plot on the top displays the evolution of the number of alive contracts that started at time zero; lines in the plot on the bottom show the evolution of the numbers of alive policies that started at time $1, 2, \ldots, 9$, respectively

abandon the contract or reach maturity, are more consistent. Therefore, actuarial reserves, discounted expectation of future disbursements, increase. Note that we consider the time interval $[0, 9]$, thus ignoring the maturity date, $T = 10$, when all policies have expired and actuarial reserves are zero, because the company has no more future payments to make.

In Figure A.6 we show the difference between asset value and liability value changing the participation rate. Evidently, the difference examined in the plot decreases when increasing the participation rate, in fact:

$$A_t - L_t = A_{t-1}(1 + R_t^P) - \sum_{i=1}^{N_M} L_{t-1,i}(1 + \max(g_i, \beta R_t^P)), \tag{A.54}$$

where the liability term increases if β becomes greater. However, in any case own funds rise over time.

In addition, Figure A.6 shows that at each time step the mean value of the difference between asset value and liability value is positive. However, in some scenarios

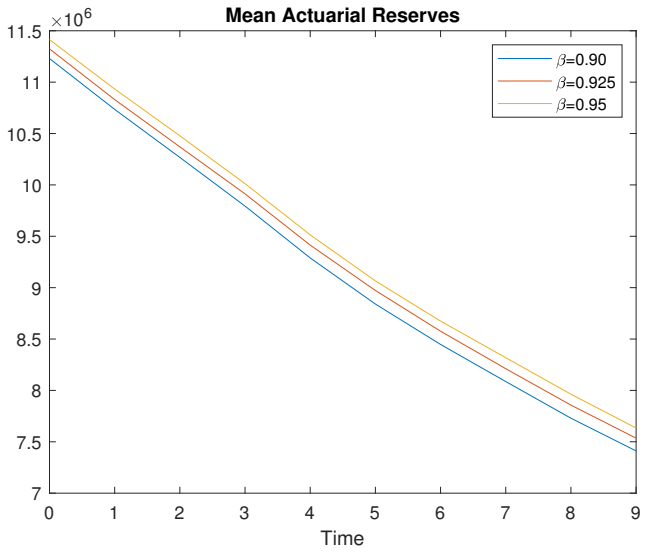

Figure A.5: Evolution of the average actuarial reserves for different values of the participation rate β

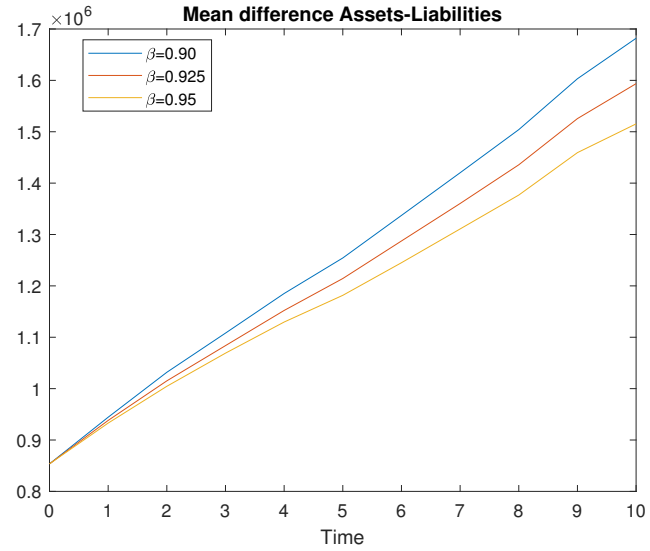

Figure A.6: Evolution of the average difference between asset value and liability value for different values of the participation rate β

own funds become negative and the company is declared defaulted. In Table A.12 we report the probability of default, defined as the ratio between the number of scenarios in which the company defaults and the total number of scenarios (10000), for three different values of the participation rate β. Obviously, probability of default rises by increasing β.

β	Probability of default
90.0%	1.10%
92.5%	1.31%
95.0%	1.68%

Table A.12: Probability of default for different values of the participation rate β

Finally, we analyse how the value of the participation rate affects the changes in the number of alive policies over time, as shown in Figure A.7. On the contrary of what happens in the right plot in Figure A.3, where the impact of the mortality model is presented, in Figure A.7 the effect of surrender and new production models can be observed. In fact, the mortality model does not depend on the participation rate, while surrender and new production models strongly depend on it (see Section A.3.1). In particular, the earnings offered by the insurance company rise when increasing β, so that less policyholders are motivated to abandon the contract, and more investors subscribe to the policy. As a result, the number of alive policies decreases more slowly in the case of larger values of the participation rate.

Death probabilities sensitivity

We have also tested our model using 2020 period life table, that is, death probabilities affected by the COVID-19 pandemic. As expected, 2020 death probabilities, reported in Table A.13, are larger than 2019 death probabilities, shown in Table A.5.

Obviously, the number of alive policies decreases faster in the case of larger death probabilities, as shown in Figure A.8.

In Figure A.9 we report the evolution over time of actuarial reserves and own

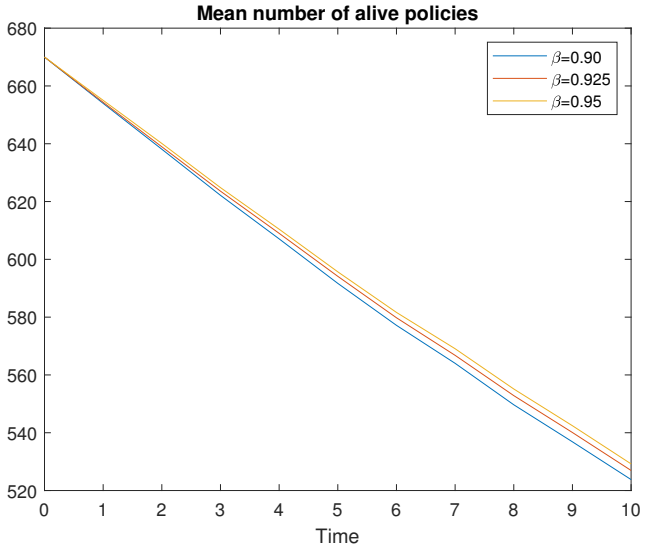

Figure A.7: Mean number of alive policies at each time for different values of the participation rate β

Age	$\mathcal{M}$ (%)	$\mathcal{F}$ (%)
$[40, 44]$	0.5879	0.3514
$[45, 49]$	0.9200	0.5625
$[50, 54]$	1.5864	0.9315
$[55, 59]$	2.6150	1.4310
$[60, 64]$	4.4282	2.2973
$[65, 69]$	7.2543	3.6888

Table A.13: 2020 period life table: death probabilities in percentage for men ($\mathcal{M}$) and women ($\mathcal{F}$) for given age intervals. Source: ISTAT (Italian National Institute of Statistics)

funds. In the case of 2020 death probabilities actuarial reserves are lower, because the company refunds policyholders sooner, therefore the refund is smaller. Moreover, own funds are larger in the case of larger death probabilities.

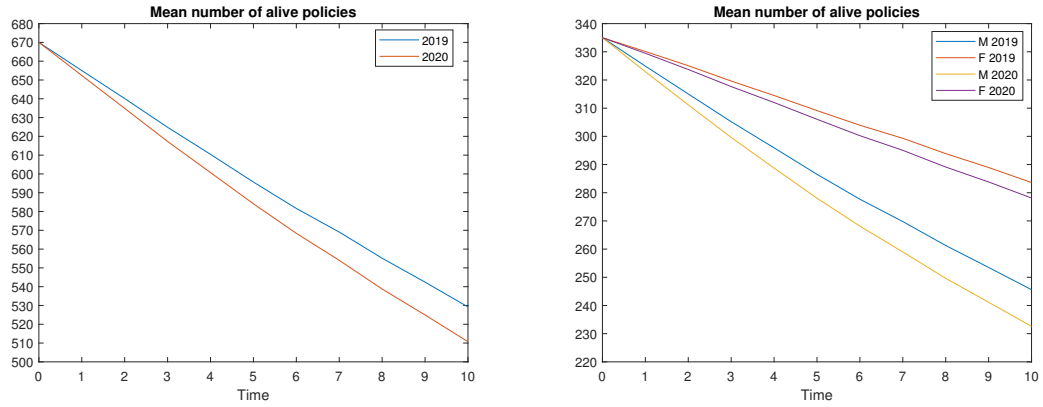

Figure A.8: Mean number of alive policies at each time with 2019 period life table and 2020 period life table

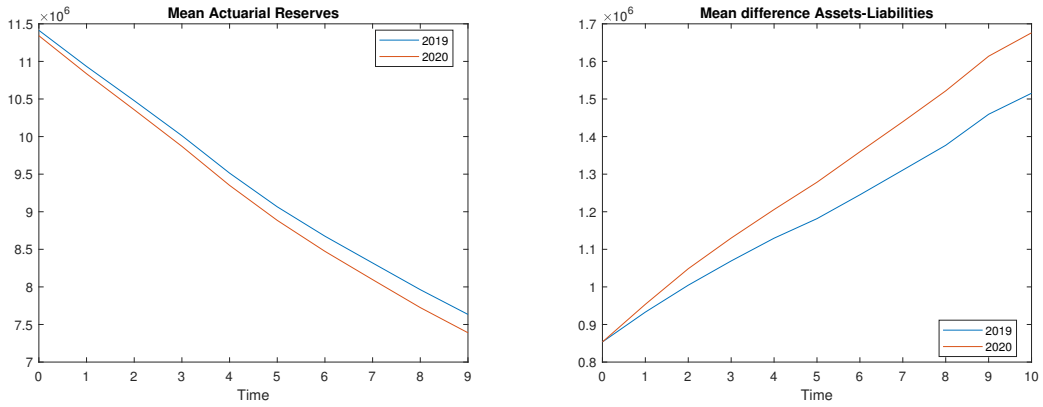

Figure A.9: Mean number of alive policies with 2019 period life table and 2020 period life table

A.9 Conclusions

In this appendix, we have built a two-stage ALM model for a life insurance company, including a policyholders' saving account model, a mortality model and a surrender model, as well as a new production model, an innovative feature with respect to existing works in literature, as far as we know. In order to handle the large number of contracts we have split them into model points, by grouping policies with similar age of the policyholder, same minimum guaranteed rate of return, and same time-to-maturity. Since an insurance company has the purpose of both ensuring its solvency and obtaining a profit, firstly, we have built a strategy for the asset portfolio rebalancing that aims to match asset duration and liability duration, and to achieve a target return. Also, we have considered several real world constraints on portfolio composition weights. From the technical point of view, the portfolio rebalancing strategy is the result of a nonlinearly constrained optimization problem, that requires the computation of future cash flows projections. According to our knowledge, we have proposed an innovation with respect to literature: when computing balance sheets projections, we have considered, in addition to future death and maturity payments, also future surrender payments and future cash flows due to new production. Next, we have proposed a second stage of portfolio rebalancing that includes sectorial optimization problems with the aim to maximize the expected value of a chosen utility function. In this way, we have built an optimal portfolio rebalancing strategy based on risk-averse decisions.

On the side of numerical tests, we have focused on the first stage of portfolio rebalancing, and we have shown how the portfolio has to be dynamically rebalanced and how the liability value associated to each model point weighs on the total value of liabilities. We have pointed out the effect of the mortality model on the evolution over time of the number of alive policies by considering separately male policyholders and female policyholders. We have proposed an analysis of the participation rate sensitivity, taking account of the evolution of actuarial reserves and of own funds. As expected, actuarial reserves increase and own funds decrease by increasing the

participation rate. Moreover, we have focused on the positive result that the mean value of own funds raises over time for any considered value of the participation rate. However, there is a small probability, depending on the participation rate, that in certain scenarios the company defaults, because own funds become negative. Finally, we have analysed how the number of alive policies varies by changing the value of the participation rate, thus showing how it depends on surrender and new production models. Indeed, the participation rate does not affect policyholders' mortality, so that the different rate of decrease in the number of alive policies with different values of the participation rate is due only to the different numbers of surrenders and of new policyholders.

Resumen extenso

En este trabajo se proponen y estudian nuevos modelos complejos de valoración de opciones *vanilla* europeas en el contexto de varias divisas (*multicurrency setting*), cuando se tienen en cuenta los ajustes de valoración debidos al riesgo de contrapartida. Además de la obtención de los modelos, se proponen diferentes técnicas numéricas para aproximación de las soluciones de los mismos, ya que no pueden ser obtenidas de manera analítica.

El interés de considerar el contexto de varias monedas, o multidivisa, proviene del hecho de que las instituciones financieras pueden operar en mercados con distintas monedas, por ejemplo cuando invierten en derivados cuyos activos subyacentes están en diferentes monedas o, estando en una moneda, la financiación o el colateral están en otras monedas. La mayor parte de la literatura sobre los ajustes de valoración asociados al riesgo de contrapartida se ha centrado en el contexto de una moneda.

La motivación de considerar ajustes de valoración asociados al riesgo de contrapartida en los precios de los derivados financieros surge a partir de la crisis financiera en 2007. Tras dicha crisis, quedó claro que cualquier marco de fijación de precios de un contrato financiero debería tener en cuenta la posibilidad de incumplimiento de cualquier contraparte involucrada en el mismo [28, 61], así como aspectos relacionados con la entrega de colateral, el riesgo de liquidez o los costos de financiamiento [52, 85]. Por lo tanto, se deben considerar diferentes ajustes de valoración debido a estos factores al fijar el precio de un derivado financiero. El conjunto de estos ajustes se denomina globalmente ajuste de valoración total o XVA (por su expresión en inglés: (*X-Valuation Adjustment*), donde "X" representa las diferentes letras que aparecen

en los ajustes de valor asociados al crédito (CVA), débito (DVA), fondeo (FVA), colateral (CollVA), capital (KVA) o marginal (MVA), por ejemplo. Los ajustes iniciales y más clásicos estuvieron motivados por los riesgos de contraparte relacionados con el crédito, la financiación y las garantías. Posteriormente se han añadido los ajustes relacionados con el capital y el marginal. Entre las referencias clásicas y más generales sobre el tema, dirigimos a los lectores a los libros [21, 28, 52] y las referencias que se citan en ellos.

En el marco de productos en una moneda, básicamente se han desarrollado tres metodologías principales. Una primera aproximación, siguiendo los artículos iniciales de Piterbarg [82] y Burgard y Kjaer [22], que obtienen formulaciones de EDPs mediante argumentos de cobertura sobre carteras adecuadas y la aplicación del lema de Itô para procesos de salto-difusión. Este enfoque en términos de formulación de EDP se ha seguido en [43], donde el problema también se escribe de manera equivalente en términos de esperanzas. Además, también se ha abordado en [4] y [3], donde se han analizado matemáticamente y resuelto numéricamente modelos EDPs para la valoración de opciones europeas con uno y dos factores estocásticos. Un segundo enfoque sigue las ideas iniciales que aparecen en [18] para obtener el CVA por medio de formulaciones basadas en esperanzas, y luego se extiende a los costos colateralizados, de cierre y de financiamiento en [78]. Además, este enfoque se ha abordado en [5, 2] para las opciones americanas, y en [15] para la dinámica de Levy, por ejemplo. Un tercer enfoque, basado en ecuaciones diferenciales estocásticas hacia atrás (BSDEs), se introdujo en [26] y [27].

Recientemente, se ha prestado atención a la extensión de los ajustes de valoración en mercados de una moneda al contexto de varias monedas [44]. Por lo tanto, comenzamos a construir un marco multidivisa, siguiendo las ideas de [44], donde se tienen en cuenta la consideración conjunta de los ajustes de CVA, FVA, CollVA y repo. Para la inclusión adicional de KVA o MVA en el XVA, se podrían considerar las ideas en [51, 50] en el caso de la moneda única.

Para ello, se suponen intensidades estocásticas de incumplimiento y se involucran

activos subyacentes denominados en distintas monedas. Nuestro enfoque se basa en el mismo marco y supuestos que en [43], aunque extendido a un entorno de múltiples monedas y con la hipótesis adicional de una intensidad de incumplimiento cero para la persona que realiza la cobertura (*hedger*). En particular, tomamos en consideración las siguientes hipótesis:

- La contraparte puede incumplir, pero la persona que hace la cobertura está libre de incumplimiento.
- Los precios de los activos subyacentes involucrados se modelan mediante procesos de difusión correlacionados.
- Los eventos de incumplimiento de los inversores no afectan la evolución de los precios de los activos subyacentes involucrados.
- El diferencial crediticio estocástico de la contraparte se modela como un proceso positivo con reversión a la media, que se correlaciona con los procesos seguidos por los precios de los activos subyacentes y, cuando estos se consideran estocásticos, con los procesos seguidos por los tipos de cambio (*FX rates*).

Siguiendo [44], primero deducimos formulaciones de ecuaciones en derivadas parciales (EDP) del problema de fijación de precios de XVA. Para ello, empleamos argumentos de cobertura, de ausencia de arbitraje y de autofinanciamiento de carteras junto con una elección del valor de mercado del derivado en caso de incumplimiento (*mark to market*), representado por M^D. Esta elección conduce a un problema lineal de EDPs, si el valor de mercado en el momento de incumplimiento es igual al precio del derivado cuando no se tiene en cuenta el riesgo de contraparte (derivado libre de riesgo), o a un problema no lineal de EDPs, cuando se considera que en el momento de incumplimiento se tiene en cuenta el valor con riesgo de contraparte (derivado con riesgo de contrapartida).

Inicialmente consideramos que los tipos de cambio entre las monedas involucradas son constantes, y a continuación consideraremos una situación más compleja y realista

en la que los tipos de cambio evolucionan de manera estocástica, proponiendo procesos adecuados para modelar esta evolución.

En concreto, en el caso de tipos de cambio constantes considerados inicialmente, los factores estocásticos son los precios de los activos subyacentes y el diferencial de crédito de la contraparte (*credit spread*). En este marco, los modelos de EDPs lineales y no lineales para obtener el XVA, representado por U, son los siguientes:

- Modelo de EDP no lineal (caso $M^D = V^D$):

$$\begin{cases} \dfrac{\partial U}{\partial t} + \mathcal{L}_{Sh}U - f^D U = h(W^D + U - C^D)^+ + (r^D + b^{D,C_0} - f^D)C^D\,, \\ U(T,S,h) = 0\,. \end{cases}$$

- Modelo de EDP lineal (caso $M^D = W^D$):

$$\begin{cases} \dfrac{\partial U}{\partial t} + \mathcal{L}_{Sh}U - \left(\frac{h}{1-R_C} + f^D\right) U = h(W^D - C^D)^+ + (r^D + b^{D,C_0} - f^D)C^D\,, \\ U(T,S,h) = 0\,. \end{cases}$$

En ambos casos el operador diferencial en derivadas parciales involucrado es

$$\begin{aligned} \mathcal{L}_{Sh} = {} & \frac{1}{2}\sum_{i,k=1}^{N} \rho^{S^i S^k}\sigma^{S^i}\sigma^{S^k} S^i S^k \frac{\partial^2}{\partial S^i \partial S^k} + \frac{1}{2}(\sigma^h h)^2 \frac{\partial^2}{\partial h^2} \\ & + \sum_{i=1}^{N} \rho^{S^i h}\sigma^{S^i}\sigma^h S^i \frac{\partial^2}{\partial S^i \partial h} + \sum_{i=1}^{N}(r^i - q^i)S^i \frac{\partial}{\partial S^i} + \alpha h(m - \log(h))\frac{\partial}{\partial h} \end{aligned}$$

cuando se usa el modelo de Vasicek exponencial para el diferencial de tipo y otro análogo en el caso de usar el modelo de CIR. Además, el precio del activo sin riesgo satisface el model clásico de EDPs de Black-Scholes:

$$\begin{cases} \partial_t W^D + \mathcal{L}_S W^D - f^D W^D = 0\,, \\ W^D(T,S) = G(S)\,, \end{cases}$$

donde $G = G(S)$ es la función de pago del derivado de tipo europeo y el operador en derivadas parciales es:

$$\mathcal{L}_S = \frac{1}{2}\sum_{i,k=1}^{N} \rho^{S^i S^k}\sigma^{S^i}\sigma^{S^k} S^i S^k \frac{\partial^2}{\partial S^i \partial S^k} + \sum_{i=1}^{N}(r^i - q^i)S^i \frac{\partial}{\partial S^i}\,.$$

El precio del derivado con riesgo de contrapartida viene dado por $V^D = W^D + U$.

En cuanto a la resolución numérica de los modelos de EDPs, abordamos la solución de las EDP lineales y no lineales solo en el caso de un derivado sobre dos activos subyacentes en monedas diferentes, con tipos de cambio de divisas constantes y diferencial de crédito de la contraparte dependiente del tiempo de modo determinista. Para ello, empleamos un método semi-Lagrangiano (también conocido como método de las características) para la discretización en tiempo, combinado con el método de elementos finitos de tipo Lagrange constante a trozos para la discretización de las variables espaciales asociadas a los factores estocásticos. La consideración conjunta de métodos semi-Lagrangianos con métodos de elementos finitos se denomina generalmente como métodos de Lagrange-Galerkin. Estas técnicas son especialmente útiles para la discretización de los llamados problemas de EDPs de convección dominante, donde los términos que contienen derivadas de primer orden (términos de convección) dominan sobre los que contienen las derivadas de segundo orden (términos de difusión). En este escenario, las técnicas propuestas evitan la presencia de oscilaciones numéricas espurias que aparecen cuando se consideran técnicas de discretización en tiempo más convencionales. Adicionalmente, se utilizan ténicas de punto fijo cuando se involucran EDPs no lineales.

En el caso de alta dimensión, los métodos numéricos deterministas convencionales conllevan un coste computacional que crece exponencialmente con el número de variables espaciales en la EDP. En ese caso, se ha optado por métodos numéricos probabilísticos para resolver las formulaciones equivalentes basadas en esperanzas.

En primer lugar, para obtener la formulación en términos de esperanzas equivalente al anterior modelo no lineal de EDPs, aplicamos el teorema no lineal de Feynman-Kac, que relaciona la solución de EDPs no lineales con la solución de BSDE. El enunciado del teorema no lineal de Feynman-Kac se remonta al artículo seminal [80]. Como el término no lineal aparece en la incógnita U y no en las derivadas de primer orden, el Teorema 1.1 en el trabajo reciente [14] se puede aplicar para formular el problema no lineal anterior en términos de una ecuación integral no lineal. Por otro

lado, el teorema lineal de Feynman-Kac (ver [81], por ejemplo) se puede aplicar al problema lineal.

En consecuencia, se obtienen las siguientes formulaciones en términos de esperanzas para calcular el valor de U en el instante inicial.

- Si $M^D = V^D$, entonces:

$$U(0,S_0,h_0) = E_0^{Q^D}\left[-\int_0^T e^{-f^D u}\cdot\left(h_u\left(W^D(u,S_u)+U(u,S_u,h_u)-C^D(u)\right)^+ + \left(r^D + b^{D,C_0} - f^D\right)C^D(u)\right)du\right].$$

- Si $M^D = W^D$, entonces:

$$U(0,S_0,h_0) = E_0^{Q^D}\left[-\int_0^T \exp\left(-\int_0^u\left(\frac{h_r}{1-R_C}+f^D\right)dr\right) \cdot\left(h_u\left(W^D(u,S_u)-C^D(u)\right)^+ + \left(r^D + b^{D,C_0} - f^D\right)C^D(u)\right)du\right].$$

En la primera formulación (que surge del modelo de EDPs no lineales), la incógnita U aparece a ambos lados de la igualdad por lo que la componente no lineal se mantiene y explicaremos su resolución numérica mediante técnicas iterativas de Picard en los siguientes párrafos. En la segunda formulación (que surge del modelo de EDPs lineal), la expresión de U es explícita de modo que se aplica un método de Monte Carlo combinado con las fórmulas de cuadratura adecuadas, siendo las compuestas las que mejores resultados proporcionan.

Las técnicas de iteración de Picard son métodos de aproximación para resolver una ecuación de punto fijo. Estos métodos se pueden aplicar para resolver modelos no lineales formulados en términos de esperanzas que se han obtenido a partir de las EDP no lineales correspondientes mediante una fórmula no lineal de Feynman-Kac. Una vez planteado el método de iteración de Picard, se debe discretizar mediante

fórmulas de cuadratura. En esta tesis, se proponen métodos de iteración de Picard para resolver las formulaciones no lineales que surgen en el cálculo de XVA mediante el uso de fórmulas de cuadratura de tipo rectángulo y trapecio simple.

Recientemente, en [37], [62] y [38], los autores proponen una familia de métodos de iteración Picard multinivel, que combinan principalmente las técnicas de Monte Carlo multinivel de [55, 56] y [46] con métodos de iteración de Picard. Como se indica en [37], la complejidad computacional aumenta como máximo linealmente en la dimensión de la PDE y cuárticamente en el inverso de la precisión prescrita. En esta tesis, en el caso del problema no lineal también aplicamos los métodos numéricos de iteración de Picard multinivel propuestos en [37] para resolver las formulaciones en esperanzas equivalentes a las formulaciones de EDPs no lineales.

El trabajo realizado en el marco de tipos de cambio constante supone una extensión de lo desarrollado en el artículo [8], al considerar modelos estocásticos para el diferencial de crédito más adecuados, que incorporan reversión a la media y positividad, además de tener sus parámetros calibrados a mercado en los ejemplos considerados.

A continuación se ha incorporado la evolución estocástica de tipos de cambio de divisa, dando lugar a modelos más complejos y realistas. Una vez introducidas las dinámicas para los tipos de cambio, se han construido las carteras adecuadas para obtener los modelos de EDPs, que incorporan tantas variables espaciales adicionales como tipos de cambio con la moneda doméstica se encuentran involucrados.

En el contexto de tipos de cambio de divisa estocásticos, ya no se aborda la resolución numérica mediante métodos deterministas de las EDPs resultantes debido al elevado número de variables espaciales incluso en los casos más sencillos.

Para aplicar los métodos numéricos probabilísticos, mediante el uso las fórmulas de Feynman-Kac adecuadas se han obtenido previamente las formulaciones en términos de esperanzas que se indican a continuación.

- Si $M^D = V^D$, entonces el XVA en el instante $t = 0$ verifica:

$$U(0, S_0, X_0, h_0) = \mathrm{E}_0^Q \Bigg[- \int_0^T e^{-f^D u} \cdot \Bigg(h_u \left(W^D(u, S_u, \bar{X}_u) + U(u, S_u, X_u, h_u) - C^{C_0}(u) X_u^{D,C_0} \right)^+ + \left(r^D + r^R + sb^{D,C_0} - f^D \right) C^{C_0}(u) X_u^{D,C_0} \Bigg) du \Bigg].$$

- Si $M^D = W^D$, el valor del XVA es:

$$U(0, S_0, X_0, h_0) = \mathrm{E}_0^Q \Bigg[- \int_0^T \exp \left(- \int_0^u \left(\frac{h_r}{1 - R} + f^D \right) dr \right) \cdot \Bigg(h_u \left(W^D(u, S_u, \bar{X}_u) - C^{C_0}(u) X_u^{D,C_0} \right)^+ + \left(r^D + r^R + sb^{D,C_0} - f^D \right) C^{C_0}(u) X_u^{D,C_0} \Bigg) du \Bigg].$$

Una vez obtenidas las formulaciones anteriores, para la resolución numérica de la primera de ellas se han aplicado los mismos métodos de iteraciones de Picard usados en el caso de tipos de cambios de divisas constantes cuando $M^D = V^D$. Para la resolución numérica de la formulación correspondiente a $M^D = W^D$, se han usado las mismas técnicas de Monte Carlo que la análoga en el caso de tipos de cambio constantes.

El trabajo realizado en el marco de tipos de cambio estocásticos supone una extensión de lo desarrollado en el artículo [89], al considerar modelos estocásticos para el diferencial de crédito más adecuados, que incorporan reversión a la media y positividad, además de tener sus parámetros calibrados a mercado en los ejemplos considerados. Por otro lado, se ha incorporado la variante de tener el colateral en bonos en lugar de efectivo.

También es importante señalar que esta tesis se ha desarrollado en el marco del Doctorado Industrial Europeo ABC-EU-XVA, que implica una estancia de investigación en un socio industrial, en este caso la compañía aseguradora Unipol Gruppo S.p.A. Durante la estancia, la autora de esta tesis ha llevado a cabo un relevante

trabajo de investigación relacionado con el desarrollo de un nuevo modelo estocástico de gestión de activos y pasivos (ALM, por su nombre en inglés: *Asset Liability Management*) para una compañía de seguros de vida, tratando tanto con una cartera de activos y una cartera de pasivos u obligaciones.

Los desarrollos y objetivos alcanzados en este trabajo de investigación aparecen recogidos en el artículo [35] y también están contenidos en el Anexo de la tesis.

El esquema seguido en el documento de esta tesis doctoral es el siguiente:

- En el Capítulo 1 modelamos el precio de un derivado de tipo europeo emitido sobre diferentes activos subyacentes que están denominados en diferentes divisas, suponiendo que los tipos de cambio de divisas son constantes. Además, asumimos que el derivado está parcialmente colateralizado en efectivo en una moneda extranjera y que la contraparte tiene una intensidad de incumplimiento estocástica, lo que se traduce en una diferencial de crédito estocástica. Mediante el uso de una estrategia de cobertura para construir una cartera autofinanciada, deducimos modelos EDPs no lineales y lineales para el precio del derivado y para el ajuste de valor total. A continuación, usamos los teoremas adecuados de Feynman-Kac para formular el problema de cálculo del XVA en términos de esperanzas. Desde el punto de vista numérico, abordamos la solución de las EDPs que modelan el valor del XVA utilizando un método de Lagrange-Galerkin bajo el supuesto de que el diferencial de crédito es una función determinista dependiente del tiempo y el derivado depende de dos activos subyacentes estocásticos, por lo que se modela con EDPs no lineales o lineales en dos variables espaciales. Por otro lado, la formulación basada en esperanzas permite el uso de técnicas de Monte Carlo para aproximar el valor del XVA con un mayor número de factores estocásticos. En el caso de los problemas no lineales, el método de Monte Carlo requiere el uso de la iteración de Picard o de técnicas de iteración de Picard multinivel. Al final del capítulo se presentan algunos ejemplos de valoración de opciones europeas, que requieren el contexto de varias monedas, mediante los modelos matemáticos y las técnicas numéricas propuestas.

- En el Capítulo 2 seguimos las mismas metodologías que en el capítulo anterior y extendemos el modelo de tipos de cambio constante al caso de tipos de cambio estocásticos. Además, suponemos que el colateral está compuesto por bonos en moneda extranjera. Los argumentos de cobertura requieren la consideración adicional de la exposición al riesgo de tipo de cambio. Los nuevos modelos obtenidos se formulan en términos de EDPs lineales y no lineales con dimensión superior al caso de tipos de cambio de divisa constantes. También se obtienen los correspondientes modelos en términos de esperanzas. En este entorno de alta dimensión, abordamos la resolución numérica de las formulaciones en términos de esperanzas mediante las mismas técnicas numéricas probabilísticas que en el capítulo anterior. En la sección de resultados numéricos, presentamos algunos ejemplos para ilustrar el comportamiento de las técnicas numéricas propuestas. En particular, analizamos el impacto de introducir estocasticidad en la dinámica de los tipos de cambio y de utilizar la garantía compuesta por bonos en lugar de efectivo.

- En el Apéndice A se construye un modelo estocástico de gestión de activos y pasivos (ALM) para una compañía de seguros de vida. Se supone que dicha compañía tiene una cartera de activos, compuesta por bonos, acciones y efectivo, conjuntamente con una cartera de pasivos, que comprende pólizas de seguro de vida con participación en beneficios. Se introduce un modelo de mortalidad y un modelo de cancelación, así como un nuevo modelo de producción. En primer lugar, con el fin de asegurar la solvencia de la empresa y la consecución de una rentabilidad competitiva, en interés tanto de los accionistas como de los asegurados, la cartera de la aseguradora se rebanlancea periódicamente de acuerdo con la solución de un problema de optimización con restricciones no lineales, que pretende igualar duraciones de activos y pasivos, sujetas a la consecución de un rendimiento objetivo. Además, se imponen varias restricciones del mundo real. Al calcular las proyecciones del balance de la empresa, se consideran no solo los pagos futuros por vencimiento y muerte, sino también los pagos futuros

por rescate y todos los flujos de efectivo debido a la nueva producción, para obtener estimaciones que sean lo más confiables posible. La estimación del momento y del número de futuros rescates, así como de futuros nuevos asegurados requiere la aproximación de esperanzas condicionadas: para ello se emplea una técnica de Monte Carlo de mínimos cuadrados. En segundo lugar, para cada clase de activo de bonos y para la clase de activo de renta variable, se propone un problema de optimización sectorial con el objetivo de maximizar el valor esperado de una función de utilidad elegida, sujeto a los resultados obtenidos en la primera etapa de rebalanceo de la cartera. Finalmente, se analiza un caso de estudio.

Resumo extenso

Neste traballo propóñense e estudan novos modelos complexos de valoración de opcións *vanilla* europeas no contexto de varias divisas (*multicurrency setting*), cando se teñen en conta os axustes de valoración debidos ao risco de contrapartida. Ademais da obtención dos modelos, propóñense diferentes técnicas numéricas para aproximación das solucións dos mesmos, xa que non poden ser obtidas de maneira analítica.

O interese de considerar o contexto de varias moedas, ou multidivisa, provén do feito de que as institucións financeiras poden operar en mercados con distintas moedas, por exemplo cando invisten en derivados cuxos activos subxacentes están en diferentes moedas ou, estando nunha moeda, o financiamento ou o colateral están noutras moedas. A maior parte da literatura sobre os axustes de valoración asociados ao risco de contrapartida centrouse no contexto dunha moeda.

A motivación de considerar axustes de valoración asociados ao risco de contrapartida nos prezos dos derivados financeiros xorde a partir da crise financeira en 2007. Tras o devandita crise, quedou claro que calquera marco de fixación de prezos dun contrato financeiro debería ter en conta a posibilidade de incumprimento de calquera contraparte involucrada no mesmo [28, 61], así como aspectos relacionados coa entrega de colateral, o risco de liquidez ou os custos de financiamiento [52, 85]. Por tanto, débense considerar diferentes axustes de valoración debido a estes factores ao fixar o prezo dun derivado financeiro. O conxunto destes axustes denomínase globalmente axuste de valoración total ou XVA (pola súa expresión en inglés: (*X-Valuation Adjustment*), onde "X" representa as diferentes letras que aparecen nos axustes de valor asociados ao crédito (CVA), débito (DVA), fondeo (FVA), colateral (CollVA),

capital (KVA) ou marxinal (MVA), por exemplo. Os axustes iniciais e máis clásicos estiveron motivados polos riscos de contraparte relacionados co crédito, o financiamento e as garantías. Posteriormente engadíronse os axustes relacionados co capital e o marxinal. Entre as referencias clásicas e máis xerais sobre o tema, diriximos aos lectores aos libros [21, 28, 52] e as referencias que se citan neles.

No marco de produtos nunha moeda, basicamente desenvolvéronse tres metodoloxías principais. Unha primeira aproximación, seguindo os artigos iniciais de Piterbarg [82] e Burgard e Kjaer [22], que obteñen formulacións de EDPs medianche argumentos de cobertura sobre carteiras adecuadas e a aplicación do lema de Itô para procesos de salto-difusión. Este enfoque en termos de formulación de EDP seguiuse en [43], onde o problema tamén se escribe de maneira equivalente en termos de esperanzas. Ademais, tamén se abordou en [4] e [3], onde se analizaron matematicamente e resolto numericamente modelos EDPs para a valoración de opcións europeas cun e dous factores estocásticos. Un segundo enfoque segue as ideas iniciais que aparecen en [18] para obter o CVA por medio de formulacións baseadas en esperanzas, e logo esténdese aos custos colateralizados, de peche e de financiamiento en [78]. Ademais, este enfoque abordouse en [5, 2] para as opcións americanas, e en [15] para a dinámica de Levy, por exemplo. Un terceiro enfoque, baseado en ecuacións diferenciais estocásticas cara atrás (BSDEs), introduciuse en [26] e [27].

Recentemente, prestouse atención á extensión dos axustes de valoración en mercados dunha moeda ao contexto de varias moedas [44]. Por tanto, comezamos a construír un marco multidivisa, seguindo as ideas de [44], onde se teñen en conta a consideración conxunta dos axustes de CVA, FVA, CollVA e repo. Para a inclusión adicional de KVA ou MVA no XVA, poderíanse considerar as ideas en [51, 50] no caso da moeda única.

Para iso, supóñense intensidades estocásticas de incumprimento e involúcranse activos subxacentes denominados en distintas moedas. O noso enfoque baséase no mesmo marco e supostos que en [43], aínda que estendido a unha contorna de múltiples moedas e coa hipótese adicional dunha intensidade de incumprimento cero para a

persoa que realiza a cobertura (*hedger*). En particular, tomamos en consideración as seguintes hipóteses:

- A contraparte pode incumprir, pero a persoa que fai a cobertura está libre de incumprimento.

- Os prezos dos activos subxacentes involucrados se modelan mediante procesos de difusión correlacionados.

- Os eventos de incumprimento dos investidores non afectan a evolución dos prezos dos activos subxacentes involucrados.

- O diferencial crediticio estocástico da contraparte se modela como un proceso positivo con reversión á media, que se correlaciona cos procesos seguidos polos prezos dos activos subxacentes e, cando estes considéranse estocásticos, cos procesos seguidos polos tipos de cambio (*FX rates*).

Seguindo [44], primeiro deducimos formulacións de ecuacións en derivadas parciais (EDP) do problema de fixación de prezos de XVA. Para iso, empregamos argumentos de cobertura, de ausencia de arbitraxe e de autofinanciamiento de carteiras xunto cunha elección do valor de mercado do derivado en caso de incumprimento (*mark to market*), representado por M^D. Esta elección conduce a un problema lineal de EDPs, se o valor de mercado no momento de incumprimento é igual ao prezo do derivado cando non se ten en conta o risco de contraparte (derivado libre de risco), ou a un problema non lineal de EDPs, cando se considera que no momento de incumprimento tense en conta o valor con risco de contraparte (derivado con risco de contrapartida).

En concreto, no caso de tipos de cambio constantes considerados inicialmente, os factores estocásticos son os prezos dos activos subxacentes e o diferencial de crédito da contraparte (*credit spread*). Neste marco, os modelos de EDPs lineais e non lineais para obter o XVA, representado por U, son os seguintes:

- Modelo de EDP non lineal (caso $M^D = V^D$):

$$\begin{cases} \dfrac{\partial U}{\partial t} + \mathcal{L}_{Sh}U - f^D U = h(W^D + U - C^D)^+ + (r^D + b^{D,C_0} - f^D)C^D\,, \\ U(T,S,h) = 0\,. \end{cases}$$

- Modelo de EDP lineal (caso $M^D = W^D$):

$$\begin{cases} \dfrac{\partial U}{\partial t} + \mathcal{L}_{Sh}U - \left(\frac{h}{1-R_C} + f^D\right) U = h(W^D - C^D)^+ + (r^D + b^{D,C_0} - f^D)C^D\,, \\ U(T,S,h) = 0\,. \end{cases}$$

En ambos os casos o operador diferencial en derivadas parciais involucrado é

$$\begin{aligned} \mathcal{L}_{Sh} = {} & \frac{1}{2}\sum_{i,k=1}^{N} \rho^{S^i S^k}\sigma^{S^i}\sigma^{S^k} S^i S^k \frac{\partial^2}{\partial S^i \partial S^k} + \frac{1}{2}(\sigma^h h)^2 \frac{\partial^2}{\partial h^2} \\ & + \sum_{i=1}^{N} \rho^{S^i h}\sigma^{S^i}\sigma^h S^i \frac{\partial^2}{\partial S^i \partial h} + \sum_{i=1}^{N}(r^i - q^i)S^i \frac{\partial}{\partial S^i} + \alpha h(m - \log(h))\frac{\partial}{\partial h} \end{aligned}$$

cando se usa o modelo de Vasicek exponencial para o diferencial de tipo e outro análogo no caso de usar o modelo de CIR. Ademais, o prezo do activo sen risco satisfai o modelo clásico de EDPs de Black-Scholes:

$$\begin{cases} \partial_t W^D + \mathcal{L}_S W^D - f^D W^D = 0\,, \\ W^D(T,S) = G(S)\,, \end{cases}$$

onde $G = G(S)$ é a función de pago do derivado de tipo europeo e o operador en derivadas parciais é:

$$\mathcal{L}_S = \frac{1}{2}\sum_{i,k=1}^{N} \rho^{S^i S^k}\sigma^{S^i}\sigma^{S^k} S^i S^k \frac{\partial^2}{\partial S^i \partial S^k} + \sum_{i=1}^{N}(r^i - q^i)S^i \frac{\partial}{\partial S^i}\,.$$

O prezo do derivado con risco de contrapartida vén dado por $V^D = W^D + U$.

En canto á resolución numérica dos modelos de EDPs, abordamos a solución das EDP lineais e non lineais só no caso dun derivado sobre dous activos subxacentes en moedas diferentes, con tipos de cambio de divisas constantes e diferencial de crédito

da contraparte dependente do tempo de modo determinista. Para iso, empregamos un método semi-Lagrangiano (tamén coñecido como método das características) para a discretización en tempo, combinado co método de elementos finitos de tipo Lagrange constante a anacos para a discretización das variables espaciais asociadas aos factores estocásticos. A consideración conxunta de métodos semi-Lagrangianos con métodos de elementos finitos denomínase xeralmente como métodos de Lagrange-Galerkin. Estas técnicas son especialmente útiles para a discretización dos chamados problemas de EDPs de convección dominante, onde os termos que conteñen derivadas de primeira orde (termos de convección) dominan sobre os que conteñen as derivadas de segunda orde (termos de difusión). Neste escenario, as técnicas propostas evitan a presenza de oscilacións numéricas espurias que aparecen cando se consideran técnicas de discretización en tempo máis convencionais. Adicionalmente, utilízanse ténicas de punto fixo cando se involucran EDPs non lineais.

No caso de alta dimensión, os métodos numéricos deterministas convencionais conlevan un custo computacional que crece exponencialmente co número de variables espaciais na EDP. Nese caso, optouse por métodos numéricos probabilísticos para resolver as formulacións equivalentes baseadas en esperanzas.

En primeiro lugar, para obter a formulación en termos de esperanzas equivailente o anterior modelo non lineal de EDPs, aplicamos o teorema non lineal de Feynman-Kac, que relaciona a solución de EDPs non lineais coa solución de BSDE. O enunciado do teorema non lineal de Feynman-Kac remóntase ao artigo seminal [80]. Como o termo non lineal aparece na incógnita U e non nas derivadas de primeira orde, o Teorema 1.1 no traballo recente [14] pódese aplicar para formular o problema non lineal anterior en termos dunha ecuación integral non lineal. Doutra banda, o teorema lineal de Feynman-Kac (ver [81], por exemplo) pódese aplicar ao problema lineal.

En consecuencia, obtéñense as seguintes formulacións en termos de esperanzas para calcular o valor de U no instante inicial.

- Se $M^D = V^D$, entón:

$$U(0,S_0,h_0) = E_0^{Q^D}\Bigg[- \int_0^T e^{-f^D u} \cdot \Big(h_u \left(W^D(u,S_u) + U(u,S_u,h_u) - C^D(u) \right)^+ + \left(r^D + b^{D,C_0} - f^D \right) C^D(u) \Big) du \Bigg].$$

- Se $M^D = W^D$, entón:

$$U(0,S_0,h_0) = E_0^{Q^D}\Bigg[- \int_0^T \exp\left(- \int_0^u \left(\frac{h_r}{1-R_C} + f^D \right) dr \right) \cdot \Big(h_u \left(W^D(u,S_u) - C^D(u) \right)^+ + \left(r^D + b^{D,C_0} - f^D \right) C^D(u) \Big) du \Bigg].$$

Na primeira formulación (que xorde do modelo de EDPs non lineais), a incógnita U aparece a ambos os dous lados da igualdade polo que a compoñente non lineal mantense e explicaremos a súa resolución numérica mediante técnicas iterativas de Picard nos seguintes parágrafos. Na segunda formulación (que xorde do modelo de EDPs lineal), a expresión de U é explícita de modo que se aplica un método de Monte Carlo combinado coas fórmulas de cuadratura adecuadas, sendo as compostas as que mellores resultados proporcionan.

As técnicas de iteración de Picard son métodos de aproximación para resolver unha ecuación de punto fixo. Estes métodos pódense aplicar para resolver modelos non lineais formulados en termos de esperanzas que se obtiveron a partir das EDP non lineais correspondentes mediante unha fórmula non lineal de Feynman-Kac. Unha vez exposto o método de iteración de Picard, débese discretizar mediante fórmulas de cuadratura. Nesta tese, propóñense métodos de iteración de Picard para resolver as formulacións non lineais que xorden no cálculo de XVA mediante o uso de fórmulas de cuadratura de tipo rectángulo e trapecio simple.

Recentemente, en [37], [62] e [38], os autores propoñen unha familia de métodos de iteración Picard multinivel, que combinan principalmente as técnicas de Monte Carlo

multinivel de [55, 56] e [46] con métodos de iteración de Picard. Como se indica en [37], a complexidade computacional aumenta como máximo linealmente na dimensión da PDE e cuárticamente no inverso da precisión prescrita. Nesta tese, no caso do problema non lineal tamén aplicamos os métodos numéricos de iteración de Picard multinivel propostos en [37] para resolver as formulacións en esperanzas equivalentes ás formulacións de EDPs non lineais.

O traballo realizado no marco de tipos de cambio constante supón unha extensión do desenvolvido no artigo [8], ao considerar modelos estocásticos para o diferencial de crédito máis adecuados, que incorporan reversión á media e positividade, ademais de ter os seus parámetros calibrados a mercado nos exemplos considerados.

A continuación incorporouse a evolución estocástica de tipos de cambio de divisa, dando lugar a modelos máis complexos e realistas. Unha vez introducidas as dinámicas para os tipos de cambio, construíronse as carteiras adecuadas para obter os modelos de EDPs, que incorporan tantas variables espaciais adicionais como tipos de cambio coa moeda doméstica atópanse involucrados.

No contexto de tipos de cambio de divisa estocásticos, xa non se aborda a resolución numérica mediante métodos deterministas das EDPs resultantes debido ao elevado número de variables espaciais mesmo nos casos máis sinxelos.

Para aplicar os métodos numéricos probabilísticos, mediante o uso as fórmulas de Feynman-Kac adecuadas obtivéronse previamente as formulacións en termos de esperanzas que se indican a continuación.

- Se $M^D = V^D$, entón o XVA no instante $t = 0$ verifica:

$$
\begin{aligned}
U(0, S_0, X_0, h_0) = \mathrm{E}_0^Q \Bigg[& - \int_0^T e^{-f^D u} \\
& \cdot \left(h_u \left(W^D(u, S_u, \bar{X}_u) + U(u, S_u, X_u, h_u) - C^{C_0}(u) X_u^{D,C_0} \right)^+ \right. \\
& \left. + \left(r^D + r^R + s b^{D,C_0} - f^D \right) C^{C_0}(u) X_u^{D,C_0} \right) du \Bigg].
\end{aligned}
$$

- Se $M^D = W^D$, o valor del XVA é:

$$U(0, S_0, X_0, h_0) = \mathrm{E}_0^Q \Bigg[- \int_0^T \exp\left(- \int_0^u \left(\frac{h_r}{1-R} + f^D \right) dr \right) \cdot \left(h_u \left(W^D(u, S_u, \bar{X}_u) - C^{C_0}(u) X_u^{D,C_0} \right)^+ + \left(r^D + r^R + sb^{D,C_0} - f^D \right) C^{C_0}(u) X_u^{D,C_0} \right) du \Bigg].$$

Unha vez obtidas as formulacións anteriores, para a resolución numérica da primeira delas aplicáronse os mesmos métodos de iteracións de Picard usados no caso de tipos de cambios de divisas constantes cando $M^D = V^D$. Para a resolución numérica da formulación correspondente a $M^D = W^D$, usáronse as mesmas técnicas de Monte Carlo que a análoga no caso de tipos de cambio constantes.

O traballo realizado no marco de tipos de cambio estocásticos supón unha extensión do desenvolvido no artigo [89], ao considerar modelos estocásticos para o diferencial de crédito máis adecuados, que incorporan reversión á media e positividade, ademais de ter os seus parámetros calibrados a mercado nos exemplos considerados. Doutra banda, incorporouse a variante de ter o colateral en bonos en lugar de efectivo.

Tamén é importante sinalar que esta tese desenvolveuse no marco do Doutoramento Industrial Europeo ABC-EU-XVA, que implica unha estadía de investigación nun socio industrial, neste caso a compañía aseguradora Unipol Gruppo S.p.A. Durante a estadía, a autora desta tese levou a cabo un relevante traballo de investigación relacionado co desenvolvemento dun novo modelo estocástico de xestión de activos e pasivos (ALM, polo seu nome en inglés: *Asset Liability Management*) para unha compañía de seguros de vida, tratando tanto cunha carteira de activos e unha carteira de pasivos ou obrigacións.

Os desenvolvementos e obxectivos alcanzados neste traballo de investigación aparecen recollidos no artigo [35] e tamén están contidos no Anexo da tese.

O esquema seguido no documento desta tese doutoral é o seguinte:

- No Capítulo 1 modelamos o prezo dun derivado de tipo europeo emitido sobre diferentes activos subxacentes que están denominados en diferentes divisas, supoñendo que os tipos de cambio de divisas son constantes. Ademais, asumimos que o derivado está parcialmente colateralizado en efectivo nunha moeda estranxeira e que a contraparte ten unha intensidade de incumprimento estocástica, o que se traduce nunha diferencial de crédito estocástica. Mediante o uso dunha estratexia de cobertura para construír unha carteira autofinanciada, deducimos modelos EDPs non lineais e lineais para o prezo do derivado e para o axuste de valor total. A continuación, usamos os teoremas adecuados de Feynman-Kac para formular o problema de cálculo o XVA en termos de esperanzas. Desde o punto de vista numérico, abordamos a solución das EDPs que modelan o valor do XVA utilizando un método de Lagrange-Galerkin baixo o suposto de que o diferencial de crédito é unha función determinista dependente do tempo e a derivada depende de dous activos subxacentes estocásticos, polo que se modela con EDPs non lineais ou lineais en dúas variables espaciais. Doutra banda, a formulación baseada en esperanzas permite o uso de técnicas de Monte Carlo para aproximar o valor do XVA cun maior número de factores estocásticos. No caso dos problemas non lineais, o método de Monte Carlo require o uso da iteración de Picard ou de técnicas de iteración de Picard multinivel. Ao final do capítulo preséntanse algúns exemplos de valoración de opcións europeas, que requiren o contexto de varias moedas, mediante os modelos matemáticos e as técnicas numéricas propostas.

- No Capítulo 2 seguimos as mesmas metodoloxías que no capítulo anterior e estendemos o modelo de tipos de cambio constante ao caso de tipos de cambio estocásticos. Ademais, supoñemos que o colateral está composto por bonos en moeda estranxeira. Os argumentos de cobertura requiren a consideración adicional da exposición ao risco de tipo de cambio. Os novos modelos obtidos formúlanse en termos de EDPs lineais e non lineais con dimensión superior

ao caso de tipos de cambio de divisa constantes. Tamén se obteñen os correspondentes modelos en termos de esperanzas. Nesta contorna de alta dimensión, abordamos a resolución numérica das formulacións en termos de esperanzas mediante as mesmas técnicas numéricas probabilísticas que no capítulo anterior. Na sección de resultados numéricos, presentamos algúns exemplos para ilustrar o comportamento das técnicas numéricas propostas. En particular, analizamos o impacto de introducir estocasticidad na dinámica dos tipos de cambio e de utilizar a garantía composta por bonos en lugar de efectivo.

- No Apéndice A construúese un modelo estocástico de xestión de activos e pasivos (ALM) para unha compañía de seguros de vida. Suponse que dita compañía ten unha carteira de activos, composta por bonos, accións e efectivo, conxuntamente cunha carteira de pasivos, que comprende pólizas de seguro de vida con participación en beneficios. Introdúcese un modelo de mortalidade e un modelo de cancelación, así como un novo modelo de produción. En primeiro lugar, co fin de asegurar a solvencia da empresa e a consecución dunha rendibilidade competitiva, en interese tanto dos accionistas como dos asegurados, a carteira da aseguradora se rebanlancea periodicamente de acordo con a solución dun problema de optimización con restricións non lineais, que pretende igualar duracións de activos e pasivos, suxeitas á consecución dun rendemento obxectivo. Ademais, impóñense varias restricións do mundo real. Ao calcular as proxeccións do balance da empresa, considéranse non só os pagos futuros por vencemento e morte, senón tamén os pagos futuros por rescate e todos os fluxos de efectivo debido á nova produción, para obter estimacións que sexan o máis confiables posible. A estimación do momento e do número de futuros rescates, así como de futuros novos asegurados require a aproximación de esperanzas condicionadas: para iso emprégase unha técnica de Monte Carlo de mínimos cadrados. En segundo lugar, para cada clase de activo de bonos e para a clase de activo de renda variable, proponse un problema de optimización sectorial co obxectivo de maximizar o valor esperado dunha función de utilidade elixida, suxeito aos

resultados obtidos na primeira etapa de rebalanceo da carteira. Finalmente, analízase un caso de estudo.

Bibliography

[1] C. Albanese, S. Crépey, R. Hoskinson, and B. Saadeddine. XVA analysis from the balance sheet. *Quantitative Finance*, 21(1):99–123, 2021.

[2] I. Arregui, A. Leitao, B. Salvador, and C. Vázquez. Efficient parallel Monte Carlo techniques for pricing American options including counterparty credit risk. *International Journal of Computer Mathematics*, 2023. Advance online publication.

[3] I. Arregui, B. Salvador, D. Ševčovič, and C. Vázquez. Total value adjustment for European options with two stochastic factors. Mathematical model, analysis and numerical simulation. *Computers & Mathematics with Applications*, 76(4):725–740, 2018.

[4] I. Arregui, B. Salvador, and C. Vázquez. PDE models and numerical methods for total value adjustment in European and American options with counterparty risk. *Applied Mathematics and Computation*, 308:31–53, 2017.

[5] I. Arregui, B. Salvador, and C. Vázquez. A Monte Carlo approach to American options including counterparty credit risk. *International Journal of Computer Mathematics*, 96(11):2157–2176, 2019.

[6] I. Arregui, B. Salvador, D. Ševčovič, and C. Vázquez. Total value adjustment for European options with two stochastic factors. Mathematical model, analysis and numerical simulation. *Computers & Mathematics with Applications*, 76:725–740, 2018.

[7] I. Arregui, R. Simonella, and C. Vázquez. Modelling and computing the total value adjustment for European derivatives in a multi-currency setting. In M. Ehrhardt and M. Günther, editors, *Progress in Industrial Mathematics at ECMI 2021*, pages 313–319. Springer International Publishing, 2022.

[8] I. Arregui, R. Simonella, and C. Vázquez. Total value adjustment for European options in a multi-currency setting. *Applied Mathematics and Computation*, 413:126647, 2022.

[9] A. R. Bacinello. Fair valuation of a guaranteed life insurance participating contract embedding a surrender option. *Journal of Risk and Insurance*, 70(3):461–487, 2003.

[10] A. R. Bacinello. Pricing guaranteed life insurance participating policies with annual premiums and surrender option. *North American Actuarial Journal*, 7(3):1–17, 2003.

[11] A. R. Bacinello. Endogenous model of surrender conditions in equity-linked life insurance. *Insurance: Mathematics and Economics*, 37(2):270–296, 2005.

[12] L. Ballotta, S. Haberman, and N. Wang. Guarantees in with-profit and unitized with-profit life insurance contracts: Fair valuation problem in presence of the default option. *Journal of Risk and Insurance*, 73(1):97–121, 2006.

[13] D. Bauer, R. Kiesel, A. Kling, and J. Ruß. Risk-neutral valuation of participating life insurance contracts. *Insurance: Mathematics and Economics*, 39(2):171–183, 2006.

[14] C. Beck, M. Hutzenthaler, and A. Jentzen. On nonlinear Feynman-Kac formulas for viscosity solutions of semilinear parabolic partial differential equations. arXiv:2004.03389v2, 2020.

[15] A. Borovykh, C. W. Oosterlee, and A. Pascucci. Efficient XVA computation under local Lévy models. *SIAM Journal on Financial Mathematics*, 9(1):251–273, 2018.

[16] S. P. Bradley and D. B. Crane. A dynamic model for bond portfolio management. *Management Science*, 19(2):139–151, 1972.

[17] A. Braun, H. Schmeiser, and F. Schreiber. Portfolio optimization under solvency II: Implicit constraints imposed by the market risk standard formula. *Journal of Risk and Insurance*, 84(1):177–207, 2017.

[18] D. Brigo and A. Capponi. Bilateral counterparty risk valuation with stochastic dynamical models and applications to CDSs. arXiv:0812.3705, 2009.

[19] D. Brigo, A. Dalessandro, M. Neugebauer, and F. Triki. A stochastic processes toolkit for risk management. *arXiv preprint arXiv:0812.4210*, 2008.

[20] D. Brigo and F. Mercurio. *Interest rate models-theory and practice: with smile, inflation and credit*. Springer Science & Business Media, 2007.

[21] D. Brigo, M. Morini, and A. Pallavicini. *Counterparty Credit Risk, Collateral and Funding with Pricing Cases for all Asset Classes*. The Wiley Finance Series, 2013.

[22] C. Burgard and M. Kjaer. PDE representations of options with bilateral counterparty risk and funding costs. *Journal of Credit Risk*, 7(3):1–19, 2011.

[23] D. R. Cariño, T. Kent, D. H. Myers, C. Stacy, M. Sylvanus, A. L. Turner, K. Watanabe, and W. T. Ziemba. The Russell-Yasuda Kasai model: An asset/liability model for a Japanese insurance company using multistage stochastic programming. *Interfaces*, 24(1):29–49, 1994.

[24] D. Castillo, A. M. Ferreiro, J. A. García-Rodríguez, and C. Vázquez. Numerical methods to solve PDE models for pricing business companies in different

regimes and implementation in GPUs. *Applied Mathematics and Computation*, 219:11233–11257, 2014.

[25] G. Consigli and M. A. H. Dempster. Dynamic stochastic programming for asset-liability management. *Annals of Operations Research*, 81:131–162, 1998.

[26] S. Crépey. Bilateral counterparty risk under funding constraints–Part I: Pricing. *Mathematical Finance*, 25:1–22, 2015.

[27] S. Crépey. Bilateral counterparty risk under funding constraints–Part II: CVA. *Mathematical Finance*, 25:23–50, 2015.

[28] S. Crépey and T. Bielecki. *Counterparty Risk and Funding: A Tale of Two Puzzles*. Chapman and Hall–CRC Press, 2014.

[29] G. B. Dantzig and G. Infanger. Multi-stage stochastic linear programs for portfolio optimization. *Annals of Operations Research*, 45(1):59–76, 1993.

[30] G. Deelstra and F. Delbaen. Convergence of discretized stochastic (interest rate) processes with stochastic drift term. *Applied Stochastic Models and Data Analysis*, 14(1):77–84, 1998.

[31] M. A. H. Dempster. *Stochastic programming*. Academic Press, 1980.

[32] M. A. H. Dempster and A. Ireland. Object-oriented model integration in a financial decision support system. *Decision Support Systems*, 7(4):329–340, 1991.

[33] Y. D'Halluin, P. A. Forsyth, and G. Labahn. A semi–Lagrangian approach for American Asian options under jump-diffusion. *SIAM Journal on Scientific Computing*, 27:315–345, 2005.

[34] M. Di Francesco. A general Gaussian interest rate model consistent with the current term structure. *International Scholarly Research Notices*, 2012, 2012.

[35] M. Di Francesco and R. Simonella. A stochastic asset liability management model for life insurance companies. *Financial Markets and Portfolio Management*, 37:61–94, 2023.

[36] N. A. Doherty and J. R. Garven. Price regulation in property-liability insurance: A contingent-claims approach. *The Journal of Finance*, 41(5):1031–1050, 1986.

[37] W. E, M. Hutzenthaler, A. Jentzen, and T. Kruse. On multilevel Picard numerical approximations for high-dimensional nonlinear parabolic partial differential equations and high-dimensional backward stochastic differential equation. *Journal of Scientific Computing*, 79:1534–1571, 2019.

[38] W. E, M. Hutzenthaler, A. Jentzen, and T. Kruse. Multilevel Picard iterations for solving smooth parabolic heat equations. *Partial Differential Equations and Applications*, Available online at https://link.springer.com/article/10.1007/s42985-021-00089-5:1–31, 2021.

[39] J. Eckert, S. Graf, and A. Kling. A measure to analyse the interaction of contracts in a heterogeneous life insurance portfolio. *European Actuarial Journal*, pages 1–26, 2020.

[40] J. L. Fernández, A. M. Ferreiro-Ferreiro, J. A. García-Rodríguez, and C. Vázquez. GPU parallel implementation for asset-liability management in insurance companies. *Journal of Computational Science*, 24:232–254, 2018.

[41] G. Fichera. Problemi elastostatici con vincoli unilaterali: il problema di Signorini con ambigue condizioni al contorno. *Atti della Accademia Nazionale dei Lincei, Ser. VII*, 7:613–679, 1964.

[42] L. Fisher and R. L. Weil. *Coping with the risk of interest-rate fluctuations: returns to bondholders from naive and optimal strategies.* Routledge, 2017.

[43] L. M. García Muñoz. CVA, FVA (and DVA?) with stochastic spreads. A feasible replication approach under realistic assumptions. *MPRA*, 2013. http://mpra.ub.unimuenchen.de/44568/.

[44] L. M. García Muñoz, F. de Lope, and J. Palomar. *Pricing Derivatives in the New Framework: OIS Discounting, CVA, DVA & FVA*. MPRA, 2015. https://mpra.ub.unimuenchen.de/62086.

[45] T. Gerstner, M. Griebel, M. Holtz, R. Goschnick, and M. Haep. A general asset–liability management model for the efficient simulation of portfolios of life insurance policies. *Insurance: Mathematics and Economics*, 42(2):704–716, 2008.

[46] M. Giles. Multilevel Monte Carlo path simulation. *Operations Research*, 56(3):607–617, 2008.

[47] I. V. Girsanov. On transforming a certain class of stochastic processes by absolutely continuous substitution of measures. *Theory of Probability & Its Applications*, 5(3):285–301, 1960.

[48] M. Grebeck and S. Rachev. Stochastic programming methods in asset-liability management. *Investment Management and Financial Innovations*, (2, Iss. 1):82–90, 2005.

[49] A. Green. *XVA: Credit, Funding and Capital Valuation Adjustments*. Wiley Finance, Chichester, 2016.

[50] A. Green and C. Kenyon. MVA: Initial margin valuation adjustment by replication and regression. *Risk*, 28(5), 2015.

[51] A. Green, C. Kenyon, and C. Dennis. KVA: Capital valuation adjustment by replication. *Risk*, 27(12), 2014.

[52] J. Gregory. *Counterparty Credit Risk and Credit Value Adjustment*. Wiley Finance, Chichester, 2012.

[53] A. Grosen and P. L. Jørgensen. Fair valuation of life insurance liabilities: the impact of interest rate guarantees, surrender options, and bonus policies. *Insurance: Mathematics and Economics*, 26(1):37–57, 2000.

[54] J. Han, A. Jentzen, and W. E. Solving high-dimensional partial differential equations using deep learning. *Proceedings of the National Academy of Sciences*, 115(34):8505–8510, 2018.

[55] S. Heinrich. Monte Carlo complexity of global solution of integral equation. *Journal of Complexity*, 14(2):151–175, 1998.

[56] S. Heinrich. Multilevel Monte Carlo methods. In *International Conference on Large-Scale Scientific Computing*, pages 58–67. Springer, 2001.

[57] P. Henry-Labordère. Counterparty risk valuation: a marked branching diffusion approach. *Risk Magazine*, 2012.

[58] P. Henry-Labordère, N. Oudjane, X. Tan, N. Touzi, and X. Warin. Branching diffusion representation of semilinear PDEs and Monte Carlo approximation. *Annales de l'Institute Henry Poincaré, Probabilité et Statistiques*, 55(1):184–210, 2019.

[59] P. Hieber, J. Natolski, and R. Werner. Fair valuation of cliquet-style return guarantees in (homogeneous and) heterogeneous life insurance portfolios. *Scandinavian Actuarial Journal*, 2019(6):478–507, 2019.

[60] J. Hull and A. White. Pricing interest-rate-derivative securities. *The Review of Financial Studies*, 3(4):573–592, 1990.

[61] J. Hull and A. White. Valuing derivatives: Funding value adjustment and fair value. *Financial Analysts Journal*, 3:1–27, 2014.

[62] M. Hutzenthaler, A. Jentzen, T. Kruse, T. Nguyen, and P. von Wurstemberger. Overcoming the curse of dimensionality in the numerical approximation of semilinear parabolic partial differential equations. *Proceedings of the Royal Society A*, 476(2244):20190630, 2020.

[63] N. Jansen. Model points for asset liability models. Master's thesis, Maastricht University Faculty of Economics and Business Administration, 2008.

[64] A. Jentzen, D. Salimova, and T. Welti. A proof that deep artificial neural networks overcome the curse of dimensionality in the numerical approximation of Kolmogorov partial differential equations with constant diffusion and nonlinear drift coefficients. *Communications in Mathematical Sciences*, 19(5):1167–1205, 2021.

[65] P. E. Kloeden and E. Platen. *Numerical Solution of Stochastic Differential Equations*. Springer, Berlin, 2011.

[66] M. Lane and P. Hutchinson. A model for managing a certificate of deposit portfolio under uncertainty. *Dempster (1980), op. cit*, pages 473–493, 1980.

[67] A. Lipton. *Mathematical Methods for Foreign Exchange*. World Scientific, London, 2001.

[68] F. A. Longstaff and E. S. Schwartz. Valuing American options by simulation: a simple least-squares approach. *The Review of Financial Studies*, 14(1):113–147, 2001.

[69] J. G. López-Salas, S. Rodríguez, and C. Vázquez. AMFR-W numerical methods for solving high dimensional SABR/LIBOR PDE models. *SIAM Journal on Scientific Computing*, 43(1):B30–B54, 2021.

[70] J. G. López-Salas and C. Vázquez. PDE formulation of some SABR/LIBOR market models and its numerical solution with a sparse grid combination technique. *Computers & Mathematics with Applications*, 75(5):1616–1634, 2018.

[71] F. R. Macaulay. From matter to "Some Theoretical Problems Suggested by the Movements of Interest Rates, Bond Yields and Stock Prices in the United States since 1856" . 1938.

[72] H. McKean. Application of Brownian motion to the equation of Kolmogorov-Petrovskii-Piskunov. *Communications on Pure and Applied Mathematics*, 28(3):323–331, 1975.

[73] M. A. Milevsky and T. S. Salisbury. Financial valuation of guaranteed minimum withdrawal benefits. *Insurance: Mathematics and Economics*, 38(1):21–38, 2006.

[74] T. Møller and M. Steffensen. *Market-valuation methods in life and pension insurance*. Cambridge University Press, 2007.

[75] J. Mossin. Optimal multiperiod portfolio policies. *The Journal of Business*, 41(2):215–229, 1968.

[76] O. A. Oleĭnik and E. V. Radkevič. *Second Order Equations with Nonnegative Characteristic Form*. AMS, Plenum Press, New York, London, 1973.

[77] C. Orozco-Garcia and H. Schmeiser. Is fair pricing possible? An analysis of participating life insurance portfolios. *Journal of Risk and Insurance*, 86(2):521–560, 2019.

[78] A. Pallavicini, D. Perini, and D. Brigo. Funding, collateral and hedging: A consistent framework including CVA, DVA, collateral, netting rules and re-hypotecation, 2011. Available at https://ssrn.com/abstract=1969114.

[79] E. Pardoux and S. Peng. Adapted solution of a backward stochastic differential equation. *Systems and Control Letters*, 14(1):55–61, 1990.

[80] E. Pardoux and S. Peng. Backward stochastic differential equations and quasilinear parabolic partial differential equations. In *Stochastic partial differential equations and their applications (Charlotte, NC,1991)*, volume 176 of *Lecture Notes Control Inf. Sci.*, pages 200–217. Springer, Berlin, 1992.

[81] A. Pascucci. *PDE and Martingale Methods in Option Pricing*. Springer Science & Business Media, 2011.

[82] V. Piterbarg. Funding beyond discounting: collateral agreements and derivatives pricing. *Risk Magazine*, 2:97–102, 2010.

[83] G. Rapuch and T. Roncalli. Dependence and two-asset options pricing. *Journal of Computational Finance*, 7(4):23–33, 2004.

[84] F. M. Redington. Review of the principles of life-office valuations. *Journal of the Institute of Actuaries (1886-1994)*, 78(3):286–340, 1952.

[85] I. Ruiz. A complete XVA valuation framework. Why the "law of one price" is dead? iRuiz Consulting, 2015.

[86] P. A. Samuelson. The effect of interest rate increases on the banking system. *The American Economic Review*, 35(1):16–27, 1945.

[87] A. Sandström. *Handbook of solvency for actuaries and risk managers: theory and practice*. CRC Press, 2016.

[88] D. F. Schrager and A. A. Pelsser. Pricing swaptions and coupon bond options in affine term structure models. *Mathematical Finance*, 16(4):673–694, 2006.

[89] R. Simonella and C. Vázquez. XVA in a multi-currency setting with stochastic foreign exchange rates. *Mathematics and Computers in Simulation*, 207:59–79, 2023.

[90] M. V. Wüthrich and M. Merz. *Financial modeling, actuarial valuation and solvency in insurance*. Springer, 2013.

[91] S. A. Zenios. Asset/liability management under uncertainty for fixed-income securities. *Annals of Operations Research*, 59(1):77–97, 1995.

[92] S. A. Zenios and W. T. Ziemba. *Handbook of Asset and Liability Management. I: Theory and Methodology*. Elsevier, 2006.

[93] S. A. Zenios and W. T. Ziemba. *Handbook of Asset and Liability Management. II: Applications and case studies*. Elsevier, 2007.